Gene therapy strategies for dominant heterogeneous disorders and the identification of a novel gene causing retinitis pigmentosa and sensorineural deafness

A thesis submitted to the University of Dublin for the degree of Doctor of Philosophy

by

Sophia Millington-Ward, M.Sc.

Department of Genetics

University of Dublin, Trinity College

Ph.D. Thesis

November, 1999

Declaration

This thesis has not been previously submitted to this or any other university for examination for a higher degree. The work presented here is entirely my own, except where noted. This thesis may be made available for consultation within the university library. It may be photocopied or lent to other libraries for purposes of consultation.

Sophia Millington-Ward

Sophia Millington-Ward M.Sc.
November, 1999

This Ph.D. thesis is dedicated to my wonderful
family and to my future husband, Nick,
who have helped me along and
supported me throughout
this difficult but
interesting
time.

Abstract

The purpose of this Ph.D. thesis has been to contribute towards the generation of therapies for inherited disorders such as retinitis pigmentosa (RP) and osteogenesis imperfecta (OI). In chapter 2, a novel mitochondrial disease mutation in the second serine tRNA gene (MTTS2) was discovered and characterised. A heteroplasmic C→A transversion at position 12258 in MTTS2 was found to cause RP in conjunction with sensorineural deafness in a large Irish kindred (Kenna et al., 1997; Mansergh et al., 1999). This study highlights yet again, the genetic heterogeneity present in many inherited disorders such as RP (Appendix B and table 2, chapter 1).

Chapter 3 explores the use of hammerhead ribozymes in mutation-independent methods of gene suppression. The generation of mutation-independent suppressors for dominant-negative disorders such as RP and osteogenesis imperfecta (OI) is imperative, as these disorders are frequently associated with immense genetic heterogeneity, making the generation of mutation-specific therapeutic agents impractical. Three mutation-independent strategies, studied in chapter 3, are based on either selective cleavage of mutant transcripts or alternatively cleavage of both mutant and wildtype transcripts and concurrent introduction of replacement genes which supply modified wildtype transcripts which are protected from cleavage. In these approaches, ribozyme mediated cleavage occurs, not at mutation sites, but at wobble positions, in untranslated regions (UTRs) of the target mRNA or at polymorphic sites. Replacement genes, which encode wildtype protein, were generated. Replacement genes were specifically altered at ribozyme cleavage sites, protecting transcripts from cleavage (Millington-Ward et al., 1997; O'Neill et al., 1999).

In chapter 4, a particularly efficient ribozyme first described in chapter 3, Rzpol1a1, was characterised in detail in terms of its kinetic profile. Rzpol1a1 targets a common polymorphic site in exon 52 of the COL1A1 transcript, a gene involved in OI. The polymorphism is sufficiently common to make Rzpol1a1 a potential therapeutic agent applicable to 1 in 5 OI patients with a dominant-negative mutation in COL1A1. Rzpol1a1 had an efficient maximum cleavage velocity (V_{max}) of 0.41 min^{-1} (Millington-Ward et al., 1999). The ability of the

ribozyme to cleave a structurally complex target transcript (in this case 371 bases) efficiently *in vitro* strongly suggests that this ribozyme is worth testing thoroughly for *in vivo* cleavage activity (see chapters 4 and 5).

In chapter 5, Rzpol1a1 was protected from ribonucleases by the incorporation of 2'-amino pyrimidines with a view to protecting the ribozyme from nucleases and delivering the pre-formed ribozyme in an exogenous fashion to either cell cultures or animal models for OI. Rzpol1a1 with protected nucleotides, while maintaining both stability in serum and cleavage specificity, was somewhat problematic to transcribe *in vitro*; ribozyme yields were low. However, there may be ways to circumvent this difficulty (see discussion section). In addition, in chapter 5, human primary fibroblast cell lines, known to express the polymorphic variants of the COL1A1 gene, were obtained and one of them characterised in terms of its ability to be transfected, using viral (adenovirus and melony leukemia virus) and non-viral (electroporation and lipids) means of gene delivery. The cell lines were only susceptible to viral transfection. Thus, a plasmid was generated carrying Rzpol1a1 driven by a CMV promoter, which will be used to generate an MLV retrovirus. The resulting virus will be studied in the characterised fibroblast cell lines and in a suitable animal model for OI.

The last decade has resulted in a substantial elucidation of the molecular etiologies of many heritable disorders. This provides knowledge of the underlying molecular pathogenesis of disease, a greater understanding of the mechanisms of many disease processes and indeed a platform on which to explore and build therapies for these disorders. The research undertaken for this Ph.D. thesis touches upon these areas outlined above. The data obtained from the study provide additional information on the molecular etiology of RP with the implication of the second mitochondrial serine tRNA in causing RP in association with sensorineural deafness. The remaining chapters explore the possible utility of ribozyme technologies in the design of therapies for genetically heterogeneous disorders such as RP and OI.

Acknowledgements

Firstly and foremost I would like to thank Pete and Jane for their great supervision, encouragement and advice. I would also like to thank the whole lab for being such a marvelous support and always being there for breakfasts, lunches and very importantly drinkies. So thanks, Pete, Jane, Paul, Marian, Denise, Avril, Niamh, Mary, Sophie, Lesley, Carmel, Brian, Gearóid and Denis. Also a thanks for people who have departed: Fiona, Michael, Peter, Alex and Val. I would like particularly to thank Fiona, Den and Irene (honorary member of the lab) for always being there for me, no matter what! I would like to thank my family and friends for their support and for putting up with me. In addition, I would like to thank the preproom lads who have ordered and fixed a million things for me over the years; not to mention kept me up to date will all the news in the department. Finally, though very importantly, I would like to thank Nick, who has been wonderful throughout, lending shoulders, helping (computer-wise for instance), and encouraging or simply spending time with me relaxing. Thanks a million all, I have loved not only the work, but also the social aspects of Ph.D. stuff.

Publications resulting from work presented in this Ph.D. thesis

Kenna P, Mansergh F, Millington-Ward S, Erven A, Kumar-Singh R, Brennan R, Farrar GJ, Humphries P. Clinical and molecular genetic characterisation of a family segregating autosomal dominant retinitis pigmentosa and sensorineural deafness. Br J Ophthalmol. 1997 Mar; 81(3):207-13.

Millington-Ward S*, O'Neill B*, Tuohy G, Al-Jandal N, Kiang AS, Kenna PF, Palfi A, Hayden P, Mansergh F, Kennan A, Humphries P, Farrar GJ. Strategems in vitro for gene therapies directed to dominant mutations. Hum Mol Genet. 1997 Sep;6(9):1415-26. *joint first authors.

Mansergh FC, Millington-Ward S, Kennan A, Kiang AS, Humphries M, Farrar GJ, Humphries P, Kenna PF. Retinitis Pigmentosa and Progressive Sensorineural Hearing Loss Caused by a C12258A Mutation in the Mitochondrial MTTS2 Gene. Am J Hum Genet. 1999 Apr;64(4):971-985.

Millington-Ward S, O'Neill B, Kiang AS, Humphries P, Kenna PF, Farrar GJ. A mutation-independent therapeutic stratagem for osteogenesis imperfecta. Antisense Nucleic Acid Drug Dev. 1999 Dec;9(6):537-42.

O'Neill B, Millington-Ward S, O'Reilly M, Tuohy G, Kiang AS, Kenna PF, Humphries P, Farrar GJ. Ribozyme-based therapeutic approaches for autosomal dominant retinitis pigmentosa. Submitted to IOVS July 1999.

Abbreviations

a	Substrate concentration
A	Adanine
a_0	Substrate concentration at time 0
AAV	Adeno acociated virus
ADA	Adenosine deaminase
adRP	Autosomal dominant RP
ARMD	Age related macular degeneration
Asn	Asparigine
$[\alpha^{32}P]dATP$	$[\alpha^{32}P]$--labeled deoxy adanine
$[\alpha^{32}P]dCTP$	$[\alpha^{32}P]$–labeled deoxycytadine
arRP	Autosomal recessive RP
Ad	Adeno virus
Ba^{2+}	Barium ion
bp	Base pair
C	Cytosine
°C	Degrees Celsius
Ca^{2+}	Calcium ion
$CaCl_2$	Calcium chloride
CAR	Cis-acting ribozyme
CEPH	Centre d'Etude du Polymorphisme Humaine
CF	Cystic fibrosis
cGMP	Cyclic 3', 5'-guanosine monophosphate
CIP	Calf intestinal phosphotase
CIPO	Chronic intestinal pseudoobstruction, myopathy and ophthalmoplegia
cM	Centi morgan ($\approx$ 1 million base)
Co^{2+}	Cobalt ion
COL1A1	Type I collagen 1a1 gene
COL1A2	Type I collagen 1a2 gene
CPEO	Chronic Progressive External Ophthalmoplegia
DEAF	Aminoglycoside-Induced Deafness
DMDF	Diabetes Mellitus and Deafness
DMEM	Dulbecco's modified eagle medium
DNA	Desoxiribonucleic acid
dNTP	Deoxy nucleotide triphosphate
dpm	Disintegrations per minute
e_0	Ribozyme concentration
ECG	Electocariographies
EDS	Ehlers-Danlos syndrome
EDTA	Ethylenediaminetetra-acetic acid
EMG	Electromyographies
ERG	Electroretinogram
FICP	Fatal infantile cadiomyopathy and MELAS-associated cardiomyopathy
G	Guanine
ΔG	Gibbs free energy
Gly	Glycine
H	Histidine

HDV	Hepatitis delta virus
His	Histidine
HIV	Human immunodeficiency virus
H_2O	Water (dihydrogen oxide)
k_1	Rate of ribozymes association
k_{-1}	Rate of ribozyme dissociation
k_2	Rate of the cleavage step of the reaction
kb	Kilobase
k_{cat}	Catalytic constant or turnover number
kDa	Kilodalton
kJ	Kilojoule
K_m	Michaelis constant
kV	Kilo volts
L	Leucine
L(0.5)	The likelihood obtained under the assumption of no linkage
$L(\Theta)$	The likelihood of the observed recombination fraction
LacZ	Gene that expressed β-galactosidase
LHON	Leber's Hereditary Optic Neuropathy
LDYT	Leber's hereditary Optic Neuropathy and Dystonia
Leu	Leucine
MHCM	Maternally inherited hypertrophic cadiomyopathy.
LIMM	Lethal infantile mitochondrial myopathy
lod	Logarithm of the odds
M	Morgan (≈ 100 million base)
MA	Milliampaire
MELAS	Mitochondrial encephalomyopathy, lactic acidosis, stroke-like episodes
MERRF	Myoclonic epilepsy and ragged red muscle fibers
Mg^{2+}	Magnesium ion
$MgCl_2$	Magnesium chloride
min^{-1}	On devided by minute
ml	Milliliter
μl	Microliter
mM	Milimolar
MM	Mitochondrial myopathy
MMC	Maternal myopathy and cardiomyopathy
Mn^{2+}	Manganese
mRNA	Messenger RNA
MCS	Multiple cloning site
mtDNA	Mitochondrial DNA
MTTS2	Second serine tRNA gene
NaOAc	Sodium acetate
NaOH	Sodium hydroxide
NARP	Neurogenic muscle weakness, ataxia and RP
ng	Nanogram
nm	Nanometer
nM	Nanomolar
nt	Nucleotide(s)
NUX	N = C or G or A or U; U = uracyl; X = any base but G
OI	Osteogenesis Imperfecta
P	Proline
P	Product
PBS	Phosphate buffered saline
$P_{\infty cont}$	Amount of product at t = ∞ for the control reaction
PCR	Polymerase chain reaction

PDE	Phosphodiesterase
pKa	$-\log Ka$ and Ka = acidconstant (mol/L)
pmoles	Picomoles
PNA	Peptide nucleic acid
Pro	Proline
$P_{\infty test}$	Amount of product at $t = \infty$ for the test reaction
QTPCR	Quantitative RTPCR
R	G or A
RDS	Retinal degeneration slow
RFLP	Restriction fragment length polymorphism
Rho	Rhodopsin
RNA	Ribonucleic acid
ROM-1	Rod outer segment membrane protein gene
RP	Retinitis Pigmentosa
rRNA	Ribosomal RNA
RTPCR	Reverse transcription PCR
rUTP	Ribo uridine triphosphate
Rz	Ribozyme
RzS	Ribozyme Substrate complex
s	Second
S	Substrate
SCID	Severe combined immunodificiency disease
SDS	Sodium dodecyl sulphate
Ser	Serine
SNP	Single nucleaotide polymorphism
Sr^{2+}	Serine ion
SSCPE	Single strand conformation polymorphism electrophoresis
Θ	Recombination fraction
T	Thymidine
$t_{1/2}$	Substrate halflife
T_{α}	Transducin α
TEMED	N, N, N, N,-tetramethylethylenediamine
TES	Tris/EDTA/SDS solution
tRNA	Transfer RNA
[-]TRSV	Tobacco Ringspot Virus Satellite
U	Uracyl
UTR	Untranslated region
US	Usher Syndrome
v	Velocity of a reaction
V_{max}	Limiting rate of a reaction or maximum velocity of a reaction
VNTR	Variable number of tandem repeats
x	RzS concentration
xlRP	X chromosome linked RP
Y	C or U
Z	Lod-score
$Z(\Theta)$	The lod-score at a given Θ
Zmax	Maximum lod-score

General Introduction

1.1. Gene therapy, introduction

Gene therapies are therapies directed towards genetic disorders. Theoretically they can be divided into two types. Somatic gene therapies are based on the suppression of genes, the addition of genes, the alteration of genes or a combination of strategies at a somatic cell level. Germline gene therapies on the other hand would require a therapy to be carried out at a germline stage, resulting in the alteration of all cells of an organism. The prospect of gene therapies has been a cause of much excitement since the late 1980's, when the molecular etiologies of many inherited disorders started to be elucidated. With the help of newly identified genetic markers such as restriction fragment length polymorphisms (RFLPs) and microsatellites, high-resolution genetic maps were being generated. With these maps and new techniques such as the polymerase chain reaction (PCR), and single strand conformation polymorphism gel electrophoresis (SSCPE) linkages between disease loci for many inherited disorders and genetic markers were being established (section 1.14 and section 2 discuss these methodologies in detail). Subsequently, many genes within the critical region of genetic linkages have been sequenced and disease-causing mutations identified.

For instance, in section 2 of this Ph.D. thesis a family, family ZMK, segregating retinitis pigmentosa (RP) and sensorineural deafness was studied. Initially the disease was thought to be autosomal dominant or x-linked dominant. However, linkage analysis excluded over 92% of the genome from harboring the disease gene. It subsequently emerged that the disorder could possibly be mitochondrially inherited as the only instance of male to offspring transmission of the disease in pedigree ZMK was brought into question (see chapter 2 for details). Finally a mutation, not present in 270 controls from the same ethnic background, was identified at a highly conserved position in the second serine tRNA gene of the mitochondrion (see chapter 2). Thus, the genetic basis of many diseases, such as the disease segregating in family ZMK, is now known. However a great deal more study needs to be carried out in order to understand the underlying mechanisms, causing the disease.

The clarification of the underlying genetic basis of many genetic disorders has enabled researchers, for the first time, to consider the possibility of gene therapy seriously. Permission for the first human gene-therapy trials was granted in the early 1990s, but it was not until the mid 1990s that the first results of these trials were published. In 1995 Blaese et al., and Bordignon et al., reported the results of the first human clinical trials for severe combined immunodeficiency disease (SCID), that is caused by an adenosine deaminase (ADA) deficiency. Both studies used *ex vivo* retroviral-mediated transfer of the ADA gene to T cells, bone marrow cells and to peripheral blood lymphocytes of 2 children with ADA. Notably, the patients' number of T lymphocytes and humoral immune responses normalised. Treatment in both studies was discontinued after 2 years, however, ADA continued to be expressed in T cells due to integration of the gene into the genome of the patients. Similar studies have been repeated a number of times and it has now been shown that, while the transduced ADA cDNA continued to be expressed in T lymphocytes and myeloid cells in a few patients, there was no significant improvement in immune function. This disappointing effect may be due to the low efficiency of stem cell transduction with retroviral vectors (reviewed in Hershfield, 1998).

In 1992 Rosenfeld et al., transferred the normal human CFTR gene, the gene that causes cystic fibrosis (CF), into cotton rats. This was an *in vivo* transfer utilising a replication-deficient recombinant adenoviral (Ad) vector. RNA could be detected for up to 6 weeks. Crystal et al., (1994) successfully carried out the same experiment on 4 humans with CF. However the patients soon developed immune responses towards the vector. The initial problems with Ad vectors due to immunological responses, have not been resolved fully although second and third generation vectors utilising viruses such as lentiviruses, adenoviruses, adeno-associated viruses and herpes simplex viruses, which elicit a reduced response, have been developed (Klimatcheva et al., 1999; Crystal, 1999; Morsy and Caskey, 1999; Lalwani et al., 1996; Fink et al., 1996; Bonini et al., 1997; Alvarez and Curiel, 1997). In addition, many other problems such as how to administer therapies safely and efficiently have still to be resolved. Scientists around the world are actively investigating both modified viral vectors for gene delivery and various non-viral vectors such as liposomes and synthetic polymers such as dendrimers (Urdea and Horn, 1993) (paragraph 1.13).

The majority of gene therapy studies to date have focussed on the development of therapies for cancers and infectious diseases such as HIV (paragraph 1.6 for details). Gene therapies for Mendelian disorders have, however, also been studied quite extensively. Initially, gene therapies for recessive Mendelian disorders were focused on, as in theory the disease phenotype may be ameliorated by simply adding a gene encoding a missing protein. In contrast, dominant gain of function mutations may require the switching off of a disease-causing gene while leaving the wildtype allele intact. In addition, if haploinsufficiency were to cause some disease pathology, the introduction of a second wildtype allele may also be required. Another complication in relation to the development of therapies for dominant disorders is allelic heterogeneity. There are, for instance, over 100 mutations in the gene encoding rhodopsin known to cause retinitis pigmentosa (RP) and over 150 mutations in the type I human collagen 1A1 and 1A2 genes known to cause osteogenesis imperfecta (OI). To develop a specific therapy for each known mutation may therefore not be time or cost effective. Thus mutation independent strategies will most likely be a more realistic approach to gene therapies for such heterogeneous disorders. RP and OI will be discussed in detail in sections 1.7 to 1.10 of this chapter.

When devising a mutation independent therapeutic strategy for genetic disorders, one can target the primary defect causing the disease; that is try to suppress a dominant negative gene or supply a recessive gene. Alternatively, a secondary effect associated with the disease process may be targeted. For instance, in the case of RP and most retinal degenerations, is has been well documented that photoreceptor cells die through apoptosis (programmed cell death). In the context of work carried out during this Ph.D., RP will be focussed on as a model disease in this section. For example, in retinal degeneration slow (rds) mice, retinal degeneration (rd) mice and transgenic mice carrying either a Pro347Ser or Q244ter mutant rhodopsin gene photoreceptor cell death is known to occur by apoptosis (see 1.12 for details on animal models of RP) (Chang et al., 1993; Portera-Cailliau et al., 1994). Thus by preventing the apoptotic pathway from either commencing or reaching completion, theoretically it may be possible to retard many retinal degenerations. There is some evidence that bcl-2 over-expression reduces apoptotic photoreceptor cell death in mouse models for different retinal degenerations (i.e. the rd mouse and a mouse expression a C-terminal truncated form of rhodopsin. In addition bcl-2 over-expression had a protective effect on albino mice exposed to sustained illumination from photoreceptor degeneration (Chen et al., 1996).

However, a similar study in the same year demonstrated no photoreceptor cell protection from light-induced apoptosis by over-expression of bcl-2 in rd mice and mice carrying a dominant rhodopsin mutation, (Joseph and Li, 1996). In addition, the absence of p53 delays apoptotic photoreceptor cell death in the rds mouse (Ali et al., 1998). However, the absence of c-fos may prevent light-induced apoptotic cell death of photoreceptors in retinal degenerations and the expression of aberrant expression levels of c-fos accompanies photoreceptor cell death in the rd mouse (Hafezi et al., 1997; Rich et al., 1997). However, c-fos is by no means the only factor influencing the apoptotic pathway in the rd mouse, as the retinal degeneration in this mouse also occurs in the absence of c-fos (Hafezi et al., 1998). In another study, p35 (baculovirus cell survival protein) expression retarded retinal degeneration in Drosophila with an autosomal dominant mutation in rhodopsin (Davidson and Steller, 1998).

A second way in which to modify photoreceptor cell death associated with many retinal degenerations is by using growth factors and neurotrophic factors to enhance the life of photoreceptor cells. In one study the effects of brain-derived neurotrophic factor (BDNF) were examined in a feline animal model of retinal detachment. Most animals receiving BDNF had well-organised outer segments that were longer than those in controls. BDNF did not reduce overall cell death in the detachments or death of photoreceptors by apoptosis. However, the results of the study suggest that BDNF may aid in the recovery of the retina after reattachment by maintaining surviving photoreceptor cells and perhaps by promoting outer segment regeneration (Lewis et al., 1999).

In a second study, repeated intravitreal injections of a ciliary neurotrophic factor analogue, either axokine or human BDNF, were carried out in order to study long-term effects on photoreceptor survival in hereditary retinal degeneration in an autosomal dominant feline model of rod-cone dystrophy. Axokine significantly prolonged photoreceptor survival and reduced the presence of apoptotic cells. BDNF and sham-injected eyes were not significantly different from untreated eyes. Thus, axokine and not BDNF delays photoreceptor loss in this retinal degeneration (Chong et al., 1999). However, cataract and mild retinal folds were found in all axokine-treated eyes in both dystrophic and normal animals.

In another study the intraocular gene transfer of an adenovirus carrying ciliary neurotrophic factor (CNTF) prevented the death and increased the responsiveness of rod photoreceptors in the rds mouse (Cayouette et al., 1998).

In one study the survival of purified rat photoreceptors in culture was stimulated directly by fibroblast growth factor-2 (FGF-2). In control cultures 36% of the originally seeded photoreceptors were alive after 5 days *in vitro*. Notably in the presence of 20 ng/ml FGF-2 this number doubled to 62% (Fontaine et al., 1998).

Another exciting field of retinal therapy, which also targets the secondary effect of various mutations, is retinal reconstruction using retinal transplantation. Professor Ray Lund's research group carried out experiments on rats with inherited eye diseases. Cells were taken from nerves in the leg and injected into the retina. These 'peripheral' nerve cells have the ability to regenerate and within six weeks, basic tests showed that the animals' eyesight had improved radically. One in three people over 60 have macular degeneration cause by cells in the macula dying. Thus initial studies would suggest that retinal transplantations may be instrumental in treating both RP and macular degeneration (Whiteley et al., 1998).

The studies described above clearly indicate that a number of therapeutic approaches for retinopathies are actively being explored. For example it may be necessary to amend the primary genetic lesion to provide long term therapeutic benefit. At present we do not know if it will be necessary to modify the primary defect or to modulate some secondary effects associated with the disease pathology or indeed to use a combination of these approaches to provide therapeutic benefit. Given that we now know the precise underlying genetic lesion causing the disease pathology for many inherited retinal degenerations one aim of the present study was to explore mutation-independent therapeutic approaches, which amend the primary genetic defect.

Three mutation independent strategies for dominant-negative heterogeneous disorders, such as RP and OI will be discussed in detail in chapter 3 of this thesis. The three strategies utilise hammerhead ribozymes as suppression effectors (paragraph 1.3.1) and target the primary genetic defects causing RP and OI. The first method utilises untranslated regions (UTRs) of RNA. Ribozymes are generated which target UTRs at specific sites and suppress both the wildtype and mutant alleles of a given gene. Concurrently a replacement gene is provided which has an altered UTR at the ribozyme cleavage site, so that replacement transcripts are masked from suppression.

The second mutation independent strategy also discussed in chapter 3 is based on the wobble hypothesis or the degeneracy of the genetic code. Ribozymes are designed which target RNA specifically at wobble positions of the genetic code; present in both the wildtype and mutant allele. Concurrently a replacement gene with an altered base at the wobble position is provided; replacement transcripts expressed from the gene are in principle masked from suppression.

The third mutation independent strategy studied in chapter 3 of this thesis is based on the occurrence of naturally occurring intragenic polymorphisms. Ribozymes were generated which differentiate between the alleles of a polymorphism and selectively suppress one allele. Therefore, if in a patient, the suppressible polymorphism is present on the same allele as a disease mutation, such a suppressor may selectively suppress the mutant allele. In cases where haploinsufficiency does not give rise to disease pathology the suppression step may be sufficient to provide therapeutic benefit and the reintroduction of a wildtype allele may not be necessary. In such cases the reintroduction of a wildtype allele may not be necessary.

Interestingly, the possible role of polymorphism in both genomics-driven drug design and the fine mapping of polygenic disorders has clearly been recognised by the scientific community as demonstrated by the new aims of the United States human genome project 1998-2003. One of the new goals (goal 3) of the project is the generation of a comprehensive natural sequence variation map. The most common polymorphism in the human genome is the single nucleotide polymorphism (SNP). When two haploid genomes are compared, on average an SNP occurs every kb. Thus SNPs, being abundant, stable and widely distributed across the genome are excellent candidates for mapping complex traits such as cancer diabetes and mental illness. By 2003 an SNP map of at least 100,000 markers (that is one SNP per 30,000 nucleotides) will be generated and made publicly available. This should not only help in the identification of susceptibility loci, it may also help in the understanding of certain types of drug-resistance which some patients seem to carry and which may be associated with polymorphism(s) (Collins et al., 1998). It is of note that the mutation independent strategies outlined above for autosomal dominant disorders may also potentially be useful in the generation of gene therapies for polygenic or susceptibility diseases and indeed may possibly help combat some genomics-based drug resistance in the future.

There is a range of methods to suppress gene expression, which can be utilised in the development of therapies for dominantly inherited disorders. Suppression effectors assessed to date include antisense DNA and RNA, DNA and RNA ribozymes including multi-target ribozymes (minizymes, connected or shotgun ribozymes), or triple helix forming oligonucleotides and peptide nucleic acids which are known to inhibit gene expression. RNA ribozymes are studied in detail in chapters 3 to 5 and are discussed in sections 1.3 to 1.6. Antisense nucleic acids will be discussed in greater detail in section 1.2. Triple helix forming oligonucleotides are small DNA sequences that can recognise specific sequences by the major grooves in double stranded DNAs. These oligonucleotides can under experimental conditions inhibit DNA transcription and replication, generate site-specific mutations, cleave DNA and induce homologous recombination (Chan and Glazer, 1997). Peptide nucleic acids (PNA) are nucleic acids in which the entire sugar-phosphate backbone has been replaced by an N-aminoethylglycine-based polyamide structure. PNAs bind DNA and RNA with higher affinity than natural oligonucleotides and have the unique ability to displace one strand of a DNA double-helix (Uhlmann, 1998). Triple helix forming oligonucleotides and PNAs will not be discussed further in this thesis, as they were not used in any of the suppression strategies explored during the course of my Ph.D. studies.

After a suitable suppression effector has been chosen for a gene therapy study, the suppressor needs to be assessed for specificity and efficiency; initially *in vitro* and subsequently in cell culture and animal models. The *in vitro* efficiency of a ribozyme, for instance, can be described using classic Michaelis-Menten kinetic parameters and can be used as a broad predictor of potential *in vivo* activity. Ribozyme kinetics will be explored in detail in section 1.5 and chapter 4 of the thesis.

Finally, prior to a gene therapy being tested on patients it must be studied extensively in cell culture and animal models. In the context of this Ph.D. thesis, the use of ribozymes in cell culture and animal models for RP and OI will be focused on in section 1.11 and 1.12 of this chapter. In addition, chapter 5 explores the potential utility of a hammerhead ribozyme targeting a polymorphism in the COL1A1 gene (a gene known to cause OI when mutated) in cell culture and an animal model for OI. Various modifications, which can be made to ribozymes, to enhance either their efficiency or their stability *in vivo* will also be explored in chapter 5 of this Ph.D. thesis.

A wide range of suppression effectors has been developed for future gene therapies for dominant-negative disorders. Additionally, appropriate cell systems and animal models have been devised to enable testing of therapies. However, the immense genetic heterogeneity associated with many dominant disorders has not been addressed adequately to date. During the course of this Ph.D. thesis mutation independent strategies for gene suppression were explored in detail in chapters 3 to 5.

In chapter 3 many mutation-independent hammerhead ribozymes, which target human rhodopsin, peripherin/*RDS* and the two type one collagen transcipts, genes involved in RP and OI, were designed and tested *in vitro*. In chapter 4 the most efficient ribozyme, Rzpol1a1, targeting a polymorphic site of the COL1A1 transcript was characterised in detail kinetically and was shown to be extremely efficient. In chapter 5 suitable cell lines to test Rzpol1a1 activity were obtained and tested in terms of their ability to be transfected by non-viral and viral means. In addition, a viral MLV construct was generated with Rzpol1a1 driven by a CMV promoter. This will be used to generate an MLV virus carrying Rzpol1a1.

1.2. Suppression effectors/ antisense nucleic acids

Antisense nucleic acids are single strands of nucleic acids, either DNA or RNA, which are complementary to a target sequence. These oligonucleotides suppress the target sequence by hybridising to it, thus preventing other interactions needed for expression (e.g. transcription, splicing or translation), or by stimulating nucleases to degrade the hybrid (either DNA:RNA or RNA:RNA), or by deactivating the target by cleaving it (e.g. ribozymes).

There are multiple uses for antisense in research. Firstly antisense molecules can suppress mutant alleles that cause a disease or are contributing to multifactorial disorders. Other uses of antisense molecules are that they can interfere with oncogenic transformation (Scherr et al., 1997) or viral infections (e.g. HIV). Further useful functions of antisense in research include the down-regulation of genes with the aim of characterising their function and the use of antisense in the elucidation of complex cellular mechanisms such as apoptosis. Furthermore, antisense may be used to suppress normal physiological responses is humans, which may, for example, cause organ rejection after surgery or may cause drug resistance. When trying to suppress a disease pathology, antisense is more likely to be effective in situations where the pathology is dosage sensitive. An unresolved hazard of

antisense is that suppression based on hybridisation may not be specific, causing suppression of the wrong protein or control region. This may be particularly hazardous when the antisense sequence used for suppression has some homology to a number of genes. For example, various human collagen genes are extremely homologous and the three cone opsin genes and the rhodopsin gene exhibit high levels of homology. It will therefore be highly preferable to target antisense molecules to unique sequences in the genome. The human genome project should provide useful information in this regard. There has been some evidence that antisense RNAs directed towards the 5'UTRs of genes may give the greatest inhibition, although 3'UTRs and translated regions have also been known to cause a reduction of gene expression (Ch'ng et al., 1989).

Historically, the first antisense oligonucleotide to be artificially created was DNA designed to selectively modify a target nucleic acid (Belikova et al., 1967). In 1988 the discovery that antisense RNA is used as a natural suppressor in eukaryotic and prokaryotic gene-expression led to an entirely new field of research (Takayama and Inouye, 1990) and indeed the many applications of antisense in control of gene expression are still being elucidated. For example, researchers have found that antisense RNA helps regulate plasmid copy number in bacteria (Aiba et al., 1987; Actis et al., 1999). In another example the transformation of antisense, sense and a promoter-less construct of the coding sequence of the elicitin gene into the oomycete plant pathogen Phytophthora infestans resulted in the transcriptional silencing of the transgenes (sense, antisense and promoter-less construct) and the endogenous elicitin gene. The gene remained silenced in nontransgenic homokaryotic progeny from the silenced heterokaryons, demonstrating that the presence of transgenes is not essential for maintaining the silenced status of the endogenous gene. The exact mechanism, however, is still unknown (van West et al., 1999).

The ability to clone DNA into plasmids containing bacterio phage promoters such as Sp6, T7 and T3, which was developed largely in the 70s, led to the successful expression of specific RNA sequences *in vitro*, greatly facilitating studies of antisense RNA. The field of antisense grew rapidly in the 80s and 90s. At one point during this development it was believed that antisense technologies would produce viable treatment for many disorders. As with many technologies a number of complications have arisen which are briefly discussed here. One problem of using antisense RNA is the instability of this molecule and the slow uptake of antisense

into the cytoplasm and nucleus. Better uptake can be achieved by associating antisense RNA with lipids, such as lipofectAMINE (GibcoBRL), now commercially available. A way of stabilising small RNAs is by chemically modifying RNA in various ways. A list of problems and solutions associated with the use of antisense RNAs is given in table 1. One special type of antisense RNA molecule is the ribozyme. Ribozymes are small catalytic molecules with a conserved core sequence and unconserved antisense arms, which bind target RNA. Under specific circumstances ribozymes can elicit sequence specific cleavage of target RNAs. Further details of ribozymes are provided below.

1.3. Suppression effectors/ ribozymes

Ribozymes are small ribonucleic acid (RNA) molecules that form a new class of metaloenzyme. They can have various very specific shapes and cleave the phosphodiester backbone of RNA at specific target sites. They require divalent metal ions (e.g. $MgCl_2$) in order to perform cleavage reactions and to stabilise themselves. The first ribozyme to be discovered was in the ciliated protozoan, *Tetrahymena thermophila*, and was a self-splicing rRNA catalysing the splicing of its intron (Kruger et al., 1982). The first ribozyme to be characterised was 400 bases of RNA comprising the part of RNase P ribozymes that can cleave pre-tRNAs. RNase P is mostly made up of protein but about 20% of it is comprised of RNA. In 1993 a group in Yale showed that it was the RNA component of RNase P that catalyses this cleavage and not the protein component (Guerrier-Takada et al., 1993). Apart from intron splicing ribozymes and RNase P there are now a further 4 known categories of ribozymes; hammerhead ribozymes, hairpin ribozymes, Hepatitis delta viral RNA and Neurospora mitochondrial VS RNA.

1.3.1. Hammerhead ribozymes

Haseloff and Gerlach first described a hammerhead ribozyme in the tobacco ringspot virus, which undergoes self-catalysed cleavage during replication. However the exact sequence of the catalytic core that elicits this cleavage was not isolated at that stage (Haseloff and Gerlach, 1989). Hammerhead ribozymes, called so because of their shape, *trans*-cleave RNA at NUX sites (N = A, U, G or C and X = A, U or C). With two antisense arms they first bind RNA and then cleave the phosphodiesterase bonds of the RNA molecules to give 5'hydroxyl and 2'-3'-cyclic phosphate termini. They, like any ribozyme, require metal ions for their enzymatic reactions, but are flexible as to which metal ions they can utilise; Mg^{2+}, Mn^{2+}, Co^{2+},

Sr^{2+} and Ba^{2+} all for instance function as coenzymes (Dahm and Uhlenbeck, 1991). In 1994 the exact structure of the hammerhead ribozyme was elucidated (Pley et al., 1994). It contains 24 highly conserved bases flanked by its two antisense arms. Together these bases form three stem-like structures (figure 1). Additionally, various researchers have found that the rate of hammerhead ribozyme catalysis can vary greatly from target site to target site and indeed from ribozyme to ribozyme (Zoumadakis et al., 1994) (see 1.5). These findings mirror the observations presented in this Ph.D. thesis, where a large variance in the catalytic rate was found between ribozymes. The specific nature of cleavage elicited by hammerhead ribozymes would suggest that the consensus sequence of the catalytic core is important in this process. Indeed many studies have investigated, via site specific mutagenesis of the consensus bases, the degree of sequence variability available while still maintaining ribozyme cleavage activity (Ruffner et al., 1990). In addition, cleavage rates vary depending on the permutation of the NUX cleavage site. At 37°C, the NUC motif was found to be cleaved most efficiently, with the AUC motif being cleaved best (Zoumakakis and Tabler, 1995).

1.3.2. Hairpin ribozymes

The original hairpin ribozyme to be discovered was in the minus strand of the Tobacco Ringspot Virus Satellite ([-]TRSV) RNA (Prody et al., 1986; Haseloff and Gerlach, 1989). Hairpin ribozymes are larger than hammerhead ribozymes and require alkaline earth metals like Mg^{2+}, Ca^{2+} or Sr^{2+} for efficient cleavage (Chowrira et al., 1993). They consist of four helical domains and five loops (figure 2) (Hampel and Tritz, 1989; Berzal-Herranz et al., 1993). Much like hammerhead ribozymes, hairpin ribozymes bind the substrate using two antisense arms, allowing for specificity and cleavage in trans. Substrate requirements are more complicated than for hammerhead ribozymes, however, any RNA molecule is still expected to contain many potential target sites. In summary, substrate requirements are the following: a GUC substrate cleavage site is required (G = guanine, U = uracyl and C = cytosine), substrates should have a C or a U at position -2 and preferably a G or A at position -3 (figure 2).

1.3.3. Hepatitis delta virus (HDV) and Neurospora mitochondrial VS RNA

HDV RNAs contain a self-cleavage site thought to be necessary during rolling circle replication (Wu et al., 1989). Their secondary structure has not yet been elucidated, though three models have been proposed: cloverleaf (Wu et al., 1989), pseudoknot (Perrotta and Been, 1990) and axehead (Branch and Robertson, 1991). None of

these models is similar to the catalytic domains described above for other ribozymes. Like all ribozymes known to date, HDVs require divalent cations for cleavage (Wu et al., 1989) and cleavage results in products with 2'3'-cyclic phosphate and 5'-OH termini (Branch and Robertson, 1991).

VS RNA is single-stranded circular RNA of 881 nucleotides. (Saville and Collins, 1990). The cleavage products again comprise of termini with 2'3'-cyclic phosphate and 5'-OH and VS RNAs again require divalent cations for cleavage. The catalytic core has been found to comprise 154 nt. (Guo et al., 1993).

All *trans*-acting ribozymes cleave target RNA after binding the target using antisense arms. Logically therefore, RNA must, in the case of hammerhead ribozymes, not only contain the required target NUX site, but also be accessible to the ribozyme. Areas in target RNAs that contain a high level of intermolecular base pairing are thought not to be very accessible to ribozymes. To determine whether a site in a target RNA is suitable for ribozyme cleavage one can perform various experiments such as RNase H mapping (Frank and Goodchild, 1997). Another, more rapid, method for determining accessible sites uses computer algorithms, although the data generated in this way is not believed to be as accurate as that generated via RNase H mapping. One such computer program, MFOLD or PlotFOLD (Zuker, 1989), attempts to specifically identify areas in target RNA that are likely to hybridise with the ribozyme. The output is presented as plots of the most likely secondary structure of the RNA for various internal energy (ΔG) levels. Naturally, plots of the RNA with lower internal energies are more likely to represent the conformation of an RNA molecule at a given time. Typically approximately the 10 most likely RNA conformations in terms of energy are analysed and open loop structures which are present in all or most of these conformations are designated as potential ribozyme target sites.

1.4. Multitarget ribozymes; connected and shotgun ribozymes and minizymes

1.4.1. Connected and shotgun ribozymes

Several groups of researchers have been investigating multitarget ribozymes (Chen et al., 1992; Weizacker et al., 1992). Joining several ribozyme sequences in tandem within a vector makes one type of multitarget ribozyme, the connected type. This type is transcribed as a single RNA. A second type of multitarget ribozyme can be made by combining cis-acting ribozymes (CARs) separated by trans-acting

ribozymes so several trans-acting ribozymes are trimmed at the 5' and 3' ends by the CARs, thus freeing multiple trans-acting ribozymes (shotgun type).

1.4.2. Minizymes

A hammerhead minizyme is like a hammerhead ribozyme, but instead of a stem-loop 2 region (figure 1) it contains a short oligonucleotide linker. Sometimes two minizymes can form divalent structures with two catalytic centres (figure 3) (Amontov et al., 1996; Sugiyama et al., 1996; Kuwabara et al., 1996; Sioud et al., 1997). In this way it is possible to design two minizymes to form one dimer that is capable of cleaving RNA at two different target sites. Minizymes, like all ribozymes are dependent on the presence of divalent cations such as $MgCl_2$ for cleavage.

1.5. Ribozyme Reaction Rates

Some of the same rules that apply to protein enzymes also apply to ribozymes. They bind the target molecule in order to make bimolecular reactions unimolecular, they stabilise the transition state of a substrate and destabilise the ground state (Cech et al., 1992; Narlikar et al., 1995; Pan et al., 1993; Cech et al., 1993; Hertel et al., 1994). Usually, enzyme catalysed reactions show a first-order dependence of rate on substrate concentration at very low concentrations, however, as the concentration of enzyme increases the rate approaches a limit, known as the saturation limit. Adding more enzyme will not increase the reaction rate and the reaction becomes of zero order with respect to substrate. Michaelis and Menten (Michaelis and Menten, 1913) were the first to develop enzyme kinetics in the way that we know it today. They exercised proper control of pH and used initial rates rather than whole time courses. They proposed that the first step in a reaction is the binding of a substrate (S) to an enzyme, in this case a ribozyme (Rz), to form a ribozyme-substrate complex (RzS), which then reacts to give the product (P) with the regeneration of the free ribozyme:

$$k_{-1} \ k_1 \qquad k_2$$
$$Rz + S \Leftrightarrow RzS \Rightarrow Rz + P \qquad (1.1)$$
$$K_m$$
$$(e_0 - x) \ (a_0 - x) \quad (x) \qquad (p)$$

k_1 = association rate
k_{-1} = dissociation rate
k_2 = rate of cleavage step
K_m = equilibrium constant
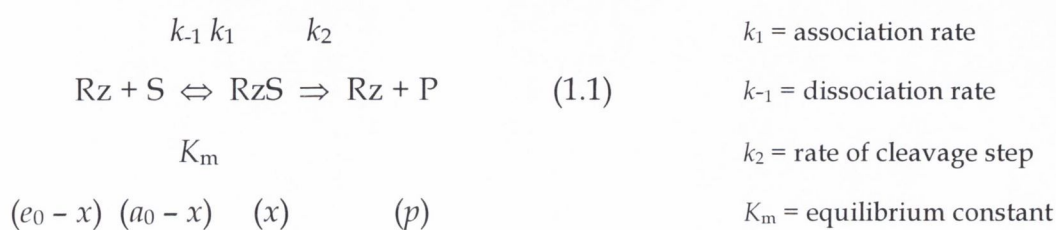
e_0 is the total concentration of enzyme and the concentration of RzS is x. Therefore the concentration of free enzyme is $e_0 - x$. The same applies to the concentration of substrate; if a_0 is the total amount of substrate then $a_0 - x$ must be the amount of free substrate, at least until there has been time for the conversion of significant amounts of S to P. Normally, a_0 is far larger than e_0 (for example, 1 mM compared with 1 nM) and one need not distinguish between the total amount of substrate and the amount of free substrate ($a_0 = a$). This may, however, not be assumed in the case of ribozyme kinetics as the amount of ribozyme (enzyme) and template (substrate) is frequently in the same order. Michaelis and Menten assumed that the first half of equation 1.1 was an equilibrium, where the equilibrium constant K_m = [enzyme] [S] / [enzymeS].

The catalytic constant k_{cat} or turnover number of an enzyme defines the capacity of the enzyme-substrate complex, once formed, to form the product, P. Values of about 10^3 s^{-1} are typical for regular enzymes; for ribozymes k_{cat} rates are generally several orders smaller. Another kinetic value of interest is the limiting rate or the maximum rate of the reaction (V_{max}). A final Michaelis – Menten value is the Michaelis constant (K_m). It has the dimensions of concentration and specifies the relative concentrations of free enzyme, free substrate and enzyme-substrate complex, under steady-state reacting conditions, before any of the parameters are rate limiting. Steady-state reacting conditions must be determined before commencing kinetic experiments. The concentration at which an enzyme is half-saturated, that is, where the velocity of the reaction (v) is equal to 0.5 V_{max}, is when $(a_0 - x) = K_m$

For experimental purposes one can vary the relative molar concentrations of substrate and ribozyme to obtain kinetic constants such as V_{max}, K_m, k_{cat} or k_{cat}/K_m. Additionally, other parameters such as temperature, pH and metal ion concentration, typically Mg^{2+}, affect the rate of the cleavage step. Kinetic experiments as described above in conditions of substrate excess are termed multiple-turnover kinetic experiments, because a ribozyme may cleave multiple target RNAs. Another type of kinetics often carried out with ribozymes is single-turnover kinetics in which the rate of cleavage is determined under single-turnover conditions; that is conditions of ribozymes excess. Experimentally, a large excess of ribozyme is added to the substrate, ensuring that saturation has taken place, and the RNAs are pre-annealed before initiating the reaction with $MgCl_2$. Thus under single-turnover conditions, ribozymes never cleave more than once at most. The

parameter obtained in this manner, k_2, is a measurement of the cleavage step, after annealing has taken place. An additional parameter that can be measured is k_{-1}. This parameter defines the rate constant of substrate dissociation and thus describes the rate at which a substrate dissociates from a ribozyme and, like k_2, is independent of ribozyme or substrate concentration.

1.5.1. Temperature of the reaction

If the ribozyme cleavage step is the rate-determining step of the reaction, increasing the temperature increases the rate of cleavage. For all ribozymes, activation energies are said to vary from 50-80 kJ/mole (Uhlenbeck, 1987; Dahm and Uhlenbech, 1991; Dahm et al., 1993), which corresponds to doubling of the reaction rate for every 10 °C increase of the reaction temperature. However, the reaction is also dependent on the binding of the ribozyme to the target RNA with antisense arms. In contrast to the above, lower temperatures favour ribozyme binding. An additional consideration is that, cleavage products may not be released efficiently by the ribozyme if reaction temperatures are too low. Therefore changes in temperature may have varying effects on overall reaction rates.

1.5.2. pH of the reaction

Typically the rate-constant of hammerhead ribozyme cleavage will increase 10-fold for each pH unit that one increases the reaction by. This is because at a neutral pH only a fraction of the 2'-hydroxyl groups will be deprotonated at any given time, as the pKa (-logKa where Ka is the acidconstant) of the 2'-hydroxyl groups in the hammerhead ribozyme is about 11.4 (Saenger, 1984). As the pH increases the fraction of deprotonated 2'-hydroxyl groups increases. Mg^{2+} reduces the pKa, however, the pKa typically still remains greater than pH 6.0-8.0. Globally pH affects all ribozymes in a similar manner. For the chemistry see section 1.3.1.

1.5.3. Mg^{2+} concentration

The natural intracellular concentration of free Mg^{2+} ions in an average mammalian cell is approximately 0.6 mM. This low abundance may prove to be a limiting factor for subsequent *in vivo* studies on ribozyme cleavage. The total concentration of Mg^{2+} in mammalian cells is about 20 mM, but most ions are bound to proteins and other substances. One positive factor is that hammerhead ribozymes can utilise other metal ions as cofactors such as Mn^{2+}, Co^{2+} and Sr^{2+} too. This will increase the concentrations of divalent metal-ions available for ribozyme cleavage. Cleavage

efficiencies for many ribozymes were evaluated at various Mg^{2+} concentrations in experiments carried out during the course of this Ph.D.

In vitro kinetic analyses of ribozyme activity can be undertaken and detailed kinetic profiles of ribozymes produced. Using *in vitro* experimental approaches great variance in ribozyme efficiencies have been observed (reviewed in Stage-Zimmermann and Uhlenbeck, 1998). Such kinetic profiles although somewhat inaccurate can act as broad predictors of potential cleavage efficiencies *in vivo* and it can therefore be valuable to screen batteries of ribozymes *in vitro* to identify those which are more likely to show effective activity *in vivo*.

1.6. Ribozyme utilities

There are multiple utilities for ribozymes, many of which have been tested in cell culture and animal models. For instance ribozymes may be used to knock out genes of unknown function in order to study the effect. Ribozymes may also be used to down-regulate genes in animal models of genetic diseases. However, most work up to date has been on ribozymes directed against various infectious agents such as the HIV-1 virus and Plasmodium falciparum and cancer genes such as the retinoblastoma gene and H-*ras* (see below for details). Much work has also been carried out on ribozymes as potential therapeutic agents for dominant-negative genes such as ribozymes against rhodopsin or COL1A1. A relatively new area in the field of ribozyme gene therapy is the ribozyme-mediated repair of mutant genes. The method requires that the ribozyme base pairs to the mutant RNA and cleaves it 5' to the mutation site. A corrected version of the 3' region of the gene is then ligated onto the 5' cleavage site to generate intact message (see below for details).

1.6.1. Ribozymes to study gene function

A new strategy to create conditional knock-out mutations using a targeted heat-inducible ribozyme was suggested by Zhao and Pick in 1993. The ribozyme method, tested in Drosophila, was proposed as an alternative to traditional mutagenesis, because mutagenesis is time-consuming, labour-intensive and not always successful. Moreover, the functions of genes that are expressed during several discrete times during development are often obscured in the later stages because of disruptions caused by the absence of early gene function. Transgenic flies expressing a ribozyme against the *fushi tarazu* (ftz) gene were generated. Because ftz is expressed during two separate developmental phases in Drosophila, ftz

function was tested separately during the two phases by timed induction of the ribozyme. Results showed that activation of the ribozyme in the blastoderm disrupted the ftz seven-stripe pattern and produced ftz-line pair-rule defects in larvae. The involvement of ftz in neurogenesis was verified by activation of the ribozyme during the early phase of formation of the central nervous system (Zhao and Pick, 1993). In another study the ribozyme-mediated strategy for gene down-regulation was utilised for the identification of gene function in zebrafish. A gene encoding a ribozyme, which targeted the known dominant zebrafish *no tail* gene, was transiently transfected into a fertilised zebrafish egg to rapidly produce high levels of ribozyme. The study clearly demonstrated the functionality of the down-regulation method of studying gene function (Xie et al., 1997).

1.6.2. Generating loss of function animal models for genetic diseases

In one study a transgenic mouse model for diabetes was generated, which expressed a ribozyme against glucokinase (GK) under the control of the insulin promoter. GK is the enzyme, which phosphorylates glucose to glucose 6-phosphate and serves as a glucose sensing mechanism for regulating insulin secretion in β cells by sensing the intercellular concentration of glucose. Transgenic mice in two independent lineages had about 30% of the normal GK activity. Insulin release in response to glucose from *in situ*-perfused pancreas was impaired. However, the plasma glucose and insulin levels of the mice remained normal. These mice are likely to be predisposed to type II diabetes and may manifest increased susceptibility to genetic and environmental diabetogenic factors. Thus, these animals provide an animal model for studying the interaction of such factors with reduced GK activity (Efrat et al., 1994).

1.6.3. Ribozymes targeting infectious agents

Another application for ribozymes, which has been studied extensively, is their ability to target infectious agents such as HIV. Monomeric and multimeric ribozymes have been generated which target the conserved regions of the HIV genome such as the tat and envelope (env) genes (reviewed in Macpherson et al., 1999).

For example Ramezani et al. engineered retroviral vectors to express monomeric and multimeric hammerhead ribozymes targeting one and nine highly conserved sites within the HIV-1 env gene coding region. A human CD4+ T lymphocyte-derived MT4 cell line was stably transduced and selected for ribozyme expression.

Compared to the control cells lacking ribozyme, HIV-1 replication was delayed in monomeric ribozyme-expressing cells. Viral replication was almost completely inhibited in multimeric ribozyme expressing cells as no viral RNA or protein could be detected in these cells and in the cell culture supernatant for up to 60 days after infection (Ramezani et al., 1997). Phase 1 clinical trials to evaluate the safety and effects in HIV-1 infected humans of autologous lymphocytes transduced with a ribozyme that cleaves HIV-1 RNA are currently underway. Preliminary results indicate that infusion of gene-altered, activated T-cells in HIV infected patients is safe and that transduced cells can persist for long intervals in HIV-infected patients. In addition results suggest ribozyme transduced cells may possess a survival advantage *in vivo* for at least 6 months (Wong-Staal et al., 1998).

Ribozymes have also been designed towards other infectious agents such as hepatitis C virus (HSV). In one study, ribozymes targeting conserved regions of the HCV RNAs were incorporated into adeno associated viral vectors and adenoviral vectors and tested for their ability to inhibit HCV core expression in a tissue culture model. Substantial inhibition of HCV gene expression was observed in tissue culture (Welch et al., 1998). Thus ribozymes have great potential in the development of anti-viral drugs against viruses such as HIV-1 and HCV.

1.6.4. Ribozymes against cancer

In one study hammerhead ribozymes were designed to cleave the mutant sequence of the dominant H-*ras* oncogene transcript. The ribozyme was delivered by an adenovirus (Ad) to neoplastic (cancer) cells. High efficiency reversion of the neoplastic phenotype was accomplished in H-*ras* expressing tumor cells (Feng et al., 1995).

In a similar study two hammerhead ribozymes targeting point mutations in the dominant N-*ras* oncogene were synthesised and their catalytic activity evaluated *ex vivo*. The ribozymes were 2'-modified to protect them against degradation by nucleases. 2'-fluoro-2'-deoxyuridine/cytidine-substituted ribozymes were nearly as active as their unmodified counterparts and had a prolonged stability in cell culture supernatant containing foetal calf serum. Ribozyme stability had been increased by introduction of terminal phosphorothioate groups without significant effects on catalytic efficiency. An assay based on the use of N-*ras*/luciferase fusion genes as a reporter system was established to detect ribozyme-mediated cleavage in HeLa cells. A reduction of nearly 60% in luciferase activity was observed in cells

expressing mutant but not wildtype N-*ras*/luciferase fusion transcripts (Scherr et al., 1997).

1.6.5. Ribozymes directed at dominant-negative and multifactorial disease genes

Kilpatrick et al., (1996) directed a hammerhead ribozyme towards the human fibrillin-1 gene; a gene known to cause Marfan syndrome when mutated. The ribozyme, delivered into cultured dermal fibroblasts by receptor-mediated endocytosis of a ribozyme-transferrin-polylysine complex, specifically reduced both cellular fibrillin mRNA levels and the deposition of fibrillin protein in the extracellular matrix, suggesting that the hammerhead ribozyme may be useful in the development of a gene therapy for Marfan syndrome.

In a different study, Grassi et al. (1997) designed five hammerhead ribozymes to the type I collagen (COL1A1) transcript. This gene, which causes osteogenesis imperfecta (OI) when mutated, was specifically cleaved at mutation sites *in vitro*, although in this study the cleavage efficiency remained relatively low for the ribozymes tested. Thus, these particular ribozymes may not be very useful as potential therapeutic agents for OI.

Trinucleotide repeat expansions (TREs) are a class of mutation characterised by a change in the size of a genomic fragment due to amplification of a repeated unit. TREs are thought to be causative of a number of genetic disorders including Huntington disease and myotonic dystrophy (MD) (reviewed in Timchenko and Caskey, 1996). In one study a group I intron ribozyme was designed to target the TRE at the 3' end of the MD protein kinase transcript, the TRE known to cause MD. The ribozyme was designed to excise twelve repeats in the TRE and ligate 5 repeats, contained within the ribozyme. The strategy was shown to be successful both *in vitro* and in mammalian cells. Thus ribozyme-mediated RNA repair may prove to be a valuable therapeutic strategy for diseases associated with repeat expansions (Phylactou et al., 1998).

1.6.6. Ribozyme-mediated repair of genes

A novel approach for ribozyme-based gene therapy is ribozyme-mediated repair of mutant transcripts. Lan et al., for example, successfully repaired sickle β-globin mRNA in erythrocyte precursor cells. Sickle cell anaemia is one of the most common recessive disorders in the world. Individuals with the disease accumulate long polymers of sickle hemoglobin in their erythrocytes, which leads to chronic

anaemia and cumulative tissue damage, eventually leading to early death. In this experiment the authors designed a trans-splicing ribozyme carrying exon 3 of the fetal γ-globin gene, a gene known to greatly impede polymerisation of the sickle hemoglobin. The ribozyme was shown successfully to bind the target RNA, release the 3' cleavage product containing the mutation and ligate in exon 3 of the γ-globin gene, thereby generating an anti-sickling γ-globin protein in cell culture (Lan et al., 1998).

1.7. Retinitis Pigmentosa

Retinitis Pigmentosa (RP) is the name given to a group of retinopathies resulting in the death of photoreceptor cells in the retina. It affects between 1 in 3000 and 1 in 7000 people (Bunker et al., 1984) and about 1.5 million people in the world have been estimated to be affected. Clinically, RP may manifest itself in various manners, from mild visual impairment at a late stage in life, to near blindness in young patients. Symptoms include night blindness, progressive loss of peripheral vision which sometimes subsequently leads to loss of central vision, waxy pallor of the optic disc, pigment depositions on the retina (hence the name RP) (figure 4), attenuated retinal vessels and a lowered or non-recordable electro-retinogram (ERG) (Heckenlively, 1988a). The ERG is an evoked response by the retina to a flash of light, which can be recorded. Responses from rod and cone photoreceptor cells can be tested separately using ERGs. By performing the test in the light-adapted state, the (photopic) ERG measures the cone system while under such conditions rods do not respond. In contrast, after a patient has been dark-adapted for at least 30 minutes, a dim flash of light below cone threshold will evoke a (scotopic) ERG from the rod system.

RP can be inherited in an autosomal dominant (adRP), autosomal recessive (arRP), x linked (xlRP), digenic or mitochondrial fashion. RP also occurs sporadically, however generally this is thought largely to represent cases of arRP (Kajiwara and Berson, 1994). The first two RP genes to be localised were xlRP genes (Bhattacharya et al., 1984; Francke et al., 1985). The first adRP locus found, mapped to chromosome 3q in a large Irish family (McWilliam et al., 1989). Since rhodopsin had previously been localised to 3q (Sparkes et al., 1986; Nathans et al., 1986) and nonsense mutations in the Drosophila opsin gene were already known to cause photoreceptor degeneration in Drosophila (Washburn and O'Tousa, 1989), this gene was considered to be a likely candidate gene for RP. This was confirmed by a linkage in the same Irish pedigree to markers close to the rhodopsin gene

(Farrar et al., 1990), and by demonstrating a mutation in this gene at codon 23 (Dryja et al., 1990a). Over 100 different mutations in rhodopsin, causing RP or congenital stationary night-blindness, have now been established. For a complete list: http://mol.ophth.uiowa.edu/MOL_WWW/Rhotab.html. It is now known that mutations in a range of other genes, many involved in phototransduction and outer segment morphogenesis, such as the human cofactor C gene, the GTPase regulator gene, the tubby-like protein 1 gene, the ATP-binding cassette transporter gene, the retinal pigment epithelium specific 65kD gene, the neural retina lucine zipper gene, the retinal outer segment membrane protein gene (ROM-1) and the second mitochondrial serine tRNA can also cause RP. Notably, mutations in ROM-1 may only cause disease pathology when found in conjunction with mutations in the peripherin/*RDS* gene. Many more RP genes have as yet not been characterised (for a complete table of all loci and genes known to cause RP and other retinopathies, see Appendix B; for a complete list of all RP loci and genes identified to date see table 2). In one gene, coding for the photoreceptor protein peripherin/*RDS* on chromosome 6p21 (Farrar et al., 1991a, b; Kajiwara et al., 1991; Jordan et al., 1992) over 40 different mutations have been characterised, that can cause inherited retinal degenerations including adRP, macular and peripheral degeneration and various macular dystrophies such as butterfly-shaped pigment dystrophy, dominant cone-rod dystrophy and diffuse retinal degeneration areolar choroidal dystrophy. For a complete on-line list see: http://mol.ophth.uiowa.edu/MOL_WWW/RDStab.html. It is clearly evident from the above that human inherited retinopathies such as RP are extremely genetically heterogeneous.

1.8. Usher syndrome

RP can occur on its own or in conjunction with other diseases (see Appendix B for a full list of retinal disorders, including RP). RP syndromes include Kearns-Sayre syndrome which manifests RP combined with cardiac conduction defects and Bardet-Biedl syndrome which manifests RP in conjunction with obesity, hypogonadism, polydactyly and mental retardation. Usher Syndrome (US) is an autosomal recessive disease in which RP is associated with congenital deafness. It is so named after a British ophthalmologist, Charles Usher, who emphasised the hereditary nature of the disorder (Usher, 1914). US was first described by Von Graefe (1858) and Liebreich (1861). The disease can be divided into various types. Type I is characterised by profound congenital deafness, vestibular a-reflexia and

early onset progressive RP (onset by age 10). Type II US patients have RP, are hard of hearing (not profoundly deaf) and have normal vestibular function (Moller et al., 1989). US type III, the rarest form of US (estimated to comprise about 2% of all US cases), in contrast is estimated to cause approximately 42 % of US cases in Finland. Patients manifest progressive hearing loss (in contrast to patients with US types I and II), vestibular hypoactivity, cataracts and RP and the disease is genetically linked to chromosome 3q21-q25 (Sankila et al., 1994). At least six genes have been implicated in type I US (types 1A-1F). Type 1A is linked to 14q (Kaplan et al., 1992), type 1B to 11q (Weil et al., 1995), type 1C to 11p (Smith et al., 1992), type 1D to 10q (Wayne et al., 1996) and type 1E to 21q (Chaib et al., 1997) and type 1F to 10q (Wayne et al., 1997). Type 1B is mapped to 11q13.5 and is caused by mutations in the myosin VIIA gene (Weil et al., 1995). Type II US maps to 1q41 (Kimberling et al., 1990; Lewis et al., 1990). Two loci have been linked to type II US; 2A has been localised to 1q41 (Kimberling et al., 1990) and is known to be caused by mutations in the USH2A gene. The USH2A protein contains motifs, that are most commonly observed in proteins comprising components of basal lamina, extracellular matrixes or cell adhesion molecules (Eudy et al., 1998a; Eudy et al., 1998b). US type 2B, although clinically similar to type 2A, is thought to manifest a milder form of RP and patients are thought to show mild vestibular abnormalities. However, type 2B is not linked to chromosome 1q41 and no linkage has been found to any other region of the genome (Pieke-Dahl et al., 1996). The family studied in chapter 2 of this Ph.D. thesis (family ZMK) present with an US-like syndrome. However, in the case of this family the disease is inherited in a mitochondrial fashion (see chapter 2 for details).

1.9. The visual transduction cycle, rhodopsin and peripherin/RDS

The roles of rhodopsin and peripherin/*RDS* in human retinopathies have been focused on in this section of the introduction for the following reasons. These two proteins were the first to be implicated in causing adRP. Moreover, the therapeutic approaches explored in this Ph.D. thesis for adRP have focused on ribozymes directed to transcripts from human rhodopsin and human peripherin/*RDS*. However, it is well established that many other proteins involved in visual transduction can when mutated cause retinal degenerations and that additionally proteins which are not directly involved in visual transduction can also result in photoreceptor cell loss when mutated (Appendix B and table 2).

1.9.1. Rhodopsin

Rod and cone photoreceptor cells are neurons in the retina, which are involved in vision. There are three types of cone photoreceptor cells, red, blue and green and one type of rod photoreceptor cell in the human retina. The genes encoding the pigment proteins in these photoreceptors all show a large amount of sequence homology, indicating a similar ancestry (Nathans et al., 1986). Cones are neurons that perceive colour; hence the necessity for red, blue and green type cones with light-sensitive red, blue and green pigments respectively, to enable a wide range of colour vision. Rod photoreceptor cells, being far more sensitive than cone photoreceptor cells, are the neurons that enable the perception of light, without distinguishing between colours. Rod and cone photoreceptor cells are morphologically similar, elongated cells (figure 5). From internally to externally they comprise of four distinct areas. Firstly there are the photoreceptor outer segment, which contains hundreds of flattened discs with rim region at the edges called the outer segment discs. These discs are constantly renewed making photoreceptor cells highly metabolically active cells. This region is responsible for carrying out phototransduction and converting light into an electrical signal, which eventually reaches the brain. A thin motile cilium connects the outer segment with a second compartment, the rod inner segment, which holds many organelles, such as mitochondria and golgi apparatuses. The third compartment is the cell body and contains the nucleus. The final region is the synaptic area through which an electric signal is transmitted to other neurons in the retina and finally to the brain. The neurotransmitter at these synapses is glutamate.

On average humans have approximately 92 million rod photoreceptor cells (so called because of their shape (figure 5)) per eye. Rod photoreceptors contain a light sensitive visual pigment molecule called rhodopsin (or visual purple) which is made of the two components, opsin (a 40 kDa protein manufactured by the rod) and 11-*cis*-retinal (a chromaphor derivative of vitamin A). Rhodopsin is a 38 kDa guanine nucleotide-binding protein (G-protein) comprising of 348 amino acids, located in the membrane of the outer segment discs of the rod photoreceptor cell and is highly sensitive to light (even dim light) of around 498 nm. After rhodopsin absorbs a photon of light, retinal isomerises from the 11-*cis* form to an all-*trans* isomer. This leads to the activation of the visual cascade (figure 6). Firstly, the excited visual pigment interacts with the α subunit of another G-protein called transducin (GDP is exchanged for GTP). The α subunit of this protein (T_α), then activates cGMP phosphodiesterase (PDE), causing the hydrolysis of cGMP to 5'-GMP. The absence

of cGMP ensures the closure of the cationic cGMP-gated channels in the plasma membrane of the photoreceptor, causing the inhibition of glutamate release at the rod synapsis and a drop in calcium ions in the outer segment. This, in turn leads to hyperpolarisation and the generation of the neural response (Streyer, 1991; Fesenko et al., 1985). It is this response that is interpreted by the brain and results in vision. After excitation, the rod returns to a dark adapted state by the shutdown of the visual cascade and the synthesis of cGMP; a process known as photoextinction. Rhodopsin is inactivated by ATP-dependent phosphorylation at the C terminus and subsequent binding to arrestin. Transducin and PDE are inactivated by the hydrolysis of GTP on Tα. Guanylate cyclase (the enzyme that converts GTP into cGMP) is activated by a drop in the concentration of calcium ions. This leads to the reopening of the cGMP gated channel and the rod is depolarised. Calcium levels return to normal and guanylate cyclase returns to its usual activity. For a comprehensive review on visual transduction see Molday 1998. Patients suffering from rhodopsin-linked RP manifest rod photoreceptor cell death. It is therefore not unexpected that patients suffering from rhodopsin-linked RP present with night blindness as one of their earlier clinical symptoms.

1.9.2. Peripherin/RDS

Peripherin/RDS, a 39 kDa trans-membrane protein comprising 346 amino acids and located in the rim of rod and cone outer segments, is believed to play a major role in the morphogenesis and structure of disc membranes in photoreceptor cells, both rods and cones. Mutations in the gene can cause adRP and various forms of macular degeneration and pattern dystrophies such as butterfly shaped pigment dystrophy and cone-rod dystrophy (Appendix B). Interestingly, in some cases, mutations in peripherin/RDS in conjunction with mutations in the rim outer segment membrane protein gene (ROM-1) can cause digenic RP. For example, digenic adRP has been found in families segregating an L185P mutation in peripherin/RDS and a null mutation in ROM-1. However, mutations in ROM-1 alone do not cause retinal degeneration (Kajiwara et al., 1994; Dryja et al., 1997). To understand this form of digenic adRP, Goldberg studied the wildtype peripherin/RDS and the L185P mutant expressed in COS-1 cells in the presence and absence of ROM-1 (Goldberg and Molday, 1996). Briefly, in cells expressing wildtype peripherin/RDS and null ROM-1, homotetramers consisting of four peripherin/RDS molecules were formed. In cells expressing L185P peripherin/RDS and normal ROM-1, heterotetramers were formed and in cells expressing L185P peripherin/RDS and null ROM-1, no tetramers were formed. Thus tetramer

formation seems to be imperative for photoreceptor cell survival. This hypothesis is further supported by the observation that in a ROM-1 knockout mouse, peripherin/*RDS* homotetramers compensate for the absence of ROM-1 and the mouse does not manifest a retinal degeneration (Clarke et al., 1998).

1.10. Osteogenesis Imperfecta, collagen and the type I collagens

In 1849 Vrolik described a severe form of diaphyseal dysplasia which he named Osteogenesis Imperfecta (OI) (Vrolik, 1849). However, it was not till the early part of this century that Bell described the disease in more detail as manifesting blue sclerotics and fragility of the bone in the first major report on OI in English literature (1928). OI is a brittle bone disorder, affecting about 1:12,000 people, which results from mutations in the COL1A1 and COL1A2 genes. Over 150 mutations have been discovered in these two genes located on chromosomes 17cen-17q24 and 7q21.3-q22.1 respectively. The resulting disease normally manifests itself in an autosomal dominant fashion (Byers et al., 1993; Wenstrup et al., 1990; Sillence et al., 1979, 1981; Prockop et al., 1994; Kuivaniemi et al., 1991). Both genes encode the two type one pro-collagen proteins, the most abundant protein in man and the major protein lending strength to bone and fibrous tissue.

The disease phenotype of OI patients varies, however, the disease can generally be divided into four major categories (types I-IV) depending on the specific mutation involved. Type I OI, the mildest and in fact often undiagnosed form of the disease, is characterised by blue sclera, brittle bones, sometimes loss of hearing, dentinogenesis imperfecta and is usually caused by null mutations in the COL1A1 gene that result in a 50% reduction in the quantity of protein produced. The more severe types of OI, types II, III and IV, are caused by mutations in COL1A1 or COL1A2 genes that result in structural deformities in the encoded protein. Type II OI results in extensive fractures and deformities causing perinatal death. Types III and IV are fairly similar disorders. They are both progressive and cause short stature, hearing loss, fracturing, blue sclera and dentinogenesis imperfecta (Sillence et al., 1979; Byers, 1989, 1990, 1993; Wenstrup et al., 1990).

Collagen is the most abundant protein in animals. In order to be classified as a collagen, a protein must form supra-molecular aggregates (fibrils, filaments or networks) which must contribute to the structural integrity of the extra-cellular matrix and must contain at least one triple-helical domain. In fibrillar collagens, each mature collagen molecule contains only one such domain. However, basement

membrane collagens or FACIT collagens contain several shorter triple-helical domains, which are separated by non-triple-helical domains. Structurally, type I collagens are involved in tendons, ligaments, skin and bone, type II collagens in hyaline cartilage and type IV in basement membranes. The structural roles of other types of collagen are less clear. One theory is that they may play important roles in the assembly process of tissues and organs during embryonic development (Gordon and Olson, 1990). Fibrillar collagens include types I, II, III, V and XI and form banded fibrils in various tissues. Each gene contains about 330 repeats of triplet sequence, Gly-X-Y- (Gly is glycine, and X and Y are often proline residues), flanked by short non-triplet containing sequence, telopeptides at each end. The proteins form stable triple-helices at 37°C which are about 300 nm rigid rod like structures with a diameter of 1.5 nm (figure 7). The molecule consists of approximately 1000 amino acids. Fibrillar collagens are produced by a variety of cells, mostly (but not all) of mesenchymal origin. After the assembly of the triple-helix, the pro-collagen molecules containing amino and carboxyl propeptide extensions flanking the central triple-helical domain are secreted from the cell into the extracellular matrix. This pro-collagen molecule is then processed to form the mature collagen (figure 7). The fibrils are then arranged in different patterns in different tissues. Parallel fibril bundles in tendon, criss-crossing layers in cornea and spiral arrangements in lamellar bone.

Type I collagen molecules, consisting of two α1 chains and one α2 chain, are products of two genes, COL1A1 and COL1A2 located on the human chromosomes 17 and 7 respectively. Each gene contains more than 50 exons. Mutations in COL1A1 and COL1A2 are known not only to cause OI, but also the autosomal dominant type VII Ehlers-Danlos syndrome (EDS) (Lehmann et al., 1994), a disease which classically causes loose-jointedness and fragile, bruisable skin that heals with peculiar 'cigarette-paper' scars (Barabas, 1966; Byers et al., 1997).

Currently there are over 150 different mutations in COL1A1 known to cause OI and over 80 in COL1A2 known to cause either EDS or OI (for a complete online list see http://www.le.ac.uk/genetics/collagen/col1a1.html). Also, there are over 40 mutations in the peripherin/*RDS* gene and over 100 mutations in the rhodopsin gene known to cause RP. In the development of gene therapies for heterogeneous disorders such as OI and RP it will be necessary to develop mutation independent therapeutic agents.

1.11. Ribozymes in cells

Naturally, after testing a ribozyme, or indeed any kind of gene therapy *in vitro*, one needs to test it *in vivo*. Human cell lines present an excellent environment for testing ribozymes in a system, which partially mirrors the *in vivo* situation, while allowing the environment to be controlled. Unfortunately, ribozyme cleavage products are extremely unstable and are immediately digested in a cellular environment. Cleavage products can not be detected in cell studies. Nevertheless hammerhead ribozymes have in many studies been shown to be active in cell culture. Bauer et al. generated stable cell lines containing double hammerhead ribozymes designed to cleave the *tat* and *rev* transcripts of HIV-1. When the transduced cultures were infected with HIV-1 virus, viral replication was inhibited up to 1000x (Bauer et al., 1997). Benedict et al. (1998) generated a ribozyme which targeted the retinoblastoma gene (Rb) mRNA. The Rb susceptibility gene serves as a tumor suppressor gene encoding the nuclear phosphoprotein which is necessary for normal cell cycle function. Stably transfected mouse fibroblasts showed reductions in Rb mRNA levels of over 70%, abnormal morphology and loss of contact inhibition. Modifications to ribozymes are often required to obtain efficient cleavage *in vivo*. For example, lengthening antisense arms will stabilise ribozyme-substrate complexes. Adding groups such as phosphorothioates may further stabilise the molecules by protecting them from nuclease degradation (Chowrira and Burke, 1992; Heidenreich et al., 1994). It has been well documented that the cleavage of long target RNAs by ribozymes is much less efficient than cleavage of short oligonucleotide substrates because of higher order structure in the long target RNA. This may theoretically be due to intra-molecular base pairing with the target RNA, which could prevent the base pairing between the ribozyme and the cleavage site or due to steric hindrance because of the tertiary structure of large target RNAs. There is some evidence that the former is the case and that steric interference is unlikely to affect hammerhead ribozyme cleavage (Campbell et al., 1997). Long targets are more efficiently cleaved by ribozymes with longer stem sequences; however, dissociation of the cleavage products is strongly decreased with such hammerhead ribozymes (11, 12). There are currently two ways to overcome this problem. Firstly, the addition of non-specific nucleic acid binding proteins can increase the catalytic turnover due to their annealing activity. For example facilitation of hammerhead ribozyme catalysis by nucleocapsid protein of HIV-1 (NCp7) and the heterogeneous nuclear ribonucleoprotein A1 (A1) has been demonstrated (Bertrand and Rossi, 1994). Secondly, the addition of

oligonucleotides capable of interacting with the substrate RNA adjacent to the 5' or 3'-end of the ribozyme, so called facilitator molecules, has been found to enhance turnover of hammerhead ribozymes. Facilitators can comprise of either DNA or RNA (Goodchild, 1992; Denman, 1996; Nesbitt and Goodchild, 1994). In one study facilitator-effects were determined *in vitro*. Generally the facilitator-effects increased with the length of the facilitator molecule and RNA facilitators had greater effects than DNA on the same substrate sequence. Interestingly, 3'-end facilitators were found to increase the turnover of the ribozyme and 5' facilitators to decrease the rate of turnover (Jankowsky and Schwenzer, 1996a). In a similar *in vitro* study it was demonstrated that facilitators not only increased the rate of the cleavage step, but also pre-formed the substrate, accelerating substrate association. 3'-end facilitator accelerated both of these rates. 5'-end facilitators increased the association rate, but could either increase or decrease the rate of cleavage depending on the length of the substrate; they increased the rate of cleavage of long substrates and decreased the rate of cleavage of short substrates (Jankowsky and Schwenzer, 1996b). In summary, varying effects have been found using facilitators but overall they are believed to aid ribozyme:substrate association.

1.11.1. Cell lines expressing Rhodopsin and peripherin/RDS

Unfortunately photoreceptor cells, as a model for RP, do not grow in culture, as they are non-dividing cells. Retinoblastoma cell-lines, however, grow in culture and some of these are known to express some of the photoreceptor cell specific proteins (Fong et al., 1988; Donoso et al., 1985; Bogenmann et al., 1988; Di Polo et al., 1995). These cancerous cells are, naturally, not true photoreceptor cells, as they divide. Retinoblastoma cells are generally thought to be derived from photoreceptor precursor cells, i.e. neurectodermal cells (Griegel et al., 1990). One such retinoblastoma cell line, Y79 (McFall et al., 1977), expresses rod α, β and γ-PDE (three subunits comprising rod phosphodiesterase), rod transducin α (T_α), rhodopsin and cone α'-PDE (Di Polo et al., 1995). Y79 cells have not, as yet, been tested for peripherin/*RDS* expression. To my knowledge no stable cell lines have ever been made using Y79, however, transient expression experiments have been carried out with these cells (Di Polo et al., 1995). Similarly transient expression studies have also been carried out successfully in another retinoblastoma cell line, WERI (Shao-Ling Fong et al., 1993). Due to the lack of appropriate cell lines expressing high levels of retinal specific proteins some colleagues in this lab have initiated the generation of stable COS-7 cell lines (African Green Monkey kidney

cells) expressing human peripherin/*RDS*, and both human and mouse rhodopsin genes (Oprian, 1993). Such cell lines will be valuable for testing the ribozyme-based therapeutic approaches for RP, which are under development and described in chapter 3 of this Ph.D. thesis.

1.11.2. Cell lines expressing type I collagens

The precursor proteins of the COL1A1 and COL1A2 genes are expressed in fibroblasts and mesenchymal progenitor cells present in bone marrow. These cells are loosely interspersed in the extra-cellular matrix and secrete many proteins, such as the type I collagens, into the matrix. There are many commercially available human fibroblast cell lines, although most of them are not immortal. One cell line, originally derived from human skin and with a finite life span, is IBR3 (Taylor et al., 1975; Arlett et al., 1988). This cell line grows in monolayers and is easy to maintain. However, fibroblast cell lines are relatively easy to generate in the lab from human skin tissue. Indeed, many such cell lines are available. Dr. Marcia Willing, for instance, has kindly donated three fibroblast cell lines to this lab derived from human OI patients (Willing et al., 1994; chapter 5). Mesenchymal progenitor cells are cells with multilineage potential (Pittenger et al., 1999). These cells, which are thought to be able to replicate as undifferentiated cells and to have the potential to differentiate into different lineages of mesenchymal tissues such as bone cartilage, fat, tendon, muscle and marrow stroma, may be extracted from bone marrow and grown in cell culture. The addition of appropriate growth factors induces the cells to differentiate into the various mesenchymal tissues mentioned above (Pittenger et al., 1999; chapter 5). As with the cell lines described above expressing retinal proteins, these cell lines expressing type I collagens will be extremely valuable in the evaluation of therapeutic approaches for diseases such as OI involving mutations in the type I collagen genes.

1.12. Ribozymes in vivo and animal models

One of the most appropriate environments for testing gene therapies is in animal models. Initially, small mammals with short life cycles and gestation periods, such as mice, are preferable, as they are cheaper to breed. However, given promising results in small mammals experimental procedures frequently would then have to be evaluated in larger mammals. Notably, in the context of this Ph.D. thesis, hammerhead ribozymes have been shown to be functional in a number of animal models. For instance, adeno-virus-mediated expression of ribozymes against

human growth hormone in transgenic mice producing the human transcript resulted in a 96% reduction of transcript over a period of several weeks (Lieber and Kay 1996).

In another study, a nuclease-resistant hammerhead ribozyme decreased stromelysin mRNA levels in rabbit synovial fluid following exogenous delivery to the knee joint. The animal used in the study was a rabbit model of interleukin 1-induced arthritis and the targeted gene, the matrix metalloproteinase stromelysin, is believe to be a key mediator in arthritic diseases. Thus inhibiting the gene may be a valid therapeutic approach for arthritis. Not only were the protected ribozymes found to be stable within the knee joint, the synovial interleukin 1-induced stromelysin mRNA was reduced, suggesting that this ribozyme may be a potentially be useful in the treatment of some types of arthritic diseases (Flory et al., 1996).

Heterozygous mutations in the glucokinase gene have been found in patients with autosomal dominantly inherited maturity-onset diabetes of the young (MODY). This raises the possibility that a decrease in β-cell GK activity may impair the insulin secretory response of these cells to glucose. A ribozyme-based study demonstrated ribozyme-mediated attenuation of pancreatic β-cell glucokinase (GK) transgene expression in transgenic mice resulting in impaired glucose-induced insulin secretion. Thus mouse models for MODY were generated, which expressed a ribozyme against GK under the control of the insulin promoter. Insulin release in response to glucose from in situ-perfused pancreas was impaired, but interestingly, plasma glucose and insulin levels of the mice remained normal. Thus these mice may be predisposed to diabetes and may manifest increased susceptibility to genetic and environmental diabetogenic factors, providing an animal model for studying the interaction of such factors with reduced GK activity (Efrat et al., 1994).

In addition, efficient ribozyme-mediated reduction of bovine α-lactalbumin expression was demonstrated in double transgenic mice expressing a bovine α-lactalbumin (α-lac) ribozyme and the bovine (α-lac) transgene. High expression of the ribozyme was detected by Northern blot, leading to significant reduction (up to 78%) of target mRNA levels. This study once more demonstrates the feasibility of ribozyme-mediated down-regulation of transcripts in transgenic animals (L'Huillier et al., 1996).

Another example of ribozymes utilised *in vivo* was provided by work carried out by Larsson et al. (1994). In this study a ribozyme (Rz) targeting the mouse 2-microglobulin (β2M) mRNA, which had previously been shown to be efficient in cell culture, was used to generate a transgenic mouse. Ribozyme expression was accompanied by a reduction of the β2M mRNA levels in heterozygous mice (Rz+/-). The effect was most pronounced in lung with a greater than 90% reduction of the target gene.

Thus ribozymes have been shown to be active in animals in many studies. Given that ribozyme based therapeutic approaches may be used for diseases such as RP and OI it is pertinent to address whether appropriate animal models are available to test therapeutic approaches in (see below).

1.12.1. Animal models for rhodopsin related RP

Many animal models for human inherited retinopathies exist; both naturally occurring animals (such as rds mice, see below) and animal models generated using transgenic and targeting technologies (for example various knockout mice and transgenic mice carrying dominantly or recessively inherited rhodopsin mutations exist).

A number of mouse models for human rhodopsin associated RP have been generated and include mice carrying a Pro23His (C to A transversion at codon 23) human rhodopsin transgene (Dryja et al., 1990; Olsson et al., 1992). This C→A missense mutation at codon 23 is the most common mutation among patients with adRP in North America, most likely due to a founder effect (Berson et al., 1991; Dryja et al., 1991). This transgenic mouse contains a human rhodopsin transgene from a patient with adRP. Notably, these mice manifest photoreceptor degeneration similar to human adRP. Various mouse lines were generated with this transgene and the least severely affected lines were also the ones that expressed the lowest levels of the transgene. Interestingly, the same group also generated two transgenic mice with wildtype human rhodopsin, one of which expressed approximately equal amounts of human and murine rhodopsin and manifested no retinopathy and one of which expresses about 5 times more human than murine rhodopsin and manifested an RP-like retinal degeneration. This indicates that, at lease in mice, over-expression of normal human rhodopsin can lead to RP, stressing strong dosage dependence. This finding has clear implications

for the tight control of levels of gene expression necessary in therapies involving delivery of the rhodopsin gene.

A second model for rhodopsin linked RP is the serine 6 mouse. This mouse expresses a mutant Pro347Ser (P347S) rhodopsin gene and displays a retinal degeneration similar to autosomal dominant RP in humans. By 5 weeks after birth the mice have lost about 35% of their photoreceptor cells (Weiss et al., 1995). There is some evidence that the mutation impairs the transport of rhodopsin from the inner segments to the outer segments. Thus it is possible that the photoreceptor degeneration occurs because of a failure to renew outer segments at a normal rate, leading to a progressive shortening of outer segments (Li et al., 1996).

The Q344ter transgenic mouse, which contains a nonsense mutation at position 344 of the mouse rhodopsin gene resulting in photoreceptor cell death is another mouse model for rhodopsin-linked RP. The photoreceptor cell death is thought to be due to the inefficient transportation of rhodopsin to or retention of rhodopsin in the outer segment (Sung et al., 1994).

Another very useful mouse for the study of rhodopsin related RP is the rhodopsin knockout mouse (Humphries et al., 1997), which carries a targeted disruption in the murine rhodopsin gene. The Rho -/- mouse cannot form rod outer segments. At 3 months the photoreceptor nuclei are entirely lost. The Rho +/- mouse maintains photoreceptor cell function but shows a small degree of structural disorganisation of inner and outer rod photoreceptor segments. This mouse as it has a recessive retinopathy will be particularly useful in evaluating replacement approaches involving gene delivery of rhodopsin to Rho-/- mice.

A somewhat larger animal model for rhodopsin-linked RP is a transgenic pig (Petters et al., 1997) that expresses a mutated rhodopsin gene (Pro347Leu), known in man to cause RP. The pigs show severe early onset rod cell degeneration followed by later onset cone degeneration. These characteristics are remarkably similar to the analogous disease in man. The pig may be particularly useful in that its profile of rod and cone photoreceptor cells mirrors that in human retinas more closely than that present in nocturnal animals such as mice.

An interesting model for rhodopsin linked RP is a transgenic rat containing a human rhodopsin transgene with an autosomal dominant mutation (P23H) (Lewin et al., 1998). This is the most common mutation in the US, affecting 12% of American RP patients (Olsson et al., 1992). A recent study demonstrated the utility

of a hammerhead ribozyme and a hairpin ribozyme targeting rhodopsin in this rat. The ribozymes, which targeted an artificially introduced NUX ribozyme cleavage site present in the transgenic rat, were delivered by recombinant adeno-associated virus (AAV) into the retina of transgenic rats containing the P23H mutation. Subsequent to AAV-ribozyme administration, the rate of photoreceptor degeneration was retarded for at least three months in treated rats (Lewin et al., 1998). This study clearly demonstrates the potential application of ribozymes for autosomal dominantly inherited disorders such as adRP. Unfortunately the ribozymes used in this study will not be directly of benefit to human patients as they target the artificially created NUX site, which is not present in the human rhodopsin sequence. However, the transgenic rat provides an extremely useful animal model for gene therapy studies on P23H-linked RP and indeed for evaluation of mutation-independent gene therapy approaches such as the gene therapy strategies discussed in chapter 5.

1.12.2. Animal models for peripherin/RDS related RP

The retinal degeneration slow (rds) mouse (van Nie et al., 1978) carries a partially dominant mutation leading to abnormal rod and cone photoreceptor cell development, eventually resulting in the slow loss of both of these cell types. The rds gene is thought to be necessary for the assembly of rod outer segments and most probably principally plays a structural role in the retina. The effects of the rds mutation in heterozygous mice are thought to be caused by haploinsufficiency (Cheng et al., 1997). In contrast to heterozygous rds mice, homozygous rds/rds mice form no outer segments in either rods or cones, resulting in loss of almost all of these cells by one year post-natally. Rds/+ mice do form outer segments, however these are reduced in length and arranged in an irregular fashion. Heterozygous rds/+ mice eventually loose photoreceptors, but only very slowly. This last phenotype is thought to possibly resemble human adRP caused by some mutations in the peripherin/*RDS* gene.

Additionally, Kedzierski et al., (1997) developed and analysed a transgenic mouse expressing a human peripherin/*RDS* P216L transgene known to cause adRP in man. From their study they concluded that the resulting loss of photoreceptors in this transgenic mouse was caused both by haploinsufficiency and by a direct dominant effect of the mutant peripherin/*RDS* protein.

1.12.3. Animal models for type I collagen associated dominant OI

A mouse-model for type I OI (Bonadio et al., 1990) carries a null mutation in intron 1 of the mouse *col1a1* gene preventing any protein from being formed. Homozygous animals, which produce no col1a1 protein, are not viable. Heterozygous animals manifest defects in mineralised and non-mineralised connective tissue and progressive hearing loss. The model clearly demonstrates that at least part of the disease in mouse is caused by haploinsufficiency.

A true gain of function mouse model for OI is the minigene mouse, a transgenic mouse expressing a COL1A1 human mini-gene. The gene contains the promoter region and the 5'- and 3'- ends of the gene, but lacks 41 exons in between. In man, this in frame mutation produces a lethal form of OI. Some mouse lines expressing large amounts of the mini-gene had a lethal phenotype, while others expressing lower levels of the transgene survived, manifesting OI or osteoporosis (Khillan et al., 1991; Pereira et al., 1993).

1.13. Gene delivery

Approaches for gene therapy vary significantly for different disorders. For instance, in the case of recessive disorders the aim may be to supply a missing gene and in the case of dominant negative disorders to silence a gene which is causing a disease. However therapeutic genes may also be utilised in cancer therapies and against infectious agents such HIV viruses. During the development of a gene therapy, no matter what the aim is, there are a number of important steps, some of which are outlined below. Firstly, the genetic cause of the pathology needs to be known. Secondly, one needs to generate a therapeutic oligonucleotides, which can be tested *in vitro*, in cell culture or both. Thirdly, a method of delivering the therapeutic agent to the correct tissue must be devised. Fourthly, the therapy must be tested in a series of animal models, initially in small animals such as rodents and subsequently in primates. Only after accomplishing these steps can one consider embarking on a human clinical trial of a gene therapy. There are various approaches for gene therapy. One approach is germ line therapy in which germ line cells, i.e. a zygote, an egg cell or a sperm cell, are transformed. This method ensures that all cells in all tissues will contain the transgene and therefore that the progeny of the transgenic organism will also contain the transgene. To date this method of therapy is illegal for ethical reasons. A second approach for gene therapy is somatic. Thus, the transgene is delivered to parts of the body, preferably tissues,

which require the transgene. This method should not, in principle, affect progeny. No matter what the aim of the somatic gene therapy is, methods for efficient gene delivery must be devised. In this regard, there are two general approaches for gene delivery. The first is *ex vivo* gene therapy and the second is *in vivo*. *Ex vivo* gene therapy is carried out outside the body on some affected tissue (maintained in tissue culture), which has been removed from the organism. The transformed tissue is then replaced in the organism.

One example of a successful human *ex vivo* gene therapy was carried out on the liver of a woman with familial hypercholesterolemia (FH) (Wilson et al., 1992). The liver was then transplanted back into the female patient. FH is an autosomal dominant disorder caused by deficiency in the receptor that clears low density lipoprotein (LDL) from serum. One abnormal LDL receptor allele causes elevations in plasma LDL and patients are prone to premature coronary artery disease. One advantage of using an *ex vivo* approach for gene delivery is that the target tissue is readily accessible to the transgene. One disadvantage is that not all tissues can be removed, maintained in tissue culture and replaced into an organism. For instance, terminally differentiated neurons, such as photoreceptor cells, cannot be targeted *ex vivo*. *In vivo* gene therapy requires the delivery of a transgene directly into affected tissue of an organism or via a systemic route such as the circulatory system. Thus for both *in vivo* and *ex vivo* gene therapy approaches, vectors may be required to carry the therapeutic gene into tissues. Currently used vectors can be classified into viral and non-viral vectors.

1.13.1. Viral vectors

There are three types of recombinant virus used as gene therapy vectors: double stranded RNA viruses, double stranded DNA viruses and single stranded DNA viruses. In the context of this thesis, which mainly deals with gene therapy strategies for RP and OI, many of the examples given below are examples of virus-mediated gene transfer into ocular tissue. Examples of viral vectors being used in the treatment of OI will be given in chapter 5.

1.13.1.1. Double stranded RNA viruses, or retroviruses

There are two types of retrovirus, the lentivirus such as HIV and the C type virus such as the mouse melony leukemia virus (MLV). Both types integrate randomly (non-homologously) into host genomes, are extremely infectious and can carry up to 8 kb of foreign DNA. To date, recombinant retroviruses have been the most

commonly used viral vector in gene therapy studies, partly because of the relative ease in which they can be generated at high titers. For safety reasons, recombinant retroviruses are made replication-deficient, missing the viral genes encoding the matrix proteins, nucleocapsid proteins and core proteins (gag), the viral polymerase (pol) and the viral envelope protein (env). Thus, when generating recombinant retroviruses, a packaging cell line is required, which expresses these genes and supplies the missing proteins to the virus. C type viruses can only transverse host nuclear membranes during cell mitosis and therefore can only multiply in dividing tissues. For this reason, recombinant C type viruses are not suitable gene therapy vectors for non-dividing tissues such as neurons. Lentiviruses on the other hand can readily cross host nuclear membranes at any stage of the cell cycle and are suitable vectors for all tissues. One danger of using recombinant retroviruses for gene therapies is that the viruses may disrupt host DNA when integrating randomly into the host genome, possibly causing disorders such as cancer. A second danger in using recombinant retroviruses in gene therapies is the small possibility of including a replication-efficient retrovirus, which has recombined with the packaging cell line and picked up the missing gag, pol and env genes.

An example of the use of an HIV-based lentiviral vector in terminally differentiated (non-dividing) retinal cells was given in 1997 (Miyoshi et al., 1997) using subretinal injections (figure 8). In this study a green fluorescent protein (GFP) reporter gene driven by a cytomegalovirus (CMV) promoter was efficiently expressed in both rod and cone photoreceptor cells and the retinal pigment epithelium (RPE) of rats. In the same study a GFP gene driven by a rhodopsin promoter (from −2174) resulted in expression predominantly in photoreceptor cells. GFP expression persisted for at least 12 weeks without any apparent decrease.

1.13.1.2. Double stranded DNA viruses

There are two types of recombinant double stranded DNA virus generally used in gene therapy studies. The first is derived from the Herpes Simplex virus (HSV) and the second from the Adenovirus (Ad). Dr. Rowe, when attempting to discover the cause of the common cold, discovered Ad in adenoid cells in 1953 (reviewed in Sohier et al., 1965). Ads generally infect moist tissues such as ocular, respiratory, gastrointestinal or urinary epithelia. Recombinant double stranded DNA viral genomes remain extra-chromosomal, may carry up to 8kb of foreign DNA and generally can infect both dividing and non-dividing tissues. Recombinant double stranded DNA viruses are prepared in much the same manner as retroviruses

using a packaging cell line. Problems associated with utilising these recombinant viruses as gene therapy vectors are that the recombinant virus may become replication-efficient again by recombining with wildtype HSV or Ad. In addition, as these viruses do not integrate into a host's genome, as therapeutic agents, the virus would need to be administered repeatedly. Therefore, the host would build up an immune response to the virus. One key advantage of these viruses is that they remain extra-chromosomal, there is no risk of a disruption in the host genome due to insertional mutagenesis. In addition they are relatively easy to generate at high titers.

There are a number of examples of gene therapy studies using HSV vectors, particularly in the treatment of tumors as these viruses have been found to be cytotoxic (Kramm et al., 1997) and will naturally be more toxic to rapidly dividing tumors. In one study a group investigated the efficacy of a viral vector, hrR3 derived from HSV in destroying colon carcinoma cells *in vitro* and *in vivo*. The hrR3 vector is capable of replication and its replication is cytotoxic to cells. HrR3 also possesses the HSV-thymidine kinase gene, which converts gancyclovir into a toxic metabolite. Thus, the addition of gancyclovir to hrR3-infected cells may enhance the ability of hrR3 to destroy tumor cells. The inherent cytotoxicity of hrR3 replication effectively destroys colon carcinoma cells. However, the cytotoxicity was not found to be enhanced *in vivo* by the addition of gancyclovir. The authors concluded that in the future, more efficacious and selective HSV 1 vectors may be useful in the treatment of cancer (Yoon et al., 1998).

There are multiple examples of gene therapy studies in which Ad viruses have been used very successfully. In the context of this thesis, the following examples again focus on Ad viral delivery of genes into retinal tissue and bone cells. In 1994 two papers were published which utilised Ad vectors to transfer genes into murine retina. In the first, a replication-deficient Ad was used to mediate the transfer of the bacterial β-galactosidase (LacZ) reporter gene, driven by a CMV promoter, into the subretinal space of normal, rd and rds mice. LacZ expression was detected in the retinal pigment epithelial and photoreceptor cells (Li et al., 1994). In the second paper, another adenovirus, carrying a LacZ reporter gene driven by a CMV promoter was microinjected into the subretinal space of CD-1 mice. LacZ expression was detected up to 95 days in the retinal pigment epithelium and photoreceptor cells (Bennett et al., 1994).

The same group published another paper in 1996, in which they utilised an Ad virus containing the murine cDNA for the wildtype cGMP phosphodiesterase gene (βPDE) driven by a CMV promoter, in a gene therapy study on the rd mouse. This mouse manifests a retinal degeneration very similar to human RP due to a recessive mutation in the βPDE gene. Subretinal injections of this virus into neonate rd mice resulted in the generation of βPDE transcripts, increased PDE activity and delayed photoreceptor cell death by six weeks, demonstrating the feasibility of treating an inherited retinal degeneration by somatic gene therapy (Bennett et al., 1996).

In the same year another group published a paper in which they studied the effects of Ad gene transfer to the tissues of the anterior segment *in vitro* in rat and monkey lens organ cultures and *in vivo* by single injection into the anterior chamber of rabbits. In the *in vitro* study, intact lens cultures were exposed to Ad containing either LacZ or the firefly luciferase (luc) gene under the control of the Rous sarcoma virus promoter. Both viruses efficiently delivered the reporter genes to the ciliary processes but penetrated poorly into the capsulated lenses. However, viral receptors were detected in rat lens epithelium, and in the primary trabecular meshwork and other lens cell lines. In the *in vivo* study, the anterior chambers of eight rabbits were injected once with Ad containing LacZ driven by a CMV promoter. After 48 hours they were evaluated and gene transfer was evident in corneal endothelium, iris anterior surface and trabecular meshwork (Borras et al., 1996).

In another study the role of cell-mediated immunity in the stability of ocular Ad mediated transgene expression was evaluated. An Ad containing the LacZ gene under the control of a CMV promoter was injected intravitreally or subretinally (figure 8) into eyes of immunocompetent (+/+) and immunocompromised, congenic nude (*nu/nu*) CD-1 mice. Additional +/+ mice received subretinal injections of the same virus with co-administration of 200 mg of human immunoglobulin (Ig) G or CTLA4Ig by intraperitoneal, intravitreal or subretinal injection (figure 8). Results of the study demonstrated that LacZ expression was extended from 1 week to more than 5 weeks in the corneal endothelium, iris and trabecular meshwork of *nu/nu* mice compared with time of expression in +/+ mice when Ad was administered intravitreally. In contrast, subretinal injection resulted in only a minimal increase in transgene stability in *nu/nu* mice compared with that in +/+ mice. Neither systemic nor intraocular administration of IgG or CTLA4Ig affected the stability of

LacZ expression in the retina or retinal pigment epithelium after subretinal injection in +/+ mice. IgG and CTLA4Ig enhance the stability of transgene expression in the trabecular meshwork. Thus, a T-cell mediated immune response appears to play a role in the loss of Ad mediated expression after intravitreal but not after subretinal injection. This result implies that the subretinal space is an immune-privileged site and favorable site for gene transfer (Hoffman et al., 1997).

Another study supports the fact that immune responses limit Ad mediated gene expression in the mouse eye. In this study an Ad containing the LacZ gene driven by a Rous sarcoma virus LTR promoter was injected into one immunocompetent mouse strain, one immunosuppressed strain (BALB/c) and one immunodeficient strain (congenic nude mice, *nu/nu*). The Ad was injected subretinally, subconjunctivally or into the anterior chamber (figure 8). The results demonstrated that T cell-mediated immune responses limit the duration of Ad-mediated ocular gene expression in adult mice since LacZ gene expression was detected for at least 15 weeks in T cell-deficient *nu/nu* mice, however, the level of transgene expression did decrease over time. In contrast to the previous paper mentioned by Hoffman et al., intra-ocular Ad-mediated gene expression was not found to have a significantly greater longevity than extra-ocular expression, suggesting that the eye is not normally immune-privileged with respect to viral vectors. Re-injection of BALB/c mice resulted in a rapid decline in reporter gene expression, however, successful re-administration of virus was possible in the case of the nude mice (Reichel et al., 1998).

1.13.1.3. Single stranded DNA viruses

The main single stranded DNA virus used in gene therapy studies is the Adeno-Associated virus (AAV). This small virus belongs to the parvovirus family and is a satellite virus to other viruses, either Ad or HSV, as it requires coinfection with these viruses to replicate. AAVs were first discovered in 1966 simultaneously by Atchison and Hoggan. All cultured human cells seem to be prone to infection by AAVs and no adverse symptoms have been demonstrated so far after infection. The wildtype AAV preferentially integrates on human chromosome 19q13.4 and is not tumorgenic (Kremer and Perricaudet, 1995). Recombinant AAV vectors have a high transduction efficiency, do not integrate preferentially on chromosome 19, can carry up to 4.7 kb of foreign DNA and do not seem to elicit an immune response in the host. AAVs are generated in a packaging cell system, which contains a recombinant AAV vector DNA plasmid and which has been infected with either

wildtype Ad or wildtype HSV. Density gradient centrifugation or heat inactivation removes the wildtype Ads or HSVs. Thus, recombinant AAVs are difficult to prepare and are easily contaminated with wildtype AAV and helper Ad or HSV viruses. There are multiple examples in which AAV viruses have been used to deliver genes into all types of tissue, especially non-dividing tissues such as neuronal cells. In the context of this thesis the following examples will focus on the use of AAV vectors for gene delivery into the retina.

For example, in 1996 a recombinant AAV was utilised to deliver a LacZ gene driven by a CMV promoter. The AAV was subretinally injected into immunodeficient (nude) mice. LacZ gene expression persisted in all layers of the neuroretina as well as the retinal pigment epithelium (RPE) for at least four weeks. Interestingly the same group carried out the same experiment in wildtype animals and found that LacZ expression decreased over time. They speculate that the decrease in transcript levels appears to be as a result of an immune mediated loss of cells, possibly directed against the bacterial reporter gene LacZ, although contamination of AAV stocks with residual wildtype helper Ad could not be discounted. Thus, this limitation may be overcome by the use of AAV vectors encoding endogenous genes and by the development of more sophisticated methods for producing purified AAV stocks (Ali et al., 1996).

In a second fascinating study, AAV carrying either the LacZ or the gfp gene driven by a mouse opsin promoter was injected subretinally into mice or rats. Transgene expression in both rodents was limited exclusively to photoreceptor cells and after a single injection 2.5 million photoreceptor cells were estimated to have been transduced. The group also determined experimentally that the AAV carrying the gfp gene was free of both Ad helper virus and wildtype AAV as judged by plaque assay and infectious center assay. All test animals exhibited strong gfp expression at 6 or 8 weeks, whereas at 1-3 weeks post-injection, expression was weak. A possible cause of this slow onset of expression may be the slow conversion of input AAV DNA (single-stranded) to a transcriptionally active, double-stranded form in non-dividing photoreceptor cells. Reporter gene expression was detectable for at least 10 weeks postinjection (Flannery et al., 1997).

In 1997 a paper was published on *in vivo* recombinant AAV-mediated transduction into retinal tissue. The aim of the study was to evaluate the efficiency, cell specificity, stability and toxicity of recombinant AAV-mediated retinal transduction *in vivo* in the adult immunocompetent mouse. Thus an AAV, carrying the gfp gene

under the control of a CMV promoter, was subretinally injected into mice, which were examined (real-time) by direct observation of fluorescence by ophthalmoscopy, using excitation-barrier filters. Histologic analyses of retinal tissue were used to identify infected cells and to assess inflammation. Real-time imaging showed that AAV efficiently transduces a variety of cells of the neural retina and retinal pigment epithelium. Transgene expression was not observed until 1 week postinjection, after which the number of gfp-expressing cell increased until week 3. Transgene expression was observed for at least 11 weeks post administration. There was no clinical or histological evidence of inflammatory response. Thus, AAV-mediated retinal gene transfer is stable and efficient and is not associated with clinically or histologically detectable toxicity or immune reaction (Bennett et al., 1997).

1.13.2. Non-viral vectors and methods of gene delivery
1.13.2.1. Bacterial delivery of DNA

One non-viral vector for gene delivery, which presents some great advantages over the viral vector, is the bacterial vector. Investigators exploit mechanisms of entering and growing in cells, used by intracellular microbial pathogens, which have co-evolved with a host for millions of years. In 1995 two separate groups investigated the potential of using Shigella flexneri as a vehicle for gene delivery (by means of plasmid DNA containing the gene of interest) into mammalian cells (Sizemore et al., 1995; Courvalin et al., 1995). The S. flexneri strains used in both studies were deficient in cell-wall synthesis and required diaminopimelicacid (DAP) for growth. In the absence of DAP, the recombinant bacteria lyse in the host cytosol and release the plasmid DNA of interest. Results showed that, subsequent to addition of bacteria, up to 28% of cells contained one to five visually intact bacterial cells, with 1.7% containing five bacteria. Recently in another paper, a group exploited Listeria monocytogenes, another intracellular pathogen, to deliver plasmid DNA carrying a gfp reporter gene into the cytosol of macrophages. The recombinant L. monocytogenes expressed a Listeria-specific phage lysin, which causes L. monocytogenes to lyse inside the host cytosol and release the plasmid. The group infected the macrophages with the bacteria at a one to one ratio and found that over 0.2% of the macrophages expressed gfp (Dietrich et al., 1998). Thus in comparison to viral vectors, bacterial vectors appear to be less efficient vehicles for gene delivery. However, two advantages of using this system are that one recombinant vector can potentially carry any number of different plasmids. In addition bacteria are relatively easy to transform, grow and purify. Also, many

bacteria, such as E. coli K12, have very high plasmid copy numbers and are thus ideal candidates to optimise this method of gene delivery.

1.13.2.2. Gene transfer by in vivo electroporation or cell permeabilisation

One of the most efficient methods of introducing small molecules and genes into mammalian cells is by using electric pulses (Neumann et al., 1982). Although it is thought that the pulses create electropores, there is a lack of clear data on the exact mechanism of the permeabilisation-process. However, electropermeabilisation may arise from a change in transmembrane potential difference, which at values of 200-250 mV leads to membranes becoming transiently permeable (Teissie and Rols, 1993). Clinical trials of *in vivo* electroporation have been performed with success in the case of head and neck carcinoma and melanoma (Mir et al., 1995). The results of one phaseI/II clinical trial for the treatment of cutaneous and subcutaneous tumors using electrochemotherapy demonstrated that 50% of nodules treated with low doses of bleomycin, chemotherapy drug, followed by an electic pulse disappeared (Heller et al., 1996). Many tissues including skin, brain and liver have been shown to be susceptible to this method of gene delivery. In addition, no secondary cytotoxic effects have been observed (Titomirov et al., 1991; Nishi et al., 1996).

In one recent study on *in vivo* cell permeabilisation, mouse melanomas were injected directly with either the β-galactosidase reporter protein or a plasmid containing the LacZ reporter gene. Subsequently, electric pulses were applied with surface electrodes in contact with the skin. The efficiencies of protein and gene delivery were 20% and 4% respectively. No secondary effects on treated animals were observed (Rols et al., 1998).

Ionthophoresis is a similar method of gene delivery to electroporation. However, ionthophoresis applies a small low voltage (typically 10V or less) continuous constant current (typically 0.5mA/cm^2) and electroporation applies a high voltage (typically around 100V) pulse for a very short duration (reviewed in Banga et al., 1999). Ionthophoresis of a drug called dexamethasone (Dex) into a rat model for endotoxin-induced uveitis has had some beneficial effects in the treatment of uveitis. In this study the therapeutic efficacy of Dexamethasone (Dex) administered by ionthophoresis was compared to systemic injection and to topical application with the iontophoresis apparatus in the absence of electrical current. The study demonstrated that Dex administration by ionthophoresis allows for a therapeutic effect on the posterior as well as the anterior segment of the eye, and

may present a viable alternative to systemic administration of glucocorticoids in severe ocular inflammations (Behar-Cohen et al., 1997). It is of note that this method of drug delivery may be applicable to gene therapies too.

1.13.2.3. Gene delivery using cationic lipids

Cationic lipids are molecules which self-associate with plasmid DNA and condense it into particles, termed lipoplexes. Lipoplexes are able to interact with the cellular plasma membrane and efficiently to promote plasmid entry into cells. Lipoplex entry into the cell is believed to occur via endocytosis (Zabner et al., 1995). Cationic lipids were first utilised for gene delivery by three individual research groups in the late 1980s (P Felgner, JP Behr and L Huang). They have now been tested in several clinical trials, mostly in therapies for cancer of cystic fibrosis. Two of the main problems associated with the use of lipids in gene delivery are the relatively low transfection efficiency compared to viral methods of gene delivery and their toxicity. Another drawback to cationic lipid-mediated gene transfer is that lipolexes are unstable, which can lead to the formation of large aggregates. Naturally this creates difficulties for *in vivo* studies. Nevertheless, cationic lipids have been tested *in vivo* and have met with some success. For example, the use of cationic lipids increased the retention of DNA plasmids injected directly in mouse tumors from 50% to 90% 2 hours post-injection. However, gene expression in the tumor was not enhanced significantly, due to the fact that the lipoplexes did not diffuse from the site of injection. These mixed results may not be relevant if the delivered gene-product in required in only very small quantities to be of benefit to a patient, as, for example, may be the case for certain growthfactors or hormones.

The systemic delivery of lipoplexes into the bloodstream to reach liver, lung and kidney has been tried (Lai et al., 1997; Lai et al., 1998). In the 1997 study, three different routes of lipid-mediated gene delivery to kidney in mice were compared; through intra-renal-pelvic, intra-renal-arterial and intra-renal-parenchymal injections. A plasmid carrying the LacZ reporter gene driver by a CMV promoter was used to monitor gene expression. β-galactosidase activity was detected in cells in the cortex and outer medulla in both intra-renal-pelvic and intra-renal-arterial groups, but not in the intra-renal-parenchymal group or in noninjected control kidney. Evidence of gene transfer was observed in tubular epithelial cells, but not in glomerular, vascular, or interstitial compartments. The levels of β-galactosidase expression started to decrease 3 weeks after injection. In addition, gene transfer in the kidney was not associated with nephrotoxicity. Thus, both intra-renal-pelvic

and intra-renal-arterial injections provide transient gene transfer to the renal tubular cells and are suitable routes for kidney-targeted gene therapy (Lai et al., 1997). The 1998 study demonstrated that in the mouse model for renal tubular acidosis (CAII mice) injected with cationic liposomes complexed with the wildtype CAII cDNA driven by a CMV promoter, the disease phenotype was suppressed for 3 weeks after gene therapy and was eventually lost by 6 weeks. As in the 1997 study, immunohistochemistry studies using anti-CAII antibodies showed that CAII was expressed in tubular cells of the outer medulla and corticomedullary junction. In addition, once more the gene therapy was not associated with nephrotoxicity (Lai et al., 1998).

1.13.2.4. Gene delivery using synthetic polymers

Another non-viral method of gene delivery is via synthetic polymers. A wide range of synthetic polymers is available for exploring as gene delivery agents. For example, Starburst polyamidoamine dendrimers (dendrimers), first described in 1996 (Roberts et al., 1996), are spherical macromolecules composed of repeating polyamidoamino units. They can be produced in various sizes and are thought to interact with DNA and help it reach the cell nucleus. In one study dendrimers were efficiently used to transfer genes into murine cardiac grafts (Qin et al., 1998). In another study dendrimers increased oligonucleotide uptake into cells by 50-fold (Delong et al., 1997).

Another example of a synthetic vector is polyethyleneimine (PEI), which can be complexed to DNA to form a linear PEI/DNA complex. This complex was successfully transfected into the mouse central nervous system after an intraventricular injection of the complex. The complexes were shown to be highly diffusible in the cerebrospinal fluid of mice, diffusing from a single site of injection throughout the entire brain ventricular spaces. Reporter transgene expression was found in both neurons and glia adjacent to ventricular spaces, suggesting that this vector may be useful for gene delivery to the central nervous system (Goula et al., 1998).

There is a wide range of other synthetic polymers which are being evaluated as non-viral vectors for gene delivery including synthetic block co-polymers, synthetic virus-like particles, synthetic DNA-compacting peptides polylysine, DEAE-dextran and protamine (Wolfert et al., 1996; Erbacher et al., 1999; Schwartz et al., 1999). One clear advantage of synthetic vectors such as polymers is that their size, shape and charge can be modified with ease. Moreover, targeting ligands can be attached

to such non-viral vectors to aid tissue specific gene delivery and delivery form cytoplasm to nucleus.

1.14. Linkage studies

1.14.1. Linkage

Linkage analysis is based on the occurrence of recombination events between an area of a chromosome of interest and a known polymorphic marker. During first-division-meiosis, recombination events between homologous chromosomes occur. Due to these events, chromosomes in an offspring are in fact a patchwork of parent chromosomes. If two areas or loci on a parent chromosome are far apart, the likelihood that an offspring inherits both parts of the chromosome from one parent is 50 % (i.e. the two areas are unlinked). However, the closer together the two areas or loci are situated, the more likely it becomes that both loci will be inherited. Two loci considered to be linked if the chance of inheriting both loci is greater than 50%.

Thus, the probability of recombination between loci may provide an estimate of the distance between them; i.e. the genetic distance. The unit for this distance is given in Morgans (M); 1 centi-Morgan (cM) corresponds to approximately 1 million bases of DNA. However, recombination rates vary between sexes; women have a higher recombination rate than men and therefore a longer genetic map. Additionally, recombination rates across a chromosome do not remain uniform. For example, the recombination rate near the telomere of any chromosome is higher than that at the rest of the chromosome. Finally the occurrence of a recombination event inhibits the occurrence of a second event in the vicinity of the first event; a phenomenon called interference. Thus genetic distance is only loosely related to actual chromosome distance.

Linkage analysis in the context of a disease represents a test for the co-segregation of a disease locus with a particular polymorphism. If the disease locus and the polymorphic marker are on the same chromosome, but far apart, there is a 50% chance that they will either be found on the same strand of DNA or that they will be separated during meiosis. If, however, the disease locus and the polymorphic marker are close together or tightly linked they are unlikely to be separated during meiosis. The recombination fraction Θ is the total number of recombinants divided by the total number of offspring and will be 50 % or 0.5 if a disease and a polymorphism are unlinked. However, if they are linked, Θ will drop towards 0.0, depending on how tightly they are linked. The ascertained value for Θ between two

loci can be used to estimate a value for the genetic distance between the two loci. However, due to phenomena such as interference Θ must be converted into cM using a mapping function such as the Kosambi mapping function or the Haldane's mapping function (Haldane, 1919). There are several methods for calculating Θ. The most common is the logarithm of the odds or the lod-score (Z), which is the most likely value of Θ.

$$Z(\Theta) = \log_{10} \frac{L(\Theta)}{L(0.5)} \quad \text{or} \quad Z(\Theta) = \log_{10}[L(\Theta)] - \log_{10}[L(\Theta = 0.5)] \quad (1.2.)$$

Where $Z(\Theta)$ = the lod-score at a given Θ; $L(\Theta)$ = the likelihood of the observed recombination fraction; $L(0.5)$ = the likelihood obtained under the assumption of no linkage (Terwilliger and Ott, 1993). Morton suggested parameters for linkage and exclusion mapping in 1955 (Morton, 1955). If Z is larger than 3, linkage is suggested, if Z is below −2 the polymorphism and the disease are unlinked and if Z lies between −2 and 3, no conclusions can be drawn regarding linkage/exclusion.

Whereas two-point analysis involves calculating the likelihood of linkage between two polymorphic sites (usually a marker site and a mutation site), multipoint analysis involves the analyses of data from multiple loci and can be used if the genetic distance between two or more markers is known. Multipoint analysis can enhance exclusion/linkage mapping by enabling data for various markers to be analysed together. A range of computer programs are available to undertake two-point and multipoint analyses such LIPED, LINKAGE and FASTLINK (Ott, 1974; Suiter et al., 1983; Lathrop et al., 1984; Shaffer et al., 1996) and which are commonly used to map disease loci.

1.14.2. Software for linkage analysis

Software packages such as LIPED and LINKAGE use the recombination fraction to calculate lod-scores in two-point and multipoint analyses. These original programs have been updated with more efficient algorithms such as in the CRI-MAP and Vitesse packages (Lander and Green 1987; Donis-Keller et al., 1987; Green et al., 1989, Lander et al., 1987; O'Connell and Weeks, 1995), which has helped in the creation of a larger genetic linkage map than was originally possible (Donis-Keller et al., 1987; Gyapay et al., 1992; Buetow et al., 1994). The CRI-MAP program is more efficient than LINKAGE when full data (that is, all parental genotypes) are known. However, LINKAGE is more equipped at dealing with missing genotypes

(Weaver et al., 1992). Some specific software packages will be discussed below, but for a comprehensive review see (Bryant, 1996).

1.14.2.1. LIPED

LIPED is a software package which computes two-point lod-scores (Ott, 1974). While the package can process data from many different types of genetic markers including RFLPs and microsatellites, one serious disadvantage is that LIPED is able to process a maximum of five different alleles for each genetic marker. A second software program called MAP (Morton and Andrews, 1989) can combine two-point lod-score data generated by LIPED and other sources to construct a multilocus map.

1.14.2.2. LINKAGE

The LINKAGE package performs multipoint linkage analysis (Suiter et al., 1983; Lathrop et al., 1984). Genetic markers are divided into four types; RFLPs, microsatellites, dominant-recessive traits and quantitative phenotypes. LINKAGE performs best with small numbers of markers, usually up to five. MLINK is used to construct two-point lod-score tables; LODSCORE is used for estimating Θ, ILINK for multipoint maps and LINKMAP to insert markers into larger multipoint maps. However, it may be more practical to use MAPMAKER or CRI-MAP for large problems involving the CEPH family reference panel (reviewed in Bryant, 1996). Sex-specific maps can be generated.

1.14.2.3. CRI-MAP and MAPMAKER

CRI-MAP (Donis-Keller et al., 1987; Green et al., 1989) presents an efficient method for calculating likelihood's and is used in constructing very large multilocus linkage maps. It is specifically adept at mapping disease loci where affected carriers are disallowed and full penetrance is assumed.

MAPMAKER is a software package for constructing large multipoint maps from nuclear CEPH-style families and F2 crosses (Lander et al., 1987). However, it is not a general-purpose linkage package and cannot be used for disease mapping. Nor can it be applied to extended pedigrees. MAPMAKER is relatively slow to run, for it is possible to construct files for use in batch or background jobs

1.14.3. Polymorphic markers

As previously mentioned, linkage analysis is based on the occurrence of recombination events between a locus of interest, often a disease locus, and a

polymorphic genetic marker. One of the first markers to be utilised in linkage studies were protein markers such as the ABO blood groups and the Rhesus factor (Bradley et al., 1989). One of the first types of genetic marker to be identified was the restriction fragment length polymorphism (RFLP) (Botstein et al., 1980). With this discovery, the first crude genetic maps were generated (Donis-Keller et al., 1987). However, RFLP analysis has 3 important restrictions. Firstly, there may not be an RFLP in a relevant genetic region. Secondly, an RFLP may not be highly polymorphic, frequently being di-allelic. Finally, the analysis of RFLPs was initially very labor intensive as it involved Southern blotting. However, the advent of PCR (see below) technology in many cases circumvented this third restriction.

Subsequently, two types of highly informative polymorphic markers were discovered which have greatly enhanced linkage analysis. Both types of marker are highly polymorphic and composed of variable numbers of tandem repeats. The first is the minisatellite, which is composed of a variable number of 33bp repeat units (Jeffreys et al., 1985). The second and most useful marker for linkage analysis is the microsatellite (see below). Microsatellites can be amplified using polymerase chain reaction (PCR) and amplified products run and separated on polyacrylamide gels to differentiate between different alleles.

1.14.3.1. Microsatellites

Microsatellites consist of very short units, which, like VNTRs and minisatellites, are repeated in tandem. The units usually comprise of mono-, di-, tri- and tetra-nucleotide repeats sequences. The most common include A, AC, AAAN, AAN or AG in decreasing order of abundance (Hearne et al., 1992). The units can be repeated as such, can be interrupted with other sequence, or can appear as a combination of two types of repeat unit. Their potential as a tool in linkage analysis was discovered by Weber and May (1989) and Lit and Luty (1989) when they reported that the repeats varied in length between individuals and readily could be analysed using PCR, as most microsatellites can be amplified in less than 300 bp fragments. Large numbers of microsatellites have been characterised in the human genome. New microsatellites can be readily detected by hybridising genomic clones with oligonucleotide probes. Thus human linkage maps now mostly comprise of microsatellite markers which have been typed through reference families such as the CEPH (Centre d'Etude du Polymorphisme Humaine) reference families. Notably, microsatellites have now been characterised in huge abundance; at approximately 1cM (1 million base) intervals (Dib et al., 1996; Gyapay et al., 1994;

Collins et al., 1996) in the human genome, making linkage analysis a very efficient means of discovering the location of disease loci. The localisation of a Mendelian disorder, given the appropriate pedigrees are available, is now a relatively straightforward process. The high-resolution human linkage maps currently being generated will be extremely valuable in the future localisation of genes involved in frequent polygenic disorders using approaches such as sub-pair analysis.

1.15. Summary

In summary this Ph.D. thesis contains work on varying aspects of human genetics, leading, ultimately, towards the generation of gene therapies for disorders such as RP and OI. Chapter 2 describes the localisation of a mutation in a novel gene (MTTS2) causing mitochondrial deafness and RP. The study highlights again the heterogeneous nature of human inherited retinal degenerations. In chapter 3 the immense problem of allelic heterogeneity which is inherent in many dominant negative disorders, including RP and OI is addressed. Three novel methods of gene silencing, which are mutation-independent, were tested *in vitro*. A total of twelve hammerhead ribozymes were designed and tested for cleavage efficiency of rhodopsin, peripherin/*RDS* and the two type I collagen transcripts. In chapter 4 the most efficient ribozyme, Rzpol1a1, which targets a common polymorphic site in the COL1A1 transcript was characterised in depth using classic Michaelis-Menten enzyme kinetics. Additionally, the frequency of the polymorphism targeted by Rzpol1a1 was evaluated. Rzpol1a1 was subsequently, in chapter 5, considered for use *in vivo*. An MLV viral construct was generated with Rzpol1a1 driven by a CMV promoter. This construct will be utilised in future work for the generation of an MLV virus, which will be tested both in cell culture and in the COL1A1 minigene mouse model for OI. Prior to the generation of the MLV construct, a fibroblast cell line, known to be heterozygous for the COL1A1 polymorphism was infected with an MLV virus carrying a LacZ reporter gene and was determined to be susceptible to MLV infection. Rzpol1a1 was also generated with protected nucleotides (2'-aminopyrimidines) in an attempt to generate a nuclease resistant ribozyme, which in principle should remain intact in cells for a longer period than unprotected ribozyme. Notably, Rzpol1a1 remained intact in the presence of nucleases for at least 30 minutes while still maintaining its ability to cleave the COL1A1 transcript. The study described in the Ph.D. thesis contributes to the growing knowledge that is available on the etiologies of inherited retinopathies and

moreover explores novel therapeutic approaches for the dominantly inherited forms of human retinopathies such as RP and bone disorders such as OI.

1.16. Bibliography

Actis LA, Tolmasky ME, Crosa JH. Bacterial plasmids: replication of extrachromosomal genetic elements encoding resistance to antimicrobial compounds. Front Biosci. 1999 Jan 1;4:D43-62.

Aiba H, Matsuyama S, Mizuno T, Mizushima S. Function of micF as an antisense RNA in osmoregulatory expression of the ompF gene in Escherichia coli. J Bacteriol. 1987 Jul;169(7):3007-12.

Ali RR, Reichel MB, Kanuga N, Munro PM, Alexander RA, Clarke AR, Luthert PJ, Bhattacharya SS, Hunt DM. Absence of p53 delays apoptotic photoreceptor cell death in the rds mouse. Curr Eye Res. 1998 Sep;17(9):917-23.

Ali RR, Reichel MB, Thrasher AJ, Levinsky RJ, Kinnon C, Kanuga N, Hunt DM, Bhattacharya SS. Gene transfer into the mouse retina mediated by an adeno-associated viral vector. Hum Mol Genet. 1996 May;5(5):591-4.

Alvarez RD, Curiel DT. A phase I study of recombinant adenovirus vector-mediated intraperitoneal delivery of herpes simplex virus thymidine kinase (HSV-TK) gene and intravenous ganciclovir for previously treated ovarian and extraovarian cancer patients. Hum Gene Ther. 1997 Mar 20;8(5):597-613.

Amontov S, Nishikawa S, Taira K. Dependence on Mg2+ ions of the activities of dimeric hammerhead minizymes. FEBS Lett. 1996 May 20; 386(2-3): 99-102.

Arlett CF, Green MH, Priestley A, Harcourt SA, Mayne LV. Comparative human cellular radiosensitivity: I. The effect of SV40 transformation and immortalisation on the gamma-irradiation survival of skin derived fibroblasts from normal individuals and from ataxia-telangiectasia patients and heterozygotes. Int J Radiat Biol. 1988 Dec 1; 54(6): 911-928.

Banga AK, Bose S, Ghosh TK. Iontophoresis and electroporation: comparisons and contrasts. Int J Pharm. 1999 Mar 1;179(1):1-19.

Barabas, A. P. Ehlers-Danlos syndrome associated with prematurity and premature rupture of foetal membranes. Brit. Med. J. 1966 2: 682-684.

Bauer G, Valdez P, Kearns K, Bahner I, Wen SF, Zaia JA, Kohn DB. Inhibition of human immunodeficiency virus-1 (HIV-1) replication after transduction of granulocyte

colony-stimulating factor-mobilized CD34+ cells from HIV-1-infected donors using retroviral vectors containing anti-HIV-1 genes. Blood. 1997 Apr 1; 89(7): 2259-2267.

Behar-Cohen FF, Parel JM, Pouliquen Y, Thillaye-Goldenberg B, Goureau O, Heydolph S, Courtois Y, De Kozak Y. Iontophoresis of dexamethasone in the treatment of endotoxin-induced-uveitis in rats. Exp Eye Res. 1997 Oct;65(4):533-45.

Belikova AM, Zarytova VF, Grineva NI. Synthesis of ribonucleosides and diribonucleoside phosphates containing 2-chloroethylamine and nitrogen mustard residues. Tetrahedron Lett. 1967 Sep 1; 37: 3557-3562.

Bennett J, Duan D, Engelhardt JF, Maguire AM. Real-time, noninvasive in vivo assessment of adeno-associated virus-mediated retinal transduction. Invest Ophthalmol Vis Sci. 1997 Dec;38(13):2857-63.

Bennett J, Tanabe T, Sun D, Zeng Y, Kjeldbye H, Gouras P, Maguire AM. Photoreceptor cell rescue in retinal degeneration (rd) mice by in vivo gene therapy. Nat Med. 1996 Jun;2(6):649-54.

Bennett J, Wilson J, Sun D, Forbes B, Maguire A. Adenovirus vector-mediated in vivo gene transfer into adult murine retina. Invest Ophthalmol Vis Sci. 1994 Apr;35(5):2535-42.

Berson EL, Rosner B, Sandberg MA, Dryja TP . Ocular findings in patients with autosomal dominant retinitis pigmentosa and a rhodopsin gene defect (Pro-23-His). Arch Ophthalmol. 1991 Jan;109(1):92-101.

Berzal-Herranz A, Joseph S, Chowrira BM, Butcher SE, Burke JM Essential nucleotide sequences and secondary structure elements of the hairpin ribozyme. EMBO J. 1993 Jun 1; 12(6): 2567-2573.

Bhattacharya SS, Wright AF, Clayton JF, Price WH, Phillips CI, McKeown CM, Jay M, Bird AC, Pearson PL, Southern EM, et al., Close genetic linkage between X-linked retinitis pigmentosa and a restriction fragment length polymorphism identified by recombinant DNA probe L1.28. Nature. 1984 May 17; 309(5965): 253-255.

Blaese RM, Culver KW, Miller AD, Carter CS, Fleisher T, Clerici M, Shearer G, Chang L, Chiang Y, Tolstoshev P, et al. T lymphocyte-directed gene therapy for ADA- SCID: initial trial results after 4 years. Science. 1995 Oct 20; 270(5235): 475-480.

Bogenmann E, Lochrie MA, Simon MI. Cone cell-specific genes expressed in retinoblastoma. Science. 1988 Apr 1; 240(4848): 76-78.

Bonadio WA, Wagner V. Transgenic mouse model of the mild dominant form of osteogenesis imperfecta. Proc Natl Acad Sci U S A. 1990 Sep 1; 87(18): 7145-7149.

Bonini C, Ferrari G, Verzeletti S, Servida P, Zappone E, Ruggieri L, Ponzoni M,

Bordignon C, Notarangelo LD, Nobili N, Ferrari G, Casorati G, Panina P, Mazzolari E, Maggioni D, Rossi C, Servida P, et al. Gene therapy in peripheral blood lymphocytes and bone marrow for ADA- immunodeficient patients. Science. 1995

Borras T, Tamm ER, Zigler JS Jr. Ocular adenovirus gene transfer varies in efficiency and inflammatory response. Invest Ophthalmol Vis Sci. 1996 Jun;37(7):1282-93.

Botstein D, White RL, Skolnick M, Davis RW. Construction of a genetic linkage map in man using restriction fragment length polymorphisms. Am J Hum Genet. 1980 May 1; 32(3): 314-331.

Branch AD, Robertson HD. Efficient trans cleavage and a common structural motif for the ribozymes of the human hepatitis delta agent. Proc Natl Acad Sci U S A. 1991 Nov 15;88(22):10163-7.

Bradley DG, Farrar GJ, Sharp EM, Kenna P, Humphries MM, McConnell DJ, Daiger SP, McWilliam P, Humphries P. Autosomal dominant retinitis pigmentosa: exclusion of the gene from the short arm of chromosome 1 including the region surrounding the rhesus locus. Am J Hum Genet. 1989 Apr;44(4):570-6.

Bryant SP. Software for genetic linkage analysis: an update. Mol Biotechnol. 1996 Feb;5(1):49-61.

Buetow KH, Weber JL, Ludwigsen S, Scherpbier-Heddema T, Duyk GM, Sheffield VC, Wang Z, Murray JC. Integrated human genome-wide maps constructed using the CEPH reference panel. Nat Genet. 1994 Apr;6(4):391-3.

Kramm CM, Chase M, Herrlinger U, Jacobs A, Pechan PA, Rainov NG, Sena-Esteves M, Aghi M, Barnett FH, Chiocca EA, Breakefield XO. Therapeutic efficiency and safety of a second-generation replication-conditional HSV1 vector for brain tumor gene therapy. Hum Gene Ther. 1997 Nov 20;8(17):2057-68.

Bunker CH, Berson EL, Bromley WC, Hayes RP, Roderick TH. Prevalence of retinitis pigmentosa in Maine. Am J Ophthalmol. 1984 Mar 1; 97(3): 357-365.

Byers PH, Duvic M, Atkinson M, Robinow M, Smith LT, Krane SM, Greally MT, Ludman M, Matalon R, Pauker S, Quanbeck D, Schwarze U. Ehlers-Danlos syndrome type VIIA and VIIB result from splice-junction mutations or genomic deletions that involve exon 6 in the COL1A1 and COL1A2 genes of type I collagen. Am J Med Genet. 1997 Oct 3;72(1):94-105.

Byers PH. Brittle bones--fragile molecules: disorders of collagen gene structure and expression. Trends Genet. 1990 Sep 1; 6(9): 293-300.

Byers PH. Inherited disorders of collagen gene structure and expression. Am J Med Genet. 1989 Sep 1; 34(1): 72-80.

Byers PH. Second international symposium on the Marfan syndrome. Hum Mutat. 1993 Jan 1; 2(2): 80-81.

Campbell TB, McDonald CK, Hagen M. The effect of structure in a long target RNA on ribozyme cleabage efficiency. Nucleic Acids Res. 1997 Dec 11; 25(24): 4985-4993.

Cayouette M, Behn D, Sendtner M, Lachapelle P, Gravel C. Intraocular gene transfer of ciliary neurotrophic factor prevents death and increases responsiveness of rod photoreceptors in the retinal degeneration slow mouse. J Neurosci. 1998 Nov 15;18(22):9282-93.

Cech TR, Herschlag D, Piccirilli JA, Pyle AM. RNA catalysis by a group I ribozyme. Developing a model for transition state stabilization. J Biol Chem. 1992 Sep 5; 267(25): 17479-17482.

Cech TR. Structure and mechanism of the large catalytic RNA2: group I and group II and ribonuclease P, in the RNA World 1993 (Gestland RF. And Atkins JF. Eds.), Cold Spring Harbor Laboratory Press. Plainview, NY, 239-269.

Ch'ng JL, Mulligan RC, Schimmel P and Holmes EW. Antisense RNA comprlmintary to 3' coding and soncoding siwuences of creatine kinase is a potent inhubitor of translation in vivo. Proc. Natl. Acad. Sci. USA. 1989; 86: 10006-10010.

Chaib H, Kaplan J, Gerber S, Vincent C, Ayadi H, Slim R, Munnich A, Weissenbach J, Petit C. A newly identified locus for Usher syndrome type I, USH1E, maps to chromosome 21q21. Hum Mol Genet. 1997 Jan 1; 6(1): 27-31.

Chan PP, Glazer PM. Triplex DNA: fundamentals, advances, and potential applications for gene therapy. J Mol Med. 1997 Apr;75(4):267-82.

Chang GQ, Hao Y, Wong F. Apoptosis: final common pathway of photoreceptor death in rd, rds, and rhodopsin mutant mice. Neuron. 1993 Oct;11(4):595-605.

Chen CJ, Banerjea AC, Harmison GG, Haglund K, Schubert M. Multitarget-ribozyme directed to cleave at up to nine highly conserved HIV-1 env RNA regions inhibits HIV-1 replication – potential effectiveness against most presently sequenced HIV-1 isolates. Nucleic Acids Res. 1992 Sep 11; 20(17): 4581-4589.

Chen J, Flannery JG, LaVail MM, Steinberg RH, Xu J, Simon MI. bcl-2 overexpression reduces apoptotic photoreceptor cell death in three different retinal degenerations. Proc Natl Acad Sci U S A. 1996 Jul 9;93(14):7042-7.

Cheng T, Peachey NS, Li S, Goto Y, Cao Y, Naash MI. The effect of peripherin/RDS haploinsufficiency on rod and cone photoreceptors. J Neurosci. 1997 Nov 1; 17(21): 8118-8128.

Chong NH, Alexander RA, Waters L, Barnett KC, Bird AC, Luthert PJ. Repeated injections of a ciliary neurotrophic factor analogue leading to long-term photoreceptor survival in hereditary retinal degeneration. Invest Ophthalmol Vis Sci. 1999 May;40(6):1298-305.

Chowrira BM, Berzal-Herranz A, Burke JM. Ionic requirements for RNA binding, cleavage, and ligation by the hairpin ribozyme. Biochemistry. 1993 Feb 2; 32(4): 1088-1095.

Clarke GA, Rossant J, McInnes RR. Rom-1 is required for outer segment morphogenesis and photoreceptor viability [ARVO abstract]. Invest Ophthalmol Vis Sci 1998;39(4):S962. Abstract number 4442.

Collins A, Frezal J, Teague J, Morton NE. A metric map of humans: 23,500 loci in 850 bands. Proc Natl Acad Sci U S A. 1996 Dec 10;93(25):14771-5.

Collins FS, Patrinos A, Jordan E, Chakravarti A, Gesteland R, Walters L. New goals for the U.S. Human Genome Project: 1998-2003. Science. 1998 Oct 23;282(5389):682-9.

Courvalin P, Goussard S, Grillot-Courvalin C. Gene transfer from bacteria to mammalian cells. C R Acad Sci III. 1995 Dec;318(12):1207-12.

Crystal RG, McElvaney NG, Rosenfeld MA, Chu CS, Mastrangeli A, Hay JG, Brody SL, Jaffe HA, Eissa NT, Danel C. Administration of an adenovirus containing the human CFTR cDNA to the respiratory tract of individuals with cystic fibrosis. Nat Genet. 1994 Sep 1; 8(1): 42-51.

Crystal RG. In vivo and ex vivo gene therapy strategies to treat tumors using adenovirus gene transfer vectors. Cancer Chemother Pharmacol. 1999;43 Suppl:S90-9.

Dahm SC, Derrick WB, Uhlenbeck OC. Evidence for the role of solvated metal hydroxide in the hammerhead cleavage mechanism. Biochemistry. 1993 Dec 7; 32(48): 13040-13045.

Dahm SC, Uhlenbeck OC. Role of divalent metal ions in the hammerhead RNA cleavage reaction. Biochemistry. 1991 Oct 1; 30(39): 9464-9469.

Davidson FF, Steller H. Blocking apoptosis prevents blindness in Drosophila retinal degeneration mutants. Nature. 1998 Feb 5;391(6667):587-91.

Denman RB. Facilitator oligonucleotides increase ribozyme RNA binding to full-length RNA substrates in vitro. FEBS Lett. 1996 Mar 11;382(1-2):116-20.

Di Polo A, Farber DB. Rod photoreceptor-specific gene expression in human retinoblastoma cells. Proc Natl Acad Sci U S A. 1995 Apr 25; 92(9): 4016-4020.

Dib C, Faure S, Fizames C, Samson D, Drouot N, Vignal A, Millasseau P, Marc S, Hazan J, Seboun E, Lathrop M, Gyapay G, Morissette J, Weissenbach J. A comprehensive genetic map of the human genome based on 5,264 microsatellites. Nature. 1996 Mar 14;380(6570):152-4.

Dietrich G, Bubert A, Gentschev I, Sokolovic Z, Simm A, Catic A, Kaufmann SH, Hess J, Szalay AA, Goebel W. Delivery of antigen-encoding plasmid DNA into the cytosol of macrophages by attenuated suicide Listeria monocytogenes. Nat Biotechnol. 1998 Feb;16(2):181-5.

Donis-Keller H, Green P, Helms C, Cartinhour S, Weiffenbach B, Stephens K, Keith TP, Bowden DW, Smith DR, Lander ES, et al. A genetic linkage map of the human genome. Cell. 1987 Oct 23;51(2):319-37.

Donoso LA, Felberg NT, Augsburger JJ, Shields JA. Retinal S-antigen and retinoblastoma: a monoclonal antibody and flow cytometric study. Invest Ophthalmol Vis Sci. 1985 Apr 1; 26(4): 568-571.

Dryja TP, Hahn LB, Cowley GS, McGee TL, Berson EL. Mutation spectrum of the rhodopsin gene among patients with autosomal dominant retinitis pigmentosa. Proc Natl Acad Sci U S A. 1991 Oct 15;88(20):9370-4.

Dryja TP, Hahn LB, Kajiwara K, Berson EL. Dominant and digenic mutations in the peripherin/RDS and ROM1 genes in retinitis pigmentosa. Invest Ophthalmol Vis Sci. 1997 Sep;38(10):1972-82.

Dryja TP, McGee TL, Reichel E, Hahn LB, Cowley GS, Yandell DW, Sandberg MA, Berson EL A point mutation of the rhodopsin gene in one form of retinitis pigmentosa. Nature. 1990 Jan 25; 343(6256): 364-366.

Eagle H. 1955 Proc. Soc. Exp. Biol. Med. 1955; 89: 262.

Eagle H. and Foley GE. Cancer Res. 1958; 18: 1017.

Efrat S, Leiser M, Wu YJ, Fusco-DeMane D, Emran OA, Surana M, Jetton TL, Magnuson MA, Weir G, Fleischer N. Ribozyme-mediated attenuation of pancreatic beta-cell glucokinase expression in transgenic mice results in impaired glucose-induced insulin secretion. Proc Natl Acad Sci U S A. 1994 Mar 15;91(6):2051-5.

Erbacher P, Remy JS, Behr JP. Gene transfer with synthetic virus-like particles via the integrin-mediated endocytosis pathway. Gene Ther. 1999 Jan;6(1):138-45.

Farrar GJ, Jordan SA, Kenna P, Humphries MM, Kumar-Singh R, McWilliam P, Allamand V, Sharp E, Humphries P. Autosomal dominant retinitis pigmentosa: localization of a disease gene (RP6) to the short arm of chromosome 6. Genomics. 1991 Dec 1; 11(4): 870-874.

Farrar GJ, Kenna P, Jordan SA, Kumar-Singh R, Humphries MM, Sharp EM, Sheils DM, Humphries P. A three-base-pair deletion in the peripherin-*RDS* gene in one form of retinitis pigmentosa. Nature. 1991 Dec 12; 354(6353): 478-480.

Farrar GJ, McWilliam P, Bradley DG, Kenna P, Lawler M, Sharp EM, Humphries MM, Eiberg H, Conneally PM, Trofatter JA, et al. Autosomal dominant retinitis pigmentosa: linkage to rhodopsin and evidence for genetic heterogeneity. Genomics. 1990 Sep 1; 8(1): 35-40.

Feng M, Cabrera G, Deshane J, Scanlon KJ, Curiel DT . Neoplastic reversion accomplished by high efficiency adenoviral-mediated delivery of an anti-ras ribozyme. Cancer Res. 1995 May 15;55(10):2024-8.

Fesenko EE, Kolesnikov SS, Lyubarsky AL. Induction by cyclic GMP of cationic conductance in plasma membrane of retinal rod outer segment. Nature. 1985 Jan 24; 313(6000): 310-313.

Fink DJ, DeLuca NA, Goins WF, Glorioso JC. Gene transfer to neurons using herpes simplex virus-based vectors. Annu Rev Neurosci. 1996;19:265-87.

Fisher SK, Anderson DH, Erickson PA, Guerin CJ, Lewis GP, Linberg KA. Light and electron microscopy of vertebrate photoreceptors, in Photoreceptor cells 1993 (Hargrave PA. Editor), Academic Press INC NY, 3-36.

Flannery JG, Zolotukhin S, Vaquero MI, LaVail MM, Muzyczka N, Hauswirth WW. Efficient photoreceptor-targeted gene expression in vivo by recombinant adeno-associated virus. Proc Natl Acad Sci U S A. 1997 Jun 24;94(13):6916-21.

Flory CM, Pavco PA, Jarvis TC, Lesch ME, Wincott FE, Beigelman L, Hunt SW 3rd, Schrier DJ. Nuclease-resistant ribozymes decrease stromelysin mRNA levels in

rabbit synovium following exogenous delivery to the knee joint. Proc Natl Acad Sci U S A. 1996 Jan 23;93(2):754-8.

Foley GE. And Handler AH. Proc. Soc. Exp. Biol. Med. 1957; 94: 661.

Fong SH, Morris TA, Lee CH, Donoso LA, Fong WB. Transfection of retinoblastoma cells: localization of cis-acting elements for human interstitial retinoid-binding protein gene, in Photoreceptor cells 1993 (Hargrave PA. Editor), Academic Press INC NY, 322-330.

Fong SL, Balakier H, Canton M, Bridges CD, Gallie B. Retinoid-binding proteins in retinoblastoma tumors. Cancer Res. 1988 Mar 1; 48(5): 1124-1128.

Francke U, Ochs HD, de Martinville B, Giacalone J, Lindgren V, Disteche C, Pagon RA, Hofker MH, van Ommen GJ, Pearson PL, et al., Minor Xp21 chromosome deletion in a male associated with expression of Duchenne muscular dystrophy, chronic granulomatous disease, retinitis pigmentosa, and McLeod syndrome. Am J Hum Genet. 1985 Mar 1; 37(2): 250-267.

Frank BL. And Goodchild J. Selection of accessible sites for ribozymes on large RNA transcripts, in Ribozyme Protocols 1997 (Turner PC. Eds.), Humana Press, Totowa, New Jersey, 37-44.

Fuchs E, Coulombe PA. Of mice and men: genetic skin diseases of keratin. Cell. 1992 Jun 12; 69(6): 899-902.

Goldberg AF, Molday RS. Defective subunit assembly underlies a digenic form of retinitis pigmentosa linked to mutations in peripherin/rds and rom-1. Proc Natl Acad Sci U S A. 1996 Nov 26;93(24):13726-30.

Goldberg AF, Molday RS. Subunit composition of the peripherin/*RDS*-rom-1 disk rim complex from rod photoreceptors: hydrodynamic evidence for a tetrameric quaternary structure.. Biochemistry. 1996 May 14; 35(19): 6144-6149.

Goodchild J. Enhancement of ribozyme catalytic activity by a contiguous oligodeoxynucleotide (facilitator) and by 2'-O-methylation. Nucleic Acids Res. 1992 Sep 11;20(17):4607-12.

Gordon MK, Olsen BR. The contribution of collagenous proteins to tissue-specific matrix assemblies. Curr Opin Cell Biol. 1990 Oct;2(5):833-8.

Goula D, Remy JS, Erbacher P, Wasowicz M, Levi G, Abdallah B, Demeneix BA. Size, diffusibility and transfection performance of linear PEI/DNA complexes in the mouse central nervous system. Gene Ther. 1998 May;5(5):712-7.

Green P, Helms C, Weiffenbach B, Stephens K, Keith T, Bowden D, Smith D, Donis-Keller H. Construction of a linkage map of the human genome, and its application to mapping genetic diseases. Clin Chem. 1989 Jul;35(7 Suppl):B33-7.

Griegel S, Heise K, Kindler-Rohrborn A, Rajewsky MF. In vitro differentiation of human retinoblastoma cells into neuronal phenotypes. Differentiation. 1990 Dec 1; 45(3): 250-257.

Guerrier-Takada C, Altman S. A physical assay for and kinetic analysis of the interactions between M1 RNA and tRNA precursor substrates. Biochemistry. 1993 Jul 20; 32(28): 7152-7161.

Guo HC, De Abreu DM, Tillier ER, Saville BJ, Olive JE, Collins RA. Nucleotide sequence requirements for self-cleavage of Neurospora VS RNA. J Mol Biol. 1993 Jul 20; 232(2): 351-361.

Gyapay G, Morissette J, Vignal A, Dib C, Fizames C, Millasseau P, Marc S, Bernardi G, Lathrop M, Weissenbach J. The 1993-94 Genethon human genetic linkage map. Nat Genet. 1994 Jun;7(2 Spec No):246-339.

Hafezi F, Abegg M, Grimm C, Wenzel A, Munz K, Sturmer J, Farber DB, Reme CE. Retinal degeneration in the rd mouse in the absence of c-fos. Invest Ophthalmol Vis Sci. 1998 Nov;39(12):2239-44.

Hafezi F, Steinbach JP, Marti A, Munz K, Wang ZQ, Wagner EF, Aguzzi A, Reme CE. The absence of c-fos prevents light-induced apoptotic cell death of photoreceptors in retinal degeneration in vivo. Nat Med. 1997 Mar;3(3):346-9.

Haldane JBS. The combination of linkage values and the calculation of distances between the loci of linked factors. J Genet. 1919 8:299-309.

Hampel A, Tritz R. RNA catalytic properties of the minimum (-)sTRSV sequence. Biochemistry. 1989 Jun 13; 28(12): 4929-4933.

Haseloff J, Gerlach WL. Sequences required for self-catalysed cleavage of the satellite RNA of tobacco ringspot virus. Gene. 1989 Oct 15; 82(1): 43-52.

Hearne CM, Ghosh S, Todd JA. Microsatellites for linkage analysis of genetic traits. Trends Genet. 1992 Aug;8(8):288-94.

Heckenlively JR, Yoser SL, Friedman LH, Oversier JJ. Clinical findings and common symptoms in retinitis pigmentosa. Am J Ophthalmol. 1988 May 15; 105(5): 504-511.

Heller R, Jaroszeski MJ, Glass LF, Messina JL, Rapaport DP, DeConti RC, Fenske NA, Gilbert RA, Mir LM, Reintgen DS. Phase I/II trial for the treatment of cutaneous and subcutaneous tumors using electrochemotherapy. Cancer. 1996 Mar 1;77(5):964-71.

Hershfield MS. Adenosine deaminase deficiency: clinical expression, molecular basis, and therapy. Semin Hematol. 1998 Oct;35(4):291-8.

Hertel KJ, Herschlag D, Uhlenbeck OC. A kinetic and thermodynamic framework for the hammerhead ribozyme reaction. Biochemistry. 1994 Mar 22; 33(11): 3374-3385.

HGMD: Human gene mutation database. Online database address: http://www.uwcm.ac.uk/uwcm/mg/hgmd0.html

Hoffman LM, Maguire AM, Bennett J. Cell-mediated immune response and stability of intraocular transgene expression after adenovirus-mediated delivery. Invest Ophthalmol Vis Sci. 1997 Oct;38(11):2224-33.

Humphries MM, Mansergh FC, Kiang AS, Jordan SA, Sheils DM, Martin MJ, Farrar GJ, Kenna PF, Young MM, Humphries P. Three keratin gene mutations account for the majority of dominant simplex epidermolysis bullosa cases within the population of Ireland. Hum Mutat. 1996 Jan 1; 8(1): 57-63.

Humphries MM, Rancourt D, Farrar GJ, Kenna P, Hazel M, Bush RA, Sieving PA, Sheils DM, McNally N, Creighton P, Erven A, Boros A, Gulya K, Capecchi MR, Humphries P. Retinopathy induced in mice by targeted disruption of the rhodopsin gene. Nat Genet. 1997 Feb 1; 15(2): 216-219.

Jankowsky E, Schwenzer B. Efficient improvement of hammerhead ribozyme mediated cleavage of long substrates by oligonucleotide facilitators. Biochemistry. 1996 Dec 3;35(48):15313-21.

Jankowsky E, Schwenzer B. Oligonucleotide facilitators may inhibit or activate a hammerhead ribozyme. Nucleic Acids Res. 1996 Feb 1;24(3):423-9.

Jeffreys AJ, Wilson V, Thein SL Individual-specific 'fingerprints' of human DNA. Nature. 1985 Jul 4; 316(6023): 76-79.

Jordan SA, Farrar GJ, Kumar-Singh R, Kenna P, Humphries MM, Allamand V, Sharp EM, Humphries P. Am J Hum Genet. 1992 Mar 1; 50(3): 634-639.

Joseph RM, Li T. Overexpression of Bcl-2 or Bcl-XL transgenes and photoreceptor degeneration. Invest Ophthalmol Vis Sci. 1996 Nov;37(12):2434-46.

Kajiwara K, Hahn LB, Mukai S, Travis GH, Berson EL, Dryja TP

Mutations in the human retinal degeneration slow gene in autosomal dominant retinitis pigmentosa. Nature. 1991 Dec 12;354(6353):480-3.

Kajiwara K, Berson EL, Dryja TP. Digenic retinitis pigmentosa due to mutations at the unlinked peripherin/*RDS* and ROM1 loci. Science. 1994 Jun 10; 264(5165): 1604-1608.

Kedzierski W, Lloyd M, Birch DG, Bok D, Travis GH. Generation and analysis of transgenic mice expressing P216L-substituted *RDS*/peripherin in rod photoreceptors. Invest Ophthalmol Vis Sci. 1997 Feb 1; 38(2): 498-509.

Khillan JS, Olsen AS, Kontusaari S, Sokolov B, Prockop DJ. Transgenic mice that express a mini-gene version of the human gene for type I procollagen (COL1A1) develop a phenotype resembling a lethal form of osteogenesis imperfecta. J Biol Chem. 1991 Dec 5; 266(34): 23373-23379.

Kielty CM, Hopkinson I, Grant ME. Collagen: the collagen family: structure, assembly, and organization in the extracellular matrix. In: Connective tissue and its heritable disorders. Molecular, genetic, and medical aspects. Eds. Royce PM, Steinmann B. Wiley-Liss, New York, 1993. 103-147.

Kilpatrick MW, Phylactou LA, Godfrey M, Wu CH, Wu GY, Tsipouras P. Delivery of a hammerhead ribozyme specifically down-regulates the production of fibrillin-1 by cultured dermal fibroblasts. Hum Mol Genet. 1996 Dec;5(12):1939-44.

Klimatcheva E, Rosenblatt JD, Planelles V. Lentiviral vectors and gene therapy. Front Biosci. 1999 Jun 1;4:D481-96.

Kremer EJ, Perricaudet M. Adenovirus and adeno-associated virus mediated gene transfer. Br Med Bull. 1995 Jan;51(1):31-44.

Kruger K, Grabowski PJ, Zaug AJ, Sands J, Gottschling DE, Cech TR. Self-splicing RNA: autoexcision and autocyclization of the ribosomal RNA intervening sequence of Tetrahymena. Cell. 1982 Nov 1; 31(1): 147-157.

Kuivaniemi H, Tromp G, Prockop DJ. Genetic causes of aortic aneurysms. Unlearning at least part of what the textbooks say. J Clin Invest. 1991 Nov 1; 88(5): 1441-1444.

Kuwabara T, Amontov SV, Warashina M, Ohkawa J, Taira K. Characterization of several kinds of dimer minizyme: simultaneous cleavage at two sites in HIV-1 tat mRNA by dimer minizymes. Nucleic Acids Res. 1996 Jun 15; 24(12): 2302-2310.

Lai LW, Chan DM, Erickson RP, Hsu SJ, Lien YH. Correction of renal tubular acidosis in carbonic anhydrase II-deficient mice with gene therapy. J Clin Invest. 1998 Apr 1;101(7):1320-5.

Lai LW, Moeckel GW, Lien YH. Kidney-targeted liposome-mediated gene transfer in mice. Gene Ther. 1997 May;4(5):426-31.

Lalwani AK, Walsh BJ, Reilly PG, Muzyczka N, Mhatre AN. Development of in vivo gene therapy for hearing disorders: introduction of adeno-associated virus into the cochlea of the guinea pig. Gene Ther. 1996 Jul;3(7):588-92.

Lan N, Howrey RP, Lee SW, Smith CA, Sullenger BA. Ribozyme-mediated repair of sickle beta-globin mRNAs in erythrocyte precursors. Science. 1998 Jun 5;280(5369):1593-6.

Lander ES, Green P, Abrahamson J, Barlow A, Daly MJ, Lincoln SE, Newburg L. MAPMAKER: an interactive computer package for constructing primary genetic linkage maps of experimental and natural populations. Genomics. 1987 Oct;1(2):174-81.

Lander ES, Green P. Construction of multilocus genetic linkage maps in humans. Proc Natl Acad Sci U S A. 1987 Apr;84(8):2363-7.

Larsson S, Hotchkiss G, Andang M, Nyholm T, Inzunza J, Jansson I, Ahrlund-Richter L. Reduced beta 2-microglobulin mRNA levels in transgenic mice expressing a designed hammerhead ribozyme. Nucleic Acids Res. 1994 Jun 25;22(12):2242-8.

Lathrop GM, Lalouel JM, Julier C, Ott J. Strategies for multilocus linkage analysis in humans. Proc Natl Acad Sci U S A. 1984 Jun;81(11):3443-6.

LaVail MM. Ribozyme rescue of photoreceptor cells in a transgenic rat model of autosomal dominant retinitis pigmentosa. Nat Med. 1998 Aug;4(8):967-71.

Lehmann HW, Mundlos S, Winterpacht A, Brenner RE, Zabel B, Muller PK. Ehlers-Danlos syndrome type VII: phenotype and genotype. Arch Dermatol Res. 1994 Jan 1; 286(8): 425-428.

Lersch R, Fuchs E. Sequence and expression of a type II keratin, K5, in human epidermal cells. Mol Cell Biol. 1988 Jan 1; 8(1): 486-493.

Lewin AS, Drenser KA, Hauswirth WW, Nishikawa S, Yasumura D, Flannery JG, LaVail MM. Ribozyme rescue of photoreceptor cells in a transgenic rat model of autosomal dominant retinitis pigmentosa. Nat Med. 1998 Aug;4(8):967-71.

Lewis GP, Linberg KA, Geller SF, Guerin CJ, Fisher SK. Effects of the neurotrophin brain-derived neurotrophic factor in an experimental model of retinal detachment. Invest Ophthalmol Vis Sci. 1999 Jun;40(7):1530-44.

L'Huillier PJ, Soulier S, Stinnakre MG, Lepourry L, Davis SR, Mercier JC, Vilotte JL. Efficient and specific ribozyme-mediated reduction of bovine alpha-lactalbumin expression in double transgenic mice. Proc Natl Acad Sci U S A. 1996 Jun 25;93(13):6698-703.

Li T, Adamian M, Roof DJ, Berson EL, Dryja TP, Roessler BJ, Davidson BL. In vivo transfer of a reporter gene to the retina mediated by an adenoviral vector. Invest Ophthalmol Vis Sci. 1994 Apr;35(5):2543-9.

Li T, Snyder WK, Olsson JE, Dryja TP. Transgenic mice carrying the dominant rhodopsin mutation P347S: evidence for defective vectorial transport of rhodopsin to the outer segments. Proc Natl Acad Sci U S A. 1996 Nov 26;93(24):14176-81.

Lieber A, Kay MA. Adenovirus-mediated expression of ribozymes in mice. J Virol. 1996 May; 70(5): 3153-3158.

Liebreich, R. Abkunft aus Ehen unter Blutsverwandten als Grundvon Retinitis pigmentosa. Dtsch. Klin. 13 1861; 53.

Litt M, Luty JA. A hypervariable microsatellite revealed by in vitro amplification of a dinucleotide repeat within the cardiac muscle actin gene. Am J Hum Genet. 1989 Mar;44(3):397-401.

Macpherson JL, Ely JA, Sun LQ, Symonds GP. Ribozymes in gene therapy of HIV-1. Front Biosci. 1999 Jun 1;4:D497-505.

McFall RC, Sery TW, Makadon M. Characterization of a new continuous cell line derived from a human retinoblastoma. Cancer Res. 1977 Apr 1; 37(4): 1003-1010.

McKenna JM, Lazarus H, Foley GE. Antigenic differences among sublines of the KB cell line. Exp Cell Res. 1966 Mar 1; 41(3): 609-613.

McWilliam P, Farrar GJ, Kenna P, Bradley DG, Humphries MM, Sharp EM, McConnell DJ, Lawler M, Sheils D, Ryan C, et al. Autosomal dominant retinitis pigmentosa (ADRP): localization of an ADRP gene to the long arm of chromosome 3. Genomics. 1989 Oct 1; 5(3): 619-622.

Michaelis L, and Menten ML. Biochem. Z. 1913, 49, 333.

Mir LM, Roth C, Orlowski S, Quintin-Colonna F, Fradelizi D, Belehradek J Jr, Kourilsky P. Systemic antitumor effects of electrochemotherapy combined with histoincompatible cells secreting interleukin-2. J Immunother Emphasis Tumor Immunol. 1995 Jan;17(1):30-8.

Molday RS. Photoreceptor membrane proteins, phototransduction, and retinal degenerative diseases. The Friedenwald Lecture. Invest Ophthalmol Vis Sci. 1998 Dec;39(13):2491-513.

Moller CG, Kimberling WJ, Davenport SL, Priluck I, White V, Biscone-Halterman K, Odkvist LM, Brookhouser PE, Lund G, Grissom TJ. Usher syndrome: an otoneurologic study. Laryngoscope. 1989 Jan 1; 99(1): 73-79.

Moritz OL, Molday RS. Molecular cloning, membrane topology, and localization of bovine rom-1 in rod and cone photoreceptor cells. Invest Ophthalmol Vis Sci. 1996 Feb 1; 37(2): 352-362.

Morsy MA, Caskey CT. Expanded-capacity adenoviral vectors--the helper-dependent vectors. Mol Med Today. 1999 Jan;5(1):18-24.

Morton NE. Sequential tests for the detection of linkage. Am J Hum Genet. 1955; 7: 277-318.

Narlikar GJ, Gopalakrishnan V, McConnell TS, Usman N, Herschlag D. Use of binding energy by an RNA enzyme for catalysis by positioning and substrate destabilization. Proc Natl Acad Sci U S A. 1995 Apr 25; 92(9): 3668-3672.

Nathans J, Piantanida TP, Eddy RL, Shows TB, Hogness DS. Molecular genetics of inherited variation in human color vision. Science. 1986 Apr 11; 232(4747): 203-210.

Nathans J, Thomas D, Hogness DS. Molecular genetics of human color vision: the genes encoding blue, green, and red pigments. Science. 1986 Apr 11; 232(4747): 193-202.

Nesbitt S, Goodchild J. Further studies on the use of oligonucleotide facilitators to increase ribozyme turnover. Antisense Res Dev. 1994 Winter;4(4):243-9.

Neumann E, Schaefer-Ridder M, Wang Y, Hofschneider PH. Gene transfer into mouse lyoma cells by electroporation in high electric fields. EMBO J. 1982;1(7):841-5.

Nishi T, Yoshizato K, Yamashiro S, Takeshima H, Sato K, Hamada K, Kitamura I, Yoshimura T, Saya H, Kuratsu J, Ushio Y. High-efficiency in vivo gene transfer using intraarterial plasmid DNA injection following in vivo electroporation. Cancer Res. 1996 Mar 1;56(5):1050-5.

Nuclease-resistant ribozymes decrease stromelysin mRNA levels in rabbit synovium following exogenous delivery to the knee joint. Proc Natl Acad Sci U S A. 1996 Jan 23;93(2):754-8.

O'Connell JR, Weeks DE. The VITESSE algorithm for rapid exact multilocus linkage analysis via genotype set-recoding and fuzzy inheritance. Nat Genet. 1995 Dec;11(4):402-8.

Olsen BR. In: Cell biology of extracellular matrix. E.D. Hay, ed. Plenium Publishing Corp. in press 1991.

Olsson JE, Gordon JW, Pawlyk BS, Roof D, Hayes A, Molday RS, Mukai S, Cowley GS, Berson EL, Dryja TP. Transgenic mice with a rhodopsin mutation (Pro23His): a mouse model of autosomal dominant retinitis pigmentosa. Neuron. 1992 Nov 1; 9(5): 815-830.

Oprian DD. Expression of opsin genes in COS cells, in Photoreceptor cells 1993 (Hargrave PA. Editor), Academic Press INC NY, 301-306.

Ott J. Estimation of the recombination fraction in human pedigrees: efficient computation of the likelihood for human linkage studies. Am J Hum Genet. 1974 Sep 1; 26(5): 588-597.

Pan T, Long DM. And Uhlenbeck OC. 1993. Divalent metal ions in RNA folding and catalysis, in the RNA World 1992 (Gestland RF. And Atkins JF. Eds.), Cold Spring Harbor Laboratory Press. Plainview, NY, 271-302.

Pereira R, Khillan JS, Helminen HJ, Hume EL, Prockop DJ. Transgenic mice expressing a partially deleted gene for type I procollagen (COL1A1). A breeding line with a phenotype of spontaneous fractures and decreased bone collagen and mineral. J Clin Invest. 1993 Feb 1; 91(2): 709-716.

Perrotta AT, Been MD. The self-cleaving domain from the genomic RNA of hepatitis delta virus: sequence requirements and the effects of denaturant. Nucleic Acids Res. 1990 Dec 11;18(23):6821-7.

Petters RM, Alexander CA, Wells KD, Collins EB, Sommer JR, Blanton MR, Rojas G, Hao Y, Flowers WL, Banin E, Cideciyan AV, Jacobson SG, Wong F. Genetically engineered large animal model for studying cone photoreceptor survival and degeneration in retinitis pigmentosa. Nat Biotechnol. 1997 Oct; 15(10): 965-970.

Phylactou LA, Darrah C, Wood MJ. Ribozyme-mediated trans-splicing of a trinucleotide repeat. Nat Genet. 1998 Apr;18(4):378-81.

Pieke-Dahl S, van Aarem A, Dobin A, Cremers CW, Kimberling WJ. Genetic heterogeneity of Usher syndrome type II in a Dutch population. J Med Genet. 1996 Sep;33(9):753-7.

Pittenger MF, Mackay AM, Beck SC, Jaiswal RK, Douglas R, Mosca JD, Moorman MA, Simonetti DW, Craig S, Marshak DR. Multilineage potential of adult human mesenchymal stem cells. Science. 1999 Apr 2; 284(5411):143-7.

Pley HW, Flaherty KM, McKay DB. Three-dimensional structure of a hammerhead ribozyme. Nature. 1994 Nov 3; 372(6501): 68-74.

Portera-Cailliau C, Sung CH, Nathans J, Adler R. Apoptotic photoreceptor cell death in mouse models of retinitis pigmentosa. Proc Natl Acad Sci U S A. 1994 Feb 1;91(3):974-8.

Prockop DJ, Kuivaniemi H, Tromp G. Molecular basis of osteogenesis imperfecta and related disorders of bone. Clin Plast Surg. 1994 Jul 1; 21(3): 407-413.

Prody GA, Bakos JT, Buzayan JM, Schneider IR, and Bruening G. Autolytic processing of dimeric plant virus satellite RNA. Science 321: 1577-1580.

Qin L, Pahud DR, Ding Y, Bielinska AU, Kukowska-Latallo JF, Baker JR Jr, Bromberg JS. Efficient transfer of genes into murine cardiac grafts by Starburst polyamidoamine dendrimers. Hum Gene Ther. 1998 Mar 1;9(4):553-60.

Ramezani A, Ding SF, Joshi S. Inhibition of HIV-1 replication by retroviral vectors expressing monomeric and multimeric hammerhead ribozymes. Gene Ther. 1997 Aug;4(8):861-7.

Reichel MB, Ali RR, Thrasher AJ, Hunt DM, Bhattacharya SS, Baker D. Immune responses limit adenovirally mediated gene expression in the adult mouse eye. Gene Ther. 1998 Aug;5(8):1038-46.

Rich KA, Zhan Y, Blanks JC. Aberrant expression of c-Fos accompanies photoreceptor cell death in the rd mouse. J Neurobiol. 1997 Jun 5;32(6):593-612.

Roberts JC, Bhalgat MK, Zera RT. Preliminary biological evaluation of polyamidoamine (PAMAM) Starburst dendrimers. J Biomed Mater Res. 1996 Jan;30(1):53-65.

Rols MP, Delteil C, Golzio M, Dumond P, Cros S, Teissie J. In vivo electrically mediated protein and gene transfer in murine melanoma. Nat Biotechnol. 1998 Feb;16(2):168-71.

Rosenberg M, Fuchs E, Le Beau MM, Eddy RL, Shows TB. Three epidermal and one simple epithelial type II keratin genes map to human chromosome 12. Cytogenet Cell Genet. 1991 Jan 1; 57(1): 33-38.

Rosenberg M, RayChaudhury A, Shows TB, Le Beau MM, Fuchs E. A group of type I
keratin genes on human chromosome 17: characterization and expression. Mol Cell
Biol. 1988 Feb 1; 8(2): 722-736.

Rosenfeld MA, Yoshimura K, Trapnell BC, Yoneyama K, Rosenthal ER, Dalemans W,
Fukayama M, Bargon J, Stier LE, Stratford-Perricaudet L, et al. In vivo transfer of
the human cystic fibrosis transmembrane conductance regulator gene to the airway
epithelium.
Cell. 1992 Jan 10; 68(1): 143-155.

Rossini S, Mavilio F, Traversari C, Bordignon C. HSV-TK gene transfer into donor
lymphocytes for control of allogeneic graft-versus-leukemia. Science. 1997 Jun
13;276(5319):1719-24.

Ruffner DE, Stormo GD, Uhlenbeck OC. Sequence requirements of the hammerhead RNA
self-cleavage reaction. Biochemistry. 1990 Nov 27;29(47):10695-702.

Saenger W. Principles of Nucleic Acid Structure. Springer-Verslag, 1984, NY, 108.

Sankila EM, Pakarinen L, Kaariainen H, Aittomaki K, Karjalainen S, Sistonen P, de la
Chapelle A. Assignment of an Usher syndrome type III (USH3) gene to chromosome
3q. Hum Mol Genet. 1995 Jan 1; 4(1): 93-98.

Saville BJ, Collins RA . A site-specific self-cleavage reaction performed by a novel RNA in
Neurospora mitochondria. Cell. 1990 May 18;61(4):685-96.

Schaffer AA. Faster linkage analysis computations for pedigrees with loops or unused
alleles. Hum Hered. 1996 Jul-Aug;46(4):226-35.

Scherr M, Grez M, Ganser A, Engels JW . Specific hammerhead ribozyme-mediated
cleavage of mutant N-ras mRNA in vitro and ex vivo. Oligoribonucleotides as
therapeutic agents. J Biol Chem. 1997 May 30;272(22):14304-13.

Schwartz B, Ivanov MA, Pitard B, Escriou V, Rangara R, Byk G, Wils P, Crouzet J,
Scherman D. Synthetic DNA-compacting peptides derived from human sequence
enhance cationic lipid-mediated gene transfer in vitro and in vivo. Gene Ther. 1999
Feb;6(2):282-92.

Sillence D. Osteogenesis imperfecta: an expanding panorama of variants. Clin Orthop. 1981
Sep 1; 159: 11-25.

Sillence DO, Senn A, Danks DM. Genetic heterogeneity in osteogenesis imperfecta. J Med
Genet. 1979 Apr 1; 16(2): 101-116.

Sioud M, Opstad A, Hendry P, Lockett TJ, Jennings PA, McCall MJ. A minimised hammerhead ribozyme with activity against interleukin-2 in human cells. Biochem Biophys Res Commun. 1997 Feb 13; 231(2): 397-402.

Sizemore DR, Branstrom AA, Sadoff JC. Attenuated Shigella as a DNA delivery vehicle for DNA-mediated immunization. Science. 1995 Oct 13;270(5234):299-302.

Sohier R, Chardonnet Y, Prunieras M. Adenoviruses. Status of current knowledge. Prog Med Virol. 1965;7:253-325.

Sparkes RS, Mohandas T, Newman SL, Heinzmann C, Kaufman D, Zollman S, Leveille PJ, Tobin AJ, McGinnis JF. Assignment of the rhodopsin gene to human chromosome 3. Invest Ophthalmol Vis Sci 1986 Jul;27(7): 1170-1172.

Stage-Zimmermann TK, Uhlenbeck OC. Hammerhead ribozyme kinetics. RNA. 1998 Aug;4(8):875-89.

Stryer L. Visual excitation and recovery. J Biol Chem. 1991 Jun 15; 266(17): 10711-10714.

Sugiyama H, Hatano K, Saito I, Amontov S, Taira K. Catalytic activities of hammerhead ribozymes with a triterpenoid linker instead of stem/loop II. FEBS Lett. 1996 Sep 2;392(3):215-9.

Sugiyama H, Hatano K, Saito I, Amontov S, Taira K. Catalytic activities of hammerhead ribozymes with a triterpenoid linker instead of stem/loop II. FEBS Lett. 1996 Sep 2; 392(3): 215-219.

Suiter KA, Wendel JF, Case JS. LINKAGE-1: a PASCAL computer program for the detection and analysis of genetic linkage. J Hered. 1983 May-Jun;74(3):203-4.

Sung CH, Makino C, Baylor D, Nathans J. A rhodopsin gene mutation responsible for autosomal dominant retinitis pigmentosa results in a protein that is defective in localization to the photoreceptor outer segment. J Neurosci. 1994 Oct;14(10):5818-33.

Takayama KM, Inouye M. Antisense RNA. Crit Rev Biochem Mol Biol. 1990 Jan 1; 25(3): 155-184.

Taylor AM, Harnden DG, Arlett CF, Harcourt SA, Lehmann AR, Stevens S, Bridges BA. Ataxia telangiectasia: a human mutation with abnormal radiation sensitivity. Nature. 1975 Dec 4; 258(5534): 427-429.

Teissie J, Rols MP. An experimental evaluation of the critical potential difference inducing cell membrane electropermeabilization. Biophys J. 1993 Jul;65(1):409-13.

Terwilliger JD, Ott J. A novel polylocus method for linkage analysis using the lod-score or affected sib-pair method. Genet Epidemiol. 1993;10(6):477-82.

Timchenko LT, Caskey CT. Trinucleotide repeat disorders in humans: discussions of mechanisms and medical issues. FASEB J. 1996 Dec;10(14):1589-97.

Titomirov AV, Sukharev S, Kistanova E. In vivo electroporation and stable transformation of skin cells of newborn mice by plasmid DNA. Biochim Biophys Acta. 1991 Jan 17;1088(1):131-4.

Toulme J-J. Artificial regulation of gene expression by complementary oligonucleotides-an overview, in AntisenseRNA and DNA 1992 (Murray JAM. Editor), Wiley-Liss INC. NY, 175-194.

Uhlenbeck OC. RNA binding site of R17 coat protein. Biochemistry. 1987 Mar 24; 26(6): 1563-1568.

Uhlmann E. Peptide nucleic acids (PNA) and PNA-DNA chimeras: from high binding affinity towa*RDS* biological function. Biol Chem. 1998 Aug-Sep;379(8-9):1045-52.

Urdea MS, Horn T. Dendrimer development. Science. 1993 Jul 30;261(5121):534.

Usher CR (1914) On the inheritance of retinitis pigmentosa with notes of cases. Lond Ophthal Hosp Rep 19:130-236.

van Nie R, Ivanyi D, Demant P. A new H-2-linked mutation, *RDS*, causing retinal degeneration in the mouse. Tissue Antigens. 1978 Aug 1; 12(2): 106-108.

Van West P, Kamoun S, van 't Klooster JW, Govers F. Internuclear gene silencing in Phytophthora infestans. Mol Cell. 1999 Mar;3(3):339-48.

Vassar R, Coulombe PA, Degenstein L, Albers K, Fuchs E. Mutant keratin expression in transgenic mice causes marked abnormalities resembling a human genetic skin disease. Cell. 1991 Jan 25; 64(2): 365-380.

Von Graefe, A. Exceptionelles Verhalten des Gesichtsfeldes bei Pigmententartung der Netzhaut. Graefes Arch. Ophthal. 4 1858; 250-253.

von Weizsacker F, Blum HE, Wands JR. Cleavage of hepatitis B virus RNA by three ribozymes transcribed from a single DNA template. Biochem Biophys Res Commun. 1992 Dec 15; 189(2): 743-748.

Vrolik W. Tabulae ad illustrandam embryogenesis hominis et mammalium, tam narutalem quam abnormem. Amsterdam 1849.

Washburn T, O'Tousa JE. Molecular defects in Drosophila rhodopsin mutants. J Biol Chem. 1989 Sep 15;264(26):15464-6.

Wayne S, Der Kaloustian VM, Schloss M, Polomeno R, Scott DA, Hejtmancik JF, Sheffield VC, Smith RJ. Localization of the Usher syndrome type ID gene (Ush1D) to chromosome 10. Hum Mol Genet. 1996 Oct 1; 5(10): 1689-1692.

Wayne, S.; Lowry, R. B.; McLeod, D. R.; Knaus, R.; Farr, C.; Smith,R. J. H. Localization of the Usher syndrome type IF (Ush1F) to chromosome10. Am. J. Hum. Genet. 61 (suppl.) 1997; A300.

Weaver R, Helms C, Mishra SK, Donis-Keller H. Software for analysis and manipulation of genetic linkage data. Am J Hum Genet. 1992 Jun;50(6):1267-74.

Weil D, Blanchard S, Kaplan J, Guilford P, Gibson F, Walsh J, Mburu P, Varela A, Levilliers J, Weston MD, et al. Defective myosin VIIA gene responsible for Usher syndrome type 1B. Nature. 1995 Mar 2; 374(6517): 60-61.

Weiss ER, Hao Y, Dickerson CD, Osawa S, Shi W, Zhang L, Wong F. Altered cAMP levels in retinas from transgenic mice expressing a rhodopsin mutant. Biochem Biophys Res Commun. 1995 Nov 22;216(3):755-61.

Welch PJ, Yei S, Barber JR. Ribozyme gene therapy for hepatitis C virus infection. Clin Diagn Virol. 1998 Jul 15;10(2-3):163-71.

Wenstrup RJ, Willing MC, Starman BJ, Byers PH. Distinct biochemical phenotypes predict clinical severity in nonlethal variants of osteogenesis imperfecta. Am J Hum Genet. 1990 May 1; 46(5): 975-982.

Whiteley SJO, Sauve Y, Aviles-Trigueros M, Vidal-Sanz M, Lund RD. Extent and duration of recovered pupillary light reflex following retinal ganglion cell axon regeneration through peripheral nerve grafts directed to the pretectum in adult rats. Exp Neurol. 1998 Dec;154(2):560-72.

Willing MC, Deschenes SP, Scott DA, Byers PH, Slayton RL, Pitts SH, Arikat H, Roberts EJ. Osteogenesis imperfecta type I: molecular heterogeneity for COL1A1 null alleles of type I collagen. Am J Hum Genet. 1994 Oct;55(4):638-47.

Wilson JM, Grossman M, Raper SE, Baker JR Jr, Newton RS, Thoene JG . Ex vivo gene therapy of familial hypercholesterolemia. Hum Gene Ther. 1992 Apr;3(2):179-222.

Wolfert MA, Schacht EH, Toncheva V, Ulbrich K, Nazarova O, Seymour LW. Characterization of vectors for gene therapy formed by self-assembly of DNA with synthetic block co-polymers. Hum Gene Ther. 1996 Nov 10;7(17):2123-33.

Wong-Staal F, Poeschla EM, Looney DJ . A controlled, Phase 1 clinical trial to evaluate the safety and effects in HIV-1 infected humans of autologous lymphocytes transduced with a ribozyme that cleaves HIV-1 RNA. Hum Gene Ther. 1998 Nov 1;9(16):2407-25.

Wright AF. A searchlight through the fog. Nat Genet. 1997 Oct; 17(2): 132-134.

Wu HN, Lai MM Reversible cleavage and ligation of hepatitis delta virus RNA. Science. 1989 Feb 3; 243(4891): 652-654.

Xie Y, Chen X, Wagner TE. A ribozyme-mediated, gene "knockdown" strategy for the identification of gene function in zebrafish. Proc Natl Acad Sci U S A. 1997 Dec 9;94(25):13777-81.

Yoon SS, Carroll NM, Chiocca EA, Tanabe KK. Cancer gene therapy using a replication-competent herpes simplex virus type 1 vector. Ann Surg. 1998 Sep;228(3):366-74.

Yu Q. and Burke JM. Design of hairpin ribozymes for in vitro and cellular applications, in Ribozyme Protocols 1997 (Turner PC. Eds.), Humana Press, Totowa, New Jersey, 161-169.

Zabner J, Fasbender AJ, Moninger T, Poellinger KA, Welsh MJ. Cellular and molecular barriers to gene transfer by a cationic lipid. J Biol Chem. 1995 Aug 11;270(32):18997-9007.

Zhao JJ, Pick L . Generating loss-of-function phenotypes of the fushi tarazu gene with a targeted ribozyme in Drosophila. Nature. 1993 Sep 30;365(6445):448-51.

Zoumadakis M, Neubert WJ, Tabler M. The influence of imperfectly paired helices I and III on the catalytic activity of hammerhead ribozymes. Nucleic Acids Res. 1994 Dec 11; 22(24): 5271-5278.

Zoumadakis M, Tabler M. Comparative analysis of cleavage rates after systematic permutation of the NUX consensus target motif for hammerhead ribozymes. Nucleic Acids Res. 1995 Apr 11;23(7):1192-6.

Zucker M. Computer prediction of RNA structure. Methods Enzymol. 1989 Jan 1; 180: 262-288.

Figure 1.

Substrate

Stem 1

5' N N N N N N N *N U X* N N N N N N N N N   3'

3' N N N N N N N N **A**   N N N N N N N N N   5'

Stem 3

C

A

U

A   G

A

G   N

G

G   A

Ribozyme

Y — R

N — N

Stem 2   N — N

N — N
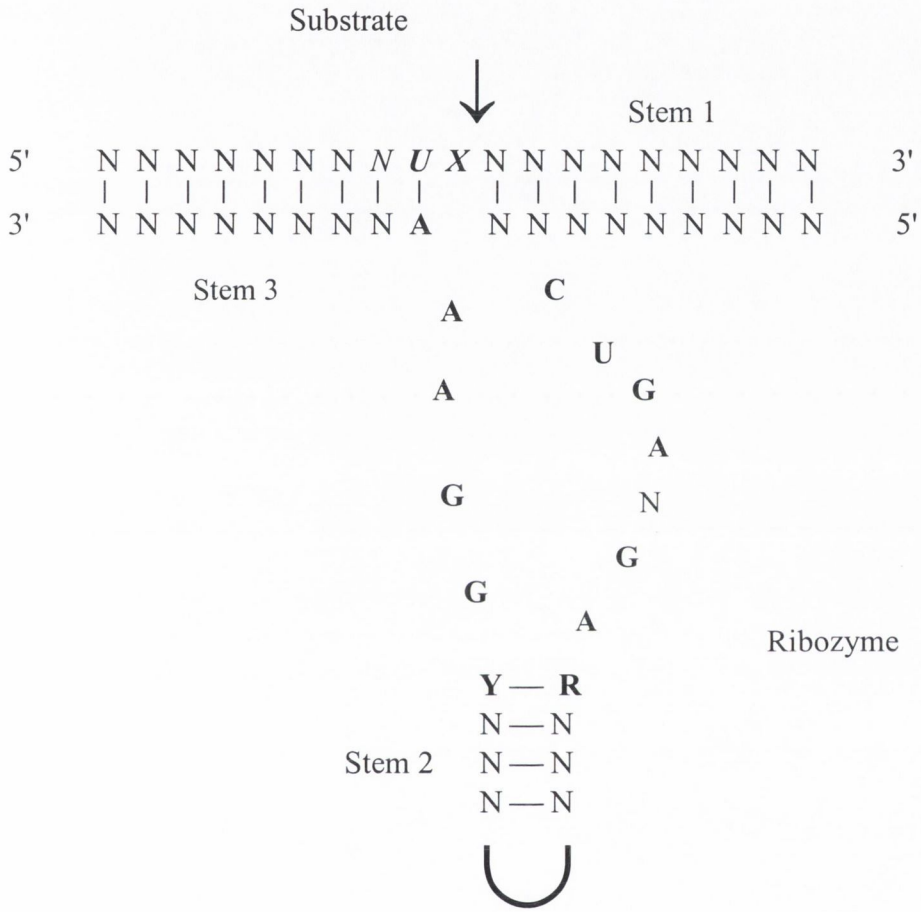
Figure 1. Hammerhead ribozyme. Hammerhead ribozymes consist of two antisense arms (stems 1 and 3) with which they bind a complementary substrate. Conserved nucleotides are shown in bold. Dashes indicate Watson-Crick base pairs. N represents any nucleotide. X represents the nucleotides C, U or A. Y represents a pyrimidine and R a purine. The arrow indicates the cleavage site in the target RNA, just after the NUX site (in italic). Stems 1-3 may be of variable length.

Figure 2.
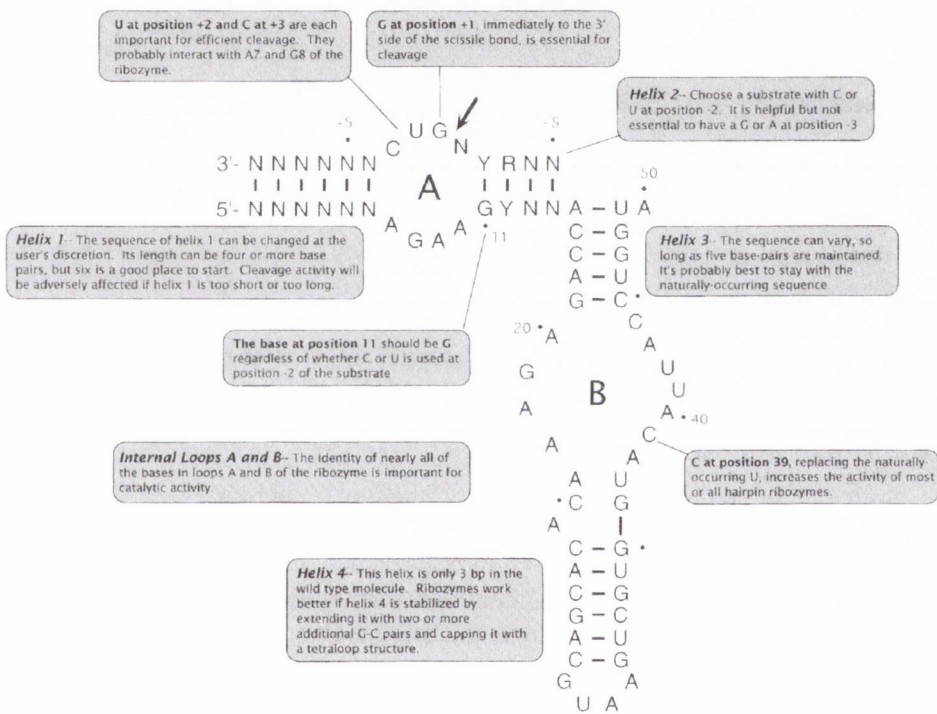
Figure 2. How to design a hairpin ribozyme. The arrow indicates the substrate GUC cleavage site and dashes indicate Watson-Crick base pairs. N is any base, R is G or A and Y is C or U (Yu and Burke, 1997). The texts within the grey boxes explain which sites within the ribozyme are necessary for retaining high catalytic activity. Copied from Yu and Burke (1997).

Figure 3.

A   B   C   D
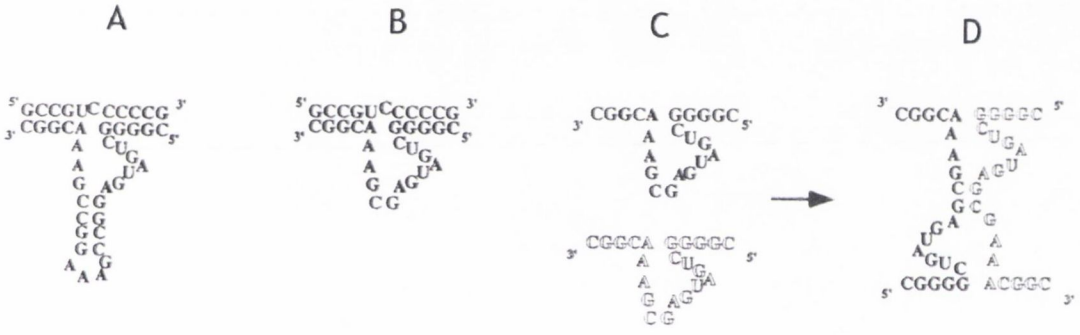
Figure 3. Structure of a hammerhead ribozyme (*A*), a minimised hammerhead ribozyme or minizyme (*B*), two minizymes designed to target the same sequence (*C*) and a minizyme dimer (*D*). For clarity the two minizymes are represented in a different font. In theory minizymes need not be identical to form dimers (Sugiyama et al., 1996; Kuwabara et al., 1996). Figure adapted from Amontov et al., 1996.

Figure 4.

A
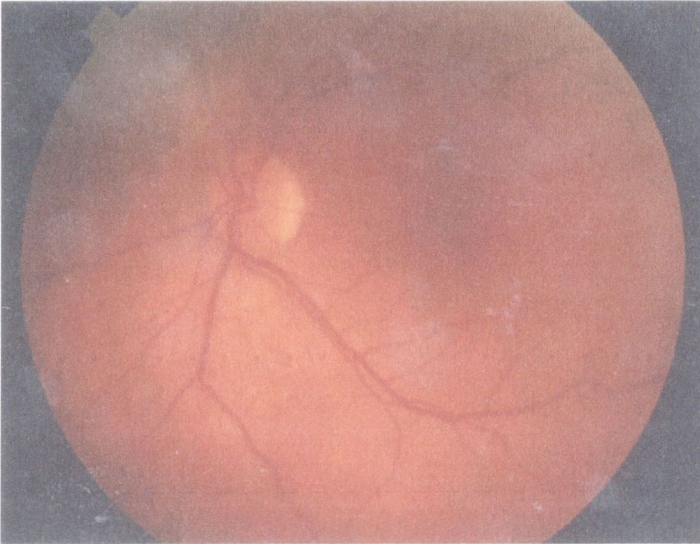
B
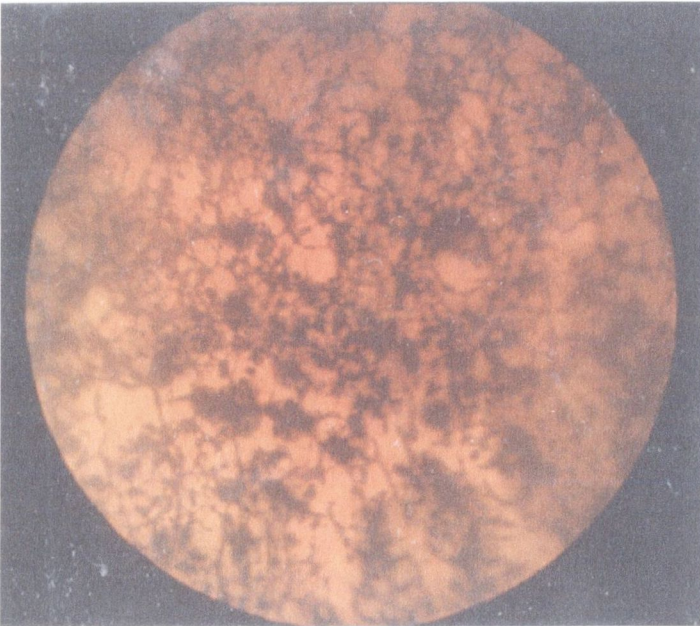
Figure 4. *A*, Fundus photograph of a retina from a healthy individual. Note the healthy pink optic disc and normal retinal blood vessels. *B*, Retina from a patient suffering from RP. Note the characteristic pigmentary depositions in the classical 'bone spicule' configuration. Neither the waxy pallor of the optic disc nor the attenuated blood vessels can be seen on this picture. Photos were kindly provided by Dr. Paul F. Kenna.

Figure 5.

Rod outer segment plasma membrane

Disks

Rim region of disks

Cytoplasmic (interdiskal) space

Intradiskal space

Connecting cilium

Mitochondria

Golgi complex

Endoplasmic reticulum

Nucleus

Synaptic vesicles

Rod outer segment

Rod inner segment

Cell body

Synaptic terminal

Incisure

Disks

Plasma Membrane

Connecting Cilium
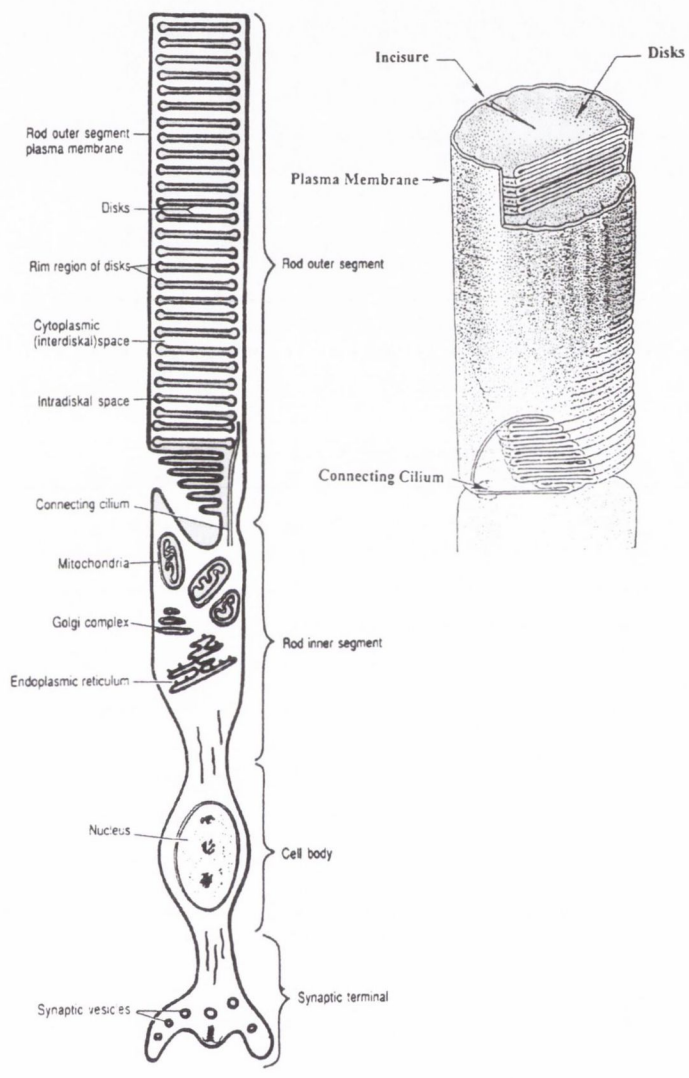
Figure 5. Diagram of a rod photoreceptor cell (Molday, 1998). The four regions of a photoreceptor cell, mentioned in the text are shown: 1, Rod outer segment with the discs; 2, Rod inner segment; 3, Cell body; 4, Synaptic terminal. In mammals rod cells are about 60 μm x 15.2 μm in size. Cone photoreceptor cells are shorter and conical. Both rhodopsin and peripherin/*RDS* are localised to the outer segment membrane discs. The arrow indicated the direction from which light enters. A diagram of the rod outer segment is shown to the right.

Figure 6.

Disk Membrane   Plasma Membrane
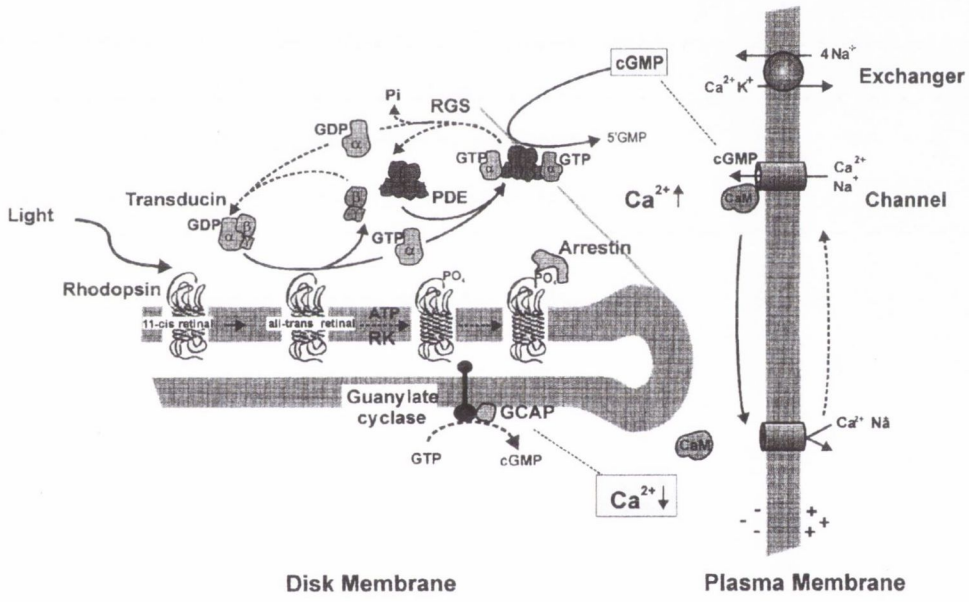
Figure 6. Diagram of the cascade of visual transduction (Molday, 1998). Light converts 11-*cis* retinal to the all-*trans* isomer of retinal resulting in the activated state of rhodopsin. Rhodopsin then catalyses the exchange of GDP for GTP on T_α. T_α subsequently interacts with PDE to release the inhibitory constraint on the enzyme. Thus PDE can catalyse the hydrolysis of cGMP to 5'GMP, which leads to a decrease in intracellular cGMP. This causes the cGMP gated channel to close and the rod cell to hyperpolarise. Intracellular Ca^{2+} levels drop as the Na/Ca-K exchanger continues to extrude Ca^{2+} from the outer segment. The shutdown of the visual cascade and the calcium mediated feedback mechanism results in photorecovery. First the phosphorylation of rhodopsin by rhodopsin kinase (RK) and the subsequent binding of arrestin occur. Then GTP gets hydrolysed to GDP on T_α and PDE returns to its inactivated state. Low intracellular Ca^{2+} concentrations lead to the activation of guanylate cyclase, and an increase in the sensitivity of the channel to cGMP as a result of the dissociation of calmodulin from the channel. As a result of the increase of cGMP the channels reopen and the cell is depolarised. In addition, the increase in Ca^{2+} converts guanylate cyclase to its normal level of activity during depolarisation. The solid arrows show the photoexcitation process and the dashed arrows show the photorecovery process (Molday, 1998).

Figure 7.

N – TERMINAL REGION   COLLAGEN FIBRIL MONOMER   C – TERMINAL REGION

15 nm   300 nm   10 nm

Pro - α1

Pro - α1

Pro - α 2

A

CLEAVAGE BY   CLEAVAGE BY
N – PROTEASE   C – PROTEASE

B
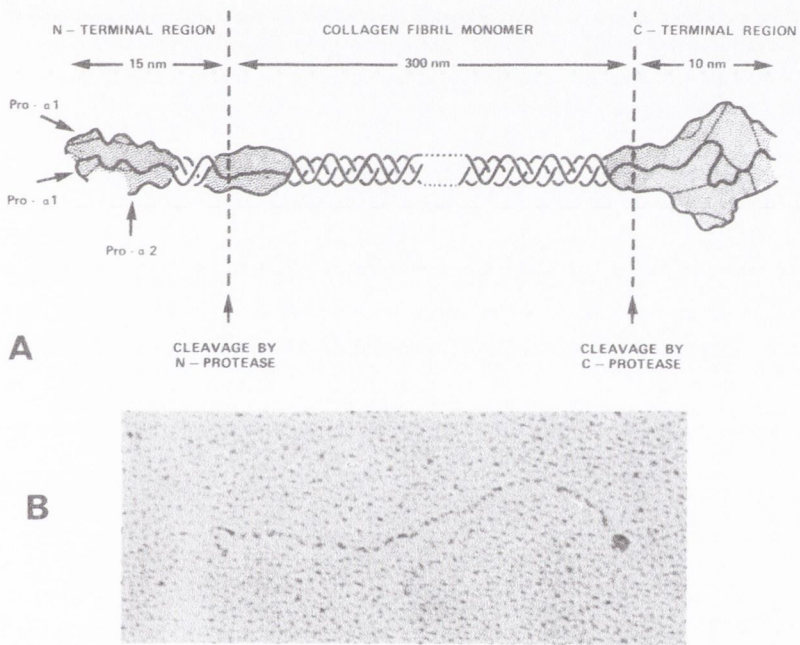
Figure 7. *A*, Diagram of a type I fibrillar pro-collagen molecule (Kielty et al., 1993). Three protein chains form stable triple-helices. These triple-helical molecules are about 300 nm rigid rod like structures with a diameter of 1.5 nm. Subsequent to post-translational modifications (hydroxilation and glycosylation) and triple-helix assembly, precursor pro-collagen molecules containing amino and carboxyl pro-peptide extensions flanking the central triple-helical domain are secreted from the cell. These extensions are removed by specific endoproteinases during extracellular processing of pro-collagen to collagen. *B*, Rotary shadowing image of type I pro-collagen. The length of the rod-like triple helix is observed and the C-terminal pro-peptide is viewed as a globular domain, while at the other end of the molecule characteristic 'hook' arrangement of the N-pro-peptide is apparent which arises as a consequence of the short helical sequence it contains (Kielty et al., 1993).

Figure 8.
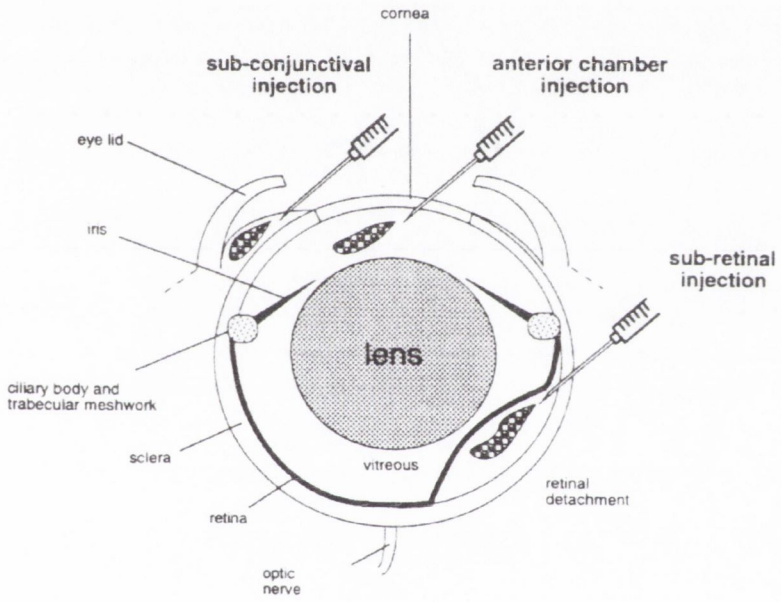
Figure 8. Schematic diagram of a mouse eye and three types of injection used for gene-delivery to mouse eyes; sub-retinal injection, anterior chamber injection and sub-conjunctival injection. Figure from Reichel et al., 1998.

Issue	Problem	Solution
Specificity	Target recognition	Length
		RNase H sensitivity
	Protein binding	Sequence
Stability	Degradation by nucleases	Phosphotriesters
		Alkylphosphorates
		α -Oligomers
		Phosphorothioates
		Phosphorodithioates
		Phosphoramidates
		2′-O-alkyl
RNase H induction	mRNA cleavage	Phosphodiester
		Phosphorothioate
Uptake	Membrane penetration	Length/charge
	Endocytosis	Hydrophobicgroups
		Polycations
		Lipoproteins
		Liposomes
Affinity	Competition with proteins	Modified bases
		Intercalating agents
		Active groups
		Modified backbone
Toxicity	Nonspecific binding	
	Mutagenicity	
	Carcinognicity	

Table 1. Various problems and solutions associated with the use of antisense RNA
(Toulme, 1992). Various methods of protection of antisense RNA are discussed in detail
in chapter 5. (table 1 is taken from "Antisense RNA and DNA" edited by Murray).

Gene symbol	locus	Protein (if known)
RP1	8q11-q13	dominant RP; protein: RP1 protein
RP2	Xp11.3	X-linked RP; protein: novel protein with similarity to human cofactor C
RP3/ RPGR	Xp21.1	X-linked RP; X-linked CSNB (possibly); protein: retinitis pigmentosa GTPase regulator
RP4/ RHO	3q21-q24	dominant RP; dominant CSNB; recessive RP; protein: rhodopsin
RP5	3q	same as RP4
RP6	Xp21.3-p21.2	X-linked RP
RP7/RDS	6p21.2-cen	dominant RP; dominant MD; digenic RP with ROM1; dominant adult vitelliform MD; protein: peripherin/RDS
RP9	7p15-p13	dominant RP
RP10	7q31.3	dominant RP
RP11	19q13.4	dominant RP
RP12	1q31-q32.1	recessive RP with para-arteriolar preservation of the RPE (PPRPE)
RP13	17p13.3	dominant RP
RP14/ TULP1	6p21.3	recessive RP; protein: tubby-like protein 1
RP15	Xp22.13-p22.11	X-linked RP, dominant
RP16	14	recessive RP (possibly)
RP17	17q22	dominant RP
RP18	1q13-q23	dominant RP
RP19	1p21-p22	recessive Stargardt disease, juvenile and late onset; recessive MD; recessive RP; recessive fundus flavimaculatus; recessive combined RP and cone-rod dystrophy; protein: ATP-binding cassette transporter - retinal
RP20/ LCA2/ RPE65	1p31	recessive Leber congenital amaurosis; recessive RP; protein: retinal pigment epithelium-specific 65 kD protein
RP21	not 9q34-qter	dominant RP with sensorineural deafness
RP22	16p12.1-p12.3	recessive RP
RP23	Xp22	X-linked RP
RP24	Xq26-q27	X-linked RP
RP25	6cen-q15	recessive RP
RP26	2q31-q33	recessive RP
RP27/ NRL	14q11.2	dominant RP; protein: neural retina lucine zipper
RP28	2p11-p16	recessive RP
ROM1	11q13	dominant RP; digenic RP with RDS; protein: retinal outer segment membrane protein 1
MTTS2	mitochondrion	RP with progressive sensorineural hearing loss; protein: serine tRNA 2 (AGU/C)

Table 2. Loci and genes known to cause RP. Table 2 is a modified version of a table by Dr. S. P. Daiger: http://www.sph.uth.tmc.edu/Retnet/disease.htm. For references see the original table.

Identification of a novel disease gene causing RP and sensorineural deafness in family ZMK

2.1. Introduction

Family ZMK is a large Irish kindred segregating classic Retinitis Pigmentosa (RP) and sensorineural deafness (figure 1). The disease is clinically very similar to the progressive autosomal recessive type III Usher syndrome (US). In family ZMK, however, the pattern of inheritance in consistent with autosomal dominant, x-linked dominant or a mitochondrial inheritance pattern (see 2.2.1). For a detailed description of US see section 1.7. For a synopsis of the genetics of US see table 1. Severity and age of onset vary considerably between affected members of family ZMK; one adolescent male was legally blind in his early twenties, while a female in her sixties manifested mild loss of night vision. However, most affected family members show loss of hearing by their teens and bad night vision and loss of the peripheral visual field in their twenties (figure 2).

Since the late 1980's, the molecular etiologies of many inherited disorders have been clarified. With the help of newly identified genetic markers such as restriction fragment length polymorphisms (RFLPs), variable numbers of tandem repeats (VNTRs) and microsatellites, high-resolution genetic maps were generated. With these maps and techniques such as Southern blotting, the polymerase chain reaction (PCR), and single strand conformation polymorphism gel electrophoresis (SSCPE), linkages between disease loci for many Mendelian disorders and genetic markers were being established (chapter 1.14 discusses polymorphic markers and linkage analysis in detail). Many genes within the critical region of genetic maps have been sequenced and disease-causing mutations identified.

A full genome search was undertaken in this laboratory to localise the disease gene in family ZMK, which initially was thought to be autosomal dominant, as a mitochondrial mode of inheritance was ruled out as a result of the inheritance of the disease through the male individual 1-1. However, this was based on 'word of mouth' rather than clinical diagnosis, as individual 1-1 was deceased before the

study was initiated. Using DNA from 29 members of family ZMK and 5 spouses (figure 1a), a battery of microsatellite markers were examined in the family with the aim of finding a linkage to the disease locus (Kumar-Singh et al., 1993a, 1993b; Kenna et al., 1997). After an extensive search through the genome a linkage was thought to have been found on 9q (Kenna et al., 1997). However, no markers were found at zero recombination with the disease locus. In addition, the markers with the highest lod-scores, D9S118 (Zmax = 3.75; Θ = 0.10) and D9S121 (Zmax = 3.41; Θ = 0.10), were unmapped at that time.

There were a number of reasons for believing that the positive lod-scores found on 9q occurred by chance. Firstly, as mentioned, no markers were found at zero recombination with the disease locus. Secondly, the unmapped markers, D9S118 and D9S121, were run through a subset of the CEPH panel in order to generate a map of chromosome 9 including these critical markers. However, on this newly generated map the markers giving the highest lod-scores and the fewest recombination events with the disease locus were closely flanked on either side by markers with lower lod-scores and more recombination events. Thirdly, multipoint analysis based on map distances from the newly generated map of 9q, excluded the disease causing gene in family ZMK from 9q (Mansergh Ph.D. thesis, 1997; Millington-Ward M.Sc. thesis, 1996; Mansergh et al., 1999).

Subsequently the author has, during the course of this Ph.D., run an additional 22 markers through the ZMK family, excluding most of the larger gaps, which had not previously been excluded by Fiona Mansergh, Sophia Millington-Ward, Rajendra Kumar Sing and Alexandra Erven. However, no linkage to the disease locus was found (Mansergh et al., 1999). Thus, in all, over 90% of the nuclear genome, including most of the known RP and deafness loci, and chromosome 9q, has been excluded from linkage in the family ZMK.

In 1998 the affected status of 4 members of family ZMK, previously thought to be unaffected, was brought into question. However, the information was obtained by personal communications and the persons in question did not approached our ophthalmologist, Dr. P. Kenna, on the matter. Thus, we decided not to broach the delicate matter of re-diagnosis with these persons. However, as the question of reduced penetrance was thereby introduced, the author decided to reanalyse all 400 microsatellite markers run in the laboratory by all the various people mentioned above, using affected members of the family only. After reanalysis no significantly positive lod-scores were obtained (tables 3a/b).

On further examination, the information on the disease status of individual 1-1 also turned out to be unsure, as no living member of the family could remember whether he or his wife had originally passed on the disease; individual 1-1 died in the 1890s. As no father to child transmission of the disease is now known to occur in this pedigree, the mitochondrion was considered a likely candidate for harboring the disease mutation. In addition, individuals with mitochondrial mutations are known in many cases to vary widely in terms of the disease symptoms they manifest (reviewed in Treem and Sokol, 1998). Mitochondrial mutations are also frequently associated with muscle abnormalities and neurological disorders (see tables 6a/b and 7). Thus, electromyographies (EMGs) and electrocariography (ECGs) were carried out on individuals 3-22, 4-4, 4-5 and 4-6 (see 2.2.1). All four individuals showed right axis deviation (ECG), suggesting the presence of a subclinical cardiomyopathy and abnormal (EMG). Also a quadriceps femoris muscle biopsy, extracted from individual 3-22 revealed abnormal quantities of mitochondria beneath the sarcolemnal membrane.

A large scale mitochondrial deletion was ruled out by Dr. Fiona Mansergh by Southern blot analysis of total DNA from affected members of the family and a PCR probe of a portion of the mitochondrial DNA (Mansergh et al., 1999). In this study 1.5kb of the mitochondrial genome was direct sequenced by the author and the remaining 15kb by Dr. Fiona Mansergh and Avril Kennan. In addition to various polymorphisms, both known and unpublished, a C→A transversion at position 12258 of the second mitochondrial serine tRNA gene (MTTS2) was discovered in family members. This mutation was not present in 270 controls, determined by Dr. Sophie Kiang. Notably, a sequence alignment carried out by the author and Dr. Fiona Mansergh of MTTS2 revealed this particular base (C12258) to be highly conserved between species (Mansergh et al., 1999). Given the observation of a mutation at position 12258 of the mitochondrial genome, it was important to establish which family members showed evidence of the presence of the mutation, to ascertain if this mutation was likely to be the disease causing mutation in family ZMK.

Heteroplasmy is the phenomenon where both mutant and wildtype genes occur within one cell. In mitochondrial disease this is very common, as a de novo mutation will, most likely, occur in one of an organism's mitochondria at a time. Thus, as egg cells contain many mitochondria, when a gamete is formed in an organism carrying a mitochondrial mutation in an egg cell, many other healthy

mitochondria will be present in addition to the mutated one. Levels of heteroplasmy are likely to vary between different members of a family segregating a heteroplasmic mtDNA mutation, depending on the chance ratio of mutant versus wildtype mtDNA present in the egg cell which formed them. Heteroplasmic mitochondrial disorders have threshold levels of mutant mitochondrial DNA (mtDNA) levels versus levels of wildtype mtDNA above which disease symptoms manifests. The threshold of wildtype mtDNA required to rescue the biochemical function of cells depends on the mutation in question. For example, in the case of point mutations in either the tRNAleu or tRNAlys, only about 15% wildtype tRNA is required to compensate for the mutant tRNAs (Katayama et al., 1991; Bower et al., 1992).

In this study the levels of heteroplasmy in family ZMK were assessed in three separate ways. Firstly, Avril Kennan sequenced the entire family over the mutation site and estimated the ratio of wildtype C to mutant A mitochondrial sequence by eye. Secondly, Avril Kennan carried out an SSCPE for all members of the family and the degree of heteroplasmy was again estimated by eye. Thirdly, the author cloned 160 PCR fragments over the mutation site, from 4 different samples, miniprepped the clones and Sophie Kiang sequenced these to determine the genotypes of the clone. The PCRs were carried out on DNAs extracted from bloods of two severely (3-22 and 4.14) and one asymptomatic individual (3-18) and from DNA extracted from a muscle biopsy of one of the severely affected members of family ZMK (3.22) (figure 1).

Thus heteroplasmy was compared between severely and mildly affected members of the family and between two tissue types, blood and muscle, of a severely affected member of the family. The data generated added to the body of evidence supporting the view that the disease causing mutation in family ZMK was mitochondrial and was indeed the C→A transversion at position 12258 of the second mitochondrial serine tRNA gene.

2.2. Materials and Methods

2.2.1. Patients and patient diagnosis

Dr. Paul Kenna in the Royal Victoria Eye and Ear Hospital in Dublin diagnosed all 29 related patients and 5 spouses. DNAs were extracted from blood using standard protocols (Fiona Mansergh Ph.D. thesis, 1997) by Dr. Paul Kenna, Dr. Rajendra Kumar-Singh, Dr. Fiona Mansergh and Mrs. Elizabeth Machlan-Sharp. In family

ZMK the sensorineural hearing loss and RP are, like in US type III, progressive. Classic RP, manifesting waxy disc pallor, arteriolar narrowing and bone spicule pigmentary depositions, are evident in older affected members of the family (figure 2).

Patients were clinically assessed in great detail with electroretinograms (ERGs) and audiometry ERGs though variable, show delayed and reduced rod and cone responses. By age 50-60 affected members of this family do not usually have detectable rod or cone responses (Kenna et al., 1996). Audiometric analysis shows moderate to severe sensorineural deafness, particularly to middle range frequencies, with evidence of 'recruitment' (marked distortion and physical discomfort by loud noise) (Kumar-Singh et al., 1993, 1993a; Kenna et al., 1997). Electromyography (EMGs) and electrocariography (ECGs) were carried out on individuals 3-22, 4-4, 4-5 and 4-6 in St. James' Hospital and the Adelaide Hospital respectively. All four individuals showed right axis deviation (ECG) and short small motor unit potentials (EMG). Also a quadriceps femoris muscle biopsy, extracted from individual 3-22 at the Adelaide Hospital in Dublin by Mr. F. Keane FRCH. Half the biopsy was used for DNA extraction (by Dr. Fiona Mansergh) and the other half was subjected to light and electron microscopy (by Ms. Anne Mynes and Dr. Michael Farrel at St. James' Hospital, Dublin). Interestingly there were unusually high numbers of mitochondria beneath the sarcolemnal membrane in the muscle sample; a matter consistent with a mitochondrial myopathy. High resolution karyotyping, performed on DNAs from four affected family members revealed no large sale chromosomal deletion or inversion (Kenna et al., 1997).

2.2.2. Oligonucleotide selection, synthesis and purification

Oligonucleotides were synthesised on an Applied Biosystems 394 DNA/RNA synthesiser by Dr. Sophie Kiang. Oligonucleotides with high polymorphic values were selected from the 1994 and 1996 Genethon maps (Dib et al., 1996; Gyapay et al., 1994) and from the online genome data base (GDB) for the purpose of running microsatellites. Oligonucleotides were purified using one chloroform extraction and subsequently drying primers in a Savant SVC200 vacuum centrifuge. The pellets were resuspended in dH_2O to a final concentration of 50 pmoles per μl. Primers for the purpose of sequencing were purified in a different manner. Briefly, primers were dried, resuspended in 100μl of dH_2O and extracted with phenol, phenol/chloroform and chloroform. Primers were then ethanol precipitated, spun at 13,000 rpm for 20 minutes and the pellets washed in 70% ethanol. Pellets were

dried and resuspended in dH$_2$O, and diluted to a final concentration of 5 pmoles/µl. Various oligonucleotides were purchased from commercial companies such as GibcoBRL and VH Bio.

2.2.3. Non-Radioactive PCR and MgCl$_2$ curve

To optimise PCRs, MgCl$_2$ curves were usually carried out at various annealing temperatures. In a 50 µl reaction 50 ng of DNA was added to 8 µl of cold dNTP mix, 5 µl of MgCl$_2$ buffer (10 mM, 12.5 mM, 15 mM, 20 mM and 25 mM), 1/6 unit of Taq polymerase and 25 pmoles of each primer (appendix A). Typically, 35 cycles of 1 minute at 94$\circ$C, 1 minute at 56$\circ$C and 1.20 minute at 72$\circ$C were carried out. If the product was more than 800 bp, the elongation time was extended to 2 minutes and if the estimated melting temperature of the primers was higher than 56$\circ$C, a higher annealing temperature was maintained.

2.2.4. Radioactive PCRs

Radioactive PCRs were carried out in 20 µl volumes containing 25 pmoles of each primer, 0.1 µl of [α^{32}P]dCTP or dATP (Amersham), 4 µl of hot dNTP mix, 1/6 unit Taq polymerase and 2 µl of the appropriate MgCl$_2$ buffer. See appendix A for solution recipes. PCRs were typically carried out for 35 cycles of 1 minute at 94$\circ$C, 1 minute at 56$\circ$C and 1 minute and 20 seconds at 72$\circ$C. To save time and materials, duplex PCRs were carried out. These were done in the same manner as above, except that two sets of primers were added to the 20 µl PCR reaction. Successful sets of primers for the purpose of running duplex PCRs on a single gel, amplify DNA fragments that differ by about 80bp in size.

2.2.5. Polyacrylamide gels and visualisation of radioactive PCRs

Prior to loading radioactive PCR samples on gels, 6 µl of formamide loading dye (appendix A) was added and samples were heated to 94$\circ$C for at least 2 minutes. The samples were run on 8% polyacrylamide and 4.65M urea gels (Sambrook et al., 1989). Polymerisation was achieved by adding 600 µl of 10% ammonium peroxodisulphate and 75 µl of TEMED. Gels were run at 2 kV and 40 mA and were dried under vacuum. Radioactivity on the gel was visualised on autoradiograph film (Afga Curix).

2.2.6. Microsatellite, selection, computer analysis and affecteds only analysis

Microsatellite data were analysed using the Linksys Data Management Package version 4.11 (Attwood and Bryant, 1988). Two point lod-scores were calculated

using LIPED version IBM PC/AT. Frequencies of the disease and normal phenotypes were set at 0.0001 and 0.9999 respectively. Full penetrance was assumed. Multipoint analyses were carried out by Dr. Fiona Mansergh (Mansergh et al., 1999) as described. A chromosome 9 map including the previously unmapped markers D9S118 and D9S121 was generated by Dr. Fiona Mansergh (Mansergh et al., 1999); the two markers were mapped using a subset of the CEPH families (Millington-Ward M.Sc. thesis, 1996; Mansergh Ph.D. thesis, 1997; Mansergh et al., 1999). Exclusions, in Kosambi centimorgan (cM), of regions from containing the disease locus were calculated from the recombination fraction (Θ) associated with a lod-score of -2 or below (Ott, 1974), using the Kosambi mapping function:

$$cM = 25 \ln \frac{(1 + 2\Theta)}{(1 - 2\Theta)}$$

2.2.7. Direct sequencing of the mitochondrion

Fiona Mansergh extracted total DNA from a quadriceps femoris muscle biopsy (carried out in the Adelaide Hospital in Dublin) of individual 3-22 (Fiona Mansergh Ph.D. thesis, 1997). This and DNA extracted from blood of individuals 3-18, 4-14 (an asymptomatic and a severely affected family member respectively) and 4-23 (a married in individual) was direct sequenced using standard protocols presented in (Fiona Mansergh Ph.D. thesis, 1997). Briefly, 5 pmoles of primer was 5' end labeled with 5 µl of γ-dATP (Amersham), 1 µl of 10x PNK buffer and 1 µl of PNK enzyme in a 10 µl volume at 37°C for at least 1 hour. The enzyme was then deactivated at 96° C for 5 minutes.

PCR primers for sequencing (in a 5'-3' orientation) were as follows:

M6651 F	GGCTTCGGAATAATCTCCCA
M7001 F	ACTACACGACACGTACTACG
M7046 R	TAGGACATAGTGGAAGTGGG
M7234 F	CCGATGCATACACCACATGA
M7339 R	TTCGAAGCGAAGGCTTCTCA
M7600 F	GCAAGTAGGTCTACAAGACG
M7670 R	TGAGGGCGTGATCATGAAAG
M7959 F	CATTATTCCTAGAACCAGGCG
M8002 R	GTCACCGTCAAGGAGTCGCA
M8273 R	GGTGCTATAGGGTAAATACG

Two PCR products, generated with M6651F and M7670R and with M7600F and M8273R respectively, were sequenced with the primers above in a forward and a

reverse orientation. The names of the primers indicate the base at which sequencing-primer starts (GenBank accession number: J01415). R stands for reverse and F for forward primer.

Resulting sequence was run on 8% polyacrylamide gels. Remaining sequence was generated by Fiona Mansergh and Avril Kennan.

2.2.8. Controls

270 controls were sequenced by automated sequencing over the 12258 mutation site by Dr. Sophie Kiang. The control DNAs, kindly provided by Dr. Lesley Mynett-Johnson, were derived from blood donated to the Irish blood transfusion board.

2.2.9. Cloning PCR products and determining levels of heteroplasmy

PCR products, amplified from DNAs extracted from bloods from individuals 3-22, 4-14 and 3-18 and from a muscle biopsy from individual 3-22 were cloned into the HindIII and XbaI sites of pcDNA3 (Invitrogen). The primers used for this purpose (in a 5'-3' orientation):

<div style="margin-left: 3em;">

Forward   CTAGAAGCTTCCGACATAATTACCGGGTTT
Reverse   TTCATCTAGATTTGTTAGGGTTAACGAGGG

</div>

Restriction enzyme sites are underlined. PCR products were digested with HindIII and XbaI (NEB), were ligated into the multiple cloning site (MCS) of the digested plasmid, pcDNA3 (Invitrogen), using rATP and ligase (Stratagene). According to standard protocols the vector was previously treated with alkaline phosphatase from calf intestine (CIPed) (Boehringer Mannheim). PCR inserts generated for cloning were digested with the same enzymes and were purified with phenol, phenol/chloroform and chloroform extractions followed by an ethanol precipitation and a 70% ethanol wash. Approximately 100 ng of vector and 100 ng, 200 ng and 500 ng of insert were ligated over night at 15°C. The Promega ligation kit was used according to the manufacturer's protocol. Ligations were transformed in XL1-blue MRA cells and resulting colonies picked, grown in LB broth and DNA isolated using standard miniprep protocols.

Briefly, 100 ml of LB broth with tetracycline (appendix A) was inoculated with 500 µl of overnight XL1-blue MRA culture. The culture was grown to an OD600 of 0.3-0.5 after which cells were left on ice for 30-60 minutes. Cells were then spun at 3000 rpm for 5 minutes in a bench-top centrifuge (Savant) and gently resuspended in 50 ml of cold 50 mM $CaCl_2$. Cells were stored on ice for 20-60 minutes and spun

at 3000 rpm for 5-10 minutes. Competent cells were gently resuspended in 10 ml of cold 50 mM CaCl$_2$. Competent cells could be stored at -70°C in 15% glycerol.

Transformations were carried out by mixing 5 µl of ligation mix with 200 µl of competent cells and leaving on ice for 30 minutes. Cells were then heat-shocked for 5 minutes at 42°C in a water bath. Immediately after heat shocking, 1 ml of LB broth was added to the transformation and the cells were left shaking gently at 37° C for 1 hour. 200 µl of transformed cells were plated on 10 cm LB plates containing appropriate antibiotics and grown over night at 37°C.

Colonies present on plates incubated over night were picked and grown over night in 10 ml of LB broth supplemented with appropriate antibiotics. 10 ml overnight cultures of clones were miniprepped in the following fashion. Cells were spun at 3000 rpm for 15 minutes, were resuspended in 400 µl of lysis solution I (appendix A) and were left at room temperature for 5 minutes. 800 µl of lysis solution II (appendix A) was added and the cells were left on ice for 5 minutes. Then, 600 µl of ice cold 3 M NaOAc pH 5.2 was added and the cells were left on ice for 10 minutes. The lysate was transferred to eppendorfs and spun at 13000 rpm for 15 minutes. The supernatant was extracted twice with phenol, once with phenol/chloroform and once with chloroform. This was then ethanol precipitated and the pellet washed with 70% ethanol. 1µl of RNacit cocktail (Stratagene) was added to minipreps to remove RNA. DNA from 40 minipreps generated using PCR products from each of the four ZMK-samples chosen for the study (DNA from 160 minipreps in all) were sequenced by Dr. Sophie Kiang on an automated sequencer (Mansergh et al., 1999).

2.3. ZMK Results

2.3.1. Linkage analysis

Linkage analysis was carried out in an Irish family (family ZMK) suffering from RP in conjunction with sensorineural deafness. The study was carried out using a battery of microsatellite markers throughout the genome. Having typed these markers through family ZMK resulting exclusions/linkages between markers and the disease locus were calculated. In previous linkage studies of family ZMK undertaken by Dr. Fiona Mansergh, the author, Dr. Rajendra Kumar Singh and Dr. Alexandra Erven a large portion of the genome, including 9q, a region previously thought to be linked to the disease, had been excluded from linkage to the disease mutation (Kenna et al., 1997; Mansergh et al., 1999; Mansergh Ph.D.

thesis, 1997; Millington-Ward M.Sc. thesis, 1996). 22 additional markers on various chromosomes were run through the family in the study presented in this thesis. Details of the microsatellite markers used in the study are presented in table 2. The lod-scores obtained at various recombination fractions with microsatellite markers are given in table 2. Resulting exclusions (in Kosambi cM) are also presented in table 1. The data generated in this study together with previous data excluded approximately 92% of the genome from harboring the disease gene segregating in family ZMK. Some examples of microsatellite autoradiographs are presented in figures 3 and 4. In summary, all the data generated using microsatellites typed through ZMK resulted in exclusions rather than linkages to the disease locus.

However, notably, the affectation status of 4 individuals, who remain anonymous for reasons of confidentiality, was brought into question in 1997, thereby initially raising the possibility of the presence of reduced penetrance in the family. Reduced penetrance had not previously been thought to be a key issue in family ZMK as many individuals in the pedigree were affected and therefore the disease looked fully penetrant. Given the introduction of the notion of reduced penetrance in ZMK all 400 microsatellite markers, which had previously been run through the family by Drs. Fiona Mansergh, Rajendra Kumar-Singh, Alexandra Erven and the author, were reanalysed using affected members of the pedigree only. Resulting 2-point lod-scores are presented in table 3a. No significant lod-scores were obtained, although 9 markers were slightly positive at zero recombination (summarised in table 3b). For instance, RHO and D3S1299 both give positive lod-scores over 1 at zero recombination, however D3S47, which is situated between these two markers excludes 7 cM to either side of it and markers D3S1291 and GLUT2 exclude 7 cM and 15 cM to either side respectively, excluding the whole area around RHO and D3S1299. The marker D5S119 gives a lod-score of 1.278 at zero recombination. However, this area is excluded by the markers CSF1R and D5S414. D10S209 gives a lod-score at zero recombination of 1.313. Again, however, the area is excluded from harboring the disease gene by markers D10S187, D10S222 and D10S587. D11S906, giving a lod-score of 0.161, is excluded by D11S937 and D11S527. The positive DRD2 on chromosome 11 (1.278) is excluded by markers D11S490, D11S29, CD3D and D11S925. D13S168 which gives a positive lod-score at zero recombination of 1.386 is excluded by marker D13S156. D17S261 which is mildly positive at zero recombination (0.705) is excluded by D17S783 and THRA1. The last positive marker at zero recombination, D18S62 (1.056), is excluded by marker

D18S877. Thus, no markers analysed through family ZMK using affected members only were significantly positive and all positive markers at zero recombination were excluded by more informative markers in the area.

2.3.2. Mitochondrial analysis

Recently, in 1997, the affectation status of yet another family member was brought into question. Individual 1-1, previously thought to be the only affected male to have produced offspring with the disorder in the family, died around the turn of the century. Despite initial hearsay it seems that no one in the family can now remember clearly whether he or his wife had suffered from RP and deafness. Thus, no male to offspring transmission of the disorder may ever have taken place in family ZMK. Since over 90% of the genome had been excluded from linkage, the ECG and EMG had been found to be abnormal in 4 family members and the light and electronmicroscopic analyses of the muscle biopsy from individual 3-22 contained an abnormally high number of mitochondria, the mitochondrial genome was considered a candidate for harboring the disease locus. In this study 1.5kb (base 6651-8273) of the mitochondrial genome was directly sequenced using DNA from four members of family ZMK. One previously reported T/C polymorphism was detected at position 6776 in the resulting sequence (figure 5). The remaining portion of the mitochondrial genome was sequence by Dr. Fiona Mansergh and Avril Kennan. A heteroplasmic C→A transversion was discovered at position 12258 of the second tRNA serine gene by Dr. Fiona Mansergh. Subsequent sequence for each member of this pedigree over the mutation site was generated by Avril Kennan and clearly demonstrated that all family members except individuals 2-3 and 2-5, who are both asymptomatic, are heteroplasmic for the mutation in DNA derived from blood. Notably the mutation was not found in 270 control DNAs, which Dr. Sophie Kiang sequenced over the mutation site. As mentioned in the introduction of this chapter, the occurrence of heteroplasmy in many mitochondrial disorders, particularly where a tRNA mutation is concerned, has been well documented (table 6a/b). Levels of heteroplasmy can differ from patient to patient and from tissue to tissue (Morgan-Hughes, 1995). The ratio of mutant to normal mitochondria in photoreceptor cells and in the inner cochlea may determine the severity of the disorder in different patients in family ZMK. Thus, varying degrees of heteroplasmy may explain the enormous variation in disease severity and age of onset noted in family ZMK. Degrees of heteroplasmy in family members were estimated in three ways. Firstly Avril Kennan sequenced blood-derived DNAs of the entire family over the mutation site and estimated the ratio of normal and

mutant DNA by eye (Mansergh et al., 1999). Secondly Avril Kennan carried out an SSCPE of PCR fragments from blood-derived DNAs over the mutation site for all family members and estimated the ratio of normal to mutant DNA by eye (Mansergh et al., 1999). Thirdly, an additional method was used to estimate levels of heteroplasmy which was deemed to be more accurate than the two methods outlined above. 40 PCR fragments which included the region over the mutation site were generated from DNA samples from individuals in ZMK and were cloned by the author into pcDNA3 (in all 160 clones were generated). The DNA samples were obtained from blood samples of individuals 3-22 (severely affected), 3-18 (asymptomatic) and 4-14 (severely affected) and from the muscle biopsy of individual 3-22. The 160 clones were miniprepped by the author and were sequenced by Dr. Sophie Kiang (table 5). The estimates of heteroplasmy obtained from the manual sequence and the SSCPE analysis revealed no correlation with affectation status and age of onset. The degrees of heteroplasmy determined by cloning by the author revealed no such correlation either. Interestingly, however, a large discrepancy was found between the ratio of mutant and wildtype mitochondrial DNAs in blood derived DNA and muscle derived DNA (25:15 and 37:3 respectively) from the same individual (individual 3-22).

Notably, the levels of heteroplasmy estimated from blood samples may not reflect the actual situation (that is the levels of heteroplasmy present in the affected tissues, for example in the retina and cochlea). The absence of a correlation between levels of heteroplasmy and severity of disease may be due to inappropriate nature of the tissue tested (that is blood).

2.4. Discussion

2.4.1. Linkage analysis

The linkage studies, which commenced in 1992 in this laboratory in family ZMK have been continued during the course of this Ph.D. and have resulted in the exclusion of about 92% of the nuclear genome. Thus most of the candidate loci, including all the US, RP and most deafness and retinopathy loci have been excluded from linkage (Kumar-Singh et al., 1993a, 1993b; Millington-Ward M.Sc. thesis, 1996; Kenna et al., 1997, Mansergh et al., 1999; Mansergh Ph.D. thesis, 1997). A suggestion of linkage to the disease mutation was found on chromosome 9q. However, no markers were at zero recombination with the disease locus, and a map generated by ourselves incorporating the two unmapped markers, D9S118

and D9S121, which had given the highest lod-scores, showed that these markers were separated from the disease locus by other markers with lower lod-scores and more recombination events. Thus, a multipoint over the 9q region incorporating these two previously unmapped markers and using map distances derived from our map excluded the region from linkage. Also, haplotype analysis showed no common allele segregating with the disease in family ZMK (Mansergh et al., 1999). Recently the affectation status of four family members was brought into question, raising the possibility of the presence of reduce penetrance. All markers previously run through the family by various researchers including the author were thus reanalysed using affected family members only. However, subsequent to 2-point analyses, no lod-scores were found that exceeded the established threshold of significance of 3.0 (tables 3a/b). Therefore after reanalyses of family ZMK using only family members whose diagnostic status was beyond doubt (that is affected members), no significant positive lod-scores were obtained with 400 markers well spread throughout the genome.

In 1998 the affectation status of individual 1-1 was brought into question. This family member deceased in the 1890s, therefore no current members of family ZMK can remember him or indeed his health status. His somewhat younger wife, who died in her late 80s is however remembered and is thought to have suffered no hearing loss or visual impairment. Thus her husband was presumed to carry the disease mutation, thereby ruling out the possibility of a maternal mode of inheritance of the disease. However, given the rather spurious nature of this evidence it is now thought, that perhaps not he, but his wife carried a mitochondrial mutation, she herself not manifesting the disease or manifesting the disease very mildly.

There are now nine reasons for suspecting a mitochondrial mode of inheritance of the disorder in family ZMK. Firstly, disease loci for RP, sensorineural and other optic disorders are prevalent on the mitochondrial genome (table 6a/b and 7). Secondly, there is no confirmed male to child transmission of the disease in family ZMK. However, again this evidence is rather spurious as most males in the family did not produce offspring, possibly for sociological reasons. Thirdly, the phenomenon of recruitment (marked distortion and physical discomfort by loud noise), observed in some affected members of the family, is more common in mitochondrial disorders (Prof. W. Kimberling, personal communication). Fourthly the ECGs carried out on four individuals, show right axis deviation (Kenna et al.,

1997). Such observation would be consistent with a mitochondrial disease (table 6a/b and 7). Fifthly, the EMG, carried out on individual 3-22 shows clear abnormalities, again consistent with mitochondrial disease (tables 6a and 7). Sixthly, analysis of the muscle biopsy from individual 3-22 reveals abnormal quantities of mitochondria (Kenna et al., 1997). Muscular abnormalities due to the function of the mitochondrion are common in mitochondrial disorders (tables 6a and 7). The seventh reason for suspecting a mitochondrial mode of inheritance of the disease in family ZMK is the suspected occurrence of reduced penetrance in a pedigree already containing such a large proportion of affected individuals (figure 1) is suggestive of a maternal mode of inheritance. In addition, the enormous variability in disease symptoms between affected individuals in family ZMK suggest an eighth reason for believing in a mitochondrial inheritance pattern in family ZMK. For example, one individual was clinically blind at age 21 and another mildly night blind in her 80s. The final reason for suspecting that the mode of inheritance in family ZMK is mitochondrial is that over 90% of the nuclear genome had been excluded from linkage by microsatellite analysis. Thus, given the nine reasons outlined above, the entire mitochondrial genome was screened for disease mutations by Dr. Fiona Mansergh, Avril Kennan and the author.

2.4.2. Mitochondrial analysis

Mitochondrial sequence was obtained for blood-derived DNAs from one severely affected family member (3-22), an asymptomatic family member (3-18) and from muscle-derived DNA from one severely affected family member (3-22). As a control a married in member was also sequenced (3-23). A number of sequence changes were observed and are presented in table 4 (see results section of details). One notable sequence change was detected at a highly conserved position (position 12258) of the second serine tRNA gene MTTS2. A sequence alignment of this gene reveals that base 12258 is conserved between widely divergent species, including opossum, vulture and frog (figure 6). Notably, this sequence change was not detected in 270 control individuals from the same ethnic background as family ZMK, suggesting that 12258A may indeed be the disease causing mutation.

The degree of heteroplasmy was determined in various family members using three methods. The first two methods (carried out by Avril Kennan) involved sequencing the entire family over the mutation site and subjecting a PCR amplification over the mutation site to SSCPE analysis. In both cases the degree of heteroplasmy was determined by eye and no correlation between degree of heteroplasmy in blood-

derived DNA and severity of the disease was determined. The third method was more accurate and was carried out by the author. Nineteen PCRs were carried out on 4 separate DNA samples. The nineteen PCRs were pooled, cloned into pcDNA3, and 40 clones derived from of each pooled PCR sample were picked, grown over night miniprepped and sequenced over the mutation site. The four samples used to generate the pooled PCR samples were blood-derived DNA from two severely affected members of the family and an asymptomatic member of the family (individuals 3-22, 4-14, and 3-18 respectively) and muscle-derived DNA from individual 3-22, who is severely affected. Sequencing of the clones (kindly carried out by Dr. Sophie Kiang) showed that there was again no correlation between affectation status and degree of heteroplasmy in blood-derived DNA. However, there was a marked variation in heteroplasmy in the samples from blood- and muscle-derived DNA from individual 3-22 (table 4). The observation of an enormous variance in levels of heteroplasmy between blood and muscle tissues, although only tested in one individual, suggests that possibly the level of heteroplasmy is dependant on the nature of the tissue. For example it may be that the degree of heteroplasmy is very different in slowly dividing and non-dividing tissues such as muscle and photoreceptor cells and rapidly dividing tissues such as blood. The same variance in heteroplasmy in the two different tissues of individual 3-22 was observed with both the SSCPE and sequence analyses (as estimated by eye). Therefore the levels of heteroplasmy observed in blood may not accurately reflect the situation present in the tissues affected in the disorder. Thus, high proportions of mutant mitochondria may be present in severely affected individuals in retinas and cochleas and low amounts in asymptomatic members of the family.

Interestingly, the same C12258A mutation was discovered in a mother and daughter from Newcastle, England, who segregate diabetes, cerebellar ataxia, cataracts and deafness (Lynn et al., 1998). The mutation in these two patients was not detected in 100 unrelated control subjects. Briefly, the researchers carried out muscle biopsies in both patients and sequenced the entire mitochondrion. The degree of heteroplasmy was estimated in muscle and blood using quantitative RTPCR (QTPCR) on DNAs extracted from muscle and using a mismatch PCR technique on DNAs extracted from blood. The levels of heteroplasmy estimated were (mutant : wildtype) 85% in the daughter and 68% in the mother in DNA extracted from muscle and 45% in the daughter and 19% in the mother in DNA extracted from blood. Southern blotting showed no evidence of major rearrangement in the mtDNA. It is of note that a number of homoplasmic

polymorphisms were also detected in this study, which were identical to the polymorphisms found in family ZMK (table 4). The results from the Newcastle study stimulated further questioning of family ZMK members. It has now been established that the index case in the above mentioned study and individual 2-11 in family ZMK were sisters (figure 1). However, notably, there is no cerebellar ataxia or diabetes in family members of ZMK. Moreover, there does not appear to be any RP present in the two patients presented in the above study. However, cataracts are often associated with RP and, as no elecroretinograms have been undertaken on the two patients in the study, they may be pre-clinical, or indeed asymptomatic, with respect to RP and therefore warrant further detailed clinical evaluation. It is also of note that the diabetes, in the patients in the Newcastle study, may have a different underlying genetic cause than the deafness in these two patients, as diabetes is a very common disorder. Nonetheless, members of family ZMK are currently being analysed for possible abnormal blood-sugar levels..

Some speculation can be made as to the exact mechanism by which the mutation in MTTS2 causes the neurological disease in family ZMK (that is RP and sensorineural deafness). Mitochondria are double membraned organelles present in the cytoplasm of cells and are characterised by having a high degree of genetic and metabolic autonomy. The function of the mitochondrion is essentially the synthesis of the high-energy molecule, adenosine triphosphate (ATP). Embedded within the inner membrane are proteins which carry out the process of oxidative phosphorylation. Mitochondria fulfil most of the energy requirements of aerobic cells by coupling electron transfer reactions with the synthesis of the ATP (reviewed in Mitchell et al., 1979). In an active cell with a high energy demand, such as a muscle cell, mitochondria supply most of the ATP required. The mitochondrial genome encodes 13 genes, all of which encode components necessary for the metabolic pathway responsible for oxidative phosphorylation. Highly metabolically active cells suffer dramatically when energy levels are withheld. For example mutations in 8 of the 13 mitochondrial genes causes the diseases Leber's Hereditary Optic Neuropathy (LHON), Neurogenic muscle weakness, Ataxia and RP (NARP), Leber's hereditary Optic Neuropathy and Dystonia (LDYT) (table 6a). Mutations in any of the 13 mitochondrial genes can cause muscle disorders such as mitochondrial myopathy (MM), NARP, chronic intestinal pseudoobstruction with myopathy and ophthalmoplegia (CIPO), maternal myopathy and cardiomyopathy (MMC), fatal infantile cadiomyopathy in conjunction with MELAS-associated cardiomyopathy (FICP), mitochondrial encephalomyopathy, lactic acidosis and

stroke-like episodes (MELAS) and many others (table 7 for a complete list). Thus most mutations in the mitochondrial genes cause different types of myopathy or neurological disorders such as RP and ataxia, suggesting that muscle and neurological tissues require high levels of ATP.

In addition to 13 genes encoding proteins, mitochondria contain 2 ribosomal RNAs (rRNAs) and 22 tRNAs, necessary for the transcription and translation of the 13 proteins encoded on this genome. Naturally mitochondrial tRNA and rRNA mutations affect the synthesis of mitochondrial proteins and hence impair the metabolic pathway responsible for generating energy (ATP). Many mutation in tRNAs have been discovered (full list see table 6b) and in each case, except for the tRNA Asp mutant that accumulates precursors with 3' extensions (Zennaro et al., 1989), the tRNAs are generated but their charging is defective, reducing their ability to bind the correct amino acid. Thus depending on the severity of the defect, the synthesis of some or all mitochondrial translation products is decreased. So far in humans, all except one mitochondrial tRNA mutation have been found to be heteroplasmic and the severity of the symptoms generally relates to the ratio of wildtype and mutant DNA. Homoplasmic mutations in the mitochondrial 12S rRNA gene can cause deafness and heteroplasmic mutations in various tRNA genes can cause Diabetes Mellitus and Deafness (DMDF), Chronic Progressive External Ophthalmoplegia (CPEO) and Maternally Inherited Deafness or Aminoglycoside-Induced Deafness (DEAF) (table 6 for a complete list).

For example an A→G mutation at nucleotide 8344 in the tRNAlys gene co-segregate with myoclonic epilepsy and ragged red fiber (MERFF) syndrome (Shoffner et al., 1990; Yoneda et al., 1990). It causes a defect in the rate of protein synthesis, which is correlated with respiration and cytochrome C oxidase deficiencies. The synthesis of larger proteins is more severely affected than that of smaller proteins and several new peptides are made; both observations are consistent with premature termination of protein synthesis (Chomyn et al., 1991).

In another example, a tRNA mutation was associated with mitochondrial myopathy, encephalopathy, lactic acidosis and stroke-like episodes (MELAS) (Goto et al., 1990; Kobayashi et al., 1990). The mutation altered a conserved base in the D-loop of the mitochondrial genome, which regulated the relative levels of rRNA to mRNA through transcription termination. *In vitro* termination of transcription is impaired by the mutation, suggesting that an alteration of the same process *in vivo* could account for the observed phenotype (Hess et al., 1991).

Thus, the mutations characterised to date in tRNAs mainly cause neurological disorders and not muscular disorders as commonly seen in patients with mutations in one of the 13 mitochondrial genes. Perhaps in non-dividing cells such as photoreceptor cells, which require high levels of ATP, mutant mitochondria inherited at birth remain in the photoreceptor cell during the lifetime of a patient, eventually leading to photoreceptor cell degeneration. In contrast to this, in dividing cells, such as muscle cells, mutant mitochondria (with malfunctioning tRNAs or rRNAs) may not divide as efficiently as wildtype mitochondria and may thus be depleted during each cell division. Thus even though muscle tissue requires more energy than, for example, a photoreceptor cell, mitochondria with mutant tRNAs or rRNAs may not cause muscle degenerations. On the other hand, tRNA mutations are mainly heteroplasmic, suggesting that homoplasmic mutations in tRNAs may frequently be fatal. The exact mechanism by which this newly identified serine tRNA mutation causes photoreceptor cell loss and sensorineural deafness is not known. However, data provided by the study strongly implicate this mutation in the disease pathology present in ZMK. Further studies may include chemical studies on the differences in charging of mutant and wildtype serine tRNAs. In addition, the exact effect of mitochondria carrying the MTTS2 mutation on cells may be studied in cell culture studies.

2.5. Summary

A novel C→A transversion at position 12258 in the second serine tRNA gene, MTTS2, has been found in family ZMK segregating RP in conjunction with sensorineural deafness (Kenna et al., 1997; Mansergh et al., 1999). This mutation is not present in over 270 control individuals. Sequence alignment shows base 12258 to be highly conserved between species, suggesting an important role for this base in serine tRNA structure and/or function. Levels of heteroplasmy, determined using a number of techniques, indicate that the mutation is heteroplasmic, with ratios of wildtype to mutant mitochondria varying significantly in blood derived DNAs between different family members and between different tissues belonging to the same individual. The ratio of normal versus mutant mitochondrial DNA present in DNA samples extracted from peripheral blood lymphocytes does not correlate with the severity of the disorder in ZMK family members. Notably, the ratio of wildtype to mutant mitochondria varies in different tissues, suggesting that the ratio observed in rapidly dividing tissues such as blood may not represent the ratio in non-dividing tissues such as photoreceptor cells and cochlea.

The identification of a novel mutation in the second serine mitochondrial tRNA gene and the implication of the mutation in a syndrome incorporating RP and sensorineural deafness, serves to highlight, yet again, the high levels of genetic heterogeneity inherent in RP and deafness. The genetic etiologies of this group of disorders has been revealed to be extremely complex over the past decade (see appendix B). The current study contributes to our understanding of this complexity and suggests that banks of DNA from patients with retinopathies and/or hearing loss should be screened not only for autosomally inherited mutations but also for mitochondrially inherited disease causing genes.

2.6. Bibliography

A common mitochondrial DNA mutation in the t-RNA(Lys) of patients with myoclonus epilepsy associated with ragged-red fibers. Biochem Int. 1990 Aug;21(5):789-96.

Bower SP, Hawley I, Mackey DA. Cardiac arrhythmia and Leber's hereditary optic neuropathy. Lancet. 1992 Jun 6;339(8806):1427-8.

Chaib H, Kaplan J, Gerber S, Vincent C, Ayadi H, Slim R, Munnich A, et al. A newly identified locus for Usher syndrome Type 1, USH1E, maps to chromosome 21q21. Hum Mol Genet 1997 6:27-31.

Chomyn A, Meola G, Bresolin N, Lai ST, Scarlato G, Attardi G.

Eudy JD, Weston MD, Yao S, Hoover DM, Rehm HL, Ma-Edmonds M, Yan D, Ahmad I, Cheng JJ, Ayuso C, Cremers C, Davenport S, Moller C, Talmadge CB, Beisel KW, Tamayo M, Morton CC, Swaroop A, Kimberling WJ, Sumegi J. Mutation of a gene encoding a protein with extracellular matrix motifs in Usher syndrome type IIa. Science 1998b Jun 12;280(5370):1753-7.

Eudy JD, Yao S, Weston MD, Ma-Edmonds M, Talmadge CB, Cheng JJ, Kimberling WJ, Sumegi J. Isolation of a gene encoding a novel member of the nuclear receptor superfamily from the critical region of Usher syndrome type IIa at 1q41. Genomics 1998a Jun 15;50(3):382-4.

GDB: The human genome database. Online database: http://www.gdb.org/

Goto Y, Nonaka I, Horai S. A mutation in the tRNA(Leu)(UUR) gene associated with the MELAS subgroup of mitochondrial encephalomyopathies. Nature. 1990 Dec 13;348(6302):651-3.

Hess JF, Parisi MA, Bennett JL, Clayton DA. Impairment of mitochondrial transcription termination by a point mutation associated with the MELAS subgroup of mitochondrial encephalomyopathies. Nature. 1991 May 16;351(6323):236-9.

In vitro genetic transfer of protein synthesis and respiration defects to mitochondrial DNA-less cells with myopathy-patient mitochondria. Mol Cell Biol. 1991 Apr;11(4):2236-44.

Kaplan J, Gerber S, Bonneau D, Rozet JM, Delrieu O, Briard ML, Dollfus et al (1992) A gene for Usher syndrome Type1 (USH1A) maps to chromosome 14q. Genomics 14:979-987.

Katayama M, Tanaka M, Yamamoto H, Ohbayashi T, Nimura Y, Ozawa T. Deleted mitochondrial DNA in the skeletal muscle of aged individuals. Biochem Int. 1991 Sep;25(1):47-56.

Kenna PF, Mansergh FC, Millington-Ward S, Erven A, Kumar-Singh R, Brennan R, Farrar GJ, et al (1997) Clinical and molecular genetic characterization of a family segregating autosomal dominant retinitis pigmentosa and sensorineural deafness. Br J Ophthalmol 81:207-213.

Kimberling WJ, Weston MD, Moller C, Davenport SHL, Shugart YY, Priluck IA, Martini A, et al (1990) Localization of Usher syndrome type II to chromosome 1q. Genomics 7:245-249.

Kobayashi Y, Momoi MY, Tominaga K, Momoi T, Nihei K, Yanagisawa M, Kagawa Y, Ohta S. A point mutation in the mitochondrial tRNA(Leu)(UUR) gene in MELAS (mitochondrial myopathy, encephalopathy, lactic acidosis and stroke-like episodes). Biochem Biophys Res Commun. 1990 Dec 31;173(3):816-22.

Kumar-Singh R, Farrar GJ, Mansergh F, Kenna P, Bhattacharya S, Gal A, Humphries P (1993a) Exclusion of the involvement of all known retinitis pigmentosa loci in the disease present in a family of Irish origin provides evidence for a sixth autosomal dominant locus. (RP8). Hum Mol Genet 2:875-878.

Kumar-Singh R, Kenna PF, Farrar GJ, Humphries P. Evidence for further genetic heterogeneity in autosomal dominant retinitis pigmentosa. Genomics. 1993b Jan;15(1):212-5.

Lewis RA, Otterud B, Stauffer D, Lalouel JM, Leppert M. Mapping recessive ophthalmic diseases: linkage of the locus for Usher syndrome type II to a DNA marker on chromosome 1q. Genomics. 1990 Jun;7(2):250-6.

Lynn S, Wardell T, Johnson MA, Chinnery PF, Daly ME, Walker M, Turnbull DM
Mitochondrial diabetes: investigation and identification of a novel mutation.
Diabetes. 1998 Nov;47(11):1800-2.

Mansergh FC, Millington-Ward S, Kennan A, Kiang AS, Humphries M, Farrar GJ,
Humphries P, Kenna PF. Retinitis Pigmentosa and Progressive Sensorineural
Hearing Loss Caused by a C12258A Mutation in the Mitochondrial MTTS2 Gene. Am
J Hum Genet. 1999 Apr;64(4):971-985.

Mansergh FC. On the molecular genetics of inherited retinopathies and glaucoma. Ph.D.
thesis 1998.

Millington-Ward S. Linkage between autosomal dominant retinitis pigmentosa in
conjunction with sensorineural deafness and microsatellite markers on chromosome
9q/ Isolation of up-stream promoter sequence of the mouse peripherin/RDS gene from
a λ-DASH II genomic library. M.Sc. thesis 1996.

Mitchell P, Moyle J, Mitchell R. Measurement of translocation of H+/O in mitochondria and
submitochondrial vesicles. Methods Enzymol. 1979;55:627-40.

MITOMAP. A human mitochondrial genome database. Online database:
http://www.tcd.ie/Secretary/Noticelist/msg00000.html

Moller CG, Kimberling WJ, Davenport SL, Priluck I, White V, Biscone-Halterman K,
Odkvist LM, Brookhouser PE, Lund G, Grissom TJ. Usher syndrome: an
otoneurologic study. Laryngoscope. 1989 Jan;99(1):73-9.

Morgan-Hughes JA, Sweeney MG, Cooper JM, Hammans SR, Brockington M, Schapira AH,
Harding AE, Clark JB. Mitochondrial DNA (mtDNA) diseases: correlation of
genotype to phenotype. Biochim Biophys Acta. 1995 May 24;1271(1):135-40.

Ott J. Estimation of the recombination fraction in human pedigrees: efficient computation
of the likelihood for human linkage studies. Am J Hum Genet. 1974 Sep;26(5):588-97.

Sambrook J, Fritsch EF, Maniatis T. Molecular cloning: a laboratory manual, 2nd ed. Cold
Spring Harbor Laboratory Press, Cold Spring Harbor, NY, 1989.

Sankila E-M, Pakarinen L, Kaariainen H, Aittomaki K, Karjalainen S, Sistonen P, de la
Chapelle A (1995) Assignment of an Usher syndrome type III (USH3) gene to
chromosome 3q. Hum Molec Genet 4:93-98.

Shoffner JM, Lott MT, Lezza AM, Seibel P, Ballinger SW, Wallace DC. Myoclonic epilepsy
and ragged-red fiber disease (MERRF) is associated with a mitochondrial DNA
tRNA(Lys) mutation. Cell. 1990 Jun 15;61(6):931-7.

Smith RJ, Lee EC, Kimberling WJ, Daiger SP, Pelias MZ, Keats BJ, Jay M, Bird A, Reardon W, Guest M, et al. Localization of two genes for Usher syndrome type I to chromosome 11. Genomics. 1992 Dec;14(4):995-1002.

Treem WR, Sokol RJ. Disorders of the mitochondria. Semin Liver Dis. 1998;18(3):237-53.

Usher CR (1914) On the inheritance of retinitis pigmentosa with notes of cases. Lond Ophthal Hosp Rep 19:130-236.

Wayne S, Der Kaloustian VM, Schloss M, Polomeno R, Scott DA, Hejtmancik JF, Sheffield VC, et al (1996) Localization of the Usher syndrome type 1D gene (USH1D) to chromosome 10. Hum Mol Genet 5:1689-1692.

Weil D, Blanchard S, Kaplan J, Guilford P, Gibson F, Walsh J, Mburu P, et al (1995) Defective myosin VIIA gene responsible for Usher syndrome type 1B. Nature 374:60-61.

Yoneda M, Tanno Y, Horai S, Ozawa T, Miyatake T, Tsuji S.

Zennaro E, Francisci S, Ragnini A, Frontali L, Bolotin-Fukuhara M. A point mutation in a mitochondrial tRNA gene abolishes its 3' end processing. Nucleic Acids Res. 1989 Jul 25;17(14):5751-64.

Figure 1A.
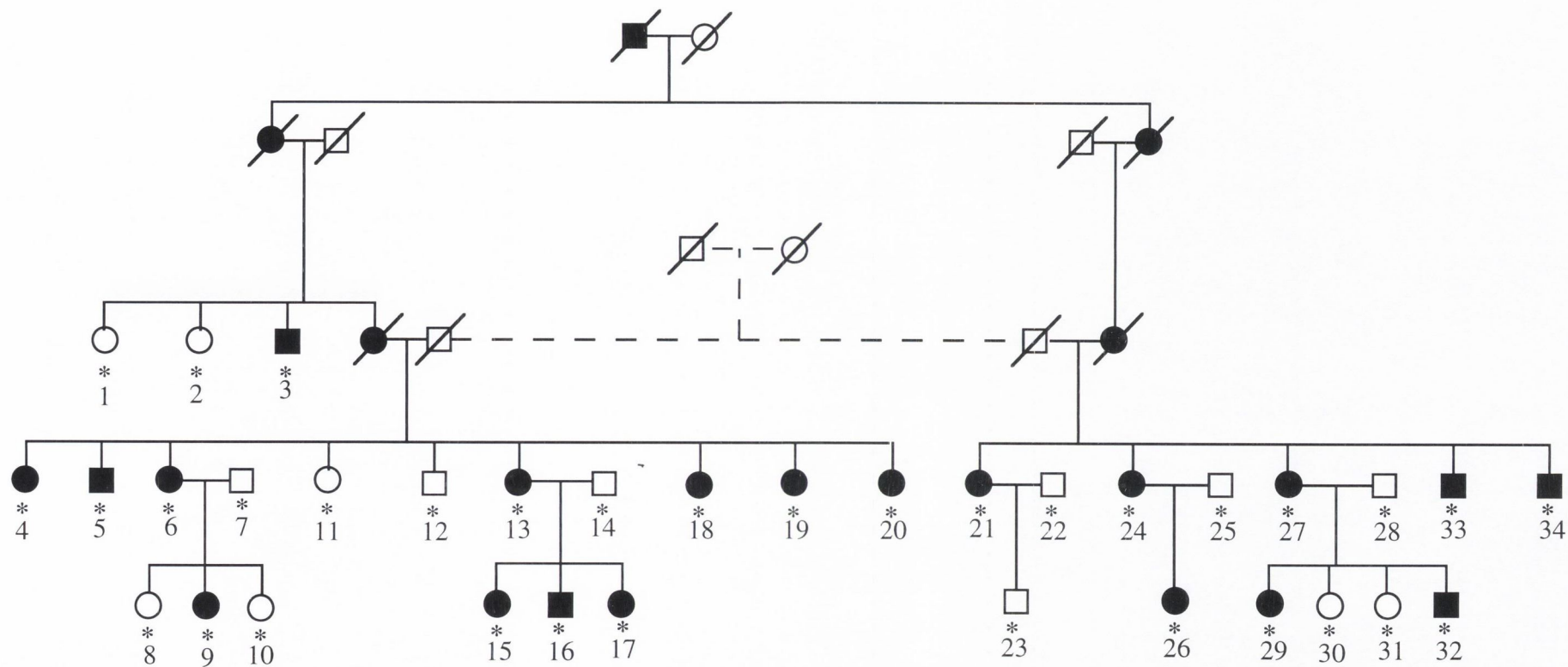
Figure 1B.
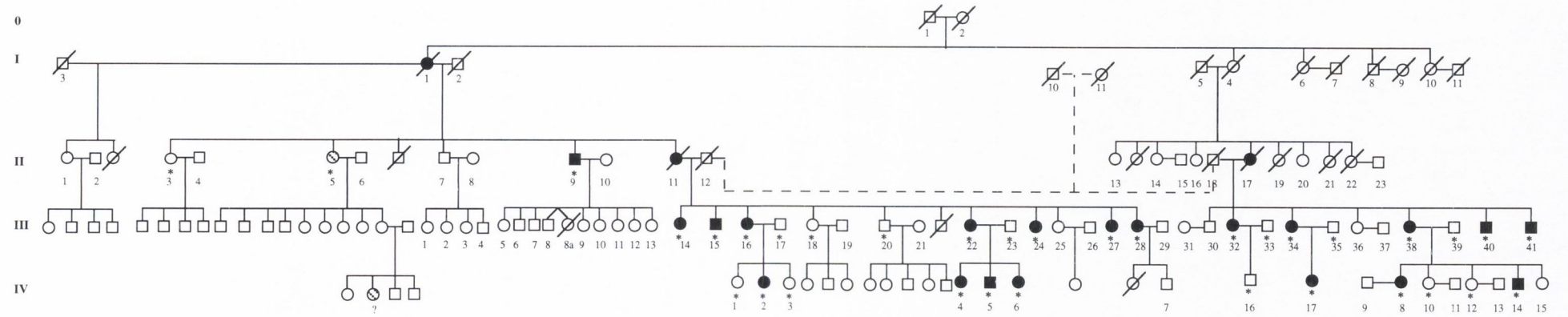
Figure 1. *A*, Partial pedigree of family ZMK with RP in conjunction with sensorineural deafness. The 34 Individuals used in the study are marked with an asterisk. The two individuals connected by a dashed line were brothers. It is unclear whether the two shade individuals are affected with the disease. Generation numbers are given to the left and individual numbers are given under each pedigree symbol. *B*, Full pedigree of family ZMK. Individuals marked with an asterisk were clinically assessed and DNA samples were obtained from them. Shaded individuals were examined clinically but their diagnoses were unsure. The individual marked by a question mark, is the affected granddaughter of an apparently unaffected grandmother (II-5). The figure was kindly lent to the author by Dr. Fiona Mansergh.

Figure 2.

A
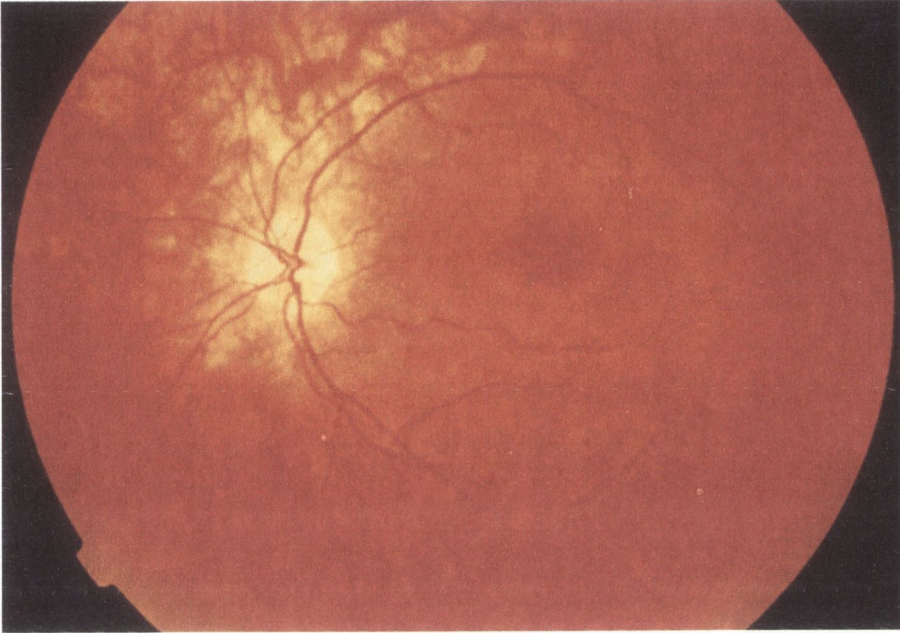
B
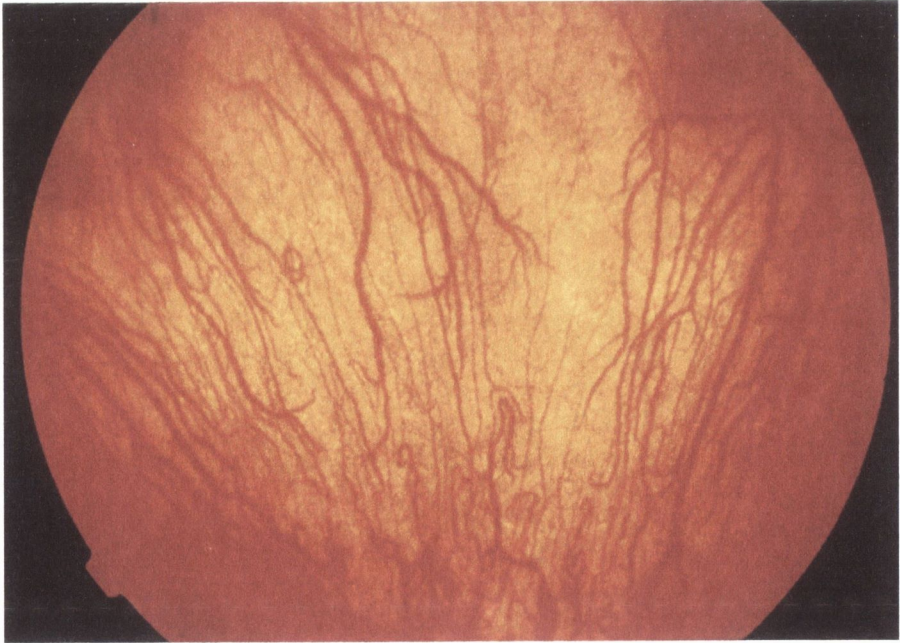
Figure 2. *A.* Fundus photograph of a retina from a mildly affected individual from family ZMK. Early stages of RP such as the thinning of the RPE and mild attenuation of the retinal blood vessels can be seen. *B.* Fundus photograph of a retina from a more severely affected individual from family ZMK. Severe thinning of the RPE and typical small pigment depositions are visible to the top right and left-hand sides of the photograph. A fundus photograph of a normal retina is shown in chapter 1 figure 4.

Figure 3.

A
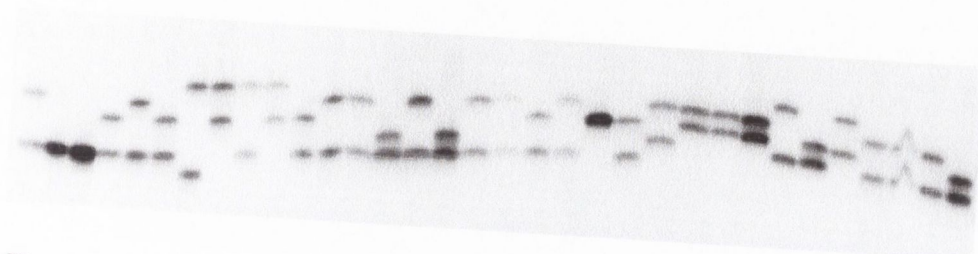
B
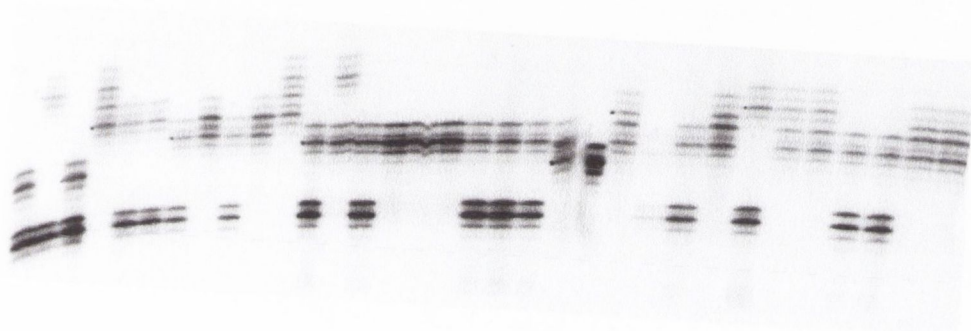
C
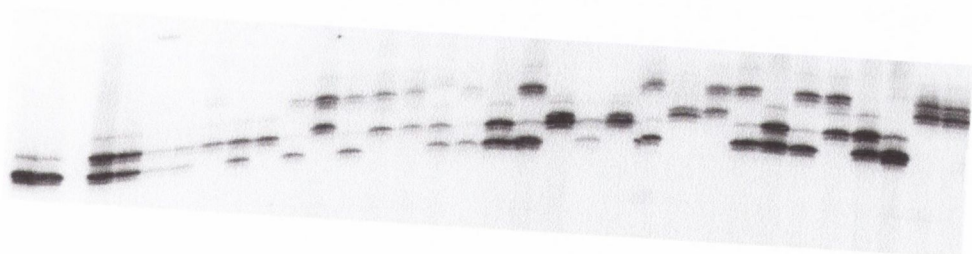
D
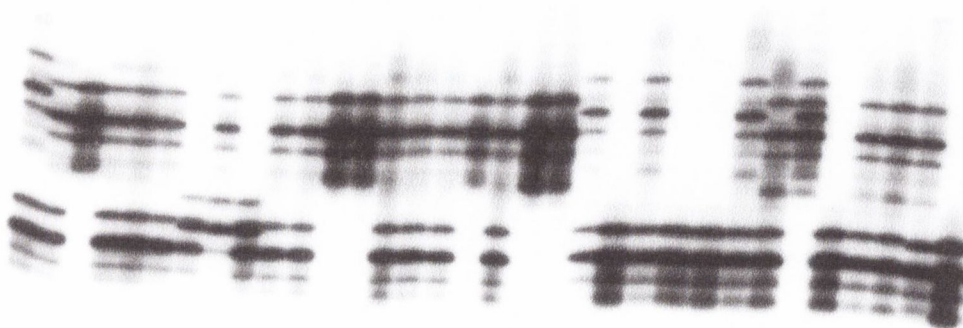
Figure 3. PCR amplification of microsatellite markers of DNAs from family ZMK run through polyacrylamide gels. *A*, D20S480. The lanes from left to right represent PCR amplifications of DNA from individuals 1-21 and 23-34 (see figure 1a). *B*, D17S1866. The lanes from left to right represent PCR amplifications of DNA from individuals 1-21 and 23-34 (see figure 1a). *C*, D19S878. The lanes from left to right represent PCR amplifications of DNA from individuals 1-21 and 23-34 (see figure 1a). *D*, SIS (chromosome 22). The lanes from left to right represent PCR amplifications of DNA from individuals 1-21 and 23-34 (see figure 1a for numbering). In *A-D* DNA from individual 22 was not amplified, becaused the laboratory ran out of DNA.

Figure 4.

A
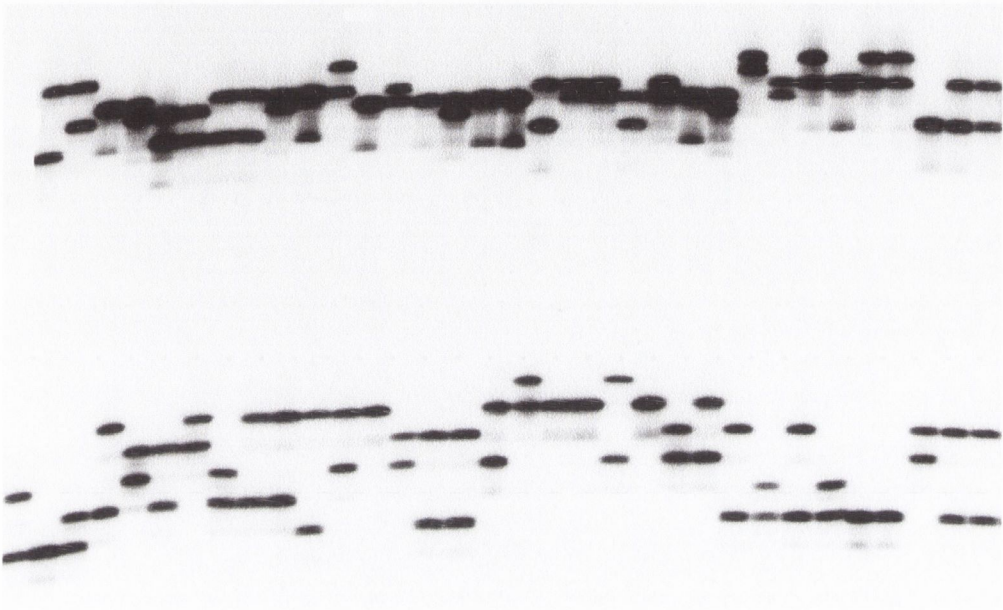
B
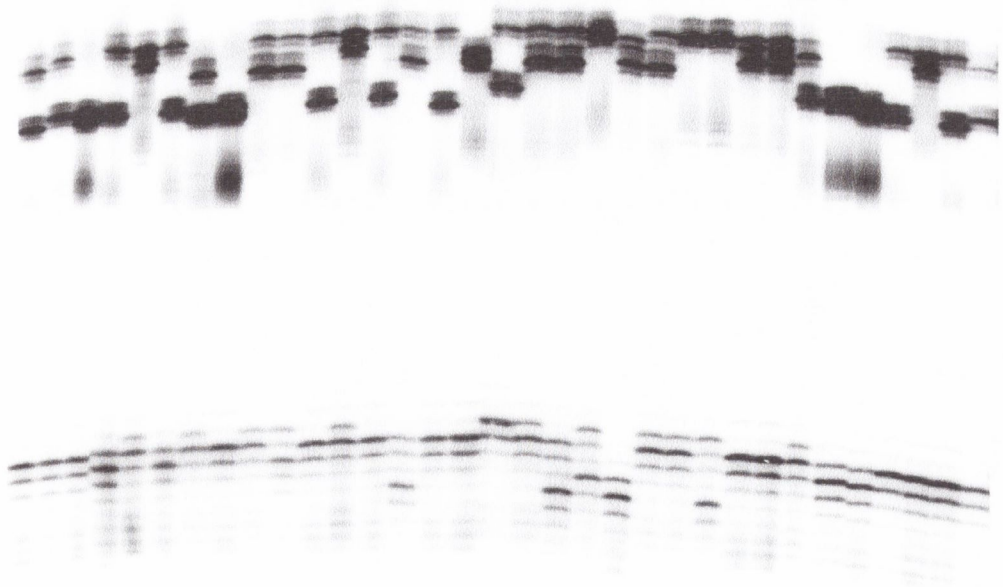
Figure 4. Duplex PCR of microsatellite markers of DNAs from family ZMK run through polyacrylamide gels. *A*, D7S820 (top) and D4S1647 (bottom). The lanes from left to right represent PCR amplifications of DNA from individuals 10-21, 23-34, and 1-9 (see figure 1a). *B*, D1S2890 (top), D1S197 (bottom). The lanes from left to right represent PCR amplifications of DNA from individuals 8-21, 23-34 and 1-7 (see figure 1a for numbering). In *A* and *B* DNA from individual 22 was not amplified, becaused the laboratory ran out of DNA.

Figure 5.

G A T C   G A T C
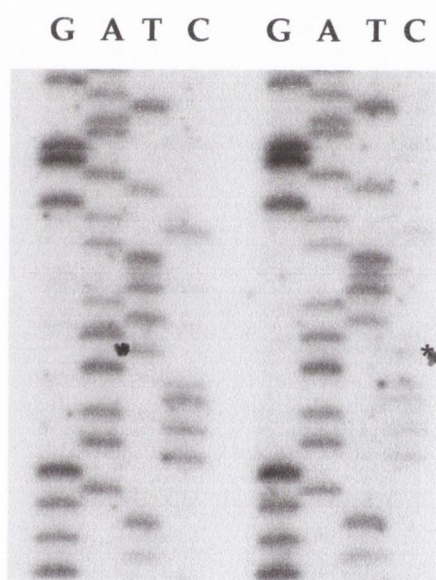
Figure 5. Direct sequence of two members of family ZMK. Left 3-23 who is married in to the family and right 3-22, who is an affected member of family ZMK. The bases G, A, T and C are shown above the appropriate lanes. The asterisks indicate the site of a known silent (H-H) polymorphism at position 6776 of the mitochondrial genome.

Species	Sequence
MTTS2 (mutation)	GAGAAAGCTCA----CAAGAACTGC-TAACT-CATGCCCCCATGTCTAAC-AA-CATGG**A**TTT-CTC
Human	GAGAAAGCTCA----CAAGAACTGC-TAACT-CATGCCCCCATGTCTAAC-AA-CATGG**C**TTT-CTC
Chimpanzee	GAGAAAGCTTA----TAAGAACTGC-TAATT-CATATCCCCATGCCTAAC-AA-CATGG**C**TTT-CTC
Gibbon	GAGAAAGCCCA----CAAGAACTGC-TAACT-CACTATCCCATGTATAAC-AA-CATGG**C**TTT-CTC
Mouse	AAGAAAGATTG----CAAGAACTGC-TAATT-CATGCTTCCATGTTTAAA-AA-CATGG**C**TTT-CTT
Rhinoceros	GAGAAAGCACT----CAAGAACTGC-TAACT-CATGCCCCCATATTTAAC-AA-TATGG**C**TTT-CTC
Cat	GAAAAAGTATG----CAAGAACTGC-TAATT-CATGCCTCCACGTATAAA-AA-CGTGG**C**TTT-TTC
Seal	GAAAAAGAATG----CAAGAACTGC-TAACT-CATGCCCCCACGTATAAA-AA-CGTGG**C**TTT-TTC
Horse	GAGAAAGTATG----CAAGAACTGC-TAATT-CATGCCCCCATGTCCAAC-AAACATGG**C**TCT-CTC
Donkey	GAGAA-GTATG----CAAGAACTGCCTAATT-CATGCTTCCGCGTCTGAC-AAACACGG**C**TCT-CTC
Opossum	GAGAATGCA-T----CAAGAACTGC-TAATT-CATGAACCCATATTTAAC-AA-TATGG**C**TTT-CTC
Platypus	GAGAGAGAA-A----TAAGAACTGC-TAATC-CTTAACTTCATGCCTAAC-CA-CATGA**C**TCTACTT
Vulture	GTTACAACCAG----CAGGAACTGC-TAACT-CTTGCATCTGAGTCTAAA-AC-CTCAG**C**CC-CCTT
Frog	GAACTTGACTGGACCTAAGAACTGC-TAATTACTTACG-CTGTG-TTCATTC--CACGG**C**TTG-TTC
	* ******* *** * * * *

Figure 6. Sequence alignment of the MTTS2 gene in various species. The asterisks indicate conserved bases. It is of note that the normal C base at position 12258, indicated with bold typeface in the table, is conserved between vertebrate species as diverse as human, mouse, platypus, vulture and frog. Drosophila, Saccheromyces Cerevisiae and Asterinia Pectinifera sequences were also examined but showed no consensus at the site of the mutation.

Type of US	Linkage	Gene
1A	14q34	Unknown
1B	11q13.5	Myosin VIIA
1C	11p15.1	Unknown
1D	10q	Unknown
1E	21q21	Unknown
1F	Unknown	Unknown
2A	1q41	USH2A
2B	10q	Unknown
3	3q21-q25	Unknown

Table 1. Summary of known US loci and the genes, if known, implicated in the disease.

marker\Θ	0.000	0.001	0.01	0.05	0.10	0.15	0.2	0.3	0.4	Θ (-2)	cM excl
D1S197	-99.99	-9.322	-4.374	-1.132	0.018	0.509	0.715	0.685	0.339	0.03	6.00
D1S2890	-99.99	-18.744	-10.812	-5.533	-3.545	-2.569	-1.970	-1.084	-0.424	0.175	36.74
D4S1647	-99.99	-22.927	-12.996	-6.313	-3.687	-2.309	-1.445	-0.340	-0.064	0.125	25.66
D6S305	-99.99	-22.894	-12.990	-6.367	-3.825	-2.536	-1.747	-0.813	-0.271	0.175	36.74
D7S820	-99.99	-10.276	-5.353	-2.146	-1.025	-0.555	-0.358	-0,311	-0.247	0.05	10.04
D14S1007	-99.99	-14.936	-8.029	-3.484	-1.816	-1.020	-0.571	-0.143	-0.016	0.09	18.20
D14S267	-99.99	-22.724	-12.800	-6.118	-3.503	-2.153	-1.327	-0.450	-0.103	0.15	30.92
D15S118	-99.99	-18.403	-10.461	-5.112	-3.013	-1.917	-1.232	-0.454	-0.098	0.125	25.56
LIPC (15)	-99.99	-6.703	-3.744	-1.800	-1.017	-0.573	-0.293	-0.039	-0.010	0.04	8.02
D16S411	-99.99	-9.167	-5.200	-2.521	-1.474	-0.933	-0.598	-0.220	-0.051	0.06	12.06
D17S789	-99.99	-11.868	-6.894	-3.512	-2.148	-1.409	-0.929	-0.363	-0.093	0.10	20.29
D17S926	-99.99	-23.261	-13.343	-6.674	-4.056	-2.675	-1.789	-0.727	-0.193	0.175	36.72
D17S928	-99.99	-1`7.364	-9.426	-4.080	-2.033	-1.028	-0.465	0.014	0.082	0.10	20.28
D17S1866	-99.99	-20.640	-11.685	-5.581	-3.179	-1.948	-1.207	-0.433	-0.125	0.125	25.56
D18S851	-99.99	-16.690	-8.784	-3.553	-1.615	-0.702	-0.224	0.062	-0.057	0.08	16.14
D19S215	-99.99	-25.355	-14.443	-7.085	-4.195	-2.688	-1.749	-0.683	-0.177	0.175	36.72
D19S222	-99.99	-9.676	-5.693	-2.972	-1.868	-1.261	-0.854	-0.341	-0.081	-0.09	18.10
D19S878	-99.99	-16.815	-8.884	-3.599	-1.596	-0.617	-0.073	0.348	0.272	0.08	16.14
D20S103	-99.99	-21.696	-12.740	-6.611	-4.114	-2.751	-1.859	-0.778	-0.224	0.175	36.74
D20S480	-99.99	-15.659	-8.715	-4.039	-2.211	-1.268	-0.696	-0.106	0.074	0.10	20.28
DXS1047	-99.99	-49.020	-30.046	-16.886	-11.332	-8.168	-5.991	-3.089	-1.233	0.30	69.32
DXS1060	-99.99	-26.177	-15.165	-7.522	-4.387	-2.689	-1.624	-0.418	0.049	0.175	36.74

Table 2. Two point lod-scores for various recombination fractions (Θ, row 1) of 22 markers run through family ZMK. In this study the initial diagnoses of all 34 members of family ZMK were utilised. The last two columns give Θ with a lod-score of less than -2 and the resulting exclusion (in cM) respectively.

Marker	0.000	0.001	0.050	0.100	0.150	0.200	0.250	0.300	0.400	0.500	Θ = -2	cM excl
D1S103 ®	-99.990	-7.560	-1.105	-0.248	0.107	0.258	0.300	0.279	0.143	0.000	0.03	6
D1S102 ®	-99.990	-9.451	-2.774	-1.655	-1.040	-0.645	-0.381	-0.204	-0.025	0.000	0.075	15
D1S189 Φ	-99.990	-15.338	-3.781	-2.020	-1.142	-0.632	-0.326	-0.148	-0.018	0.000	0.1	20
D1S193 Φ	-99.990	-1.966	1.016	1.201	1.133	0.967	0.758	0.537	0.159	0.000	0.001	0.2
D1S197 Σ	-99.990	-6.131	-0.947	-0.132	0.229	0.389	0.433	0.402	0.207	0.000	0.01	2
D1S199 Φ	-99.990	-10.115	-1.959	-0.802	-0.284	-0.033	0.070	0.085	0.020	0.000	0.05	10
D1S200 Φ	-99.990	-0.880	0.676	0.783	0.740	0.633	0.489	0.355	0.116	0.000	0	0
D1S201 Φ	-99.990	-0.373	1.007	0.998	0.879	0.726	0.561	0.397	0.116	0.000	0	0
D1S207 @	-99.990	-8.347	-1.924	-1.105	-0.785	-0.649	-0.570	-0.473	-0.209	0.000	0.05	10
D1S211 Φ	-99.990	-2.532	0.488	0.721	0.713	0.621	0.501	0.379	0.163	0.000	0.04	8
D1S213 Φ	-99.990	-5.366	-0.655	-0.142	0.013	0.044	0.036	0.022	0.013	0.000	0.01	0.2
D1S216 Φ	-99.990	-13.156	-3.295	-1.836	-1.131	-0.731	-0.490	-0.335	-0.132	0.000	0.085	17
D1S220 Φ	-99.990	-3.330	-0.253	0.036	0.096	0.083	0.051	0.020	-0.017	0.000	0.001	0.2
D1S228 Φ	-99.990	-9.400	-2.645	-1.494	-0.895	-0.546	-0.338	-0.215	-0.090	0.000	0.06	12
D1S230 @	-99.990	-8.091	-1.601	-0.706	-0.309	-0.115	-0.032	-0.015	-0.050	0.000	0.07	14
D1S235 Φ	-99.990	-5.423	-0.594	0.049	0.316	0.427	0.453	0.423	0.256	0.000	0.07	14
D1S243 Φ	-99.990	-12.888	-3.015	-1.542	-0.823	-0.417	-0.183	-0.058	0.012	0.000	0.07	14
D1S249 Φ	-99.990	-5.269	-0.578	-0.098	0.002	-0.042	-0.133	-0.203	-0.188	0.000	0.01	2
D1S255 Φ	-99.990	-2.877	0.157	0.406	0.416	0.348	0.257	0.173	0.061	0.000	0.04	8
D1S2890 Σ	-99.990	-8.108	-1.650	-0.794	-0.434	-0.267	-0.188	-0.145	-0.076	0.000	0.07	14
D1S463 Φ	-99.990	-4.983	-0.224	0.347	0.541	0.581	0.537	0.442	0.196	0.000	0.01	2
D1S547 Φ	-99.990	-8.634	-2.112	-1.187	-0.755	-0.513	-0.356	-0.241	-0.075	0.000	0.05	10
F13B®	-99.990	-0.150	1.191	1.132	0.962	0.761	0.561	0.378	0.100	0.000	0	0
D1S207 Φ	-99.990	-8.347	-1.924	-1.105	-0.785	-0.649	-0.570	-0.473	-0.209	0.000	0.05	10
D1S104 ®	-99.990	-14.360	-4.233	-2.530	-1.606	-1.014	-0.611	-0.335	-0.044	0.000	0.1	20
D1S305 Φ	-99.990	-10.824	-2.600	-1.370	-0.770	-0.429	-0.230	-0.118	-0.034	0.000	0.06	12
D1S242 Φ	-99.990	-8.643	-2.091	-1.129	-0.661	-0.389	-0.219	-0.110	-0.004	0.000	0.05	10
D1S238 Φ	-99.990	-15.891	-4.275	-2.449	-1.510	-0.941	-0.580	-0.356	-0.151	0.000	0.1	20
MYCL ®	-99.990	-4.593	0.090	0.581	0.699	0.673	0.583	0.467	0.228	0.000	0.001	0.2
D1S236 ®	-99.990	-8.942	-2.218	-1.144	-0.610	-0.309	-0.146	-0.062	-0.037	0.000	0.07	14
D1S53 Φ	-99.990	-8.415	-1.878	-0.926	-0.472	-0.222	-0.083	-0.011	0.015	0.000	0.07	14

Marker	0.000	0.001	0.050	0.100	0.150	0.200	0.250	0.300	0.400	0.500	Θ = -2	cM excl
APOB Φ	-99.990	-15.803	-4.238	-2.463	-1.570	-1.038	-0.701	-0.479	-0.204	0.000	0.125	25
CD8A Φ	-99.990	-13.143	-3.232	-1.717	-0.957	-0.511	-0.237	-0.074	0.049	0.000	0.08	16
CRYG1 Φ	-99.990	-56.694	-1.838	-1.145	-0.794	-0.565	-0.394	-0.259	-0.074	0.000	0.04	8
CTLA4 Φ	-99.990	-10.713	-2.488	-1.255	-0.657	-0.321	-0.131	-0.029	0.025	0.000	0.07	14
D2S111 Φ	-99.990	-13.232	-3.321	-1.805	-1.049	-0.608	-0.341	-0.182	-0.050	0.000	0.08	16
D2S116 Φ	-99.990	-3.362	-0.245	0.080	0.168	0.171	0.139	0.097	0.030	0.000	0.001	0.2
D2S123 Φ	-99.990	-16.727	-5.065	-3.186	-2.185	-1.544	-1.095	-0.766	-0.314	0.000	0.15	30
D2S125 @	-99.990	-8.592	-2.076	-1.148	-0.704	-0.448	-0.286	-0.177	-0.048	0.000	0.05	10
D2S131 Φ	-99.990	-15.901	-4.332	-2.539	-1.629	-1.081	-0.728	-0.484	-0.208	0.000	0.13	26
D2S139 @	-99.990	-3.175	-0.102	0.177	0.217	0.171	0.092	0.016	-0.046	0.000	0.001	0.2
D2S159 @	-99.990	-2.931	0.161	0.458	0.517	0.489	0.424	0.345	0.177	0.000	0.001	0.2
IL1A Φ	-99.990	-21.104	-6.074	-3.636	-2.333	-1.503	-0.938	-0.547	-0.111	0.000	0.17	34
D2S114 @	-99.990	-8.182	-1.732	-0.866	-0.489	-0.299	-0.194	-0.129	-0.043	0.000	0.05	10
D2S135 @	-99.990	-8.960	-2.426	-1.469	-0.986	-0.681	-0.466	-0.308	-0.104	0.000	0.07	14
2DS144 @	-99.990	-16.766	-4.842	-2.871	-1.841	-1.206	-0.789	-0.506	-0.175	0.000	0.13	26
D2S164 @	-99.990	-13.101	-3.236	-1.763	-1.049	-0.646	-0.412	-0.275	-0.129	0.000	0.08	16
D2S171 @	-99.990	-4.842	-2.871	-1.841	-1.206	-0.789	-0.506	-0.311	-0.075	0.000	0.08	16
D2S172 @	-99.990	-5.283	-0.564	-0.032	0.146	0.193	0.183	0.148	0.060	0.000	0.001	0.2
D2S177 @	-99.990	-21.016	-5.983	-3.549	-2.263	-1.458	-0.922	-0.557	-0.148	0.000	0.17	34

Marker	0.000	0.001	0.050	0.100	0.150	0.200	0.250	0.300	0.400	0.500	Θ = -2	cM excl
D3S1265 Φ	-99.990	-7.567	-0.961	-0.020	0.371	0.521	0.533	0.457	0.194	0.000	0.02	4
D3S1267 Φ	-99.990	-12.692	-2.790	-1.287	-0.556	-0.155	0.055	0.139	0.088	0.000	0.07	14
D3S1300 Φ	-99.990	-14.349	-4.462	-2.911	-2.020	-1.380	-0.902	-0.548	-0.127	0.000	0.15	30
D3S1228 ®	-99.990	-18.854	-5.505	-3.345	-2.187	-1.442	-0.926	-0.560	-0.131	0.000	0.15	30
D3S1262 Φ	-99.990	-8.020	-1.508	-0.580	-0.152	0.069	0.176	0.210	0.147	0.000	0.01	2
D3S1279 Φ	-99.990	0.070	1.456	1.445	1.316	1.146	0.957	0.763	0.377	0.000	0	0
D3S1284 Φ	-99.990	-9.746	-1.618	-0.491	0.004	0.237	0.328	0.333	0.200	0.000	0.03	6
D3S1286 Φ	-99.990	-18.166	-4.887	-2.803	-1.726	-1.065	-0.637	-0.356	-0.071	0.000	0.17	34
D3S1291 Φ	-99.990	-13.264	-3.352	-1.837	-0.076	-0.623	-0.340	-0.163	-0.003	0.000	0.09	18
D3S1297 Φ	-99.990	-8.820	-1.837	-0.753	-0.256	-0.006	0.106	0.130	0.044	0.000	0.01	2
D3S1298 Φ	-99.990	-8.663	-2.123	-1.164	-0.693	-0.418	-0.249	-0.144	-0.038	0.000	0.05	10
D3S1299 Φ	1.507	1.502	1.268	1.042	0.835	0.651	0.491	0.356	0.146	0.000	0	0
D3S1307 Φ	-99.990	-8.820	-1.838	-0.756	-0.260	-0.011	0.098	0.117	0.016	0.000	0.01	2
D3S1314 Φ	-99.990	-5.109	-0.333	0.261	0.428	0.551	0.538	0.474	0.260	0.000	0.001	0.2
D3S1595 Φ	-99.990	-8.561	-1.979	-0.981	-0.487	-0.200	-0.029	0.065	0.101	0.000	0.05	10
D3S196 Φ	-2.772	-1.286	0.178	0.278	0.279	0.250	0.209	0.163	0.072	0.000	0	0
D3S47 ®	-99.990	-12.366	-2.524	-1.081	-0.400	-0.037	0.147	0.218	0.163	0.000	0.07	14
D3S659 ®	-99.990	-12.869	-2.979	-1.489	-0.755	-0.335	-0.090	0.044	0.104	0.000	0.08	16
GLUT2 Φ	-99.990	-20.841	-5.835	-3.417	-2.136	-1.331	-0.793	-0.432	-0.063	0.000	0.15	30
RHO ®	1.251	1.247	1.049	0.858	0.682	0.522	0.381	0.262	0.093	0.000	0	0

Marker	0.000	0.001	0.050	0.100	0.150	0.200	0.250	0.300	0.400	0.500	$\Theta = -2$	cM excl
D4S1552 Σ	-99.990	-9.115	-3.643	-1.741	-1.316	-1.063	-0.875	-0.702	-0.347	0.000	0.08	16
D4S1585 Σ	-99.990	-11.252	-3.008	-1.730	-1.087	-0.682	-0.411	-0.227	-0.031	0.000	0.08	16
D4S1599 Σ	-99.990	-15.878	-4.282	-2.478	-1.548	-0.975	-0.596	-0.340	-0.063	0.000	0.125	25
D4S1647 Σ	-99.990	-4.915	-2.805	-1.706	-1.027	-0.584	-0.296	-0.118	-0.009	0.000	0.08	16
D4S171 ®	-99.990	-15.878	-4.313	-2.527	-1.607	-1.037	-0.658	-0.402	-0.132	0.000	0.12	24
D4S174 ®	-99.990	-19.134	-5.671	-3.440	-2.239	-1.470	-0.944	-0.576	-0.150	0.000	0.16	32
D4S175 Φ	-99.990	-8.708	-2.163	-1.192	-0.711	-0.426	-0.246	-0.132	-0.022	0.000	0.05	10
D4S227 ®	-99.990	-1.308	0.290	0.454	0.474	0.434	0.364	0.282	0.118	0.000	0	0
D4S231 Σ	-99.990	-11.920	-3.436	-2.023	-1.277	-0.812	-0.505	-0.297	-0.071	0.000	0.1	20
D4S412 Σ	-99.990	-16.196	-4.640	-2.854	-1.924	-1.329	-0.910	-0.601	0.207	0.000	0.13	26
D4S428 Σ	-99.990	-2.504	0.580	0.863	0.900	0.837	0.725	0.587	0.288	0.000	0.001	0.2
D4S43 Σ	-99.990	-4.141	-0.923	-0.415	-0.188	-0.099	-0.085	-0.105	-0.138	0.000	0.01	2
GABRB1 ®	-99.990	-15.878	-4.282	-2.478	-1.548	-0.975	-0.596	-0.340	-0.063	0.000	0.125	25

Marker	0.000	0.001	0.050	0.100	0.150	0.200	0.250	0.300	0.400	0.500	$\Theta = -2$	cM excl
CFSIR ®	-99.990	-6.391	-1.491	-0.774	-0.430	-0.236	-0.121	-0.053	0.005	0.000	0.02	4
D5S108 Φ	-99.990	-1.532	-0.004	0.122	0.134	0.118	0.097	0.077	0.036	0.000	0	0
D5S111 Φ	-99.990	-1.112	0.312	0.347	0.283	0.201	0.129	0.075	0.016	0.000	0	0
D5S117 Φ	-99.990	-18.364	-5.065	-2.961	-1.863	-1.176	-0.720	-0.409	-0.073	0.000	0.125	25
D5S118 Φ	-99.990	-3.755	-0.610	-0.249	-0.116	-0.057	-0.027	-0.009	0.004	0.000	0.001	0.2
D5S119 Φ	1.278	1.273	1.064	0.864	0.679	0.513	0.367	0.244	0.071	0.000	0	0
D5S210 Φ	-99.990	-5.771	-0.988	-0.388	-0.156	-0.061	-0.028	-0.020	-0.015	0.000	0.01	2
D5S211 Φ	-99.990	-13.468	-3.590	-2.093	-1.330	-0.859	-0.547	-0.335	-0.193	0.000	0.1	20
D5S39 Φ	-99.990	-15.944	-4.248	-2.374	-1.402	-0.808	-0.428	-0.187	0.026	0.000	0.125	25
D5S400 Φ	-99.990	-13.095	-3.198	-1.700	-0.962	-0.540	-0.292	-0.150	-0.037	0.000	0.08	16
D5S408 Φ	-99.990	-6.271	-1.418	-0.756	-0.456	-0.292	-0.190	0.119	0.030	0.000	0.02	4
D5S414 Φ	-99.990	-15.399	-3.816	-2.036	-1.139	-0.611	-0.287	-0.095	0.045	0.000	0.1	20
D5S416 Φ	-99.990	-12.166	-3.752	-2.251	-1.420	-0.891	-0.537	-0.299	0.050	0.000	0.12	24
D5S418 Φ	-99.990	-11.389	-2.812	-1.437	-0.760	-0.377	-0.158	-0.043	0.400	0.000	0.08	16
D5S421 Φ	-99.990	-2.909	-0.184	0.485	0.546	0.514	0.433	0.327	0.108	0.000	0.001	0.2
D5S428 Φ	-99.990	-10.835	-2.575	-1.324	-0.710	-0.360	-0.154	-0.037	0.041	0.000	0.07	14
FIB5 Φ	-99.990	-16.317	-3.878	-1.546	-0.384	0.294	0.353	0.312	0.218	0.000	0.08	16

Marker	0.000	0.001	0.050	0.100	0.150	0.200	0.250	0.300	0.400	0.500	Θ = -2	cM excl
D6S249 @	-99.990	-10.496	-2.292	-1.083	-0.507	-0.192	-0.020	-0.064	0.079	0.000	0.07	14
D6S252 @	-99.990	-0.296	1.076	1.052	0.923	0.768	0.608	0.448	0.155	0.000	0	0
D6S257 @	-99.990	-9.748	-1.614	-0.489	-0.002	0.217	0.283	0.253	0.059	0.000	0.03	6
D6S261 Σ	-99.990	-13.060	-3.173	-1.679	-0.944	-0.526	-0.280	-0.140	-0.029	0.000	0.08	16
D6S271 @	-99.990	-12.563	-2.673	-1.181	-0.456	-0.057	0.157	0.251	0.207	0.000	0.07	14
D6S281 @	-99.990	-15.941	-4.360	-2.579	-1.677	-1.130	-0.768	-0.513	-0.176	0.000	0.125	25
D6S285 @	-99.990	-13.428	-3.448	-1.883	-1.093	-0.628	-0.343	-0.173	-0.027	0.000	0.08	16
D6S291 @	-99.990	-11.243	-3.018	-1.767	-1.131	-0.741	-0.483	-0.306	-0.099	0.000	0.08	16
D6S305 Σ	-99.990	-15.904	-4.362	-2.600	-1.709	-1.167	-0.807	-0.551	-0.214	0.000	0.125	25
D6S309 @	-99.990	-8.188	-1.686	-0.782	-0.376	-0.166	-0.055	0.002	0.040	0.000	0.02	4
D6S310 @	-99.990	-12.197	-3.339	-1.815	-1.024	-0.547	-0.250	-0.070	0.062	0.000	0.08	16
D6S87 @	-99.990	-3.311	-0.126	0.253	0.380	0.404	0.376	0.317	0.161	0.000	0.001	0.2
D6S89 ®	-99.990	-5.989	-1.159	-0.519	-0.244	-0.108	-0.040	-0.007	0.014	0.000	0.02	4
RDS ®	-99.990	-7.409	-0.977	-0.136	0.203	0.339	0.366	0.329	0.161	0.000	0.01	2
D6S206 @	-99.990	-22.504	-5.912	-3.305	-1.963	-1.151	-0.639	-0.327	-0.097	0.000	0.15	30
D6S251 @	-99.990	-5.690	-0.908	-0.317	-0.082	0.026	0.071	0.080	0.045	0.000	0.01	2

Marker	0.000	0.001	0.050	0.100	0.150	0.200	0.250	0.300	0.400	0.500	Θ = -2	cM excl
CFTR ®	-99.990	-13.295	-3.374	-1.840	-1.061	-0.596	-0.307	-0.132	0.000	0.000	0.08	16
D7S1818 Φ	-99.990	-8.321	-1.816	-0.907	-0.496	-0.285	-0.173	-0.114	-0.048	0.000	0.01	2
D7S466 ®	-99.990	-8.567	-2.059	-1.134	-0.691	-0.433	-0.267	-0.154	-0.076	0.000	0.05	10
D7S471 ®	-99.990	-18.416	-5.087	-2.951	-1.831	-1.139	-0.688	-0.394	-0.107	0.000	0.125	25
D7S485 Φ	-99.990	-5.041	-0.257	0.317	0.508	0.539	0.483	0.379	0.130	0.000	0.001	0.2
D7S486 ®	-99.990	-16.357	-4.723	-2.876	-1.906	-1.295	-0.879	-0.583	-0.208	0.000	0.14	28
D7S493 Φ	-99.990	-6.424	-1.550	-0.849	-0.511	-0.313	-0.188	-0.105	-0.015	0.000	0.01	2
D7S495 Φ	-99.990	-8.090	-1.637	-0.766	-0.389	-0.206	-0.117	-0.075	-0.034	0.000	0.03	6
D7S505 Φ	-99.990	-3.820	-0.665	-0.292	-0.147	-0.080	-0.047	-0.030	-0.013	0.000	0.001	0.2
D7S507 Φ	-99.990	-15.743	-4.162	-2.377	-1.470	-0.923	-0.570	-0.338	0.085	0.000	0.125	25
D7S514 ®	-99.990	-9.141	-2.548	-1.480	-0.888	-0.508	-0.262	-0.113	-0.009	0.000	0.07	14
D7S517 Φ	-99.990	-5.802	-0.939	-0.280	-0.000	0.124	0.164	0.157	0.082	0.000	0.01	2
D7S460 Φ	-99.990	-11.334	-3.097	-1.784	-1.079	-0.637	-0.351	-0.171	-0.011	0.000	0.08	16
D7S523 ®	-99.990	-13.274	-3.359	-1.830	-1.057	-0.594	-0.304	-0.124	0.028	0.000	0.08	16
D7S530 Φ	-99.990	-9.333	-2.735	-1.726	-1.206	-0.876	-0.642	-0.461	-0.191	0.000	0.07	14
D7S550 Φ	-99.990	-7.419	-0.951	-0.090	0.263	0.401	0.416	0.353	0.117	0.000	0.01	2
D7S820 Σ	-99.990	-5.734	-0.905	-0.285	-0.059	0.001	-0.026	-0.088	-0.146	0.000	0.01	2

Marker	0.000	0.001	0.050	0.100	0.150	0.200	0.250	0.300	0.400	0.500	Θ = -2	cM excl
ANK1 ®	-99.990	-8.178	-1.178	-0.786	-0.383	-0.182	-0.083	-0.041	-0.019	0.000	0.01	2
D8S198 Σ	-99.990	-2.785	0.314	0.608	0.652	0.597	0.494	0.372	0.139	0.000	0.001	0.2
D8S201 ®	-99.990	-8.969	-2.382	-1.350	-0.804	-0.463	-0.246	-0.114	-0.011	0.000	0.07	14
D8S257 Σ	-99.990	-6.237	-1.389	-0.722	-0.413	-0.413	-0.134	-0.069	-0.006	0.000	0.02	4
D8S260 Σ	-99.990	-10.470	-2.316	-1.162	-0.634	-0.362	-0.224	-0.164	-0.119	0.000	0.06	12
D8S261 Σ	-99.990	-10.637	-2.532	-1.412	-0.915	-0.661	-0.524	-0.437	-0.267	0.000	0.07	14
D8S264 ®	-99.990	-12.940	-3.094	-1.647	-0.957	-0.580	-0.372	-0.261	-0.142	0.000	0.08	16
D8S265 Σ	-99.990	-9.660	-2.822	-1.659	-1.050	-0.680	-0.441	-0.282	-0.099	0.000	0.08	16
D8S272 Σ	-99.990	-8.447	-1.966	-1.073	-0.673	-0.460	-0.329	-0.233	-0.083	0.000	0.05	10
D8S275 Σ	-99.990	-3.814	-0.666	-0.283	-0.128	-0.053	-0.013	0.008	0.024	0.000	0.001	0.2
D8S277 Σ	-99.990	-9.253	-2.465	-1.340	-0.768	-0.434	-0.234	-0.118	-0.023	0.000	0.07	14
D8S283 Σ	-99.990	-10.524	-2.380	-1.210	-0.655	-0.349	-0.177	-0.088	-0.037	0.000	0.07	14
D8S373 Σ	-99.990	-18.277	-4.976	-2.872	-1.777	-1.101	-0.659	-0.368	-0.074	0.000	0.125	25
D8S556 Σ	-99.990	-14.517	-4.217	-2.457	-1.519	-0.931	-0.543	-0.119	0.013	0.000	0.125	25
D8S87 ®	-99.990	-3.659	-0.486	-0.112	0.019	0.059	0.059	0.045	0.017	0.000	0.001	0.2
D8S265 Σ	-99.990	-9.660	-2.822	-1.659	-1.050	-0.680	-0.441	-0.282	-0.099	0.000	0.07	14
MYC Σ	-99.990	-14.642	-4.703	-3.057	-2.071	-1.380	-0.887	-0.536	-0.134	0.000	0.15	30

Marker	0.000	0.001	0.050	0.100	0.150	0.200	0.250	0.300	0.400	0.500	Θ = -2	cM excl
D10S107 Φ	-99.990	-3.855	-0.595	-0.138	0.057	0.143	0.169	0.160	0.091	0.000	0.001	0.2
D10S109 Φ	-99.990	-13.980	-4.118	-2.632	-1.878	-1.405	-1.067	-0.800	-0.365	0.000	0.13	26
D10S111 Φ	-99.990	-5.897	-1.102	-0.497	-0.242	-0.111	-0.038	-0.004	-0.014	0.000	0.01	2
D10S179 Φ	-99.990	-16.966	-4.845	-2.780	-1.684	-1.002	-0.557	-0.268	-0.003	0.000	0.13	26
D10S187 Φ	-99.990	-12.994	-3.097	-1.601	-0.862	-0.435	-0.181	-0.037	0.044	0.000	0.08	16
D10S198 Φ	-99.990	-1.399	0.089	0.195	0.197	0.169	0.132	0.096	0.039	0.000	0	0
D10S209 Φ	1.313	1.308	1.074	0.854	0.658	0.490	0.345	0.220	0.037	0.000	0	0
D10S214 Φ	-99.990	-4.723	-1.233	-0.653	-0.366	-0.205	-0.113	-0.064	-0.029	0.000	0.02	4
D10S216 Φ	-99.990	-5.569	-0.743	-0.131	0.097	0.171	0.170	0.134	0.043	0.000	0.005	1
D10S217 Φ	-99.990	-12.334	-1.088	-0.230	-0.089	0.079	0.140	0.135	0.095	0.000	0.005	1
D10S222 Φ	-99.990	-13.884	-3.866	-2.249	-1.400	-0.872	-0.526	-0.297	-0.064	0.000	0.12	24
D10S558 Φ	-99.990	-13.327	-3.430	-1.932	-1.184	-0.739	-0.454	-0.264	-0.051	0.000	0.1	20
D10S570 Φ	-99.990	-14.238	-3.707	-1.993	-1.129	-0.620	-0.305	-0.112	0.040	0.000	0.1	20
D10S583 Φ	-99.990	-16.966	-4.845	-2.780	-1.684	-1.002	-0.557	-0.268	-0.003	0.000	0.13	26
D10S587 Φ	-99.990	-13.659	-3.711	-2.160	-1.372	-0.898	-0.594	-0.391	-0.151	0.000	0.13	26
D10S590 Φ	-99.990	-2.056	-0.468	-0.250	-0.146	-0.088	-0.057	-0.042	-0.027	0.000	0.001	0.2
D10S89 Φ	-99.990	-5.985	-1.077	-0.365	-0.041	0.119	0.185	0.189	0.091	0.000	0.03	6

Marker	0.000	0.001	0.050	0.100	0.150	0.200	0.250	0.300	0.400	0.500	$\Theta = -2$	cM excl
CD3D ®	-99.990	-9.631	-1.495	-0.369	0.118	0.335	0.402	0.376	0.190	0.000	0.04	8
D11S1324 Φ	-99.990	-13.247	-3.324	-1.799	-1.026	-0.565	-0.277	-0.099	0.043	0.000	0.08	16
D11S1344 Φ	-99.990	-13.554	-3.567	-1.983	-1.162	-0.662	-0.346	-0.151	0.004	0.000	0.1	20
D11S29 ®	-99.990	-9.626	-1.484	-0.351	0.144	0.370	0.444	0.422	0.220	0.000	0.03	6
D11S35 ®	-99.990	-7.535	-1.086	-0.237	0.101	0.225	0.237	0.190	0.066	0.000	0.03	6
D11S419 ®	-99.990	-4.340	-1.073	-0.598	-0.366	-0.229	-0.141	-0.083	0.019	0.000	0.03	6
D11S490 ®	-99.990	-9.999	-1.829	-0.667	-0.140	0.122	0.235	0.255	0.149	0.000	0.03	6
D11S527 Φ	-99.990	-12.705	-3.411	-1.744	-0.905	-0.419	-0.134	0.024	0.102	0.000	0.08	16
D11S528 ®	-99.990	-3.623	-0.481	-0.132	-0.025	-0.003	-0.011	0.022	0.015	0.000	0.001	0.2
D11S534 Φ	-99.990	-12.731	-2.882	-1.429	-0.731	-0.340	-0.115	0.011	0.087	0.000	0.06	12
D11S836 ®	-99.990	-4.443	-0.961	-0.408	-0.152	0.024	0.033	0.047	0.021	0.000	0.001	0.2
D11S874 ®	-99.990	-1.495	0.433	0.661	0.679	0.609	0.495	0.362	0.115	0.000	0	0
D11S900 Φ	-99.990	-5.564	-0.738	-0.117	0.124	0.211	0.217	0.181	0.070	0.000	0.01	2
D11S901 Φ	-99.990	-7.120	-0.705	0.102	0.405	0.501	0.487	0.411	0.183	0.000	0.01	2
D11S906 Φ	0.161	0.159	0.038	-0.058	-0.114	-0.129	-0.115	-0.084	--0.021	0.000	0	0
D11S910 Φ	-99.990	-2.297	0.799	1.083	1.108	1.020	0.868	0.676	0.255	0.000	0.001	0.2
D11S912 Φ	-99.990	-1.814	1.169	1.357	1.295	1.135	0.932	0.713	0.295	0.000	0	0
D11S914 Φ	-99.990	-0.871	0.523	0.530	0.437	0.324	0.221	0.142	0.053	0.000	0	0
D11S917 Φ	-99.990	-9.405	-1.295	-0.193	0.271	0.468	0.515	0.470	0.243	0.000	0.03	6
D11S920 Φ	-99.990	-3.937	-0.511	-0.025	0.157	0.213	0.205	0.166	0.062	0.000	0.01	2
D11S925 Φ	-99.990	-12.788	-2.923	-1.455	-0.748	-0.359	-0.145	-0.040	0.009	0.000	0.08	16
D11S927 Φ	-99.990	-2.701	0.389	0.676	0.716	0.658	0.551	0.424	0.177	0.000	0.001	0.2
D11S934 Φ	-99.990	-5.390	-0.333	0.380	0.646	0.714	0.665	0.543	0.201	0.000	0.001	0.2
D11S935 Φ	-99.990	-2.685	0.434	0.730	0.752	0.658	0.506	0.334	0.045	0.000	0.001	0.2
D11S937 Φ	-99.990	-13.340	-3.430	-1.924	-1.166	-0.712	-0.421	-0.227	-0.022	0.000	0.1	20
D11S968 Φ	-99.990	0.104	1.467	1.422	1.254	1.037	0.805	0.576	0.189	0.000	0	0
D11S969 Φ	-99.990	-1.901	1.118	1.319	1.255	1.076	0.832	0.553	0.055	0.000	0.001	0.2
DRD2 ®	1.278	1.273	1.064	0.863	0.679	0.513	0.367	0.244	0.071	0.000	0	0
HBE1 Φ	-99.990	-8.439	-1.902	-0.956	-0.501	-0.242	-0.090	-0.004	0.042	0.000	0.05	10
D11S1309 Φ	-99.990	-2.211	0.836	1.080	1.076	0.970	0.808	0.614	0.207	0.000	0.001	0.2
TH ®	-99.990	-15.408	-3.825	-2.037	-1.133	-0.598	-0.267	-0.067	0.078	0.000	0.1	20

Marker	0.000	0.001	0.050	0.100	0.150	0.200	0.250	0.300	0.400	0.500	Θ = -2	cM excl
D12S341 Σ	-99.990	-11.606	-3.328	-2.025	-1.337	-0.899	-0.597	-0.383	-0.118	0.000	0.1	20
D12S342 Σ	-99.990	-6.136	-1.275	-0.604	-0.300	-0.139	-0.053	-0.010	0.011	0.000	0.03	6
D12S357 Σ	-99.990	-17.711	-4.454	-2.389	-1.338	-0.711	-0.323	-0.093	0.065	0.000	0.12	24
D12S364 Σ	-99.990	-10.724	-2.539	-1.337	-0.760	-0.435	-0.243	-0.130	-0.034	0.000	0.06	12
D12S43 ®	-99.990	-16.728	-5.067	-3.170	-2.143	-1.475	-1.007	-0.667	-0.234	0.000	0.15	30
D12S78 Σ	-99.990	-14.547	-4.355	-2.591	-1.629	-1.015	-0.602	-0.322	-0.034	0.000	0.13	26
D12S79 Σ	-99.990	-18.015	-4.741	-2.661	-1.594	-0.949	-0.543	-0.291	-0.070	0.000	0.13	26
D12S81 Σ	-99.990	-15.639	-4.048	-2.255	-1.341	-0.791	-0.443	-0.223	-0.022	0.000	0.12	24
D12S87 Σ	-99.990	-13.514	-3.605	-2.086	-1.309	-0.829	-0.506	-0.283	-0.038	0.000	0.1	20
D12S90 Σ	-99.990	-5.346	-0.630	-0.119	0.020	0.017	-0.045	-0.110	-0.113	0.000	0.001	0.2
IGF1 ®	-99.990	-16.558	-4.618	-2.635	-1.600	-0.966	-0.558	-0.296	-0.046	0.000	0.13	26

Marker	0.000	0.001	0.050	0.100	0.150	0.200	0.250	0.300	0.400	0.500	Θ = -2	cM excl
D13S156 Φ	-99.990	-8.436	-1.837	-0.855	-0.397	-0.159	-0.044	-0.002	-0.015	0.000	0.04	8
D13S158 Φ	-99.990	-16.862	-5.225	-3.272	-2.164	-1.426	-0.909	-0.542	-0.118	0.000	0.15	30
D13S168 Φ	1.386	1.381	1.154	0.940	0.742	0.560	0.397	0.258	0.071	0.000	0	0
D13S173 Φ	-99.990	-6.661	-1.740	-1.001	-0.626	-0.397	-0.247	-0.147	-0.039	0.000	0.04	8
D13S175 Φ	-99.990	-3.835	-0.713	-0.371	-0.250	-0.193	-0.151	-0.110	-0.036	0.000	0.001	0.2
D13S218 Φ	-99.990	-1.640	-0.140	-0.017	0.004	-0.006	-0.023	-0.040	-0.047	0.000	0	0
D13S221 Φ	-99.990	-19.372	-5.837	-3.575	-2.344	-1.551	-1.007	-0.625	-0.178	0.000	0.17	34
D13S285 Φ	-99.990	-12.927	-3.034	-1.545	-0.812	-0.394	-0.148	-0.011	0.067	0.000	0.08	16
D13S71 Φ	-99.990	-10.759	-2.563	-1.354	-0.774	-0.453	-0.270	-0.168	-0.071	0.000	0.06	12
FLT1 Φ	-99.990	-1.409	0.084	0.188	0.186	0.152	0.110	0.070	0.014	0.000	0	0
D13S328 Φ	-99.990	-2.347	0.714	0.967	0.966	0.862	0.704	0.517	0.143	0.000	0.001	0.2

Marker	0.000	0.001	0.050	0.100	0.150	0.200	0.250	0.300	0.400	0.500	Θ = -2	cM excl
D14S1007 Σ	-99.990	-7.961	-1.427	-0.519	-0.130	0.042	0.101	0.100	0.048	0.000	0.04	8
D14S261 Σ	-99.990	-0.695	0.731	0.771	0.700	0.590	0.466	0.340	0.123	0.000	0	0
D14S267 Σ	-99.990	-18.637	-5.293	-3.147	-2.009	-1.293	-0.812	-0.484	-0.119	0.000	0.15	30
D14S288 Σ	-99.990	-9.949	-1.800	-0.658	-0.151	0.091	0.188	0.196	0.090	0.000	0.04	8
D14S43 Φ	-99.990	-2.563	0.453	0.660	0.618	0.481	0.312	0.152	-0.019	0.000	0.001	0.2
D14S45 Φ	-99.990	-13.305	-3.441	-1.953	-1.196	-0.730	-0.423	-0.219	-0.021	0.000	0.1	20
D14S592 Φ	-99.990	-8.708	-2.183	-1.224	-0.745	-0.456	-0.269	-0.145	-0.017	0.000	0.05	10
D14S68 Σ	-99.990	-10.814	-2.666	-1.504	-0.953	-0.646	-0.466	-0.355	-0.203	0.000	0.08	16
P1 Φ	-99.990	-6.089	-1.215	-0.543	-0.249	-0.105	-0.039	-0.013	-0.004	0.000	0.02	4

Marker	0.000	0.001	0.050	0.100	0.150	0.200	0.250	0.300	0.400	0.500	$\Theta = -2$	cM excl
D15S122 Σ	-99.990	-8.817	-2.322	-1.393	-0.935	-0.647	-0.440	-0.283	-0.080	0.000	0.06	12
D15S165 Φ	-99.990	-3.009	-0.013	0.274	0.321	0.286	0.225	0.164	0.069	0.000	0.001	0.2
D15S211 Φ	-99.990	-16.190	-4.548	-2.698	-1.725	-1.113	-0.700	-0.416	-0.096	0.000	0.13	26
D15S652 Φ	-99.990	-13.511	-3.619	-2.103	-1.332	-0.859	-0.545	-0.329	0.082	0.000	0.1	20
D15S659 Φ	-99.990	-12.457	-2.597	-1.144	-0.454	-0.084	0.106	0.180	0.119	0.000	0.06	12
D15S87 Σ	-99.990	-0.994	0.453	0.515	0.471	0.396	0.313	0.235	0.103	0.000	0	0
FES ®	-99.990	-9.715	-2.928	-1.799	-1.197	-0.813	-0.549	-0.359	-0.119	0.000	0.07	14

Marker	0.000	0.001	0.050	0.100	0.150	0.200	0.250	0.300	0.400	0.500	$\Theta = -2$	cM excl
D16S265 Φ	-99.990	-5.557	-0.785	-0.200	0.027	0.120	0.147	0.137	0.065	0.000	0.001	0.2
D16S287 Φ	-99.990	-2.988	0.061	0.312	0.327	0.268	0.189	0.120	0.037	0.000	0.001	0.2
D16S403 Φ	-99.990	-15.811	-4.209	-2.403	-1.475	-0.909	-0.541	-0.298	-0.046	0.000	0.12	24
D16S406 Φ	-99.990	-6.874	-2.057	-1.405	-1.059	-0.788	-0.550	-0.352	-0.088	0.000	0.05	10
D16S411 Σ	-99.990	-6.186	-1.337	-0.682	-0.400	-0.259	-0.182	-0.134	-0.067	0.000	0.03	6
D16S422 Φ	-99.990	-13.720	-3.818	-2.295	-1.517	-1.034	-0.704	-0.464	-0.149	0.000	0.12	24
D16S521 Φ	-99.990	-19.972	-5.576	-3.343	-2.153	-1.400	-0.893	-0.543	-0.144	0.000	0.15	30

Marker	0.000	0.001	0.050	0.100	0.150	0.200	0.250	0.300	0.400	0.500	$\Theta = -2$	cM excl
CA14 ®	-99.990	-4.792	-1.226	-0.632	-0.348	-0.195	-0.113	-0.070	-0.031	0.000	0.03	6
D17S1866 Σ	-99.990	-13.093	-3.199	-1.711	-0.984	-0.572	-0.334	-0.200	-0.093	0.000	0.08	16
D17S784 Σ	-99.990	-10.642	-2.455	-1.247	-0.661	-0.327	-0.130	-0.018	0.050	0.000	0.06	12
D17S789 Σ	-99.990	-6.582	-1.641	-0.912	-0.560	-0.353	-0.221	-0.134	-0.039	0.000	0.02	4
D17S801 Σ	-99.990	-11.320	-3.047	-1.773	-1.134	-0.752	-0.509	-0.349	-0.154	0.000	0.08	16
D17S926 Σ	-99.990	-15.854	-4.238	-2.414	-1.478	-0.913	-0.554	-0.324	-0.095	0.000	0.12	24
D17S928 Σ	-99.990	-15.020	-3.485	-1.740	-0.882	-0.393	-0.110	0.042	0.100	0.000	0.08	16
D17S261 @	0.705	0.702	0.566	0.442	0.335	0.243	0.167	0.107	0.028	0.000	0	0
D17S783 @	-99.990	-14.721	-4.679	-2.991	-2.063	-1456	-1.030	-0.717	-0.292	0.000	0.15	30
D17S796 @	-99.990	-7.907	-1.428	-0.540	-0.155	0.026	0.099	0.113	0.060	0.000	0.04	8
D17S806 @	-99.990	-14.018	-3.735	-2.058	-1.209	-0.710	-0.406	-0.225	-0.072	0.000	0.1	20
D17S849 ®	-99.990	-15.592	-3.981	-2.188	-1.286	-0.754	-0.424	-0.219	-0.031	0.000	0.1	20
D17S938 @	-99.990	-15.509	-3.917	-2.118	-1.208	-0.669	-0.341	-0.148	-0.012	0.000	0.1	20
D17S945 ®	-99.990	-15.323	-3.761	-2.002	-1.127	-0.619	-0.315	-0.143	-0.037	0.000	0.1	20
THRA1 ®	-99.990	-13.423	-3.574	-2.109	-1.386	-0.957	-0.680	-0.491	-0.239	0.000	0.1	20

Marker	0.000	0.001	0.050	0.100	0.150	0.200	0.250	0.300	0.400	0.500	Θ = -2	cM excl
D18S34 ®	-99.990	-11.133	-2.894	-1.647	-1.028	-0.662	-0.472	0.264	0.067	0.000	0.08	16
D18S464 Φ	-99.990	-3.849	-0.689	-0.310	-0.163	-0.103	-0.079	-0.068	-0.040	0.000	0.01	2
D18S51 Φ	-99.990	-10.380	-2.127	-0.899	-0.322	-0.025	0.112	0.146	0.065	0.000	0.05	10
D18S53 Φ	-99.990	-1.302	0.171	0.260	0.243	0.198	0.149	0.104	0.041	0.000	0	0
D18S59 Φ	-99.990	-15.716	-4.116	-2.308	-1.383	-0.822	-0.462	-0.230	-0.007	0.000	0.12	24
D18S62 Φ	1.056	1.052	0.867	0.694	0.537	0.399	0.281	0.183	0.051	0.000	0	0
D18S70 Φ	-99.990	-10.217	-2.059	-0.900	-0.372	-0.103	0.028	0.077	0.059	0.000	0.05	10
D18S851 Φ	-99.990	-15.524	-3.960	-2.194	-1.308	-0.784	-0.460	-0.258	-0.060	0.000	0.1	20
D18S877 Φ	-99.990	-18.638	-5.305	-3.166	-2.031	-1.312	-0.824	-0.486	-0.106	0.000	0.15	30

Marker	0.000	0.001	0.050	0.100	0.150	0.200	0.250	0.300	0.400	0.500	Θ = -2	cM excl
D19S180 ®	-99.990	-5.566	-0.750	-0.127	0.116	0.201	0.204	0.159	0.029	0.000	0.01	2
D19S210 Φ	-99.990	-10.429	-2.202	-0.990	-0.427	-0.140	-0.007	0.031	-0.012	0.000	0.05	10
D19S214 @	-99.990	-10.014	-1.867	-0.714	-0.196	0.057	0.164	0.183	0.095	0.000	0.04	8
D19S215 Σ	-99.990	-18.224	-4.933	-2.831	-1.738	-1.063	-0.622	-0.331	-0.042	0.000	0.13	26
D19S216 Φ	-99.990	-15.821	-4.204	-2.387	-1.453	-0.884	-0.518	-0.281	-0.047	0.000	0.12	24
D19S217 Φ	-99.990	-12.997	-3.106	-1.611	-0.877	-0.458	-0.214	-0.078	-0.007	0.000	0.08	16
D19S221 Φ	-99.990	-18.160	-4.849	-2.729	-1.624	-0.944	-0.504	-0.221	0.030	0.000	0.13	26
D19S222 Σ	-99.990	-7.180	-2.147	-1.287	-0.808	-0.502	-0.301	-0.172	-0.045	0.000	0.05	10
D19S225 Φ	-99.990	-1.616	-0.086	0.069	0.116	0.122	0.110	0.088	0.038	0.000	0	0
D19S49 ®	-99.990	-0.991	0.457	0.516	0.465	0.383	0.293	0.208	0.074	0.000	0	0
D19S878 Σ	-99.990	-10.172	-2.006	-0.838	-0.306	-0.039	0.084	0.120	0.067	0.000	0.05	10

Marker	0.000	0.001	0.050	0.100	0.150	0.200	0.250	0.300	0.400	0.500	Θ = -2	cM excl
D20S103 Σ	-99.990	-13.963	-3.962	-2.348	-1.492	-0.950	-0.585	-0.334	-0.063	0.000	0.12	24
D20S110 Σ	-99.990	-4.094	-0.791	-0.310	-0.095	0.009	0.051	0.060	0.031	0.000	0.005	1
D20S189 @	-99.990	-7.612	-1.180	-0.337	0.017	0.177	0.237	0.238	0.138	0.000	0.005	1
D20S27 ®	-99.990	-8.077	-1.516	-0.568	-0.134	0.084	0.183	0.207	0.130	0.000	0.03	6
D20S480 Σ	-99.990	-13.934	-3.975	-2.389	-1.550	-1.015	-0.648	-0.389	-0.090	0.000	0.12	24
D20S851 Φ	-99.990	-15.762	-4.154	-2.337	-1.408	-0.849	-0.497	-0.276	-0.066	0.000	0.12	24
D20S175 @	-99.990	-2.015	-0.425	-0.202	-0.093	-0.034	-0.005	0.006	0.000	0.000	0.001	0.2

Marker	0.000	0.001	0.050	0.100	0.150	0.200	0.250	0.300	0.400	0.500	Θ = -2	cM excl
APP Φ	-99.990	-13.027	-3.118	-1.605	-0.849	-0.408	-0.147	-0.007	0.042	0.000	0.08	16
D21S11 Φ	-99.990	-13.414	-3.587	-2.126	-1.398	-0.957	-0.663	-0.456	-0.179	0.000	0.1	20
D21S167 ®	-99.990	-3.874	-0.710	-0.332	-0.183	-0.111	-0.070	-0.042	-0.008	0.000	0.001	0.2
D21S172 Φ	-99.990	-12.477	-2.630	-1.176	-0.485	-0.115	0.077	0.156	0.128	0.000	0.07	14
D21S215 Φ	-99.990	-5.285	-0.475	0.127	0.347	0.408	0.382	0.305	0.104	0.000	0.01	2
D21S265 Φ	-99.990	-8.956	-2.239	-1.169	-0.633	-0.328	-0.153	-0.061	-0.013	0.000	0.05	10
D21S266 Φ	-99.990	-6.341	-1.478	-0.777	-0.437	-0.245	-0.134	-0.073	-0.023	0.000	0.005	1
D21S270 Φ	-99.990	-15.911	-4.277	-2.435	-1.481	-0.900	-0.527	-0.289	-0.059	0.000	0.12	24
D21S65 Φ	-99.990	-8.078	-1.571	-0.643	-0.212	0.015	0.126	0.160	0.084	0.000	0.07	14

Marker	0.000	0.001	0.050	0.100	0.150	0.200	0.250	0.300	0.400	0.500	Θ = -2	cM excl
D22S156 ®	-99.990	-15.406	-3.798	-1.995	-1.081	-0.542	-0.215	-0.027	0.076	0.000	0.1	20
D22S283 Σ	-99.990	-10.801	-2.631	-1.457	-0.906	-0.603	-0.426	-0.316	-0.168	0.000	0.07	14
D22S420 Φ	-99.990	-3.354	-0.271	0.019	0.078	0.062	0.027	-0.002	-0.016	0.000	0.001	0.2

Marker	0.000	0.001	0.050	0.100	0.150	0.200	0.250	0.300	0.400	0.500	Θ = -2	cM excl
DMD ®	-99.990	-17.165	-5.463	-3.545	-2.493	-1.790	-1.273	-0.874	-0.314	0.000	0.18	36
DXS1047 Σ	-99.990	-32.774	-10.869	-17.148	-5.062	-3.650	-2.613	-1.818	-0.699	0.000	0.23	46
DXS1060 Σ	-99.990	-26.177	-7.522	-4.387	-2.698	-1.624	-0.902	-0.418	0.049	0.000	0.18	36
DXS6797 Φ	-99.990	-18.546	-5.169	-2.995	-1.835	-1.101	-0.610	-0.281	-0.068	0.000	0.14	38
DXS6800 Φ	-99.990	-24.155	-7.389	-4.618	-3.106	-2.118	-1.422	-0.917	-0.283	0.000	0.2	40
DXYS154 Φ	-99.990	-18.546	-5.169	-2.995	-1.835	-1.101	-0.610	-0.281	0.035	0.000	0.14	28
MAOA ®	-99.990	-7.072	-2.123	-1.366	-0.975	-0.728	-0.553	-0.418	-0.199	0.000	0.05	10
DXS989 @	-99.990	-20.776	-5.754	-3.332	-2.049	-1.242	-0.705	-0.346	-0.006	0.000	0.15	30

Table 3a. Two point lod-scores for various recombination fractions (Θ, row 1) of 298 markers (column 1) run through family ZMK by Fiona Mansergh (Φ), Sophia Millington-Ward (Σ), Alexandra Erven (@) and Rajendra Kumar-Singh (®). These data were obtained by analysing current data (table 2) and previous data, using affected members of family ZMK only. The last two columns represent Θ with a lod-score of less than -2 and the resulting exclusion (Kosambi cM) to either side of the marker respectively. Notably, no table is presented in this thesis for markers and exclusions on chromosome 9 as Fiona Mansergh undertook the affected only analysis of the 62 markers typed on chromosome 9 and presented the resulting data in her thesis.

Marker	Lod-score at zero recombination
D3S1299	1.507
RHO (chromosome 3)	1.251
D5S119	1.278
D10S209	1.313
D11S906	0.161
DRD2 (chromosome 11)	1.278
D13S168	1.386
D17S261	0.705
D18S62	1.056

Table 3b. Positive lod-scores found at zero recombination when microsatellite markers run through family ZMK were reanalysed, using affected members of the family only. None of the markers are above the accepted threshold of significance (3).

Position	Consensus	ZMK	Gene	Amino Acid
533*	A	G	Control	-
6776*	T	C	MTCO1	H-H
11953	C	T	MTND4	L-L
12258	**C**	**A**	**MTTS2**	-
13404	T	C	MTND5	I-I
14272*	C	G	MTND6	F-L
14569*	G	A	MTND6	P-P
14766*	A	G	MYCYB	I-T
16239*	C	G	Control	-
16519*	T	C	Control	-
16569	T	C	Control	-

Table 4. Mitochondrial sequence variations found in family ZMK members. Note: The putative disease-causing mutation in the serine tRNA gene is highlighted in bold. Additional sequence variations were found both in 'married-in' members of family ZMK and across all four individuals sequenced including the unaffected control individual (data not presented). Many of the variations from the consensus sequence presented above are either previously reported sequence variations, indicated with *, or do not alter encoded amino acids. Notably, no mutations in the control region of the mtDNA are known to cause disease (MITOMAP, 1999).

Individual	Affection status	Tissue	Ratio A:C
3-22	Severely affected	Muscle	37:3
3-22	Severely affected	Blood	25:15
3-18	Asymptomatic	Blood	16:24
4-14	Severely affected	Blood	24:16

Table 5. Estimated levels of heteroplasmy are provided for members of family ZMK. A is the mutated variant, C is the normal base. Tissue refers to the type of tissue from which DNA was extracted. Unaffected members of the family have been referred to as asymptomatic, given that some individuals are still young and that there is evidence for a widely variable age of onset and penetrance in the pedigree. The ratios of clones, cloned from PCR samples, containing the mutant A base and wildtype C base are shown for four DNA samples extracted from bloods and muscle.

Locus	Disease	Nucleotide Position	Nucleotide Change	Amino Acid Change	Homoplasmy	Heteroplasmy
MTND1	LHON	3394	T-C	Y-H	+	-
MTND1	LHON	3460	G-A	A-T	+	+
MTND1	LHON	4136	A-G	Y-C	+	-
MTND1	LHON	4160	T-C	L-P	+	-
MTND1	LHON	4216	T-C	Y-H	+	-
MTND2	LHON	4917	A-G	D-N	+	-
MTND2	LHON	5244	G-A	G-S	-	+
MTCO1	LHON	7444	G-A	Term-K	+	-
MTATP6	LHON	9101	T-C	I-T	+	-
MTCO3	LHON	9738	G-T	A-T	+	-
MTCO3	LHON	9804	G-A	A-T	+	-
MTND4L	LHON	10663	T-C	V-A	+	-
MTND4	LHON	11778	G-A	R-H	+	+
MTND5	LHON	13708	G-A	A-T	+	-
MTND5	LHON	13730	G-A	G-E	-	+
MTND6	LHON	14484	T-C	M-V	+	+
MTCYB	LHON	15257	G-A	D-N	+	-
MTCYB	LHON	15812	G-A	V-M	+	-
MTATP6	NARP	8993	T-G	L-R	-	+
MTATP6	NARP/Leigh disease	8993	T-C	L-P	-	+
MTND6	LDYT	14459	G-A	A-V	+	+

Table 6a. Reported mitochondrial DNA base substitutions involved in LHON (Leber's Hereditary Optic Neuropathy), NARP (Neurogenic muscle weakness, Ataxia and RP; alternate phenotype at this locus is reported as Leigh Disease) and LDYT (Leber's hereditary Optic Neuropathy and Dystonia).

Locus	Disease	Nucleotide Position	RNA	Homoplasmy	Heteroplasmy
MTTL1	DMDF	3243	tRNALeu (UUR)	-	+
MTTI	CPEO	4298	tRNA Ile	-	+
MTTN	CPEO	5692	tRNA Asn	-	+
MTTN	CPEO	5703	tRNA Asn	-	+
MTTL2	CPEO	12308	tRNA Leu (CUN)	nd	nd
MTTL2	CPEO	12311	tRNA Leu (CUN)	+	+
MTTL2	CPEO	12315	tRNA Leu (CUN)	-	+
MTRNR1	DEAF	1555	rRNA 12S	+	-
MTTS1	DEAF	7445	tRNA Ser (UCN)	+	+

Table 6b. Reported mitochondrial rRNA and tRNA mutations involved in DMDF (Diabetes Mellitus and Deafness), CPEO (Chronic Progressive External Ophthalmoplegia) and DEAF (Maternally Inherited Deafness or Aminoglycoside-Induced Deafness).

Disease	Locus
NARP	MTATP6
MM	MTCYB, MTTF, MTTL1MTTM, MTTW, MTTN, MTTS1, MTTL2, MTATT, MTTT, MTTP
MERRF	MTTK
CIPO	MTTS1
MMC	MTTL1
FICP	MTTI
MELAS	MTND1, MTCO3, MTND4, MTCYB, MTTV, MTTL1
LIMM	MTTT
MHCM	MTTG

Table 7. Mitochondrial disease associated with muscular abnormalities. NARP: neurogenic muscle weakness, ataxia, and RP. MM: mitochondrial myopathy. MERRF: myoclonic epilepsy and ragged red muscle fibers. CIPO: chronic intestinal pseudoobstruction with myopathy and ophthalmoplegia. MMC: maternal myopathy and cardiomyopathy. FICP: fatal infantile cadiomyopathy in conjunction with MELAS-associated cardiomyopathy. MELAS: mitochondrial encephalomyopathy, lactic acidosis and stroke-like episodes. LIMM: lethal infantile mitochondrial myopathy. MHCM: maternally inherited hypertrophic cadiomyopathy.

3. Hammerhead ribozymes *in vitro*

3.1. Introduction

A potential gene therapy for a recessive disorders, caused by the absence of a protein, will in theory require the introduction of a wildtype gene. Dominant disorders, however, can arise in three ways. Firstly, a dominant disorder may be due to a reduction in wildtype protein (i.e. haploinsufficiency), secondly it may arise directly from the mutant protein (i.e. gain of function mutation or dominant negative mutation) or thirdly a combination of both may cause disease pathology. Dominant negative disorders such as many forms of Osteogenesis Imperfecta (OI) and Retinitis Pigmentosa (RP) will require the selective silencing of mutant alleles, while maintaining expression of the wildtype alleles. There is a range of suppression effectors from which to choose when designing a gene therapy for such disorders, such as antisense DNA and RNA, DNA and RNA ribozymes, peptide nucleic acids and triple helix forming oligonucleotides, each with advantages and disadvantages (see sections 1.1 to 1.3). In this chapter RNA ribozymes were investigated as suppressors for the dominant negative forms of OI and RP (sections 1.7 to 1.10).

Hammerhead ribozymes are small catalytic RNAs that cleave target RNA at very specific sites (Haseloff and Gerlach, 1989). With two antisense arms they bind target RNA and, in the presence of cofactors, typically divalent cations (usually Mg^{2+}), cleave target RNA at NUX (N = any base; U = uracyl; X = any base except guanine) sites, present in target RNA (see figure 1, chapter 1 and section 1.3.1). The efficiency of ribozyme cleavage may depend on a number of things. For instance, target RNA that is readily accessible to ribozymes will more easily be bound and cleaved than inaccessible target sites (Fedor and Uhlenbeck, 1990). Thus methods have been devised to identify such suitable areas in target RNAs (see section 1.3.3).

One such method involves the use of a computer program called PlotFOLD (Zuker, 1989). The secondary structure of RNA contains large areas, which are hybridised internally and which are interspersed with loop-like structures of single stranded RNA (figure 2). It is within these loops that RNA may form Watson and Crick

basepairs with ribozymes. PlotFOLD uses mathematical algorithms, which attempt to identify loops in RNA. Output is presented in plots of the most likely RNA secondary structure for various internal energy (ΔG) levels. Naturally, RNA plots with lower ΔGs are more likely to represent accurate RNA conformations at a given time, though RNA conformations are thought to be fluid and to alter continuously. One should therefore attempt to design hammerhead ribozymes towards loop-like structures, which are consistently predicted to occur within as may different ΔG plots as possible.

A second issue to consider when designing hammerhead ribozymes is the length of the antisense arms. Long antisense arms will enable ribozymes to recognise and bind targets easily. However, long antisense arms may not render the ribozyme sufficiently specific, causing unwanted down-regulation of other RNAs. Also, dissociation after cleavage may not occur or may be slow and may thus increase the ribozyme turnover time. Short antisense arms will readily dissociate from cleavage products, but may not enable ribozymes to recognize and bind targets easily within the large quantity of other DNAs and RNAs, which surround the ribozyme. Generally, it has been found that ribozymes with longer stems 3 and shorter stems 1 (figure 1) cleave more efficiently than a ribozymes with the reverse (Hendry and McCall, 1996).

Another issue for consideration when designing a hammerhead ribozyme is the sequence of the actual NUX target site. Zoumadakis and Tabler (1995) tested the 12 permutations of NUX and calculated the cleavage rate constants *in vitro*. The rates were found to vary quite considerably depending on the sequence of the target site. Their findings are summarised below. Target sites are given in order of efficiency: AUC, GUC, UUC, AUA, GUA, AUU, CUC, UUA, GUU, CUA, CUU, UUU. Cleavage efficiencies of UUU target sites were found to be 40 times lower than of AUC sites. A similar study revealed somewhat different results. Shimayama et al., (1995) found that all mutations of the GUC cleavage site reduce the efficiency of cleavage. A at the first or third base position of the NUX site increased K_m (the affinity of the ribozyme for the substrate, see section 1.5) by 35 or 30 fold respectively, while the effect on k_{cat} (the cleavage efficiency, see section 1.5) was small. U at the first or third base position of the NUX site decreased k_{cat} by 8 or 15 fold respectively while the effect on K_m was small. The effect of C at the first base of the NUX site was relatively small on both kinetic parameters. In short, Shimayama et al., (1995) concluded that with respect to cleavage efficiency, the

more efficient target sites were GUC, CUC, UUC, GUU, AUA, AUC, GUA, UUU, UUA, CUA, AUU, CUU.

A further issue for consideration when designing a hammerhead ribozyme is the sequence of the catalytic core (see chapter 1 figure 1). The catalytic core contains 11 highly conserved bases, two partially conserved bases and one unconserved base. The unconserved base (figure 1, underlined) has been studied in depth and has been found to influence cleavage efficiency substantially. U is the most efficient, followed by G, A, and C, which have a 60%, 50% and 20% activity compared to U (Ruffner et al., 1990). In stem 2 there is catalytically a strong preference for a G-C base (see figure 1, underlined) (Tuschl and Eckstein, 1993). The length of stem 2 also has some influence on the catalytic efficiency of hammerhead ribozymes. Stems of less than two base pairs have been found to be significantly less active (Tuschl and Eckstein, 1993). However, the length and composition of the loop in stem 2 seems not to influence hammerhead ribozyme activity (Thomson et al., 1994).

OI is a brittle-bone-disorder caused by mutations in either of the type I collagen genes, COL1A1 and COL1A2. Type I collagen, the most abundant protein in man, lends strength to bone and fibrous tissue. Null-mutations cause a very mild form of the disorder due to haploinsufficiency (type I OI) and will not be discussed further in this thesis. More serious forms of OI (types II-IV) arise from dominant gain of function frameshift mutations and point mutations resulting in a structural abnormality of the collagen protein. The collagen fibers, i.e. the bundles of collagen that give bone and fibrous tissue strength, become brittle causing symptoms which range from mildly brittle bones to perinatal death (see section 1.10).

RP is the name given to a group of retinopathies, which result in photoreceptor cell death. Clinically, patients may manifest night blindness, waxy pallor of the optic disc, pigment depositions on the retina (see figure 4 chapter 1) and attenuated retinal vessels (see section 1.6 for details). RP can be inherited in an autosomal dominant (gain of function) (adRP), autosomal recessive (arRP, due to haploinsufficiency), x linked (xlRP) or digenic fashion. It also occurs sporadically, but generally this is thought to represent arRP, adRP manifesting partial penitrance or perhaps digenic RP. Notably, *de novo* mutations may also appear as sporadic cases of RP. However, I will focus on autosomal dominant forms of RP in this chapter of the thesis. The first two genes to be implicated in adRP were the rod photoreceptor cell pigment, rhodopsin (see sections 1.7 and 1.9.1), and the

structural rod and cone protein peripherin/*RDS* (see section 1.7 and 1.9.2) (Farrar et al., 1990; Dryja et al., 1990; Farrar et al., 1991a, b; Kajiwara et al., 1991; Jordan et al., 1992). However, other RP causing genes have now been identified (see appendix B for a complete list of cloned and/or mapped genes causing retinal diseases and chapter 1 table 2 for a complete list of the known loci and genes linked to RP).

However, like many dominant negative disorders, OI and RP are extremely heterogeneous; over 150 different mutations in the COL1A1 and COL1A2 genes are known to cause OI and over 100 mutations in the rhodopsin gene and 40 in the peripherin/*RDS* gene are known to cause RP. Thus, due to restrictions in terms of time, money and indeed in terms of design-potential, mutation-independent methods of gene-suppression (chapter 1.1) will be required for the development of gene therapies for such disorders.

Recently three general mutation-independent methods of gene-suppression were suggested and tested *in vitro* as a means of circumventing the immense allelic heterogeneity often associated with dominant disorders (Millington-Ward et al., 1997). Two general strategies for gene suppression and one mutation-specific strategy for suppression, all of which utilised hammerhead ribozymes, were studied during the course of this Ph.D. Hammerhead ribozymes were used because they are extremely specific (see sections 1.2 and 1.3). Also hammerhead ribozymes are the best-characterised ribozyme and the most flexible in terms of design (see section 1.3).

In an attempt to optimise the catalytic activity of ribozymes in this study, all ribozymes were designed with a U at the unconserved position of the catalytic core and C-G at the semi-conserved positions in stem 2 (figure 1). Stem 2 contained 4 base pairs with a 4 base loop. The lengths of stems 1 and 3 varied between 6-8 and 7-8 bases (see 3.2.5), depending on the sequence composition; in general, where sequences comprised many pyrimidines shorter stems 1 and 3 were used. The exact compositions of the NUX sites are summarised in table 1.

In addition, in an attempt to mimic an *in vivo* situation as accurately as possible, long, structured RNA targets were used to test ribozyme cleavage. All target transcripts were over 350 bases, indeed, in many cases over 900 bases long. Many studies in the literature utilise short unstructured RNAs of 20-30 bases in length to test ribozyme catalytic activity, and due to the absence of secondary and tertiary

structures in these transcripts find higher catalytic activities than may perhaps be expected in an *in vivo* situation (Drenser et al., 1998; Vaish et al., 1997; Zaug et al., 1998). However, despite the length of our target RNAs, many of the ribozymes tested in this chapter compare very favourably to ribozymes in other studies.

The first strategy of gene suppression studied in this chapter was a disease specific strategy, in which three ribozymes were specifically designed to cleave rhodopsin RNA at three autosomal dominant mutation sites, while leaving the wildtype human rhodopsin RNA intact. These mutations, known to cause adRP, at codons 23, 51 and 255 (Inglehearn et al., 1991; Dryja et al., 1991) of human rhodopsin, create NUX ribozyme cleavage sites and occur in predicted open-loop structures in the RNA.

The second strategy utilises the untranslated regions (UTRs) of RNA. Three ribozymes were designed to cleave human rhodopsin, human type 1 COL1A2 and human peripherin/*RDS* transcripts in 5'UTR sequences. In addition, a ribozyme was designed to cleave human rhodopsin in 3'UTR sequence. cDNAs with modified UTR sequences, which did not contain the ribozyme NUX target site, were generated to replace the gene. The third strategy explored in this study utilises intragenic polymorphism. Three ribozymes were designed to cleave one polymorphic variant of human type I COL1A1 and COL1A2, while leaving the other polymorphic variant intact. The three strategies outlined above have been tested and shown to work *in vitro* (Millington-Ward et al., 1997). Two ribozymes, Rz8 and Rzpol1A1, targeting the human peripherin/*RDS* 5'UTR and a human COL1A1 polymorphism respectively, were quantified with respect to extent of cleavage achieved, to evaluate whether to proceed to *in vivo* studies with these ribozymes.

An extensive search was carried out to identify suitable polymorphisms in the human rhodopsin and peripherin/*RDS* genes for hammerhead ribozyme-based therapies. A suitable polymorphism must be common, occur in an open-loop structure of target RNA and create an NUX target site. To this end restriction digest analysis and single strand conformation polymorphism electrophoresis (SSCPE) were carried out. Unfortunately, no suitable polymorphisms were revealed within the rhodopsin or peripherin/*RDS* gene. The ever increasing quantity of human DNA sequence that is becoming available will greatly facilitate the identification of suitable intragenic polymorphisms for this type of ribozyme-based therapeutic approach.

In this chapter, one mutation-specific and two mutation-independent strategies for gene suppression using hammerhead ribozymes were investigated in detail *in vitro*. All three methods were found to elicit sequence specific cleavage of target RNAs, although the ribozymes varied greatly in cleavage efficiency. Mutation-independent strategies will be necessary in gene therapy drug development because of the heterogeneous state of most dominant negative disorders and because not all mutation sites lend themselves to gene suppression. The genes chosen for the study were human rhodopsin and peripherin/*RDS* and human COL1A1 and COL1A2; genes known to cause adRP and OI. However, it is of note that these mutation-independent strategies may not only be extremely valuable for dominant gain of function single gene disorders, but also for complex traits such as bipolar disease and Alzheimer's disease. It is also of note that the mutation-independent strategies outlined in this chapter need not necessarily be explored using hammerhead ribozymes but could potentially use other suppressing agents such as antisense and peptides.

3.2. Materials and Methods

3.2.1. Predicting RNA Secondary Structures

Oligonucleotides required for PCR amplifications were selected, synthesised and purified as in section 2.2.2. PCRs and $MgCl_2$ curves were carried out as in section 2.2.3. Two-dimensional secondary RNA structures of human rhodopsin, human peripherin/*RDS* and human collagens 1A1 and 1A2 were predicted using PlotFOLD (figure 2) (Zuker, 1989). Ribozymes were designed to target predicted open-loop structures in the RNA target sequence, as these are thought to be more accessible for ribozymes to bind and cleave. Because RNA can have various conformations, depending on the internal energy level of the molecule, the loops were assessed for at least 6 different possible conformations with different internal energies.

3.2.2. Finding and Assessing Common Polymorphisms

Previously, Westerhausen et al. found a CCC/CTC intragenic polymorphism at position 3210 in human COL1A1. One of these variants, CTC (T-allele) contains an NUX hammerhead ribozyme cleavage site, while the other (C-allele) does not. PlotFOLD predicted this polymorphic site to be in an open-loop structure of the COL1A1 RNA and hence potentially to be accessible to ribozymes (see 3.2.1) (figure 2d). In this study, 11 unrelated individuals from the CEPH panel were assessed for the polymorphism by sequencing PCR products over the polymorphic site.

To assess whether a Ban I polymorphism (G/T) in intron 4 of the human rhodopsin gene (position 4335) (Sung et al., 1991) was common, DNA of 20 individuals from the Irish blood bank was PCR amplified (see section 2.2.3), subsequently digested with Ban I and run on an agarose gel. Dr. Lesley Mynett-Johnson generously provided these DNAs from the blood bank.

Primers used for the amplification were:

      F   TCCCATCTTCATGAGCATCC

      R   TCTCCGAGGAACCCTTTACC

A third polymorphism, which was assessed for allele frequency, and which occurs in a predicted open-loop structure in the human peripherin/*RDS* RNA, (Ile32Val position 611) was tested using SSCPE analysis (Keen and Inglehearn, 1996). Primers used to amplify the region were

      F   CTCTTCAACATCATCCTCTT

      R   ATTGCTGATCCACTGAATCT

A radioactive PCR (see 2.2.4. Radioactive PCRs, page 89) was carried on DNA's extracted from 20 individuals from the blood bank (kindly donated by Dr. Lesley Mynett-Johnson). SSCPE was undertaken on PCR products amplified from the 20 DNAs described above. PCR fragments were run on various percentages (6%-9%) of acrylamide gel, without urea, under constant cooling with a fan heater, at 6W. The loading dye used was made by adding 50 µl of 10 M NaOH, 0.03 g of bromophenol blue and 0.03 g of xylene cyanol to 50 ml of formamide.

3.2.3. Cloning and transforming

All except two of the DNA fragments were cloned into the multiple cloning site (MCS) of the expression vector pcDNA3 (Invitrogen), to allow for subsequent expression either *in vitro* from the T7 promoter or in mammalian cells from the CMV promoter. Human Peripherin/*RDS* was cloned into MCS of Bluescript and was kindly provided by Dr. Gabriel Travis. Dr. Wolfgang Baehr kindly donated human rhodopsin cDNA with an incomplete 5'UTR. Using PCR directed mutagenesis and a HindIII (in pcDNA3) BstEII (in exon 4 of human rhodopsin) cassette, Dr. Jane Farrar inserted the full length 5'UTR into Dr. Baehr's clone. For a diagram of primer directed mutatgenesis see figure 1a. This new full length rhodopsin cDNA was digested and inserted in the HindIII and EcoRI sites of pcDNA3 by Dr. J. Farrar. Vectors were digested with suitable enzymes and treated

with alkaline phosphatase from calf intestine (CIPed) (see section 2.2.9). Inserts were digested and purified and ligations and transformations were carried out (see section 2.2.9).

3.2.4. Automated Sequencing

All clones and various PCR fragments were sequenced by Dr. Sophie Kiang, Avril Kennan, Gearoid Tuohy and the author on an Applied Biosystems (ABI) 373A DNA sequencer using standard protocols.

3.2.5. Constructs
3.2.5.1. Ribozymes

All ribozymes (Rz) used in these experiments were hammerhead ribozymes, which were synthesised by VhBio as two single stranded forward and reverse oligonucleotides. These were purified using OPC columns (Applied Biosystems), after which the forward and the reverse strand were annealed by heating 10-15 µg of each in a 40 µl reaction with 25 mM NaCl to 94°C for 3 minutes and leaving over night at room temperature. All annealed oligonucleotides were cloned into the HindIII and XbaI sites of the pcDNA3 MCS. Ribozymes were designed as in figure 1b.

3.2.5.2. Disease Specific Mutation
Human rhodopsin with Gly51Val mutation

A single base change (GlyGGC51ValGTC; Dryja et al., 1991) was introduced into human rhodopsin using primer driven mutagenesis and a HindIII to BstEII cassette.

Human rhodopsin with Pro23Leu mutation

A single base change (ProCCC23LeuCTC; Dryja et al., 1991) was introduced into human rhodopsin by Arpad Palfi using primer driven mutagenesis using HindIII and BstEII cassette.

Human rhodopsin with del255 mutation

A three base pair deletion (Del255ATC; Inglehearn et al., 1991) was introduced into human rhodopsin using primer driven mutagenesis and a HindIII to AcyI cassette by Patrick Hayden.

Ribozyme 20

Ribozyme 20 (Rz20) was designed to cleave a CUC mutation site in the human
rhodopsin RNA at position 361-363. Arpad Palfi cloned Rz20. Antisense arms are
underlined.

Rz20:   <u>UACUCGAA</u>CUGAUGAGUCCGUGAGGACGAA<u>AGGCUGC</u>

Ribozyme 10

Ribozyme 10 (Rz10) was designed to cleave a GUC mutation site in the human
rhodopsin RNA at position 475-477 and was cloned by Najma Al Jandal. Antisense
arms are underlined.

Rz10:   <u>GGACGGU</u>CUGAUGAGUCCGUGAGGACGAA<u>ACGUAGAG</u>

Ribozyme 255

Ribozyme 255 (Rz255) was designed to target an AUG mutation site in the human
rhodopsin RNA at position 4161-4163 and was cloned by Patrick Hayden.
Antisense arms are underlined.

Rz255: <u>AUGACCAU</u>CUGAUGAGUCCGUGAGGACGAA<u>AUGACCA</u>

Ribozyme 447

Ribozyme 447 (Rz447) was designed to target a GUC target site at position 445-447
of the human rhodopsin RNA. Antisense arms are underlined.

Rz447: <u>UGGGGAA</u>CUGAUGAGUCCGUGAGGACGAA<u>ACCAGCAC</u>

3.2.5.3. UTR

Human rhodopsin cDNA (4B)

Human rhodopsin cDNA with full-length 5'-UTR was cloned into the HindIII and
EcoRI sites of pcDNA3 by Dr. G. Jane Farrar and Dr. W. Baehr (3.2.3). Using
primer driven PCR mutagenesis and a HindIII (in pcDNA3) to BstEII (in exon IV
of human rhodopsin) PCR cassette the full 5'-UTR was inserted into the clone. To
understand the base-numbering system, see accession number K02281.

Hybrid replacement human rhodopsin with a shortened 5'-UTR (5A)

The human full rhodopsin clone (see above) was generated by Dr. G. Jane Farrar
by deleting all but the 21 bases of the 5'-UTR immediately 5' to the ATG start site
and was cloned into the EcoRI site in pcDNA3.

Hybrid replacement human rhodopsin in the 3'-UTR (8A)

Full human rhodopsin with a T>G (CTT>CTG) transition at base 1393-1395 in the
3'UTR was generated. The mutation destroys the CTT ribozyme cleavage site. The

mutation was introduced into clone 4B (see above) by primer driven PCR mutagenesis and a BstEII (in exon IV of human rhodopsin) to XhoI (in pcDNA3) PCR cassette.

Human peripherin cDNA (6B)

Human peripherin full cDNA, including the 5'-UTR, was kindly provided by Dr. Gabriel Travis. The gene had been cloned into the EcoRI site of Bluescript in a 5'-3' orientation allowing subsequent *in vitro* expression from the T7 promoter.

Hybrid replacement peripherin cDNA (7A)

Hybrid human peripherin cDNA was kindly generated by Dr. G. Jane Farrar using primer driven PCR mutagenesis of a BamHI (in the 5'-UTR sequence) to BglII (in the coding sequence of the above cDNA) DNA fragment. The clone contains full human peripherin coding sequence, human 5-UTR sequence till the BamHI site at position 76 and mouse *RDS* 5'-UTR sequence until the ATG start site (position 84-250 of mouse cDNA sequence).

Human collagen 1A2 template for UTR work (1B)

The 5'-UTR and exon 1 of human COL1A2 genomic DNA was amplified and cloned into the HindIII and XhoI sites of the pcDNA MCS.

Human collagen 1A2 hybrid replacement for UTR work (2A)

Hybrid replacement collagen 1A2 was generated by primer driven mutagenesis and contains the 5'-UTR of human collagen 1A1 and exon 1 of human collagen 1A2

Ribozyme 18

Ribozyme 18 (Rz18) was designed to cleave human type I collagen 1A2 RNA in the 5'-UTR at a GUC site at position 448-450 (Accession number: J03464). Antisense arms are underlined.

Rz18: <u>ACAUGCA</u>CUGAUGAGUCCGUGAGGACGAA<u>ACUCCUUG</u>

Ribozymes 8 and 9

Ribozymes 8 and 9 (Rz8 and Rz9) were designed to cleave human peripherin/*RDS* 5'-UTR-RNA sequence at CUA and GUU at positions 234-236 and 190-192 respectively (Accession number: M62958). Antisense arms are underlined (Cloned by Gearoid Tuohy).

Rz8: <u>CCAAGUG</u>CUGAUGAGUCCGUGAGGACGAA<u>AGUCCGG</u>

Rz9: <u>CAAACCUU</u>CUGAUGAGUCCGUGAGGACGAA<u>ACGAGCC</u>

Ribozyme 15

Ribozyme 15 (Rz15) was designed to cleave human rhodopsin RNA at an AUU site (position 249-251) (Accession number: K02281). Antisense arms are underlined.

Rz15: <u>ACCAAG</u>CUGAUGAGUCCGUGAGGACGAA<u>AUGCUGC</u>

Ribozyme 25

Ribozyme 25 (Rz25) was designed to cleave human rhodopsin RNA at a CUU site at position 1393-1395 (Accession number: K02281) in the 3'UTR. Antisense arms are underlined.

Rz25: <u>GGGGGA</u>CUGAUGAGUCCGUGAGGACGAA<u>AGGUGUAG</u>

3.2.5.4. Polymorphism

Pol1a1 T and Pol1a1 C

Exon 52 of Human collagen 1A1 genomic DNA was amplified and sequenced (see above). Clones containing the T and C allele of a common polymorphism at position 3210 were cloned into the HindIII and XbaI sites of pcDNA3 (Accession number: K01228).

Colpol1A2, 1 (G902, T907) and 2 (A902, A907)

cDNA (position 229-1107) of human type I collagen 1A2 was cloned into the HindIII and XbaI sites of the MCS of pcDNA3. This cDNA clone, called clone 1, has a GUC ribozyme target site at position 907, but has a non-cleavable CUG site at position 902) (Accession Number: Y00724).

Clone 2 with adanine residues at positions 902 and 907 was generated by PCR mutagenesis utilising a HindIII to XbaI cassette. This clone has a CUA ribozyme target site at position 902, having lost the site at 907 (GAC). Clones 1 and 2 are polymorphic variants of one another.

Ribozyme 902

Ribozyme 902 (Rz902) was designed to cleave human type I collagen 1A2 at a CUA ribozyme target site (position 900-902) in clone 2 (see above). Antisense arms are underlined.

Rz902: <u>GGUCCAG</u>CUGAUGAGUCCGUGAGGACGAA<u>AGGACCA</u>

Ribozyme 907

Ribozyme 907 (Rz907) was designed to cleave human type I collagen 1A2 at the GUC ribozyme target site (position 906-908) in clone 1 (see above).

Antisense arms are underlined.

116

Rz907: <u>CGGCGG</u>CUGAUGAGUCCGUGAGGACGAA<u>ACCAGCA</u>

Ribozyme pol1a1

Ribozyme pol1a1 (Rzpol1A1) was designed to cleave human type I collagen 1A1 at a CUC ribozyme target site (position 3209-3211) in the clone with the T allele (see above). Antisense arms are underlined.

Rzpol1A1: <u>UGGCUUUU</u>CUGAUGAGUCCGUGAGGACGAA<u>AGGGGGU</u>

3.2.6. In vitro transcription of RNA

Constructs were linearised and expressed *in vitro* using the Promega Ribomax expression kit and standard protocols. Frequently different restriction enzymes were utilised so resulting transcripts would by of different lengths and therefore distinguishable on polyacrylamide gels. Radiolabeling of RNA was achieved by incorporating [αP^{32}]rUTP (Amersham) in the expression reaction (Gaughan et al., 1995, Millington-Ward et al., 1997). Resulting RNA was run on 4% polyacrylamide gels and was purified from these using 0.3 M sodium acetate and 0.2% SDS. The enzymes used to linearise the clones and the expected size of the RNA products are given in table 1.

3.2.7. Cleavage of RNA

RNA hammerhead ribozyme cleavage reactions were performed under standard conditions at 37°C. MgCl$_2$ curves (0-15mM) for the cleavage reactions were performed in order to optimise the MgCl$_2$ concentration in the reaction (normally for 3 hours). Timepoints of up to 5 hours were taken for cleavage reactions using the pre-determined optimal MgCl$_2$ concentration. Radiolabeled target RNAs, replacement hybrid RNAs and cleavage products were run on 4-8% polyacrylamide gels and were visualised on autoradiograph film (see section 2.2.5). The expected sizes of cleavage products are given in table 1.

3.2.8. DNA Ladder

MspI cut pBR322 was end-labeled using standard protocols. This was used as a rough size estimate for RNA in all the experiments (figure 4a). DNA and RNA do not, however, migrate at exactly the same speed; hence the marker serves as a means to roughly estimate RNA size.

3.2.9. Maximum quantity of target cleavage by ribozyme

Maximum quantity of cleavage by a ribozyme (maximum extent of cleavage) was assessed for Rz8 and Rzpol1a1 using various molar ratios of ribozyme to template

RNA in cleavage reactions. Ratios of template to ribozyme varied between 1:1, 1:2, 1:5, 1:10, 1:50, 1:100, 1:200, 1:250 and 1:500. The formula used to work out the molar ratio of ribozyme to template RNA was the following:

$[(e/f)] \times [(b \times d) / (a \times c)]$

a = length of ribozyme

b = length of target RNA

c = the ratio of hot to cold rUTP used in the expression of the ribozyme

d = the ratio of hot to cold rUTP used in the expression to the template

e = the number of disintegrations of the ribozyme used in the reaction

f = the number of disintegrations of the template used in the reaction

Disintegrations per minute (dpm) were counted in a liquid scintillation counter. Subsequent gels were radioactively quantified using an instant imager (Packard). Background was corrected for by counting equal areas of uncleaved and product RNAs.

3.3. Results

In this chapter mutation-specific and mutation-independent strategies for gene suppression were studied for dominant-negative gene therapies. The mutation-independent methods of gene suppression were designed in an attempt to overcome the heterogeneity, frequently associated with autosomal dominant disorders including RP, OI and epidermolysis bullosa (EB). The strategies were tested utilising hammerhead ribozymes, though in theory other suppression affectors, such as peptide nucleic acids and antisense could be used. Hammerhead ribozymes were chosen in this project because of their sequence specificity, the ease whith which they can be generated and their flexibility in target seqence (see sections 1.3-1.5). In addition hammerhead ribozymes have on many occasions been utilised with success in cell culture and animal models (see sections 1.6, 1.11 and 1.12). It is of note that designing a mutation-specific suppressor, such as a ribozyme, towards each separate mutation, causing a dominant heterogeneous disorder, may not be possible in terms of time and cost. Some individual mutations may only occur in a single small family. Also, in terms of design, it may not be possible to generate suppressors towards mutation sites. For instance, hammerhead ribozymes have strict sequence requirements necessary for efficient cleavage, such as the presence of an NUX site (most mutations do not create NUX sites), situated in an open-loop structure, which is accessible to the ribozyme. Some other suppressors currently in

use, such as hairpin ribozymes, have ever more stringent requirements (see chapter 1, figure 2 and section 1.3.2).

However, three mutations in the human rhodopsin gene, known to cause adRP, created hammerhead ribozyme NUX target sites and were predicted to be situated in open-loop structures of the target RNA. Thus, these mutation sites were suitable for mutation-specific hammerhead ribozyme suppression and the wildtype rhodopsin transcript (which does not contain the NUX site) should not be cleavable by the ribozymes. Thus, three mutation dependent ribozymes targeting different mutations in human rhodopsin were generated (discussed in detail in paragraph 3.3.1). Mutant rhodopsin cDNAs were generated by PCR directed mutagenesis. All three ribozymes were shown to cleave the mutant rhodopsin RNAs and to leave wildtype rhodopsin RNAs intact. In addition, all cleavage products were of the correct size, though cleavage efficiencies varied (for details see 3.3.1; figures 3 and 4). However, as mentioned above, most mutations are not suitable for selective ribozyme cleavage. In addition, most dominant negative disorders are extremely heterogeneous as many mutations within one gene may cause similar disease pathology. Thus two methods of gene suppression utilising hammerhead ribozymes were investigated which are mutation-independent.

The first mutation-independent strategy (discussed in detail in paragraph 3.3.2) for gene suppression tested in this study involved a suppression and replacement step. Ribozymes were directed towards NUX target sites, situated in the 3' or 5'UTRs of human rhodopsin (figure 2a), peripherin/*RDS* (figure 2b), or COL1A2 (figure 2c) RNAs. Ribozymes would therefore in theory cleave both mutant and wildtype RNAs of these genes, making a replacement step necessary. Replacement genes were generated with altered UTRs at the NUX ribozyme target site, which were thus protected from ribozyme cleavage. Four ribozymes were generated, tested *in vitro*, and shown to cleave wildtype RNAs while leaving replacement RNAs intact. In addition, the maximum extent for cleavage of one of these ribozymes was determined with a view to use the ribozyme in subsequent *in vivo* studies.

The second mutation-independent strategy for gene suppression in this study involved the suppression of mutant alleles at polymorphic sites situated on the same allele as mutation sites. Thus, if haploinsufficiency were not to play a large role in the disease pathology, a replacement step may not be necessary. This method was tested for three ribozymes, which targeted polymorphic sites in human COL1A1 (figure 2d) and COL1A2 (figure 2c) (discussed in detail in paragraph

3.3.3). In each case ribozymes were shown to selectively cleave one of the polymorphic variants, while leaving the other intact. With a view to possibly using one of these ribozymes in subsequent *in vivo* studies, the maximum extent of cleavage was determined.

Thus, one mutation-specific and two mutation-independent methods of gene suppression were tested *in vitro* using twelve different hammerhead ribozymes targeting four human genes (rhodopsin, peripherin/*RDS*, COL1A1 and COL1A2). All cleavage NUX sites were predicted with PlotFOLD to occur in accessible open-loop structures of target RNAs (figure 2). Ribozyme cleavage of target RNAs and replacement RNAs were tested *in vitro* at various MgCl$_2$ concentrations and for varying times (figures 3-9, paragraphs 3.3.1-3.3.3). All cleavage products were of the predicted sizes and all replacement RNAs were protected from cleavage and remained intact. Details are given below.

3.3.1. Disease Specific Mutation (codons 23, 51 and 255)

The first mutation-specific ribozyme (Rz447), was generated to cleave human rhodopsin RNA at a mutation site (GlyGGC51ValGTC at position 445-447/GUC), known to cause adRP in humans. Wildtype rhodopsin RNA (4B) which does not contain the mutant NUX target site, should thus in theory be protected from cleavage by Rz447. Rz447 was digested with XbaI and expressed *in vitro*. A mutant rhodopsin clone (GlyGGC51ValGTC) and the wildtype human rhodopsin were digested with BstEII and AcyI respectively. Both constructs were expressed *in vitro*. Resulting RNAs were mixed together at various Mg^{2+} concentrations (figure 3a) and for varying times (figure 3b). Template and ribozyme were added together in a molar ratio of 1 to 30. As expected the ribozyme specifically cut mutant rhodopsin transcript while leaving wildtype transcript intact. However, the cleavage efficiency was relatively low and about 30% of the mutant RNA remained intact after 5 hours. The Mg^{2+} concentration appeared not to have any influence on the cleavage efficiency of Rz447 (figure 3a).

The second mutation-specific ribozyme designed and tested during the course of this Ph.D. was Rz255, designed to target a known rhodopsin deletion (causing adRP) at codon 255. Rz255 was designed to target and cleave the AUG site flanking the deletion on either side while leaving the wildtype transcript intact. Codon 255 of human rhodopsin was deleted from the wildtype gene by PCR directed mutagenesis (clone Del255ATC). The clone was digested with AcyI and

expressed *in vitro*. In addition, the wildtype human rhodopsin was digested with BstEII and expressed *in vitro*. Rz255 was digested with XbaI and was expressed *in vitro*. Resulting RNAs were mixed together with various concentrations of MgCl₂, incubated for 3 hours and run on an acrylamide gel (figure 3c). Rz255 cleaves Del255ATC specifically while leaving the wildtype rhodopsin transcript intact. All cleavage products were of the predicted size. Interestingly, the MgCl₂ concentration does seem to influence the cleavage efficiency of Rz255. At a higher concentrations of Mg²⁺(15mM), Rz255 cleaves more efficiently than at the lower concentrations. Thus, using a 15mM concentration of MgCl₂, a timepoint was carried out in the presence of a 150x molar excess of Rz255 (figure 3d). After 5 hours most of the template had been cleaved, however, a residual amount of mutant transcript remained intact. Non cleavage of the wildtype RNA (4B) by Rz255 was demonstrated in a separate experiment (data not shown).

The third ribozyme generated to target a specific mutation was ribozyme 20 (Rz20), designed to target and cleave an adRP mutation site (ProCCC23LeuCUC) at position 361-363 of human rhodopsin, while leaving wildtype rhodopsin RNA intact (accession number K02281). Mutant Pro23Leu cDNA was generated by PCR directed mutagenesis, digested with BstEII and expressed *in vitro*. In addition, Rz20 was digested with XbaI and was expressed *in vitro*. Resulting RNAs (with a 40x excess of Rz20) were mixed together at various MgCl₂ concentrations and subsequently run on polyacrylamide gels. As expected, the mutant RNA was cleaved specifically. Cleavage products were of the predicted sizes. Non-cleavage of wildtype human rhodopsin was determined in a different experiment (data not shown). In a timepoint experiment only a residual amount of mutant RNA remained uncleaved after 5 hours (figure 4b), demonstrating the relatively high efficiency of Rz20. However, as most adRP mutations do not create NUX sites, necessary for ribozyme cleavage, and do not occur in accessible predicted open-loop structures of RNA and as many mutations within one given gene may cause a disease phenotype, it is not always either possible or practical to design disease-specific ribozymes. A more general approach would be to target an open-loop structure, not at a mutation site, but at a wobble position of a target transcript and to re-administer the gene with the base at that particular wobble position altered, so it is protected from cleavage by the ribozyme. With this in mind, Rz10 was designed to cleave the human rhodopsin transcript at a third base wobble position at a GUC (position 475 to 477) of human rhodopsin in a large predicted open-loop structure of the RNA (figure 2a). Mutant Pro23Leu DNA and wildtype human

rhodopsin were digested with BstEII and AcyI respectively and were expressed *in vitro*. Rz10 was digested with XbaI and was also expressed *in vitro*. Resulting RNAs were incubated together for different periods of time and were run on a polyacrylamide gel (figure 4c). Rz10 was again a highly efficient ribozyme, leaving very little of the mutant rhodopsin target uncleaved after 5 hours. All products were of the predicted size. The mutation-independent strategy, based on the wobble hypothesis and demonstrated with Rz10 has been studied in this laboratory in depth by Brian O'Neill, but was not further tested during the course of this Ph.D. (Millington-Ward et al., 1997). Notably, the most common mutation to cause adRP in the United States (12% of cases) is the Pro23His mutation. The mutant transcript generated for testing Rz20 and Rz10 carried not the Pro23His, but the less common Pro23Leu mutation, because Dr. Bill Hauswirth was investigating the use of ribozymes against the Pro23His mutation already (personal communication).

3.3.2 UTR cleavage and replacement

In addition to the mutation-specific method of gene suppression discussed in 3.3.1, two mutation-independent strategies of gene suppression were studied. The first of these was based on UTRs. Two mutation-independent ribozymes, ribozymes 8 and 9, were designed to cleave the human peripherin/*RDS* transcript in the 5'UTR (positions 234-236 (GUA) and 190-192 (GUU) respectively). Peripherin/*RDS* was chosen to demonstrate the utility of the mutation-independent strategy, because it is known to cause, amongst other diseases, adRP. Rz8 and Rz9 were digested with XbaI and were expressed *in vitro*. Clones 6B (human peripherin/*RDS*) and 7A (human peripherin/*RDS* hybrid (replacement), with part of the 5'UTR sequence replaced with mouse peripherin 5'UTR sequence) were cut with BglII and AvrII respectively and expressed *in vitro*. Resulting RNAs were mixed with Rz8 RNA in both magnesium chloride and timepoint reactions, to test for specific cleavage. The exact magnesium chloride concentration used in the reaction made a slight difference to the cleavage efficiency of Rz8. Cleavage efficiencies seemed to be somewhat higher at higher MgCl$_2$ concentrations. Most of 6B was cleaved while 7A, lacking the target site in the 5'UTR of human peripherin/*RDS*, remained intact (figure 5a). In the timepoint reaction with Rz8, again 7B remained intact, while 6B was almost fully cleaved after 180 minutes (figure 5b). Almost the same results were obtained in a magnesium chloride curve and timepoint with 6A, 7A and Rz9. This ribozyme, however, seems to cleave even more efficiently, leaving very little of 6A transcript uncleaved after 180 minutes. In addition, Rz9 does not seem to be sensitive to MgCl$_2$ concentration (figures 5c/d). Magnesium chloride curves and

timepoints of Rz8 and Rz9 were carried out in collaboration with Brian O'Neill. (Brian O'Neill expressed RNAs and set up cleavage reactions, and the author gel-purified RNAs and ran polyacrylamide gels).

In addition, the maximum extent of cleavage of 6B by Rz8 was tested *in vitro*, in order to assess whether this ribozyme should be used in later *in vivo* experiments. Various molar ratios of 6B and Rz8 were used in three-hour cleavage reactions and resulting samples run on a polyacrylamide gel (figure 5e). The resulting gel was quantified and a graph plotted (figure 5f and 5g). As is clearly shown in figure 5, a 50 fold molar excess of ribozyme is needed to cleave half the template. However, using a Rz8 molar excess of 200 fold, over 70% of 6B is cleaved. Thus, 30% of the target transcript remains intact, which possibly may impair later *in vivo* cleavage experiments.

The second gene chosen to illustrate the first mutation-independent strategy of gene suppression, based on UTR, was human rhodopsin, a gene known to cause adRP. Hammerhead Rz15, designed to cleave the human rhodopsin transcript in the 5' UTR was generated. In addition, a hybrid (replacement) rhodopsin transcript with a shortened 5'UTR and not containing the cleavage site was generated. Rz15 was designed to cleave human rhodopsin RNA in a predicted loop structure at position 249-251. However, the loop was not predicted to be either very large or to have a large amount of integrity between different RNA conformations. A series of magnesium chloride curve experiments was carried out with Rz15 and human rhodopsin RNA. Saturating levels of ribozyme were added in each experiment.

In the first experiment 4B (full human rhodopsin construct) and 5A (replacement human rhodopsin construct with a shortened 5' UTR) were digested with BstEII and expressed *in vitro*. Rz15 was cut with XbaI and also expressed *in vitro*. Resulting RNAs were mixed together and magnesium chloride curves were carried out (figure 6a/b). Non-cleavage of 5A transcript was demonstrated in a separate experiment (data not shown). In the second experiment carried out with Rz15, 4B and 5A were digested with AcyI and resulting RNAs were mixed separately with Rz15 RNA. The reason that 4B and 5A RNA was not mixed together was that the sizes of the RNAs would have been too similar to distinguish on a polyacrylamide gel. Again magnesium chloride curves were carried out (figure 6c). In the third experiment, clone 4B was digested with BstEII and 5A with FspI. Resulting RNAs were mixed together with Rz15 RNA. Magnesium chloride curves were carried out (figure 6d). All RNAs and cleavage products were of the predicted size and the

MgCl$_2$ concentration seemed not to influence the cleavage efficiency of Rz15. 5A, having a shortened 5'UTR and therefore not containing the cleavage target site, was not cleaved by Rz15 in any of the experiments. In each experiment 4B was cleaved by Rz15, however, only partially. This is consistent with the predicted inconsistency of the open-loop structure of 4B around the ribozyme target NUX site and may be caused by the ribozyme's difficulty in approaching or binding the target site. AcyI was the only enzyme used that cuts 4B after the rhodopsin stop codon. Resulting RNA is therefore full length and the most likely to have a three dimensional structure similar to the rhodopsin transcript found in photoreceptor cell.

The last ribozyme targeting UTR sequence of the human rhodopsin transcript designed and tested during this Ph.D. was Rz25, targeting the 3'UTR. This ribozyme was added in equal amounts to wildtype human rhodopsin transcript (4B) and incubated for various times at 37°C. However, cleavage, although specific, was very inefficient (figure 7c). In addition, non-cleavage of replacement 8A transcript was demonstrated (data not shown).

The third gene chosen to highlight the first mutation-independent strategy, based on UTR was human COL1A2, a gene known to cause dominant OI. Thus, ribozyme 18, designed to cleave human type I collagen 1A2 at a GUX site at position 448-450 of the 5'UTR, was generated. Rz18 was digested with XbaI and expressed *in vitro*. A construct containing the 5'UTR and exon 1 of the human collagen 1A2 cDNA (clone1B) was digested with XhoI and expressed *in vitro*. In addition, a hybrid replacement construct containing exon 1 of the human collagen 1A2 (clone 2A) cDNA and the 5'UTR of human collagen 1A1, was digested with XhoI and expressed *in vitro*. Magnesium chloride curves and timepoint reactions were carried out for Rz18 and clones 1B and 2A (figure 7a/b). In both experiments, saturating levels of Rz18 were used (molar ratio of target RNA to Rz18 was 1:50). Both experiments clearly demonstrate that Rz18 is not efficient at cleaving the target transcript, though Rz18 does seem to function at low magnesium chloride concentrations. The reason that cleavage is so incomplete may, possibly, be that the target NUX site is predicted to be situated in a very small open-loop structure. All cleavage products were of the expected size. The initial rate of the cleavage reaction was determined from the slope of a graph of % product versus time and was estimated to be 1.0×10^{-4} min^{-1} (data not shown).

3.3.3. Polymorphism

3.3.3.1. Finding common polymorphisms

The second mutation-independent strategy for gene suppression, studied during this Ph.D., was based on the selective silencing of one polymorphic allele at a polymorphic site. For a polymorphic site to be a suitable ribozyme target site, it must be situated in a large open-loop structure of target RNA, create a ribozyme cleavage NUX site and must, importantly, occur frequently in the population. The first genes that were investigated to establish if they harbor such polymorphisms were human rhodopsin and peripherin/*RDS*. Using the computer program PlotFOLD it was predicted that two human rhodopsin and peripherin/*RDS* polymorphisms, previously described in the literature, were fortuitously situated in open-loop structures of these two transcripts. Thus these polymorphisms represented possible candidate sites for designing mutation-independent ribozymes towards.

The first candidate polymorphism (Ile32Val) was situated at position 611 of the human peripherin/*RDS* gene. SSCPE analyses were carried out on PCRs from DNA samples purified from 20 individuals from the Irish population. The PCRs, which spanned the area of the peripherin/*RDS* gene containing the Ile32Val polymorphism, were subjected to SSCPE analysis in an attempt to determine the frequency of this polymorphism. No shifts were found, even though a control sample (kindly provided by Dr. Fiona Mansergh) shifted in the expected manner (data not shown).

The second polymorphism which was analysed for its allele frequency was situated in intron 4 of the human rhodopsin gene. This polymorphism destroys a BanI restriction site. Therefore, BanI digests were carried out on PCRs, containing the polymorphic site, amplified from DNA samples from 20 unrelated Irish individuals. Unfortunately, the polymorphism was not detected in these 20 samples and the polymorphism was therefore considered to be too rare for further study.

Thus, no common polymorphisms were discovered in either the human rhodopsin or the human peripherin/*RDS* gene. However, additional genes, which could be targeted by hammerhead ribozymes, were investigated for the presence of frequent polymorphisms situated in open-loop structures of the target RNA and which created ribozyme cleavage (NUX) sites. In the context of this Ph.D., two genes

known to cause OI, the type I collagen genes (COL1A1 and COL1A2), were investigated.

3.3.3.2. Rzpol1a1

Westerhausen et al., (1991) first described a C/T polymorphism at position 3210 in the human collagen 1A1 gene. One polymorphic variant (the T-allele) contains a ribozyme NUX target site, while the other (the C-allele) does not. They assessed the frequency of the polymorphism in 18 individuals. 11 were homozygous T, 5 were heterozygous and 2 were homozygous for the C-allele. We assessed an additional 11 unrelated individuals from the CEPH panel for the polymorphism. Of the total of 58 alleles, 42 were T and 16 were C. The frequencies for the T- and C-alleles, p and q respectively, are therefore estimated to be $p = 0.72$ and $q = 0.28$, suggesting that the frequency of heterozygotes is 0.4032 (2pq). In addition, RNA PlotFOLD predicted that the C3210T polymorphism is situated in an, extremely large conserved loop structure of the COL1A1 RNA (figure 2c). Thus, this polymorphism fulfilled all three criteria necessary for being a suitable hammerhead ribozyme site for this mutation-independent strategy. Rzpol1a1, was therefore designed to cleave one polymorphic allele, the T-allele, while leaving the other polymorphic allele, the C-allele, intact. To determine the specificity of Rzpol1a1 cleavage a $MgCl_2$ curve was carried out with Rzpol1a1, the T-allele RNA (figure 8a) and the C-allele RNA (figure 8b). As expected Rzpol1a1 cleaved the T-allele RNA and left the C-allele RNA intact. In addition, a time-point cleavage reaction was carried out with Rzpol1a1 and the T- and C-allele RNAs respectively (figure 8c/d). This demonstrated that Rzpol1a1 was not only specific, but also very efficient at cleaving the T-allele transcript; after 30 minutes most of the template had been cleaved. Therefore, with a view to possibly using Rzpol1a1 in future *in vivo* studies, the maximum extent of cleavage of the T-allele RNA by Rzpol1a1 was determined. Various molar ratios of T-allele RNA and Rzpol1a1 were used in three-hour cleavage reactions (figure 8e). The resulting gel was quantified and a graph showing cleavage efficiency for various molar ratios of Rzpol1a1 to target RNA plotted (figure 8f). As is clear from figure 8e/f, Rzpol1a1 is extremely efficient, cleaving 90% of the template COL1A1 RNA with only a 5 fold molar excess of ribozyme. Interestingly, the reaction seems to show asymptotic behaviour, reaching 93% cleavage, suggesting that 7% of the COL1A1 transcript may not be suitable for cleavage by Rzpol1a1. This may possibly be due to 7% of the COL1A1 transcript having an alternative conformation, which is not accessible to Rzpol1a1. However, the cleavage efficiency achieved is sufficiently high to make Rzpol1a1 an extremely

interesting ribozyme as a potential mutation-independent therapeutic agent for COL1A1 associated OI and hence warranting further study (Millington-Ward et al., 1999).

3.3.3.3. Colpol1a2, 902 and 907

Two additional polymorphic sites in the COL1A2 transcript were investigated as potentially suitable sites for ribozyme cleavage. Ribozymes 902 and 907 (Rz902 and Rz907) were designed to cleave two naturally occurring polymorphic NUX and GUX sites at positions 902 and 907 of the human COL1A2 gene. Both sites were predicted to be situated in open-loop structures of the target RNA. However, the open-loop containing the Rz902 target site was not consistently predicted to occur at all the ΔG levels. The ribozymes were cloned and expressed *in vitro* after linearisation. In addition, two polymorphic variants of the human COL1A2 gene, A and B, containing respectively G (902), T (907) and A (902), A (907) were cloned, linearised and expressed *in vitro*. Rz902, clone A and clone B RNAs were mixed together at various $MgCl_2$ concentrations. Rz902, although able to cleave clone B RNA specifically while leaving clone A RNA intact, was not efficient at any of the $MgCl_2$ concentrations tested (figure 9a). This is consistent with the predictions of RNA secondary structure, in which the loop targeted by Rz902 was not always present for different RNA energy levels.

A $MgCl_2$ curve of Rz907, clone A RNA and clone B RNA was also carried out. Again Rz907 cleaved the target site in clone A specifically, while leaving clone B intact. No noticeable difference was found in cleavage efficiency at different $MgCl_2$ concentrations (figure 9b). A timepoint was then undertaken for this ribozyme, demonstrating almost complete cleavage after 5 hours (figure 9c).

In summary, twelve hammerhead ribozymes have been designed and tested *in vitro* for cleavage of mRNAs of human rhodopsin, human peripherin, human COL1A1 and COL1A2. Three of these were designed to cleave human rhodopsin at dominant mutation sites known to cause adRP in humans. The ribozymes successfully cleave the target RNAs at the expected positions. However, to circumvent complications associated with the allelic heterogeneity associated with many dominant disorders, including RP, two general approaches for gene suppression were tested successfully *in vitro*, one utilising intragenic polymorphism and the other UTRs. Each of the remaining 9 ribozymes elicited specific cleavage of target transcripts, although cleavage efficiencies varied substantially. One ribozyme in particular, Rzpol1a1 targeting a polymorphic site in

human COL1A1, was extremely efficient *in vitro* and may potentially be very useful as a mutation-independent therapeutic agent for COL1A1 associated OI.

3.4. Discussion

In the development of gene therapies for dominant negative disorders it will be necessary to devise methods of suppressing mutant alleles. However, many dominant disorders, such as RP, OI, epidermolysis bullosa (EB) and hypertrophic cardiomyopathy, are heterogeneous in their etiologies. For instance over 100 and 40 mutations in rhodopsin and peripherin/*RDS* respectively are known to cause RP. In addition, over 150 mutations in COL1A1 and COL1A2 are known to cause OI. Many of these mutations are extremely rare making the generation of gene therapies based on targeting specific mutations unlikely. Many mutations may not lend themselves to selective suppression by therapeutic agents such as antisense RNA, DNA or ribozymes. Antisense RNAs and DNAs, for instance, may not be able to distinguish between wildtype and mutant alleles, as these may, in many cases, only differ by a single base. Hammerhead ribozymes on the other hand require specific and accessible target NUX sites, which most mutations do not create. Some mutation sites such as the Pro23Leu, Del255 and Gly51Val mutations in human rhodopsin, known to cause adRP and which have been investigated in this chapter, create suitable ribozyme NUX cleavage sites which occur in open-loop structures of the target RNA (figures 3 and 4). However, statistically this situation is not likely to occur very frequently. Unfortunately, antisense arms of a ribozyme (stems 1 and 3, see figure 1) are in many cases unlikely to be able to discriminate between single base changes. Dr. Fiona Mansergh tested this approach using a hammerhead ribozyme targeting a human rhodopsin mutation, Met207Arg, and found that the ribozyme cleaved both the mutant and wildtype alleles (personal communication). In a similar fashion, other gene suppressors such as hairpin ribozymes, antisense DNA and RNA, triple helices and peptide nucleic acids may either have more complex target sequence requirements or may not be sufficiently specific to achieve the selective silencing of a disease allele which differs by one base from the wildtype allele (see sections 1.1 to 1.3). This study, therefore, explores two strategies for suppressing mutant alleles *in vitro*, which are mutation-independent and thus in principle are applicable to many individuals with different mutations within a gene. For each of these approaches hammerhead ribozymes have been utilised.

The first strategy is based on the silencing of mutant and wildtype RNAs at NUX sites in UTRs. A replacement, hybrid gene, is generated, which is altered at the NUX site and protected from ribozyme cleavage. Replacement UTRs may be modified in a variety of ways. For example, replacement UTRs may be altered by just one or two bases so the NUX site is destroyed or may be shortened so that the NUX site and the sequence surrounding it are absent. In addition, the UTRs may be replaced with UTRs from genes with similar expression profiles. Ribozymes 15 and 25 targeting the human rhodopsin 5' and 3'UTRs respectively and ribozymes 8 and 9 targeting the 5'UTR of human peripherin/*RDS*, were all found to cleave wildtype RNAs specifically while leaving replacement RNAs intact (figures 5, 6 and 7c). Replacement RNAs, which only differ from wildtype RNAs by one base at the NUX site, theoretically make the unwanted down-regulation of replacement RNAs due to an antisense effect by stems 1 and 3 of the ribozyme (figure 1) a distinct possibility. This possible effect would require further *in vivo* study. Such an antisense effect, caused by non-functional ribozyme, which differed from a functional ribozyme in one base only (at the NUX target site), was observed *in vivo* and presented by Dr. Bill Hauswirth at the 3rd international EU meeting on New therapeutic approaches in hereditary eye diseases-"from genes to cure" at Tuebingen, Germany. Dr. Hauswirth described the use of a functional hammerhead ribozyme, targeting an artificially introduced NUX ribozyme target site in a human rhodopsin transgene, in a transgenic rat model for adRP. Subsequent to subretinal injection in the rat model with an adeno-associated viral vector (AAV) with functional and non-functional ribozyme (used as a control) a down-regulatory effect on transgene expression was observer in both cases, although the effect with the functional ribozyme was greater.

With this antisense effect in mind, Ribozyme 18, studied in this chapter of the Ph.D. thesis, was designed to cleave COL1A2 transcript in the 5'UTR. However, a replacement COL1A2 gene, containing an altered 5'UTR without the ribozyme cleavage site, was generated, which did not contain any sequence homology to the antisense arms (stems 1 and 3, see figure 1) of Rz18. The 5'UTR of COL1A2 was replaced with the 5'UTR of COL1A1, a gene with a similar expression profile, hence increasing the likelihood that transcription of the replacement gene will be correctly regulated in terms of tissue profile and levels of expression. Thus, since the replacement RNA does not contain the ribozyme cleavage site or homology to antisense arms, in principle, it should not competitively bind Rz18 and inhibit ribozyme cleavage of the target wildtype transcript. Rz18, elicited selective

cleavage of the wildtype RNA while leaving hybrid replacement transcripts intact (figure 7a/b). However, ribozyme cleavage was inefficient; the initial rate of cleavage was calculated to be 1.0×10^{-4} min^{-1}.

The mutation-independent strategy of gene suppression base on UTR relies on the concurrent administration of a replacement hybrid gene with an altered UTR sequence such that replacement transcripts are protected from suppression. There has been a substantial elucidation in recent years of the roles of 5'- and 3'UTRs on gene expression. Thus, altering UTRs in a manner, which enables tissue- and level-specific expression of replacement genes, will require careful consideration. For instance, three types of translational control on maternal mRNAs present in oocytes have emerged. The first is translational activation by cytoplasmic polyadenylation. The second is translational activation by RNA localisation and the third is regulated translational repression. In each case translational control depends on the binding trans-acting factors to sequences in the 3'UTR. Recently some of these factors have been identified, shedding light on the molecular mechanisms that mediate translational control (reviewed in Seydoux, 1996). Thus changing sequences within the 3'UTR, which interact with these factors, may potentially alter important features controlling gene expression and levels of translation. In addition, sequences in the 3'UTR and the poly-A tail can have dramatic effects on translational initiation frequency, that is the frequency that an mRNA is translated. This can have particularly profound effects in early development.

The 5'UTR, on the other hand, can determine which initiation pathway is used to bring the ribosome to the initiation codon, how efficiently initiation occurs and which initiation site is selected. In addition 5'UTR-mediated control can be accomplished via sequence-specific mRNA binding proteins (reviewed in Gray and Wickens, 1998). Again, changing the 5'UTR within these regions may alter such 5'-mediated control. Translation of mRNAs with long 5'UTRs, containing AUG sites and complex secondary structures, can severely hamper ribosomal scanning; a process necessary for translation. These characteristics are commonly found in mRNAs encoding regulatory proteins like proto-oncogenes and growth factors. Mutations in the 5'UTR or the occurrence of alternative 5'UTRs have been implicated in the progression of various forms of cancer, including melanoma and prostate cancer (Liu et al., 1999; Crocitto et al., 1997). Interestingly, the translational efficiency of mRNAs with long 5'UTRs can vary depending on the

sequence of the 5'UTR, which provides post-transciptional regulation (reviewed in van der Velden and Thomas, 1999). In summary, 5'- and 3'UTR sequences play important roles in the regulation of gene expression and therefore modifications to replacement genes would have to be designed carefully taking into consideration such mechanisms for control of gene expression.

A similar mutation-independent strategy for gene suppression utilising UTRs has been tested in cell culture (Kilpatrick et al., 1996). A hammerhead ribozyme directed towards the 5'UTR of fibrillin-1, a gene involved in Marfan syndrome, was delivered to cultured dermal fibroblasts using a ribozyme-transferrin-polylysine complex. It is notable that in this study both fibrillin-1 mRNA and protein levels were reduced.

The second mutation-independent approach for gene suppression studied in this Ph.D. thesis, also utilising hammerhead ribozymes, is based on the presence of intragenic polymorphisms in the human genome. In this method a ribozyme is directed to cleave transcripts from one polymorphic variant of the gene. This approach was tested with three ribozymes, which target three polymorphisms in the human COL1A1 and COL1A2 transcripts. In each case the ribozymes were found to specifically cleave one polymorphic variant while leaving the other intact (figures 8 and 9).

The polymorphism strategy may not be possible to design for all diseases using ribozymes, as suitable polymorphisms must occur in accessible areas of target RNAs to enable ribozyme binding (i.e. in open-loop structures of target RNAs). In addition, polymorphisms must occur frequently in the population and must create NUX ribozyme target sites. However, in situations where such a suitable polymorphism were available and a patient were heterozygous for such a polymorphism, and carried the cleavable polymorphic variant on the same allele as the mutation, a gene replacement step may not be necessary. Suppression of the mutant by targeting one allele of the polymorphism may provide therapeutic benefit. However, if haploinsufficiency causes sufficient disease pathology, a gene replacement step would still be necessary. For example, haploinsufficiency of CBFA2 causes familial thrombocytopenia with propensity to develop acute myelogenous leukemia (Song et al., 1999) and reduced expression of the G209A alpha-synuclein allele is associated with familial parkinsonism (Markopoulou et al., 1999). In addition, GATA4 haploinsufficiency in patients with an interstitial deletion of chromosome region 8p23.1 causes congenital heart disease (Pehlivan et

al., 1999). However, in cases where genes encode structural proteins, such as fibrillin-1 (associated with Marfan syndrome) and both type I collagens (associated with OI), haploinsufficiency is frequently associated with a very mild disease phenotypes, which frequently remain undiagnosed (Aoyama et al., 1994; De Paepe, 1998).

A third mutation-independent therapeutic strategy for gene suppression, touched on in paragraph 3.3.1, was based on the degeneracy of the genetic code. Rz10 in 3.3.1 was designed to cleave human rhodopsin RNA at a wobble position and a hybrid replacement construct was generated with the wobble base altered, thereby disrupting the NUX cleavage site. However, the replacement gene would in theory code for wildtype rhodopsin protein. One advantage of this third approach includes a greater choice of target sequence for suppression. Since genes are generally far larger than 5'- or 3'UTRs, they are more likely to harbor suitable ribozyme cleavage (NUX) sites in accessible regions of the target RNA than UTRs or, indeed, polymorphic sites are. In addition, it is unlikely that the alteration of a third base site in a gene will affect gene expression, whereas alterations in UTRs may possibly alter the expression of the replacement gene.

Some additional complications that may be encountered while exploring the utility of using ribozymes *in vivo* are that ribozymes may not be expressed at sufficiently high levels *in vivo* to make a substantial difference in target transcript levels or that the ribozyme catalytic activity may not be great enough to down-regulate target gene expression. In addition, competitive inhibition, caused by cellular RNA, DNA and the replacement RNA, all present in a cell, may greatly reduce the ribozyme's catalytic efficiency *in vivo*. It is therefore imperative to select ribozymes which are very catalytically active *in vitro*, for subsequent *in vivo* studies. It is of note that the catalytic efficiencies of the 12 ribozymes tested in this chapter varied significantly. Table 2 outlines the relative efficiencies of the ribozymes studied estimated by eye, the target NUX sequence and the size and consistency of the open-loop structure in the target RNA. As mentioned previously the catalytic core in all the ribozymes explored in this thesis was identical. Two research groups have tested the relative efficiencies of ribozyme cleavage by testing cleavage of all twelve permutations of the NUX site. However, these groups obtained significantly different results (see section 3.1). As can be seen from table 2, however, in the present study cleavage efficiencies seem to be largely dependent on the size and consistency of the open-loop structure and not so much on the sequence of the NUX

site. In general, the larger and more consistent the loop is, the more efficient the ribozyme was found to be. This would certainly suggest that the computer program PlotFOLD provides relatively good predictions of RNA secondary structure. The only exception to the above was Rz447; cleavage of the human rhodopsin transcript by Rz447 was found to be rather inefficient despite the size and integrity of the open-loop targeted by Rz447. However, it is of note that though Rz447 cleaves within a large open-loop structure, one of the antisense arms is not within the loop region and may reduce the binding efficiency of the ribozyme.

For future *in vivo* studies it may be necessary to reduce the competitive binding effect, described by Dr. Bill Hauswirth in Tuebingen and mentioned above, of any hybrid replacement transcript to the ribozyme. For instance, the complementary region to the ribozyme antisense arms in the hybrid replacement genes could be altered at wobble positions so as to decrease their binding capacity to the ribozyme while still coding for wildtype amino acids. Yet another possible problem associated with ribozymes *in vivo* is possible a-specific antisense inhibition and potentially even aspecific cleavage of other RNA molecules. The human genome project and computer programs such as BLAST, which can search sequence databases for sequence homology, may in time help researchers in selecting appropriate sites for designing suppession agents towards. Naturally, problems associated with the administration of gene therapies remain at large. Non-viral methods of gene delivery *in vivo* are still not very efficient compared to viral gene-delivery. However, recombinant viruses such as Adenoviruses (Ad) may elicit immune responses or be cytotoxic (for example Herpes Simplex virus). (section 1.13). However, new recombinant viruses such as HIV based viruses and Adeno Associated viruses (AAV) are being generated constantly and improved on to avoid some of these complications (see section 1.13 for detailed discussions on gene delivery).

It is of note that, the mutation-independent strategies for gene therapy, in this study utilising hammerhead ribozymes towards mutant alleles associated with single-gene disorders, may, in addition, be useful in the suppression of mutant alleles associated with polygenic disorders, such as mental illnesses, and neurological disorders such as Parkinson's disease and Multiple Sclerosis. Complex trates are most likely significantly more common than single-gene disorders and with time more multiple-gene disorders will be characterised.

In summary, in this chapter mutation-specific and mutation-independent strategies for gene suppression have been tested *in vitro*. Mutation-independent methods of gene suppression will be necessary, to overcome the immense heterogeneity inherent in many dominant negative disorders. Notably, the ribozymes tested *in vitro*, varied immensely in terms of their cleavage efficiencies, although the catalytic cores of all ribozymes were identical. It is therefore optimal to test ribozymes extensively *in vitro* for cleavage efficiency before proceeding with a ribozyme to *in vivo* studies.

To this end Rzpol1a1 targeting human COL1A1 RNA and Rz10 targeting human rhodopsin, both found to be highly efficient *in vitro*, will be used for further studies *in vivo* by the author and Brian O'Neill respectively.

3.5. Summary

Many dominant-negative disorders, such as RP, OI, epidermolysis bullosa (EB), Charcot-Marie-Tooth disease and some forms of cancer, are very heterogeneous; many different mutations within the same gene give rise to similar disease pathologies. Thus, when designing gene therapies for these disorders, it may not be practical to generate mutation-specific therapies. In this chapter, not only mutation-specific, but mutation-independent methods of gene suppression were tested *in vitro* using hammerhead ribozymes. Two of the mutation-independent strategies were based on the suppression of both mutant and wildtype alleles in UTRs or at wobble positions of the target transcript. A replacement gene was then generated which had been altered at the site of cleavage, masking it from ribozyme suppression. The third mutation-independent method of gene suppression was based on the selective suppression of a mutant RNA transcript by a hammerhead ribozyme at a polymorphic site. Thus the wildtype allele, which does not contain the suitable polymorphism for ribozyme cleavage, is left intact by the ribozyme. In all, three mutation-specific ribozymes, targeting rhodopsin mutation sites, known to cause RP were generated and tested *in vitro*. Selective cleavage of the mutant transcripts was demonstrated and wildtype rhodopsin transcript was left intact. In addition 5 ribozymes were designed to target human rhodopsin, peripherin/*RDS* and COL1A2 transcripts in either the 5' or 3' UTRs. In each case a replacement (hybrid) transcript was generated which was left intact by the ribozymes, while wildtype alleles were cleaved specifically. To demonstrate the third mutation-independent method of gene suppression, three hammerhead ribozymes were generated which cleaved one polymorphic variant of either the COL1A1 or COL1A2

gene and left the other polymorphic allele intact. As with the other ribozymes tested, target RNAs were cleaved at the polymorphic site and non-cleavage of the other polymorphic variant was demonstrated, however, cleavage efficiencies varied greatly. In addition, in some cases a residual amount of target transcript remained intact, even after prolonged incubation with the ribozyme. These ribozymes may therefore not be as suitable for *in vivo* studies. However, one extremely efficient ribozyme was discovered, Rzpol1a1, which targets a common polymorphic site in the COL1A1 gene. This ribozyme cleaves the target COL1A1 transcript fully after 3 hours and indeed most of the target transcript is cleaved after 5 minutes. This ribozyme warrants further *in vitro* characterisation with a view to using it in *in vivo* studies; both in cell culture and animal models.

3.6. Bibliography

Aoyama T, Francke U, Dietz HC, Furthmayr H. Quantitative differences in biosynthesis and extracellular deposition of fibrillin in cultured fibroblasts distinguish five groups of Marfan syndrome patients and suggest distinct pathogenetic mechanisms. J Clin Invest. 1994 Jul;94(1):130-7.

Crocitto LE, Henderson BE, Coetzee GA. Identification of two germline point mutations in the 5'UTR of the androgen receptor gene in men with prostate cancer. J Urol. 1997 Oct;158(4):1599-601.

De Paepe A. Heritable collagen disorders: from phenotype to genotype. Verh K Acad Geneeskd Belg. 1998;60(5):463-82; discussion 482-4.

Drenser KA, Timmers AM, Hauswirth WW, Lewin AS. Ribozyme-targeted destruction of RNA associated with autosomal-dominant retinitis pigmentosa. Invest Ophthalmol Vis Sci. 1998 Apr;39(5):681-9.

Dryja TP, Hahn LB, Cowley GS, McGee TL, Berson EL . Mutation spectrum of the rhodopsin gene among patients with autosomal dominant retinitis pigmentosa. Proc Natl Acad Sci U S A. 1991 Oct 15;88(20):9370-4.

Dryja TP, McGee TL, Reichel E, Hahn LB, Cowley GS, Yandell DW, Sandberg MA, Berson EL. A point mutation of the rhodopsin gene in one form of retinitis pigmentosa. Nature. 1990 Jan 25;343(6256):364-6.

Farrar GJ, Kenna P, Jordan SA, Kumar-Singh R, Humphries MM, Sharp EM, Sheils DM, Humphries P . A three-base-pair deletion in the peripherin-*RDS* gene in one form of retinitis pigmentosa. Nature. 1991a Dec 12;354(6353):478-80.

Farrar GJ, Kenna P, Redmond R, Shiels D, McWilliam P, Humphries MM, Sharp EM, Jordan S, Kumar-Singh R, Humphries P Autosomal dominant retinitis pigmentosa: a mutation in codon 178 of the rhodopsin gene in two families of Celtic origin. Genomics. 1991b Dec;11(4):1170-1.

Farrar GJ, McWilliam P, Bradley DG, Kenna P, Lawler M, Sharp EM, Humphries MM, Eiberg H, Conneally PM, Trofatter JA, et al . Autosomal dominant retinitis pigmentosa: linkage to rhodopsin and evidence for genetic heterogeneity. Genomics. 1990 Sep;8(1):35-40.

Fedor MJ, Uhlenbeck OC. Substrate sequence effects on "hammerhead" RNA catalytic efficiency. Proc Natl Acad Sci U S A. 1990 Mar;87(5):1668-72.

Gaughan DJ, Steel DM, Whitehead AS . Ribozyme mediated cleavage of acute phase serum amyloid A (A-SAA) mRNA in vitro. FEBS Lett. 1995 Oct 30;374(2):241-5.

Gray NK, Wickens M. Control of translation initiation in animals. Annu Rev Cell Dev Biol. 1998;14:399-458.

Haseloff J, Gerlach WL . Sequences required for self-catalysed cleavage of the satellite RNA of tobacco ringspot virus. Gene. 1989 Oct 15; 82(1):43-52.

Hendry P, McCall M. Unexpected anisotropy in substrate cleavage rates by asymmetric hammerhead ribozymes. Nucleic Acids Res. 1996 Jul 15;24(14):2679-84.

Inglehearn CF, Bashir R, Lester DH, Jay M, Bird AC, Bhattacharya SS. A 3-bp deletion in the rhodopsin gene in a family with autosomal dominant retinitis pigmentosa. Am J Hum Genet. 1991 Jan;48(1):26-30.

Jordan SA, Farrar GJ, Kumar-Singh R, Kenna P, Humphries MM, Allamand V, Sharp EM, Humphries P . Autosomal dominant retinitis pigmentosa (adRP; RP6): cosegregation of RP6 and the peripherin-RDS locus in a late-onset family of Irish origin. Am J Hum Genet. 1992 Mar;50(3):634-9.

Kajiwara K, Hahn LB, Mukai S, Travis GH, Berson EL, Dryja TP. Mutations in the human retinal degeneration slow gene in autosomal dominant retinitis pigmentosa. Nature. 1991 Dec 12;354(6353):480-3.

Keen TJ, Inglehearn CF . Mutations and polymorphisms in the human peripherin-RDS gene and their involvement in inherited retinal degeneration. Hum Mutat. 1996;8(4):297-303.

Liu L, Dilworth D, Gao L, Monzon J, Summers A, Lassam N, Hogg D. Mutation of the CDKN2A 5' UTR creates an aberrant initiation codon and predisposes to melanoma. Nat Genet. 1999 Jan;21(1):128-32.

Markopoulou K, Wszolek ZK, Pfeiffer RF, Chase BA. Reduced expression of the G209A alpha-synuclein allele in familial Parkinsonism. Ann Neurol. 1999 Sep;46(3):374-81.

Millington-Ward S, O'Neill B, Kiang AS, Humphries P, Kenna PF, Farrar GJ. A mutation-independent therapeutic stratagem for osteogenesis imperfecta. Antisense Nucleic Acid Drug Dev. In Press.

Millington-Ward S, O'Neill B, Tuohy G, Al-Jandal N, Kiang AS, Kenna PF, Palfi A, Hayden P, Mansergh F, Kennan A, Humphries P, Farrar GJ . Strategems in vitro for gene therapies directed to dominant mutations. Hum Mol Genet. 1997 Sep;6(9):1415-26.

Pehlivan T, Pober BR, Brueckner M, Garrett S, Slaugh R, Van Rheeden R, Wilson DB, Watson MS, Hing AV. GATA4 haploinsufficiency in patients with interstitial deletion of chromosome region 8p23.1 and congenital heart disease. Am J Med Genet. 1999 Mar 19;83(3):201-6.

Ruffner DE, Stormo GD, Uhlenbeck OC. Sequence requirements of the hammerhead RNA self-cleavage reaction. Biochemistry. 1990 Nov 27;29(47):10695-702.

Seydoux G. Mechanisms of translational control in early development. Curr Opin Genet Dev. 1996 Oct;6(5):555-61.

Shimayama T, Nishikawa S, Taira K . Generality of the NUX rule: kinetic analysis of the results of systematic mutations in the trinucleotide at the cleavage site of hammerhead ribozymes. Biochemistry. 1995 Mar 21;34(11):3649-54.

Song WJ, Sullivan MG, Legare RD, Hutchings S, Tan X, Kufrin D, Ratajczak J, Resende IC, Haworth C, Hock R, Loh M, Felix C, Roy DC, Busque L, Kurnit D, Willman C, Gewirtz AM, Speck NA, Bushweller JH, Li FP, Gardiner K, Poncz M, Maris JM, Gilliland DG. Haploinsufficiency of CBFA2 causes familial thrombocytopenia with propensity to develop acute myelogenous leukaemia. Nat Genet. 1999 Oct;23(2):166-75.

Sung CH, Davenport CM, Hennessey JC, Maumenee IH, Jacobson SG, Heckenlively JR, Nowakowski R, Fishman G, Gouras P, Nathans J. Rhodopsin mutations in autosomal dominant retinitis pigmentosa. Proc Natl Acad Sci U S A. 1991 Aug 1;88(15):6481-5.

Thomson JB, Tuschl T, Eckstein F. Activity of hammerhead ribozymes containing non-nucleotidic linkers. Nucleic Acids Res. 1993 Dec 11;21(24):5600-3.

Tuschl T, Eckstein F. Hammerhead ribozymes: importance of stem-loop II for activity. Proc Natl Acad Sci U S A. 1993 Aug 1;90(15):6991-4.

Vaish NK, Heaton PA, Eckstein F. Isolation of hammerhead ribozymes with altered core sequences by in vitro selection. Biochemistry. 1997 May 27;36(21):6495-501.

van der Velden AW, Thomas AA. The role of the 5' untranslated region of an mRNA in translation regulation during development. Int J Biochem Cell Biol. 1999 Jan;31(1):87-106.

Westerhausen AI, Constantinou CD, Prockop DJ . A sequence polymorphism in the 3'-nontranslated region of the pro alpha 1 chain of type I procollagen. Nucleic Acids Res. 1990 Aug 25;18(16):4968.

Zaug AJ, Grosshans CA, Cech TR. Sequence-specific endoribonuclease activity of the Tetrahymena ribozyme: enhanced cleavage of certain oligonucleotide substrates that form mismatched ribozyme-substrate complexes. Biochemistry. 1988 Dec 13;27(25):8924-31.

Zoumadakis M, Tabler M . Comparative analysis of cleavage rates after systematic permutation of the NUX consensus target motif for hammerhead ribozymes. Nucleic Acids Res. 1995 Apr 11;23(7):1192-6.

Zuker M. Computer prediction of RNA structure. Methods Enzymol. 1989;180:262-88.

Figure 1a.

Substrate

↓

Stem 1

5' N N N N N N N *N U X* N N N N N N N N N 3'
    | | | | | | | | | | | | | | | | | |
3' N N N N N N N N A   N N N N N N N N N 5'

Stem 3   A   C

                        U

                          G

              A   A

              G   **U**

                      G

              G   A

              C-G
              C-G   Ribozyme
Stem 2 G-C
              G-C
              A   G
                A A
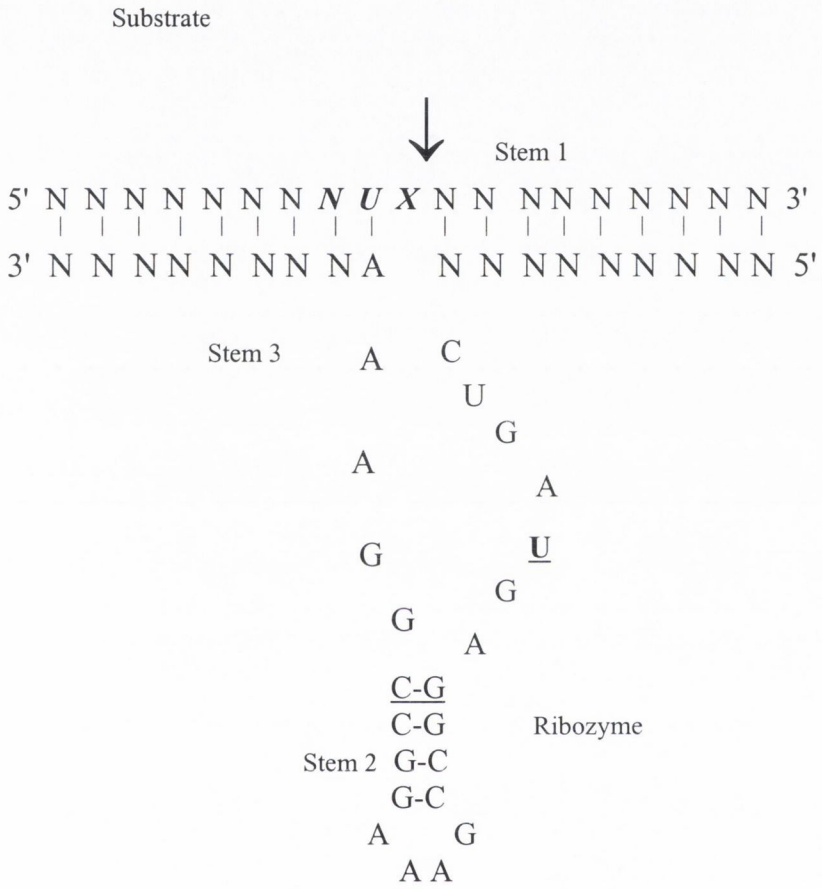
Figure 1a. Hammerhead ribozyme structure used for all ribozymes. Hammerhead ribozymes consist of two antisense arms with which they bind a complementary substrate and 24 highly conserved nucleotides. Dashes indicate Watson-Crick base pairs. N means any base. The arrow indicates the cleavage site in the target RNA, just after the NUX site, which is in italics. At the position of the only unconserved base in the catalytic core (underlined and in bold print) we used a Uracyl residue. Stems 1-3 of the ribozyme are shown. We generated all our ribozymes with the C-G (underlined in stem 2), because these, though not conserved, are known to be the most active residues at these two positions.

Figure 1b
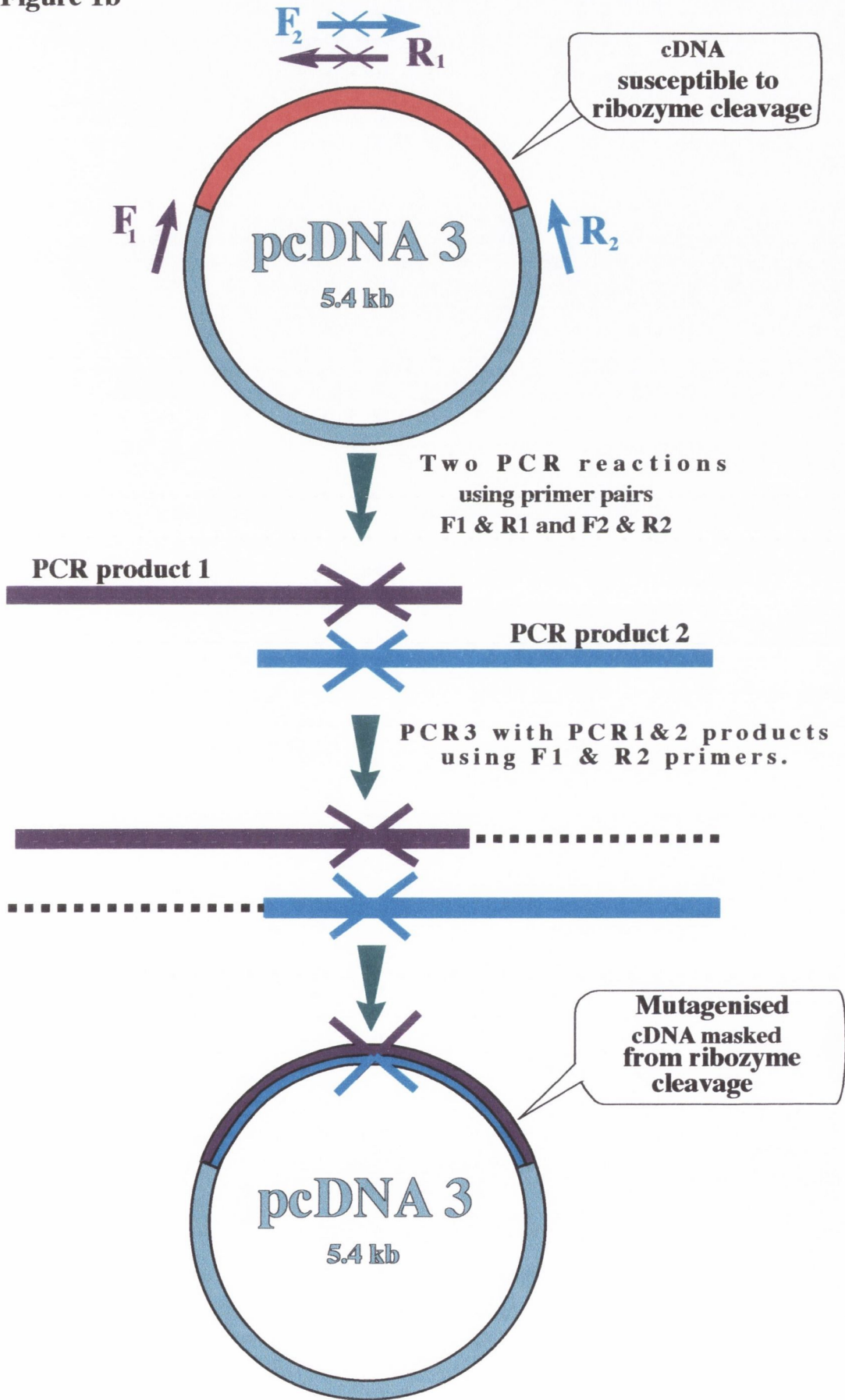
Figure 1b. Diagram of PCR directed mutagenesis. Two PCR amplifications are carried out with primer pairs F_1 and R_1 (Blue), and F_2 and R_2 (purple). However, F_2 and R_1, which overlap in at least 20 nucleotides, have base missmatches at the site one wishes to mutaginise (indicated with an X). The two resulting PCR products are gel-isolated (in order to remove any residual primers) and used as template DNA for a third PCR amplification, which is carried out with primers F_1 and R_2.

Figure 2.
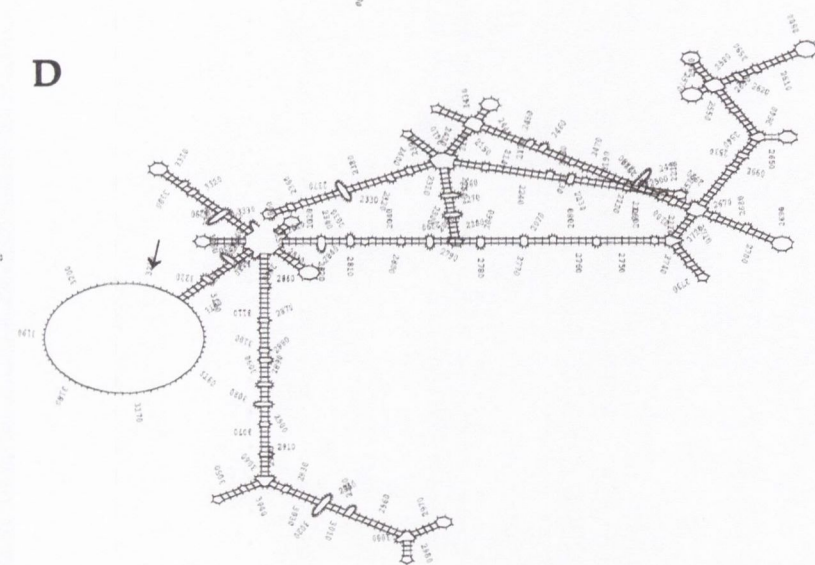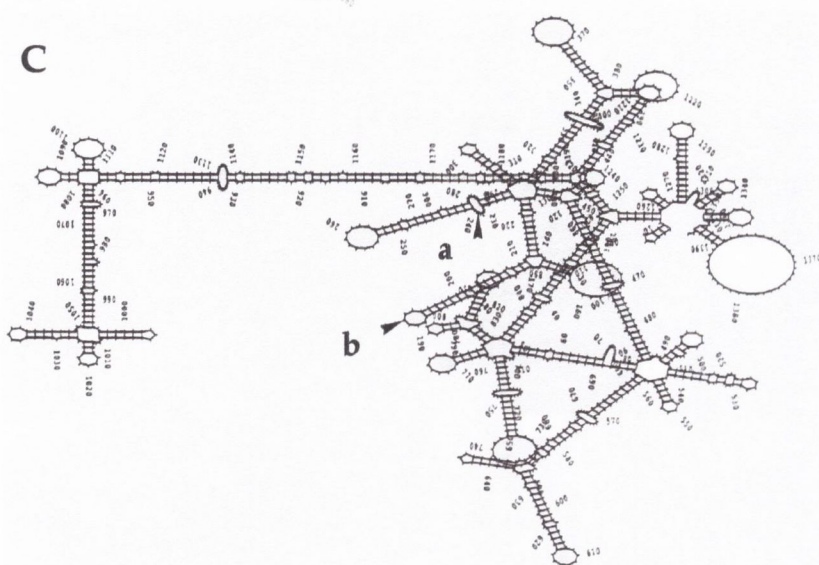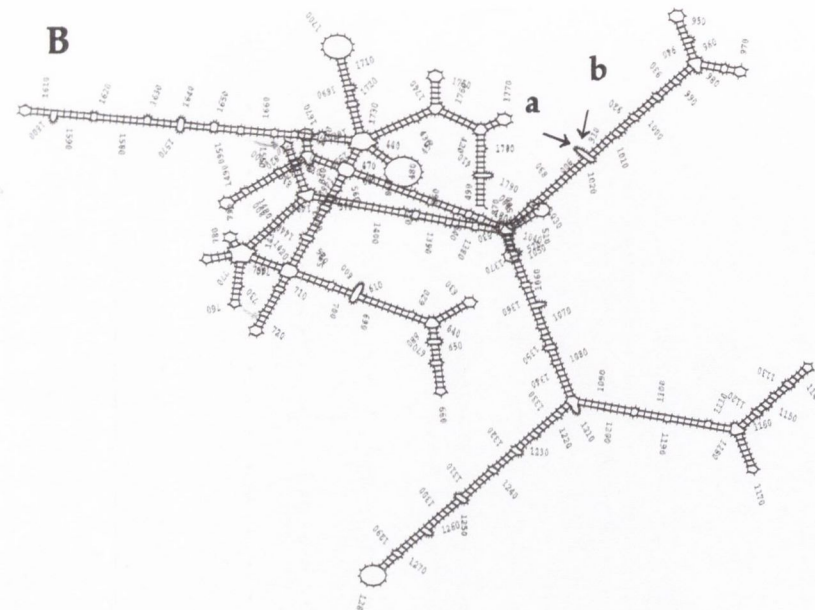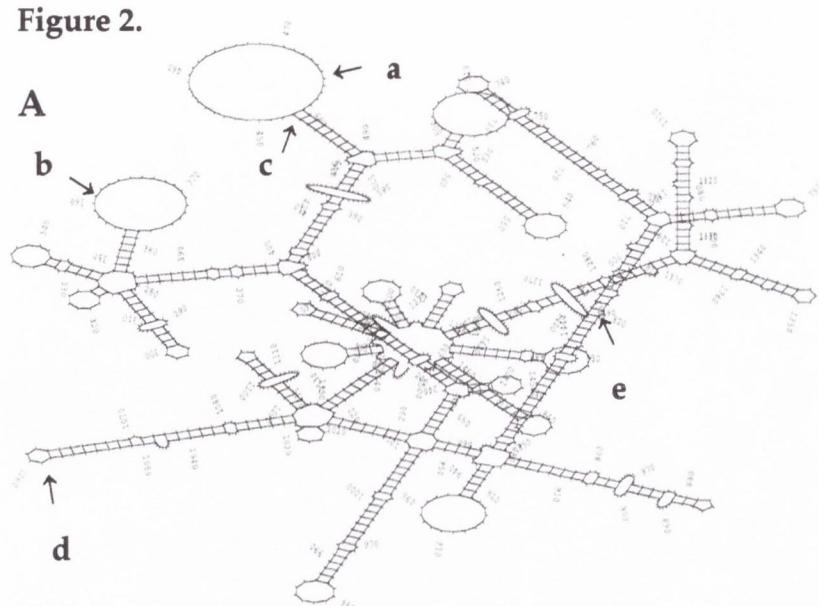
Figure 2. The most probable secondary structure of RNAs predicted using PlotFOLD (Zuker, 1989). *A*, human rhodopsin. Arrows a-e indicate the cleavage sites in the rhodopsin transcript by Rz10, Rz20, Rz447, Rz225 and Rz25 respectively. The cleavage site of Rz15 is not indicated as this region of the transcript has not been plotted here. *B*, human peripherin/*RDS* transcript. Arrows a an b indicate the cleavage sites in the transcript by Rz8 and Rz9 respectively. *C*, human COL1A2 transcript. Arrows a and b indicate the cleavage sites of Rz902 and Rz908 respectively. The cleavage site of Rz18 is not indicated as this region of the transcript has not been plotted here. *D*, human COL1A1 transcript. The arrow indicates the cleavage site in the transcript by Rzpol1a1.
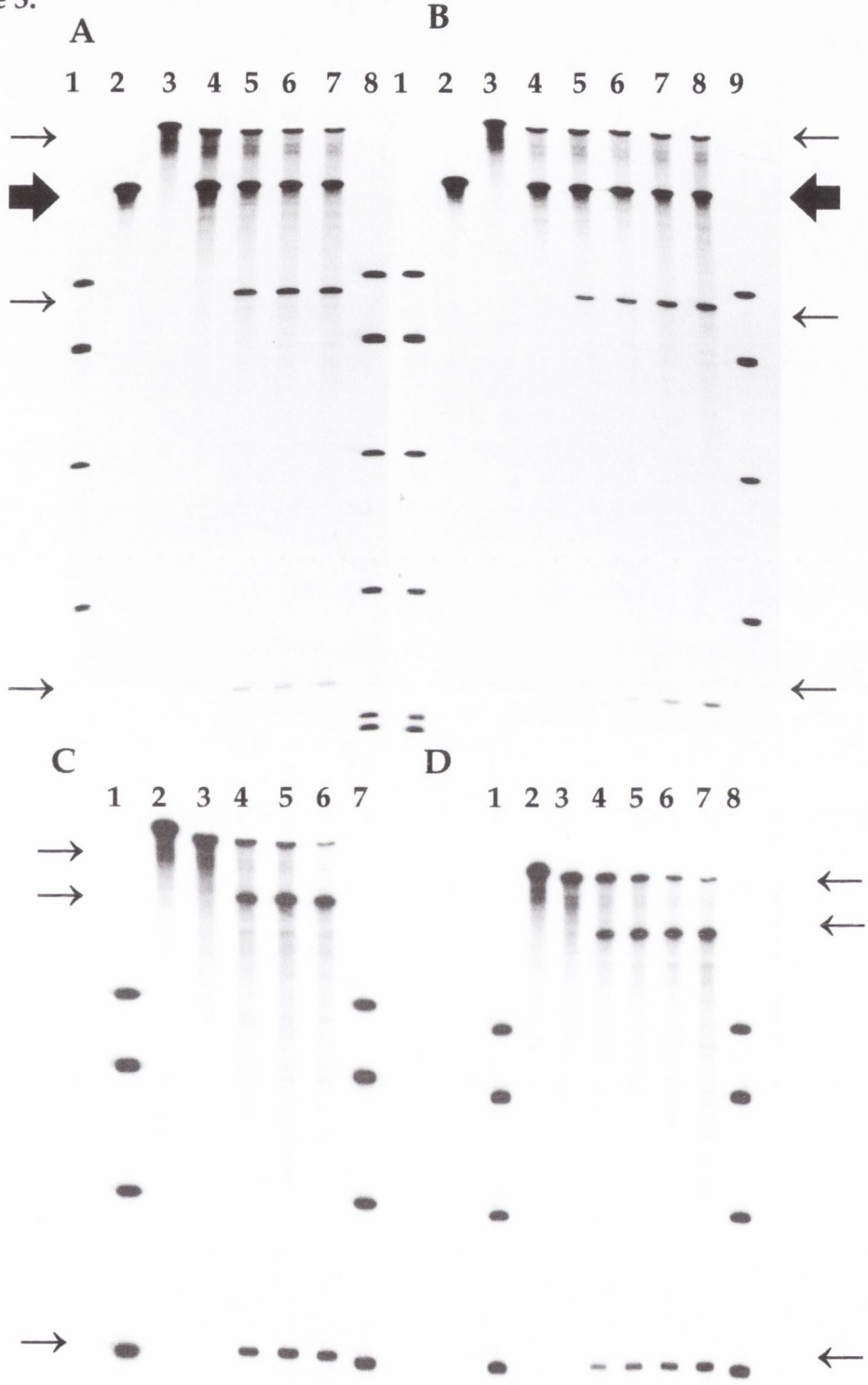
Figure 3.

Figure 3. MgCl$_2$ curves and timepoint cleavage reactions of mutant rhodopsin RNAs with Rz447 and Rz255. From top to bottom mutant RNA and cleavage products are highlighted with arrows. Wildtype rhodopsin RNA (4B) is highlighted with an enlarged arrow. *A,* MgCl$_2$ curve of Rz447, 4B transcript and mutant Gly51Val rhodopsin transcript. Lanes 1 and 8, DNA ladder; lane 2 wildtype (4B) rhodopsin transcript alone; lane 3 mutant Gly51Val rhodopsin transcript alone; lanes 4-7 cleavage reactions with Rz20 at 37°C with 0, 2.5, 5 and 10mM MgCl$_2$. *B,* Timepoint of Rz447, 4B transcript and mutant rhodopsin Gly51Val transcript. Lanes 1 and 9, DNA ladder; lane 2, wildtype (4B) rhodopsin transcript alone; lane 3, mutant Gly51Val RNA alone; lanes 4-8 cleavage reactions with Rz447 at 37°C for 0, 30, 60, 120 and 300 minutes respectively. *C,* MgCl$_2$ curve of Rz255 and mutant rhodopsin Del255ATC transcript. Lanes 1 and 7, DNA ladder; lane 2, Del255ATC RNA alone; lanes 3-6 cleavage reactions with Rz255 at 37°C with 0, 2.5, 5 and 10mM MgCl$_2$. *D,* Timepoint of Rz255 and mutant rhodopsin Del255ATC transcript. Lanes 1 and 8, DNA ladder; lane 2 Del255ATC RNA alone; lanes 3-7, cleavage reactions with Rz255 at 37°C for 0, 30, 90, 210 and 300 minutes respectively.

Figure 4.

A

622 → 527

404 →

307

242 → 238

217 → 201

190 → 180

160 →

147

123 →

110

90 →

76
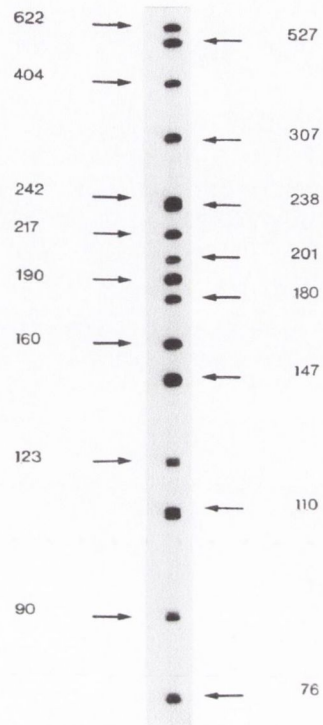
B   1 2 3 4 5 6 7 8

C   1 2 3 4 5 6 7 8
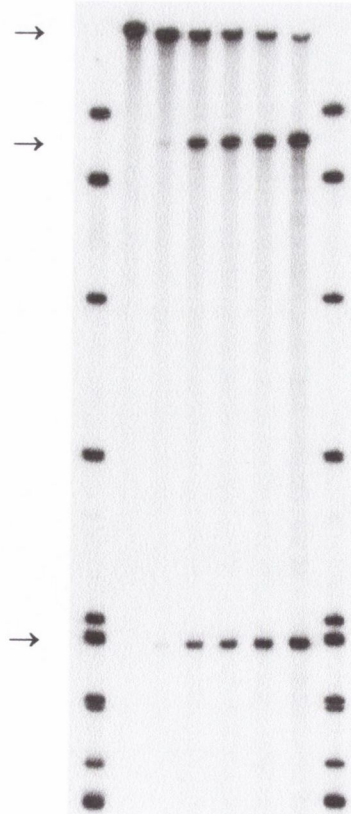
Figure 4. *A*, Diagram of end-labeled MspI cut pBR322. Sizes are indicated. The DNA was run on polyacrylamide gels to provide an estimate of sizes of RNA products on gels. *B*, timepoint reaction with mutant Pro23Leu rhodopsin RNA and Rz20. Lanes 1 and 8, DNA ladder; lane 2, mutant Pro23Leu rhodopsin transcript; lanes 3-7, cleavage reactions of mutant Pro23Leu transcript by Rz20 at 37°C for 0, 30, 60, 120 and 300 minutes respectively. From top to bottom mutant RNA and cleavage products are highlighted with arrows. *C*, timepoint reaction with mutant Pro23Leu rhodopsin RNA and Rz10. Lanes 1 and 8, DNA ladder; lane 2, mutant Pro23Leu rhodopsin transcript; lanes 3-7, cleavage reactions of mutant Pro23Leu transcript by Rz10 at 37°C for 0, 30, 60, 120 and 300 minutes respectively. From top to bottom mutant RNA and cleavage products are highlighted with arrows.

Figure 5a.
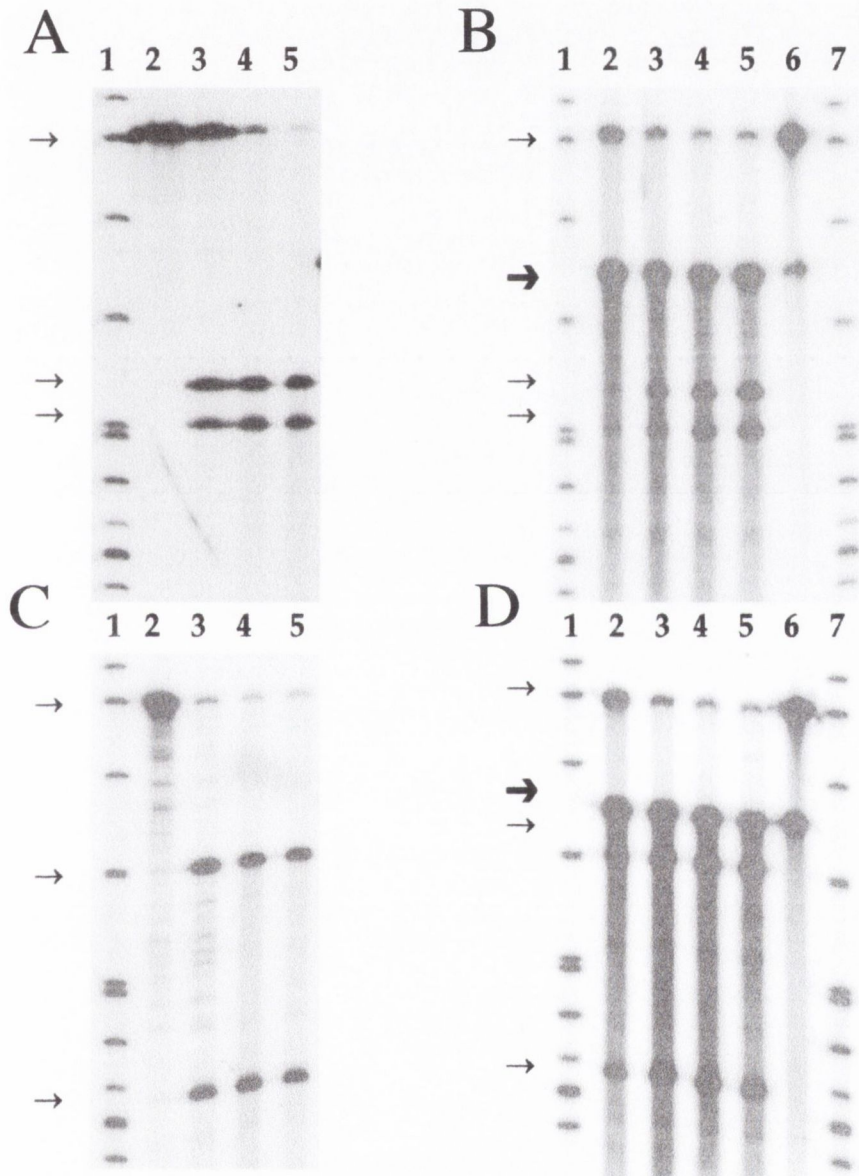
Figure 5a. MgCl$_2$ curves and timepoint cleavage reactions of Rz8 and Rz9 targeting the 5'UTR of wildtype human peripherin/*RDS* (6B) RNA. In all figures 6B RNA and cleavage products are highlighted with arrows. Replacement (7A) transcript is highlighted with an enlarged arrow. *A*, MgCl$_2$ curve of Rz8 and 6B transcript. Lane 1, DNA ladder; lanes 2-5, cleavage reactions at 37°C with Rz8 with 0, 5, 10 and 15mM MgCl$_2$. *B*, timepoint reactions of Rz8, 6B RNA and replacement peripherin/*RDS* (7A) transcript. Lanes 1 and 7, DNA ladder; lanes 2-5, cleavage reactions with Rz8 at 37°C for 0, 60, 120, and 180 minutes respectively; Lane 6, wildtype and replacement RNAs alone. *C*, MgCl$_2$ curve of Rz9 and 6B transcript. Lane 1, DNA ladder; lanes 2-5, cleavage reactions at 37°C with Rz9 with 0, 5, 10 and 15mM MgCl$_2$. *D*, timepoint reactions of Rz9, wildtype peripherin/*RDS* 6B transcript and replacement peripherin/*RDS* 7A transcript. Lanes 1 and 7, DNA ladder; lanes 2-5, cleavage reactions with Rz9 at 37°C for 0, 60, 120, and 180 minutes respectively; Lane 6, 6B and 7A RNA on their own.

Figure 5b.
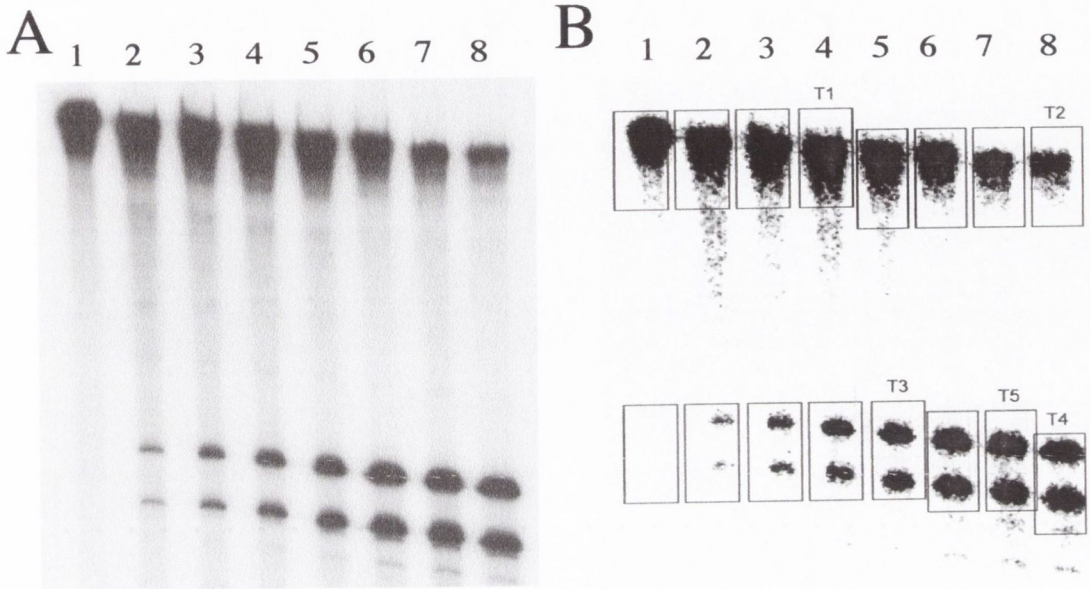
C

T1: 136,768
103,695
104,293
121,261

T2: 92,630
70,648
46,938
36,090

T3: 3,522
12,353
19,742
35,520
47,162

T4: 79,036

T5: 70,811
84,877
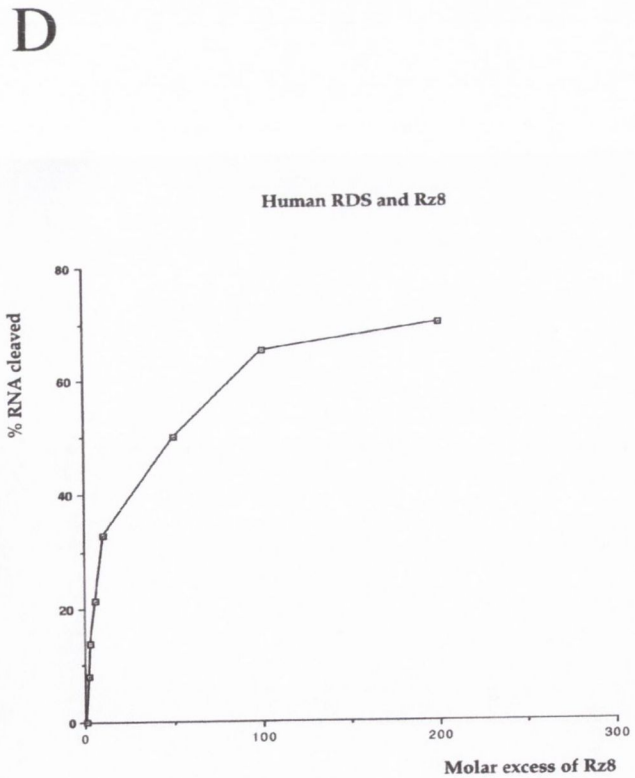
Figure 5b. *E*, Maximum extent of cleavage of wildtype peripherin/*RDS* 6B transcript by Rz8. Lanes 1-8 represent 3 hour cleavage reactions at 37°C with molar ratios of 6B RNA:Rz8 of 1:0, 1:1, 1:2, 1:5, 1:10, 1:50, 1:100 and 1:200 respectively. F, Reading given by the Packard instant imager of gel in 5*E*. *G*, Graph of maximum extent of cleavage of 6B by Rz8. The vertical axis represents the percentage cleavage of transcript and the horizontal axis represents the excess of Rz8 used over 6B RNA.

Figure 6.
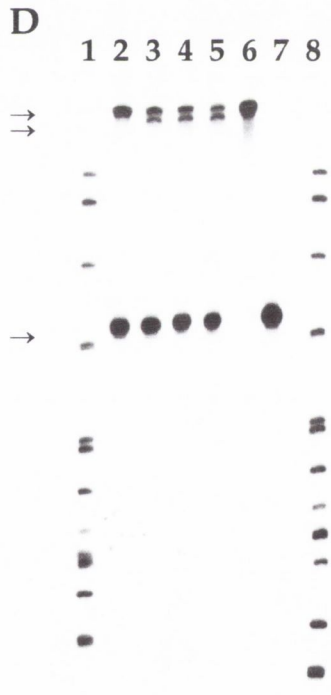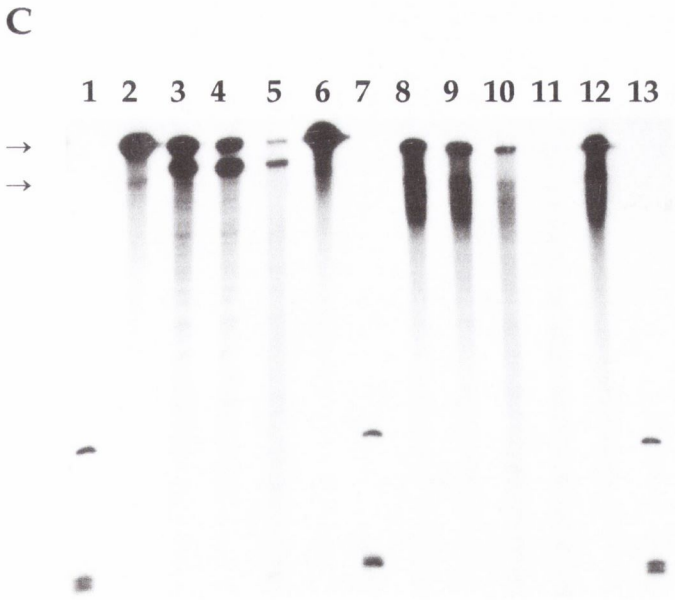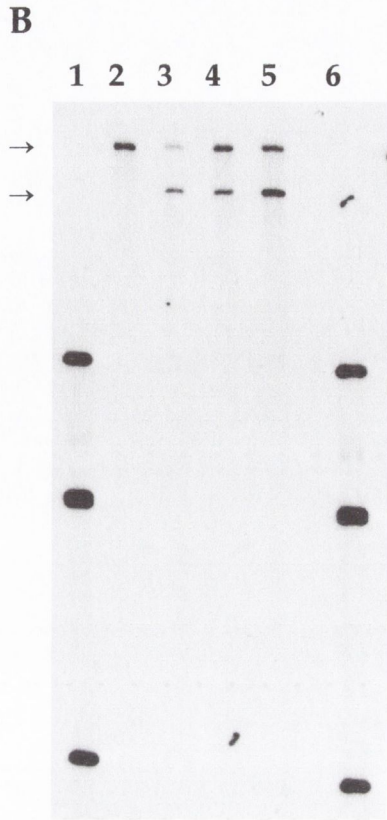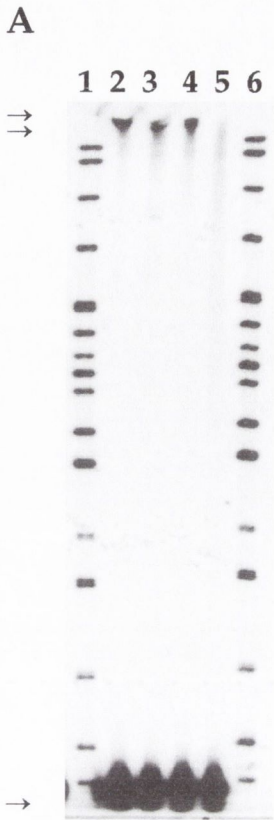
Figure 6. MgCl$_2$ curves of Rz15 targeting the 5'UTR of the wildtype human rhodopsin transcript (4B). *A*, MgCl$_2$ curve of Rz15, and 4B transcript from clone 4B digested with BstEII. Lanes 1 and 6, DNA ladder; lanes 2-5 cleavage reactions with Rz15 at 37°C with 0, 5, 10 and 15mM MgCl$_2$. From top to bottom 4B RNA, the larger cleavage product and the ribozyme are highlighted with arrows. The smaller cleavage product can not be distinguished from the ribozyme in size. *B*, MgCl$_2$ curve of Rz15, and 4B transcript from clone 4B digested with BstEII. Lanes 1 and 6, DNA ladder; lanes 2-5 cleavage reactions with Rz15 at 37°C with 0, 5, 10 and 15mM MgCl$_2$. From top to bottom 4B RNA and the larger cleavage product are highlighted with arrows. The smaller cleavage product can not be seen in this figure. *C*, MgCl$_2$ curves of Rz15 and transcript from clone 4B digested with AcyI and replacement rhodopsin transcript from clone 5A digested with AcyI. Lanes 1, 7 and 13, DNA ladder; lanes 2-5 cleavage reactions of 4B transcript with Rz15 at 37°C with 0, 5, 10 and 15mM MgCl$_2$, lane 6 4B transcript alone; lanes 8-11, cleavage reactions of 5A transcript with Rz15 at 37°C with 0, 5, 10 and 15mM MgCl$_2$. Lane 12, 5A transcript alone. From top to bottom rhodopsin transcripts and the larger cleavage products are highlighted with arrows. 4B transcript is clearly cut by Rz15 while replacement 5A RNA is not. *D*, MgCl$_2$ curve of Rz15, wildtype rhodopsin 4B transcript from clone 4B digested with BstEII and replacement rhodopsin 5A transcript from clone 5A digested with FspI. Lanes 1 and 8, DNA ladder; lanes 2-5 cleavage reactions with Rz15 at 37°C with 0, 5, 10 and 15mM MgCl$_2$. Lane 6, 4B transcript alone. Lane 7, 5A transcript alone. From top to bottom, wildtype 4B transcript, the larger cleavage product and the replacement 5A transcript are highlighted with arrows.
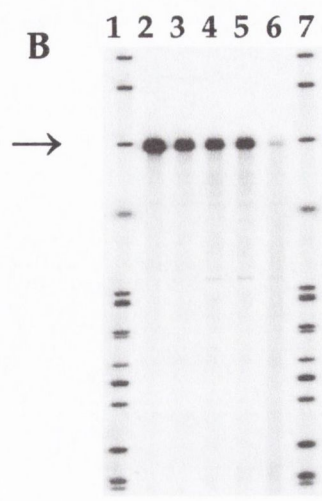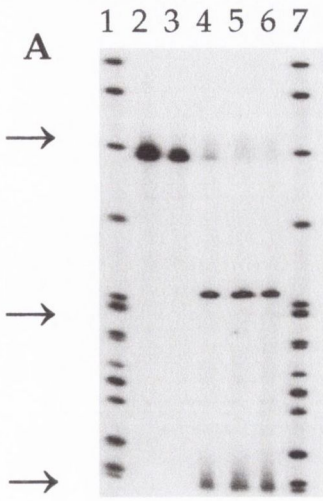
Figure 7.
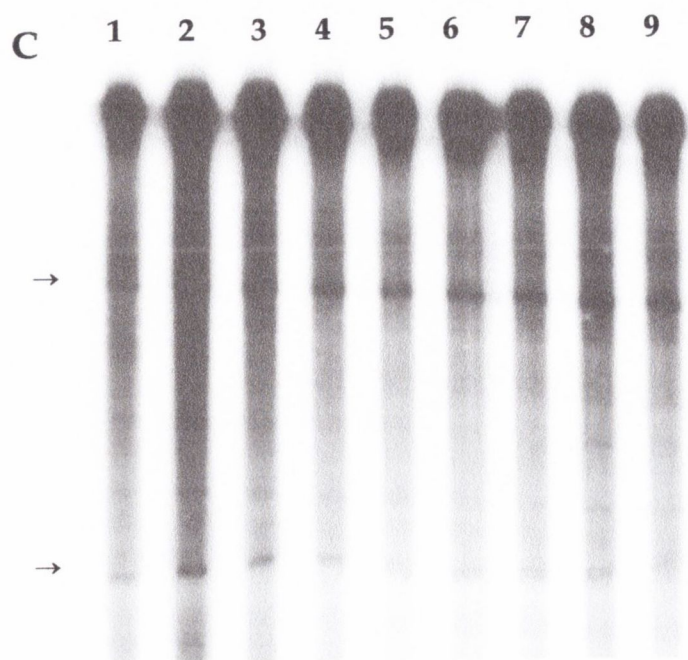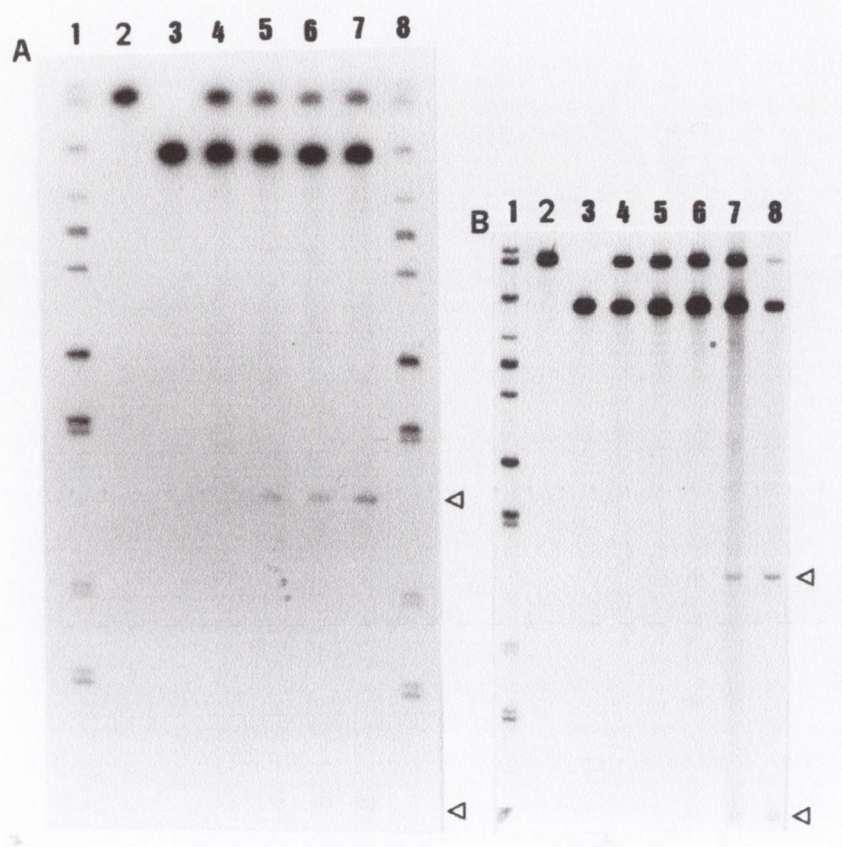
Figure 7. *A*, MgCl$_2$ curve of Rz18, wildtype COL1A2 transcript and hybrid COL1A2 transcript. Lanes 1 and 8, DNA ladder; lane 2 wildtype COL1A2 transcript alone; lane 3, hybrid replacement COL1A2 transcript alone; lanes 4-7 cleavage reactions with Rz18 at 37°C with 0, 2.5, 5 and 10mM MgCl$_2$. *B*, Timepoint of Rz18, wildtype COL1A2 transcript and replacement COL1A2 transcript. Lane 1, DNA ladder; lane 2, wildtype COL1A2 transcript alone; lane 3 hybrid COL1A2 transcript alone; lanes 4-8 cleavage reactions with Rz18 at 37°C for 0, 30, 60, 180 and 300 minutes respectively. C, Timepoint cleavage reaction of Rz25 and wildtype human rhodopsin transcript (4B). Lanes 1-9 represent cleavage reactions for 1, 2, 5, 7.5, 10, 20, 30, 60 and 180 minutes respectively. Cleavage products are highlighted with arrows.

Figure 8.
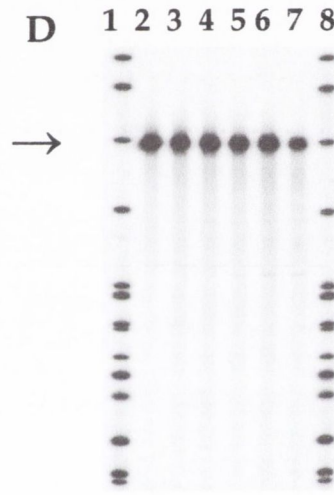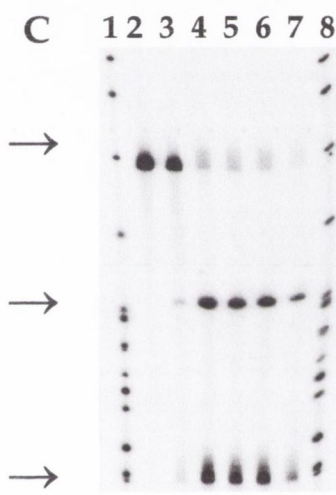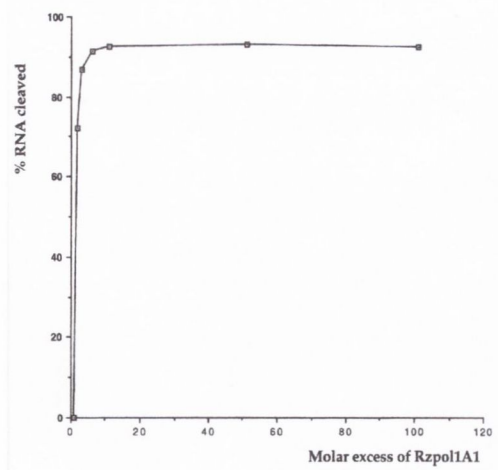
Figure 8. $MgCl_2$ curves and timepoint cleavage reactions of COL1A1 polymorphic site with Rzpol1a1. T-allele or C-allele RNA and cleavage products are highlighted from top to bottom with arrows. *A*, $MgCl_2$ curve of Rzpol1a1 and T-allele transcript. Lanes 1 and 7, DNA ladder; lane 2 T-allele RNA alone; lanes 3-6 cleavage reactions with Rzpol1a1 at 37°C with 0, 5, 10 and 15mM $MgCl_2$. *B*, $MgCl_2$ curve of Rzpol1a1 and C-allele RNA. Lanes 1 and 7, DNA ladder; lanes 3-6 cleavage reactions with Rzpol1a1 at 37°C with 0, 5, 10 and 15mM $MgCl_2$. *C/D*, timepoint cleavage reactions of Rzpol1a1 with T-allele RNA and C-allele RNA respectively. Lanes 1 and 8 represent DNA ladders; lanes 2-7 represent cleavage reactions at 37°C for 0, 30, 60, 120 and 300 minutes. *E*, Maximum extent of cleavage of T-allele RNA by Rzpol1a1. Lanes 1-8 represent 3 hour cleavage reactions at 37°C with molar ratios of clone 6B:Rz8 of 1:0, 1:1, 1:2, 1:5, 1:10, 1:50 and 1:100 respectively. *F*, Graph of maximum extent of cleavage of T-allele RNA by Rzpol1a1. The vertical axis represents percentage T-allele transcript cleaved and the horizontal axis the molar excess of Rzpol1a1 over T-allele RNA used in the cleavage reaction.

Figure 9.
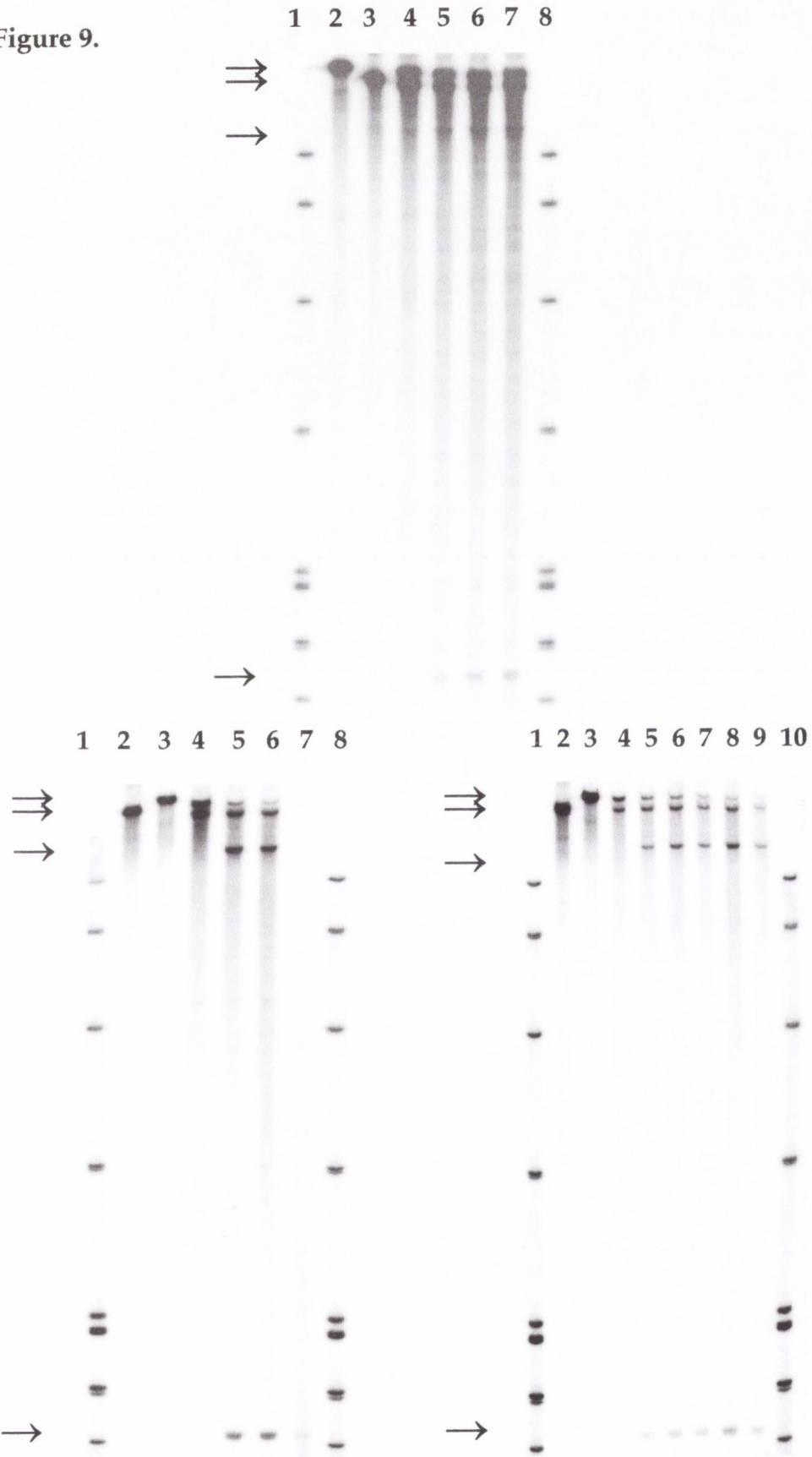
Figure 9. MgCl$_2$ curves and timepoint reactions of two polymorphic sites in the COL1A2 transcript by Rz902 and Rz907. *A*, Lanes 1 and 8, DNA ladder; lane 2, RNA from COL1A2 clone B; lane 3, RNA from COL1A2 clone A; lanes 4-7 COL1A2 RNAs of clone A and B and Rz902 incubated with 0, 5, 10, and 15 mM MgCl$_2$ for 3 h at 37°C. From top to bottom RNA from clone B and A and the two cleavage products from clone B are highlighted with arrows. *B*, Lane 1 and 8, DNA ladder; lane 2, RNA from COL1A2 clone B; lane 3, RNA from COL1A2 clone A; lanes 4-7 COL1A2 RNAs of clone A and B and Rz907 incubated with 0, 5, 10, and 15 mM MgCl$_2$ for 3 h at 37°C. From top to bottom RNA from clone A and B and the two cleavage products from clone A are highlighted with arrows. *C*, Lanes 1 and 10, DNA ladder; lane 2, RNA from the human COL1A2 clone B of the 907 polymorphism; lane 3, RNA from COL1A2 clone A of the 907 polymorphism; lanes 4-9, COL1A2 RNAs from clones A and B and Rz907 incubated with 10 mM MgCl$_2$ at 37°C for 0, 30, 60, 120, 180 and 300 minutes respectively. From top to bottom RNA from clones A and B , and the two cleavage products from clone A transcript are highlighted by arrows.

	Enzyme	uncleaved RNA size	NUX site	cleavage products size
UTR				
4B	BstEII	851		61, 790 (Rz15)
	AcyI	1183		61, 1122 (Rz15)
5A	BstEII	841		
	AcyI	1173		
	FspI	300		
Rz15	XbaI	60	AUU	
6B	BglII	489		238, 251 (Rz8)
	BglII	489		194, 295 (Rz9)
7A	AvrII	331		
Rz8	XbaI	60	CUA	
Rz9	XbaI	60	GUU	
1B	XhoI	217		127, 90 (Rz18)
2A	XhoI	256		
Rz18	XbaI	60	GUC	
4B	PCR	406		166, 240 (Rz25)
8A	PCR	406		
Rz25	XbaI	60	CUU	
Disease specific mutation				
Gly51Val	BstEII	851		254, 597 bases (Rz447)
Pro23Leu	BstEII	851		170, 681 bases (Rz20)
Del255	AcyI	1183		865, 318 bases (Rz255)
4B	BstEII	851		61, 790 bases (Rz10)
4B	AcyI	1183		
Rz447	XbaI	60	GUC	
Rz20	XbaI	60	CUC	
Rz10	XbaI	60	GUC	
Rz255	XbaI	60	AUC	
Polymorphism				
pol1a1 C	XbaI	381		
pol1a1 C	BbsI	514		
pol1a1 T	XbaI	381		245, 136 bases
Rzpol1A1	XbaI	60	CUC	
clone A	XbaI	888		689, 199 bases (Rz907)
	MvnI	837		
clone B	XbaI	888		683, 105 (Rz902)
	MvnI	837		
Rz902	XbaI	60	CUA	
Rz907	XbaI	60	GUC	

Table 1. Transcript and cleavage product sizes. Enzymes used to linearise plasmid DNA prior to expression are indicated. The NUX target sites are given.

Ribozyme	NUX site	Loop size (bases)	consistency	% cleavage estimated by eye
Rzpol1a1	CUC	68	yes	95
Rz10	GUC	33	yes	85
Rz20	CUC	22	yes	85
Rz447	GUC	33	yes, one arm not in loop	70
Rz255	AUC	42	no	70
Rz9	GUU	6	yes	70
Rz8	CUA	8	yes	70
Rz15	AUU	5	no	50
Rz907	GUC	3	no	50
Rz902	CUA	4	no	30
Rz18	GUC	4	yes	10
Rz25	CUU	20	no	5

Table 2. Hammerhead ribozymes studied in this chapter from top to bottom in order of cleavage efficiency. The exact cleavage NUX site, the size of the open-loop structure in the target RNA, and the consistency of the open-loop structure are given. In addition, an estimate has been made of the maximum amount of cleavage (in percent) of target transcripts by the various ribozymes.

4. Characterisation of a Mutation-Independent ribozyme for Osteogenesis Imperfecta

4.1. Introduction

Osteogenesis Imperfecta (OI) is a dominant disorder involving the development of brittle bones. Affecting 1/12000 people, it is known to arise from mutations in either of the type I pro-collagen genes, COL1A1 and COL1A2 (Sillence et al. 1979). The severity of the disease is dependent upon the position and type of mutation. Null mutations cause relatively mild phenotypes due to haploinsufficiency. More severe forms of OI result from frameshift mutations, especially when located in the first exons of the gene. (Sillence et al., 1979, 1981; Wenstrup et al., 1990; Kuivaniemi et al., 1991; Byers et al., 1993; Prockop et al., 1994). Currently over 150 and 80 OI causing mutations have been defined in the COL1A1 and the COL1A2 genes respectively (HGMD, 1998) (for details on COL1A1, COL1A2 and OI, see section 1.10). In addition, 18 mutations in the COL1A2 gene have been shown to cause type VIIB Ehler's Danlos syndrome (HGMD, 1998). Thus the generation of mutation-independent therapeutic strategies would be highly preferable when designing gene therapies for type I collagen disorders (see section 1.1 and chapter 3 for details on mutation independent strategies for gene therapy).

A range of techniques is now available for gene suppression. For example, hammerhead ribozymes are small catalytic RNAs that can, in the presence of divalent cations (usually $MgCl_2$), cleave RNA at NUX sites (N = any nucleotide, U = Uracyl, X = any nucleotide but Guanine). Cleavage efficiencies are thought to depend on the ribozyme core sequence, the length and composition of antisense arms and the tertiary structure of the target mRNA, that is its accessibility for the ribozyme. Cleavable areas in mRNA can be revealed using, amongst other techniques, RNase H mapping, ribozyme expression libraries and computer programs such as RNAPlotfold (Zuker 1989; Lieber and Strauss, 1995; Birikh et al. 1997b). Ribozymes are discussed in detail in sections 1.3 to 1.6.

Ribozymes can, like protein enzymes, follow Michaelis-Menten kinetics (Fedor and Uhlenbeck, 1992); the constants V_{max} and K_m indicating the maximum velocity of the cleavage reaction and the affinity of the ribozyme for the target RNA respectively, can be determined from initial rates of cleavage under multiple-turnover conditions. The rate of the cleavage step k_2, and the dissociation rate k_{-1}, (materials and methods) can be determined under single-turnover conditions (see section 1.5). Kinetic profiles of ribozymes *in vitro* can be used as broad predictors of efficiencies *in vivo* (Birikh et al., 1997a).

Recently, hammerhead ribozymes have been designed to selectively cleave three mutant collagen transcripts. Cleavage *in vitro*, though selective, was inefficient, possibly due to the inaccessibility of the mutation sites for the ribozymes (Grassi et al. 1997).

Many disease mutations do not create hammerhead ribozyme NUX target sites or, in addition, are not accessible to ribozymes, and hence do not lend themselves to selective ribozyme suppression. Moreover the vast array of diverse mutations which can give rise to similar disease pathologies makes the generation of mutation-specific therapies most probably unrealistic. Therefore mutation-independent strategies for suppression of dominant gain-of-function mutations would be preferable and have indeed been proposed previously (Millington-Ward et al., 1997; section 1.1 and chapter 3). These approaches utilise hammerhead ribozymes, however, in principle, the same strategies could be used in conjunction with other agents including antisense DNA/RNA or triple helix forming oligonucleotides. In essence the approach explored in the current study involves the utilisation of the polymorphic nature of the genetic code. To date polymorphism has provided an invaluable tool enabling the generation of high-resolution genetic linkage maps (section 1.14). Recently however, additional novel applications for polymorphisms have been recognised and have been highlighted by the recent inclusion of the creation of a comprehensive polymorphism database containing over 100,000 polymorphisms as a new aim of the human genome project (Collins et al., 1998). Undoubtedly there is now a growing realisation that polymorphism will play a central role in genomics driven drug-design, modulation of disease severity, efficacy of various drugs in patients with different haplotypes and in mapping multifactorial traits such as cancer and mental-illness (Persidis, 1998). As demonstrated in the current study, polymorphisms may provide a powerful means

of directing gene therapeutic agents specifically to disease alleles in a mutation-independent manner.

In the present study a hammerhead ribozyme (Rzpol1a1, figure 1b/c) has been designed to overcome heterogeneity in COL1A1-associated OI. Rzpol1a1 cleaves COL1A1 RNA at a common polymorphic ribozyme target site, C3210T (Westerhausen et al., 1991; accession number K01228), situated in a predicted open-loop structure of the transcript (figure 1a). The heterozygosity index for this polymorphism indicates that over 40% of individuals (ascertained from Europe and the US) are predicted to be heterozygous for this polymorphism. A detailed kinetic profile of Rzpol1a1 has been established *in vitro*; V_{max}, K_m, k_2 and k_{-1} were determined. Additionally, inhibitory effects on cleavage by cellular RNA, the alternative polymorphic variant (C-allele) RNA, cleavage products and DNA were assessed *in vitro* together with the stability of Rzpol1a1 at 37°C. This detailed kinetic profile of Rzpol1a1 indicates that Rzpol1a1 elicits efficient cleavage of 3210T; hence this ribozyme may potentially be a valuable single therapeutic agent for OI caused by diverse gain-of-function mutations in COL1A1 (Millington-Ward et al., 1999). Moreover the study clearly demonstrates the increasing potential role of pharmacogenetics in future drug development.

4.2. Materials and Methods

4.2.1. COL1A1 and Rzpol1a1 RNA

In chapter 3 cDNAs derived from both polymorphic variants (C/T position 3210) of the human COL1A1 gene (comprising bases 2977-3347; accession number K01228) were cloned at the Hind III and XbaI sites of the expression vector pcDNA3 (Invitrogen). In this chapter clones were linearised with BclI and XbaI respectively, transcribed *in vitro* and purified as previously described (Millington-Ward et al. 1997). C- and T-allele RNAs were 428 and 381 bp respectively. Rzpol1a1 (figure 1b/c) was designed to cleave T-allele RNA at its polymorphic CUC site. Rzpol1a1 was generated by cloning annealed forward and reverse oligonucleotides (Gibco/BRL), into the Hind III and XbaI sites of pcDNA3. In this chapter Rzpol1a1 was linearised with XbaI, transcribed *in vitro* and purified. Molar ratios of ribozyme and target RNAs were determined by liquid scintillation counting (1500 TRI-CARB).

4.2.2. Determining steady-state intervals

RNAs were combined in molar ratios of T-allele RNA:Rzpol1a1 from 1:10-1:0.01 (T-allele RNA and Rzpol1a1 of 22.9 nM and 229.3-0.2 nM) with 100 mM Tris pH 8.0. Reactions were heated to 90°C for two minutes and transferred to ice. Reactions were initiated at 37°C with 10mM MgCl$_2$. Aliquots were removed at various times and quenched with equal volumes of stopmix (80% formamide, 10mM EDTA). Samples were separated on polyacrylamide gels and counted on a Packard Instant Imager as in chapter 3.

4.2.3. Inhibition of ribozyme-induced T-allele cleavage by cellular RNA, C-allele RNA and DNA

Incubations were carried out for 8.5 minutes; a time frame experimentally determined to be within the steady-state interval. A 400x weight excess (determined spectrophotometrically) of cellular RNA was added to reactions to assess inhibition. Molar ratios of T-allele RNA:Rzpol1a were varied between 0.1:1 to 10:1 (T-allele RNA and Rzpol1a1 of 8.2 nM and 0.8 to 83.4 nM), however for multiple-turnover kinetics only ratios of 1.25:1 to 10:1 1 (T-allele RNA and Rzpol1a1 of 8.3 nM and 0.8 to 6.7 nM) were analysed. In addition to assessing inhibition by cellular RNA, the inhibitory effect of the uncleavable C-allele was examined. Molar ratios of C-allele RNA:Rzpol1a1 were kept constant at 1:1. Molar ratios of T-allele RNA:Rzpol1a1 varied between 0.1:1 to 10:1 (T-allele RNA and Rzpol1a1 of 8.2 nM and 0.8 to 83.4 nM), however again for multiple-turnover kinetics only ratios of 1.25:1 to 10:1 (T-allele RNA and Rzpol1a1 of 8.3 nM and 0.8 to 6.7 nM) were analysed. In an experiment to determine inhibitory effects on ribozyme cleavage by DNA, varying amounts of herring sperm DNA (0x, 10x, 50x, 100x, 200x, and 500x, determined spectraphotometrically), which had been fragmented by autoclaving it for one hour, was added to cleavage reactions. These reactions contained T-allele RNA:Rzpol1a1 of 1:1 and were carried out for 8 minutes.

4.2.4. Determining catalytic constants

Multiple- and single-turnover kinetic data are presented in Lineweaver-Burk plots. The constants K_m, a measurement for the affinity of the ribozyme for the target RNA and V_{max}, the maximum velocity of the cleavage reaction, were determined under multiple-turnover conditions using the following equations (Cornish-Bowden and Wharton, 1990).

$$K_\mathrm{m} = \frac{\Sigma v^2 \Sigma v/a - \Sigma v^2/a \Sigma v}{\Sigma v^2/a^2 \Sigma v - \Sigma v^2/a \Sigma v/a} \qquad V_\mathrm{max} = \frac{\Sigma v^2/a^2 \Sigma v^2 - (\Sigma v^2/a)^2}{\Sigma v^2/a^2 \Sigma v - \Sigma v^2/a \Sigma v/a}$$

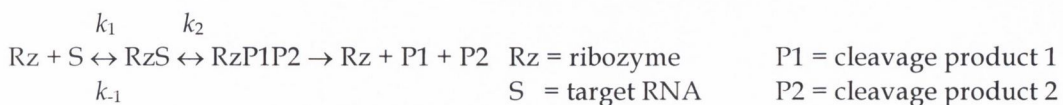a = concentration of substrate
v = rate of the reaction

4.2.5. Inhibition of ribozyme activity by cleavage products

Cleavage reactions were undertaken as described above. Aliquots of 2μl were removed from reactions containing molar ratios of T-allele:Rzpol1a1 of 1:0.1 (T-allele RNA and Rzpol1a1 of 9.8 nM and 1.0 nM) and 1:100 (T-allele RNA and Rzpol1a1 of 9.8 nM and 1012.2 nM) at 10, 20 and 30 minutes and quenched. At 31 minutes half the original amount of template was added to the reactions. Additional aliquots were removed at 41, 51 and 61 minutes. Given that at 30 minutes, as empirically determined, 88.7% of the original T-allele had been cleaved when a 100x excess of Rzpol1a1 was present, and in addition that 30% of Rzpol1a1 had been removed by sampling, the ratio of T-allele:Rzpol1a1 at 31 minutes was 1:120.8, (T-allele RNA and Rzpol1a1 of 0.7 nM and 83.8 nM) (at zero minutes it was 1:100). In contrast, when the ratio of T-allele RNA to Rzpol1a1 was 1:0.1 at time zero, 7.3% of the RNA had been cleaved after 30 minutes. Therefore, the ratio of T-allele RNA:Rzpol1a1 at 31 minutes after sampling and addition of extra template was 1:0.06094 (T-allele RNA and Rzpol1a1 of 13.3 nM and 0.8 nM).

To determine how active Rzpol1a1 remained after incubation at 37°C for one hour prior to initiating reactions, timepoints were carried out at 5, 10, 20, 30 and 40 minutes for pre-incubated and non-pre-incubated Rzpol1a1 at molar ratios of T-allele:Rzpol1a1 of 1:0.1 (T-allele RNA and Rzpol1a1 of 9.7 nM and 0.1 nM) and 1:100 (T-allele RNA and Rzpol1a1 of 9.7 nM and 974.4 nM).

4.2.6. Single-turnover kinetics; determining $t_{1/2}$, k_2 and k_{-1}

The half-life of T-allele RNA, $t_{1/2}$, the rate of the cleavage step of the reaction, k_2, and the rate of dissociation, k_{-1} (see below), were determined under single-turnover conditions with a 100x excess of Rzpol1a1 over T-allele RNA. (in the case of k_2, concentrations of T-allele RNA and Rzpol1a1 were 22.9 nM and 2293.1 nM.

$$\text{Rz} + \text{S} \underset{k_{-1}}{\overset{k_1}{\longleftrightarrow}} \text{RzS} \overset{k_2}{\longleftrightarrow} \text{RzP1P2} \rightarrow \text{Rz} + \text{P1} + \text{P2}$$

Rz = ribozyme
S = target RNA

P1 = cleavage product 1
P2 = cleavage product 2

$t_{1/2}$ was determined over 2 half-lives from the initial rate of cleavage, indicated by the slope of a graph of the fraction of uncleaved T-allele RNA versus time. k_2 was calculated from $k_2 = \ln2/t_{1/2}$ (Hendry et al., 1997a).

k_{-1} was determined from the following equation (Hendry et al., 1997b).

$$k_{-1} = k_2 \times \frac{(P_{\infty cont} - P_{\infty test})}{P_{\infty test}}$$

$P_{\infty cont}$ = amount of product at $t = \infty$ for the control reaction
$P_{\infty test}$ = amount of product at $t = \infty$ for the test reaction

Briefly, in two tubes, labelled test and control, an excess of ribozyme (1.0 nM) over [α^{32}P]UTP labelled T-allele RNA (0.4 nM) were combined in the presence of 50 mM TrisCl pH 8.0 and dH$_2$O in a 27 µl reaction. After the RNAs had annealed for at least 30 minutes at 37 °C, the control reaction was initiated with 3 ml of 100 mM MgCl$_2$ (10mM final concentration). Samples were removed at various time intervals (1 minute etc.) and quenched. The test reaction was then initiated with MgCl$_2$ and 37.3 nM of unlabelled T-allele RNA. Again, samples were removed and quenched at similar time intervals to the control reaction. Test and control samples were separated on 8% polyacrylamide gels and bands analysed by instant imager. Amount of product at $t = \infty$ for the test and control reactions were determined from a graph of percent product versus time.

4.3. Results

4.3.1. Predicting the accessibility of the 3210 polymorphism for Rzpol1a1

The RNA secondary structure of COL1A1, predicted using the computer program RNAPlotfold, demonstrates that the 3210 polymorphism in COL1A1 is situated in a large open-loop structure of the transcript and is thus predicted to be accessible for ribozyme approach, binding and cleavage (figure 1a). Also, the open-loop structure is present in the ten most probable estimations of the two-dimensional structure of COL1A1 mRNA.

4.3.2. Rzpol1a1 functionality and specificity

The first things to establish were whether Rzpol1a1, designed to cleave the COL1A1 transcript at the 3210 C/T polymorphism, could firstly cleave the T-allele at this position and secondly left the C-allele RNA intact. Thus, a timepoint cleavage reaction with equal amounts of C-allele RNA, T-allele RNA and Rzpol1a1 was carried out (figure 2). Cleavage of the T-allele transcript was clearly

demonstrated with only a small amount of intact transcript remaining after 3 hours at 37°C. C-allele RNA, however, remained intact. Thus Rzpol1a1 is able to cleave T-allele RNA while leaving C-allele RNA intact, demonstrating the functionality of the mutation independent strategy based on polymorphism.

4.3.3. Determination of steady-state intervals for Rzpol1a1

To assess whether Rzpol1a1 may be an efficient mutation-independent suppressor for the COL1A1 transcript, the maximum velocity of the cleavage reaction V_{max} and the affinity of the ribozyme for the target RNA K_m, were determined under multiple-turnover conditions. That is under conditions of substrate excess, where the ribozyme is expected to cleave multiple substrate molecules. Multiple-turnover kinetic reactions must always be carried out during the steady-state interval when no inhibitors such as cleavage products or depleted levels of substrate are inhibiting the reaction (see section 1.5 for details). The steady-state interval of the cleavage reaction, determined from time point cleavage reactions of seven T-allele RNA:Rzpol1a1 molar ratios ranging between 1:0.1-1:100 (figure 3 a-g), was at least 10 minutes for ratios ranging between 1:0.1-1:2 (figure 4a/b) (with excess substrate). A timeframe within the steady-state interval (8.5 minutes) was chosen for subsequent multiple-turnover kinetics reactions.

4.3.4. Inhibition of ribozyme activity due to cleavage products or to ribozyme instability

To assess whether cleavage products inhibit rates of cleavage, samples were removed every 10 minutes from a reaction containing a molar ratio of T-allele RNA:Rzpol1a1 of 1:0.1. At 31 minutes half the original amount of T-allele RNA was added to the reaction. As the relative amount of T-allele had increased (methods), the rate of cleavage should exceed the original rate if no inhibition had taken place. However, as shown in figure 5a, the rate of cleavage is significantly lower. This may be due either to inhibition by cleavage products or loss of ribozyme catalytic activity at 37°C.

To test the latter scenario, reactions were carried out at two molar ratios of T-allele:Rzpol1a1 (1:0.1 and 1:100). Reactions were undertaken in duplicate with one sample containing Rzpol1a1 pre-incubated at 37°C for one hour. Cleavage profiles over time show that pre-incubation at 37°C has little effect on Rzpol1a1 activity (figures 5c/d). Hence, the observed inhibition (T-allele:Rzpol1a1 = 1:0.1) may possibly be due to the presence of cleavage products.

Steady-state intervals for 10x and 100x excess Rzpol1a1 were significantly shorter than for ratios ranging between 0.1x-2x (figure 4a). This may be a function of inhibition by cleavage products or simply a lack of intact T-allele RNA. This possibility was addressed by testing whether initial rates of cleavage could be achieved after adding extra T-allele RNA to reactions (T-allele RNA:Rzpol1a1 of 1:100) after 30 minutes. As a result of this experiment initial rates were achieved indicating that lack of T-allele RNA may cause the shortened steady-state interval (figure 5b). In addition, these results suggest that a large excess of ribozyme may enable inhibitory effects due to cleavage products observed in the previous experiment when ribozyme was limited to be overcome.

4.3.5. Michaelis-Menten constants and inhibition of cleavage by total RNA and C-allele RNA

Michaelis-Menten constants, V_{max} and K_m, provide knowledge of the efficiency, V_{max} (the maximum velocity of the cleavage reaction) and affinity of the ribozyme for the substrate (K_m). Reactions with molar ratios of T-allele RNA:Rzpol1a1 ranging from 1.25:1-10:1 were carried out for 8.5 minutes, a time-span deemed to be within the steady state interval (figure 4). Simultaneously, experiments were carried out with 400x excess cellular RNA (figure 6a/b). By comparing the V_{max} and K_m of these reactions with and without potential inhibitor under multiple-turnover conditions, one can determine the nature of potential inhibition. Competitive inhibition will result in an increased K_m (and therefore a decreased affinity of the ribozyme for the substrate) and an unaltered V_{max}. Uncompetitive inhibition will result in a reduced V_{max} and unaltered K_m. Figures 6a/b and 7a demonstrate that inhibition is taking place. V_{max} and K_m for Rzpol1a1 were determined from the formulas in paragraph 4.2.4. V_{max} was the same with and without inhibitor (0.4) whereas K_m increased with inhibitor from 9.5 to 10.3, suggesting that the inhibitory effects of total RNA on Rzpol1a1 are competitive (table 1).

The inhibition experiment was repeated with the alternative polymorphic variant as inhibitor. Equal amounts of C-allele RNA and Rzpol1a1 were combined. V_{max} and K_m were determined at 0.4 and 9.8 respectively. A Lineweaver-Burk plot shows 40% inhibition of cleavage activity by C-allele RNA (figure 7b). As with cellular RNA, the data suggest that inhibition by C-allele RNA is competitive. Additionally, an experiment was carried out to determine the possible inhibitory effects of total DNA on ribozyme activity (figure 8). Interestingly, the effect showed asymptotic behaviour, tending towards a maximum inhibitory effect of about 70%.

4.3.6. Single-turnover kinetics; determination of $t_{1/2}$, k_2 and k_{-1}

The cleavage-rate constant k_2 and the dissociation rate k_{-1} were determined under single-turnover ribozyme-saturation conditions where the ratio of template RNA:Rzpol1a1 was 1:100 (figure 3g). The half-life of the T-allele RNA, $t_{1/2}$, calculated from the initial (linear) portion of figure 7c, was 1.199 minutes, generating a k_2 of 0.58 min^{-1}. k_{-1}, determined from a P∞cont of 92.000 % and a P∞test of 79.978 %, was determined to be 0.087 min^{-1} (figure 7d; see 4.2.6 for details).

Thus a single therapeutic agent, Rzpol1a1, designed to overcome heterogeneity in COL1A1-linked OI, has been tested for efficiency of cleavage of the COL1A1 T-allele transcript under both multiple and single turnover conditions. Notably, the C-allele RNA remained intact (figure 2). Kinetic parameters V_{max}, K_m, k_2 and k_{-1} (table 1) all show Rzpol1a1 to be extremely efficient *in vitro*, while inhibitory effects by cellular RNA, cleavage products and transcript from the alternative polymorphic variant (C-allele) and DNA, have been found to be small (approximately 40%). Notably, *in vitro* ribozyme cleavage efficiencies have in general been found to correlate with efficiencies *in vivo* (Birikh et al., 1997a).

4.4. Discussion

A significant problem associated with the development of gene therapies for dominant diseases is the substantial genetic heterogeneity often associated with such disorders. In addition, individual mutations are frequently confined to individual pedigrees; in such cases designer therapies may not be viable owing to cost and difficulties in the design of therapies for specific mutations. For example, hammerhead ribozymes require very specific NUX target sites in RNA, which must preferably occur within accessible areas of target RNA in order to ensure a ribozyme cleaves its target efficiently. Thus mutation-independent therapies are likely to present a more realistic approach to therapy. Such therapies could be targeted towards the primary genetic defect or a secondary effect associated with disease pathology. In terms of the latter, it is becoming evident that many disorders, including retinitis pigmentosa (RP) and age related macular degeneration (ARMD) involve apoptosis (reviewed in Adler et al., 1999). Therefore modulating apoptosis might provide a means of therapy, independent of the individual disease mutation. In the current study a strategies for a mutation-independent therapy targeting the primary defect of COL1A1 linked OI has been explored *in vitro*; a disease in which over 150 mutations in the type I pro-collagen

gene COL1A1 are known to be involved (HGMD 1998). A very mild form of disease is manifested when null mutations occur, suggesting that suppression of a mutant allele, known to cause a severe form of OI, alone may ameliorate the disease. The approach, consisting of directing a hammerhead ribozyme (Rzpol1a1) to one allele of a polymorphism provides a novel genomics-driven means of selectively suppressing mutant alleles in a mutation-independent manner, while leaving the alternative allele coding for wildtype protein intact.

A C3210T intragenic polymorphism in human COL1A1 has previously been described (Westerhausen et al. 1990). One variant, the T-allele contains an NUX hammerhead ribozyme target site, while the C-allele does not. The frequency of the polymorphism was assessed in 18 individuals (27 T-allele, 9 C-allele) (Westerhausen et al., 1990). An additional 11 unrelated individuals from the CEPH panel were assessed in this study. Of the total 58 alleles, 42 were T (0.72) and 16 were C (0.28), suggesting a heterozygote frequency of 0.4032 (2pq). Therefore it is predicted that approximately 1 in 5 dominant-negative OI patients will be heterozygous for the 3210 polymorphism and will carry the disease mutation on the same allele as 3210T and hence Rzpol1a1 could potentially provide a therapy for these patients. Therefore this polymorphism has almost the maximum resolution possible for any 2-allele system using a single ribozyme. Moreover it is fortuitous that this polymorphism creates a ribozyme cleavage site which is predicted by RNAPlotfold to be situated in a large open-loop structure of the COL1A1 RNA (figure 1a). This, together with the heterogeneous nature of OI stimulated us to explore Rzpol1a1 as a potentially powerful mutation-independent therapeutic agent for OI.

Rzpol1a1 cleaves the T-allele of COL1A1 RNA in a sequence specific manner *in vitro*, while leaving the C-allele RNA intact (figure 2). Moreover, the results of this study indicate that Rzpol1a1 is extremely efficient in cleaving a 381 bp fragment of COL1A1 RNA *in vitro*, with a V_{max} of 0.4 min^{-1}. Maximum cleavage rates of hammerhead ribozymes for unstructured short (20bp) RNAs have typically approximated 1 min^{-1} (Zaug et al., 1988). However, significant reductions (in excess of 200 fold) in cleavage rates are typically observed for longer more complex RNA targets (Jankowsky and Schwenzer, 1996), suggesting that Rzpol1a1 is efficient at cleaving its structured target. Notably the activity of Rzpol1a1 was modified by competitors. A 400 fold weight excess of total RNA over Rzpol1a1 reduced the rate of cleavage by approximately two-fold, while a 1:1 ratio of C-allele RNA:Rzpol1a1

inhibited the cleavage rate by 40% (figure 7a/b). In both experiments the observed inhibition was competitive and could be overcome with higher concentrations of substrate. It is not surprising that competitive inhibition with the C-allele RNA was observed, since the ribozyme antisense arms are a perfect match for this allele. The fact that no uncompetitive inhibition by total RNA was observed was somewhat surprising since uncompetitive inhibition caused by the ribozyme-substrate complex binding to the inhibitor, or physical interference of RNA might have been expected. Inhibitory effects have been investigated in other studies of ribozyme kinetics and various effects have been observed. Grassi et al., (1997) found no inhibition of ribozyme activity by total RNA, and Kisich et al., (1997) found competitive and uncompetitive inhibition by cellular RNA. In addition to RNA-inhibition on ribozyme cleavage, DNA-inhibition was investigated (figure 8). Interestingly, the inhibitory effect showed asymptotic behaviour, towards a limit of approximately 70% inhibition. This effect may be due to aggregation of DNA when present at high concentrations. This in turn may lead to a clumping effect of the DNA with 'gaps' containing no DNA in-between. Thus, when more DNA is added to such a solution of DNA clumps, the 'gaps' may not reduce much in size and the inhibition caused by the additional DNA may be relatively low. In addition to exploring cleavage rates and inhibition, the cleavage rate constant and dissociation constant, k_2 and k_{-1}, were determined under single-turnover conditions, where the ribozyme is in excess of the target RNA, and were found to be 0.58 min^{-1} and 0.087 min^{-1} respectively (figure 7c/d). These figures fall within the range determined for many other hammerhead ribozymes (Stage-Zimmerman and Uhlenbeck, 1998). k_2 for short unstructured RNA targets (30 bases) ranges between 0.3 and 2.5. The rate of dissociation, k_{-1}, which depends greatly on the length and composition of ribozyme antisense arms, though not often studied can vary widely; values greatly exceeding k_2 or indeed far smaller have been observed (Stage-Zimmerman and Uhlenbeck, 1998).

In the current study, in addition to inhibition observed with competitor RNA, inhibition by cleavage products was observed in the presence of limiting amounts of ribozyme (figure 5a), however inhibition was overcome using a large excess of ribozyme (figure 5b). In contrast to the situation *in vitro*, the product inhibition observed at low ribozyme concentrations is unlikely to occur *in vivo*, since such cleavage products lack either a 5' cap or 3' polyA tail and are therefore unstable. Additionally, the stability of Rzpol1a1 at 37°C was assessed and this ribozyme was found to be extremely stable at 37°C (figure 5c/d), a situation that does not apply to

all RNAs. Rzpol1a1 had not lost activity after 3 hours at 37°C. Perhaps the ribozyme secondary structure with internal base-pairing stabilises Rzpol1a1. The maintenance of activity of Rzpol1a1 at 37°C suggested that the inhibition observed may be due to inhibition by cleavage products (as discussed above) rather than loss of activity at 37°C.

4.5. Summary

In conclusion, the hammerhead ribozyme Rzpol1a1 has been shown to elicit selective highly efficient cleavage of one allele of a polymorphism in the human COL1A1 transcript. The common nature of the polymorphism suggests that a single therapeutic agent would in principle be applicable to 20% of OI patients with gain-of-function mutations in the COL1A1 gene. Thus one single potential cure (Rzpol1a1) would benefit many patients (20%) with different mutations in the COL1A1, in which over 100 different mutations are known to cause OI (Millington-Ward et al., 1999). An exponential increase in characterisation of intragenic polymorphisms, which is a necessary consequence of the human genome project given its restated aims for 2003, that is the listing of 100,000 human SNPs in a special database, will greatly expedite the exploitation of polymorphism in innovative allele-specific drug designs. The power of SNPs to undertake linkage studies, to direct therapeutic agents in an allele-specific manner and to understand the molecular basis of variable responses of patients to many drugs has been realised not only in the academic community (in the guise of the human genome project) but additionally by a number of commercial companies. Not least among these are: Isis Pharmaceuticals, who mainly generate antisense technology and Surgen, which is a joint-venture company of GENSET and the Royal College of Surgeons in Ireland (RCSI). This company has the following two main aims. The first aim is to discover novel genetic variants, which can improve drug development; mainly by identifying a protein or protein region as a target for drug action. The second aim is to discover novel genetic variants, which can improve clinical practise; mainly by allowing gene diagnosis to assist in therapeutic decision making.

The current study clearly demonstrates how valuable SNPs, such as COL1A1 C3210T, may be in circumventing the inherent diversity in the genetic etiology of OI. It is of note that a similar pharmacogenetic approach, exploiting intragenic polymorphisms and using a range of therapeutic suppressors such as antisense or

ribozymes, could be adopted for many heterogeneous dominantly-inherited genetic disorders and complex traits with dominant-negative genetic factors.

4.6. Bibliography

Adler R, Curcio C, Hicks D, Price D, Wong F. Cell death in age-related macular degeneration. Mol Vis. 1999 Nov 3;5:31.

Allay JA, Dennis JE, Haynesworth SE, Majumdar MK, Clapp DW, Shultz LD, Caplan AI, Gerson SL (1997) LacZ and interleukin-3 expression in vivo after retroviral transduction of marrow-derived human osteogenic mesenchymal progenitors. Hum Gene Ther 8(12): 1417-1427

Bauer G, Valdez P, Kearns K, Bahner I, Wen SF, Zaia JA, Kohn DB (1997) Inhibition of human immunodeficiency virus-1 (HIV-1) replication after transduction of granulocyte colony-stimulating factor-mobilized CD34+ cells from HIV-1-infected donors using retroviral vectors containing anti-HIV-1 genes. Blood 89(7): 2259-2267

Birikh KR, Berlin YA, Soreq H, Eckstein F (1997b) Probing accessible sites for ribozymes on human acetylcholinesterase RNA. RNA 3(4): 429-437

Birikh KR, Heaton PA, Eckstein F (1997a) The structure, function and application of the hammerhead ribozyme. Eur J Biochem 245(1): 1-16

Byers PH (1993) Second international symposium on the Marfan syndrome. Hum Mutat 2(2): 80-81

Collins FS, Patrinos A, Jordan E, Chakravarti A, Gesteland R, Walters L. New goals for the U.S. Human Genome Project: 1998-2003. Science. 1998 Oct 23;282(5389):682-9.

Cornish-Bowden A and Wharton CW (1990) Simple Enzyme Kinetics. In Rickwood D (eds) Enzyme kinetics. IRL Press, Oxford, p 14.

Fedor MJ, Uhlenbeck OC (1992) Kinetics of intermolecular cleavage by hammerhead ribozymes. Biochemistry 31(48): 12042-12054

Grassi G, Forlino A, Marini JC (1997) Cleavage of collagen RNA transcripts by hammerhead ribozymes in vitro is mutation-specific and shows competitive binding effects. Nucleic Acids Res 25(17): 3451-3458

Hendry P, McCall MJ, Lockett TJ (1997) Characterizing Ribozyme Cleavage Reactions. In: Turner PC (eds) Ribozyme Protocols. Humana Press, New Jersey pp 221-229

HGMD. The Cardiff Human Gene Mutation Database. Online database: http://www.1e.ac.uk.genetics.collagen.collagen.html

Khillan JS, Olsen AS, Kontusaari S, Sokolov B, Prockop DJ (1991) Transgenic mice that express a mini-gene version of the human gene for type I procollagen (COL1A1) develop a phenotype resembling a lethal form of osteogenesis imperfecta. J Biol Chem 266(34): 23373-23379

Kilpatrick MW, Phylactou LA, Godfrey M, Wu CH, Wu GY, Tsipouras P (1996) Delivery of a hammerhead ribozyme specifically down-regulates the production of fibrillin-1 by cultured dermal fibroblasts. Hum Mol Genet 5(12): 1939-1944

Kisich KO, Freedland SJ, Erickson KL (1997) Factors altering ribozyme-mediated cleavage of tumor necrosis factor-alpha mRNA in vitro. Biochem Biophys Res Commun 236(1): 205-211

Kuivaniemi H, Tromp G, Prockop DJ. Mutations in collagen genes: causes of rare and some common diseases in humans. FASEB J. 1991 Apr;5(7):2052-60.

Lieber A, Kay MA (1996) Adenovirus-mediated expression of ribozymes in mice. J Virol 70(5): 3153-3158

Lieber A, Strauss M (1995) Selection of efficient cleavage sites in target RNAs by using a ribozyme expression library. Mol Cell Biol 15(1): 540-551

Millington-Ward S, O'Neill B, Kiang AS, Humphries P, Kenna PF, Farrar GJ. A mutation-independent therapeutic stratagem for osteogenesis imperfecta. Antisense Nucleic Acid Drug Dev. In Press.

Millington-Ward S, O'Neill B, Tuohy G, Al-Jandal N, Kiang AS, Kenna PF, Palfi A, et al (1997) Strategems in vitro for gene therapies directed to dominant mutations. Hum Mol Genet 6(9): 1415-1426

Pereira RF, O'Hara MD, Laptev AV, Halford KW, Pollard MD, Class R, Simon D, et al (1998) Marrow stromal cells as a source of progenitor cells for nonhematopoietic tissues in transgenic mice with a phenotype of osteogenesis imperfecta. Proc Natl Acad Sci U S A 95(3): 1142-1147

Persidis A. Pharmacogenomics and diagnostics. Nat Biotechnol. 1998 Aug;16(8):791-2.

Prockop DJ (1994) Antisense oligonucleotides to inhibit expression of mutated and wild type genes for collagen. International application published under the patent cooperation treaty (PCT) WO 94/11494

Prockop DJ, Kuivaniemi H, Tromp G (1994) Molecular basis of osteogenesis imperfecta and related disorders of bone. Clin Plast Surg 21(3): 407-413

Sillence D (1981) Osteogenesis imperfecta: an expanding panorama of variants. Clin Orthop 159: 11-25

Sillence DO, Senn A, Danks DM (1979) Genetic heterogeneity in osteogenesis imperfecta. J Med Genet 16(2): 101-116

Sokolov BP, Ala-Kokko L, Dhulipala R, Arita M, Khillan JS, Prockop DJ (1995) Tissue-specific expression of the gene for type I procollagen (COL1A1) in transgenic mice. Only 476 base pairs of the promoter are required if collagen genes are used as reporters. J Biol Chem 270(16): 9622-9629

Wenstrup RJ, Willing MC, Starman BJ, Byers PH (1990) Distinct biochemical phenotypes predict clinical severity in nonlethal variants of osteogenesis imperfecta. Am J Hum Genet 46(5): 975-982

Westerhausen AI, Constantinou CD, Prockop DJ (1990) A sequence polymorphism in the 3'-nontranslated region of the pro alpha 1 chain of type I procollagen. Nucleic Acids Res 18(16): 4968

Willing MC, Pruchno CJ, Atkinson M, Byers PH (1992) Osteogenesis imperfecta type I is commonly due to a COL1A1 null allele of type I collagen. Am J Hum Genet 51(3): 508-515

Zuker M (1989) Computer prediction of RNA structure. Methods Enzymol 180: 262-288, Oct 20; 270 (5235): 470-475

Figure 1.

A

B

Substrate

Stem 1

```
5'  A C C C C  CUC  A A A A G C C A  3'
    | | | | | | |      | | | | | | | |
3'  U G G G G G A      U U U U C G G U  5'
```

Stem 3

```
            A   C
                U
                 G
        A          A
                   U
                 G
        G     A
        C-G
        A-U        Ribozyme
Stem 2  G-C
        G-C
      A     G
        G U
```

C

Substrate

X

Stem 1

```
5'  A C C C C  CCC  A A A A G C C A  3'
    | | | | | | |      | | | | | | | |
3'  U G G G G G A      U U U U C G G U  5'
```

Stem 3

```
            A   C
                U
                 G
        A          A
                   U
                 G
        G     A
        C-G
        A-U        Ribozyme
Stem 2  G-C
        G-C
      A     G
        G U
```
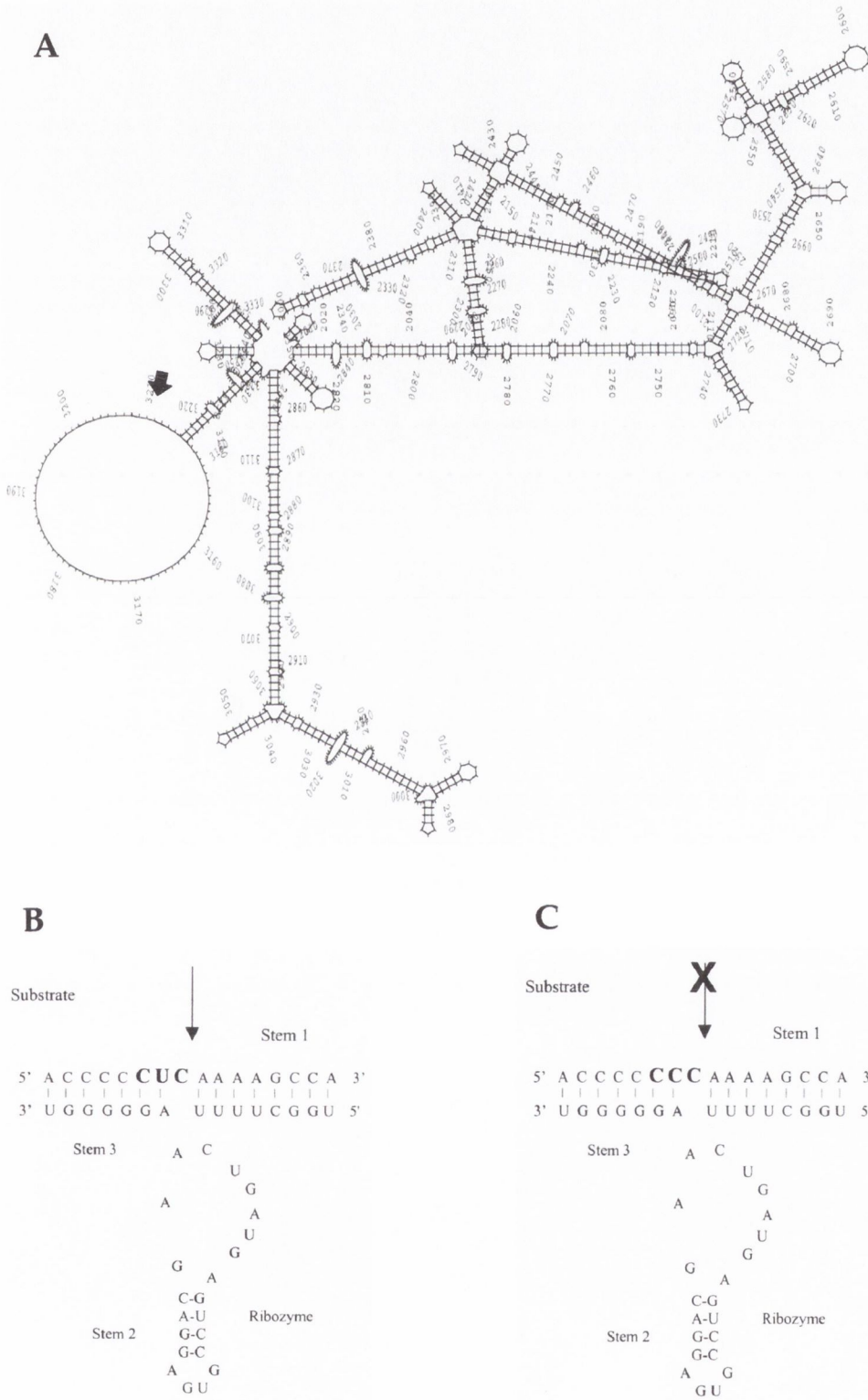
Figure 1. *A*, RNAPlotfold of COL1A1 RNA. The Ribozyme cleavage site, indicated with an arrow, is situated in a large open-loop structure of the RNA; *B*, diagram of hammerhead ribozyme Rzpol1a1. The two antisense arms (stems 1 and 3) and the double-stranded region (stem 2) are shown. The NUX target site of the substrate RNA is highlighted in bold print, with an arrow indicating the exact position of cleavage of the T-allele polymorphic variant of COL1A1. *C*, diagram of Rzpol1a1 (as in *B*) showing non-cleavage of the C-allele polymorphic variant of the COL1A1 transcript.

Figure 2.
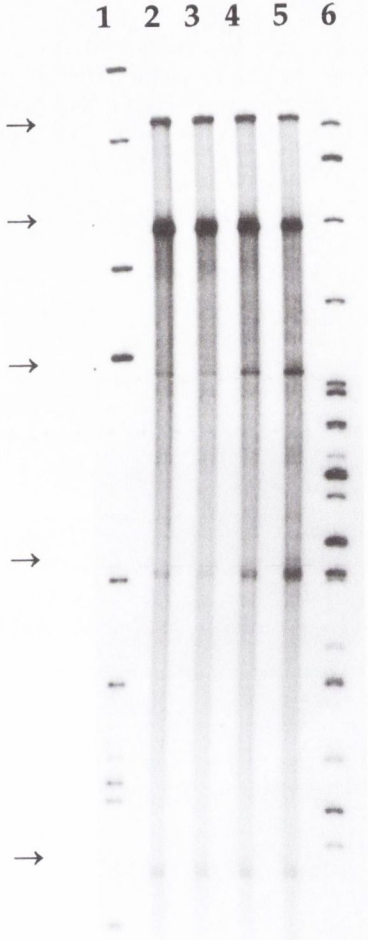
Figure 2. Cleavage timepoints of T-allele RNA, C-allele RNA and Rzpol1a1. Lanes one and six represent Sal3A cut Puc19 and MspI cut pBR322 DNA size markers. From top to bottom the T-allele RNA, C-allele RNA, two cleavage products and the ribozyme are highlighted. Cleavage products of the T-allele RNA were of predicted sizes. However, as can clearly be seen, the C-allele RNA remains intact.

Figure 3.
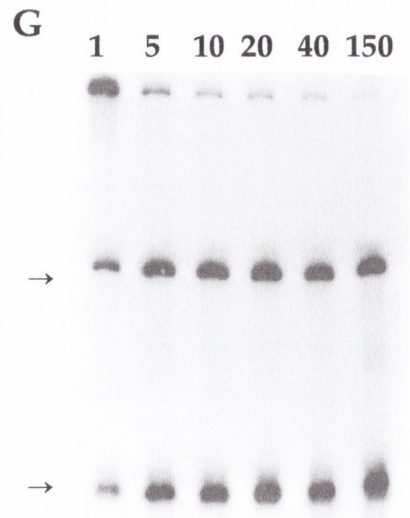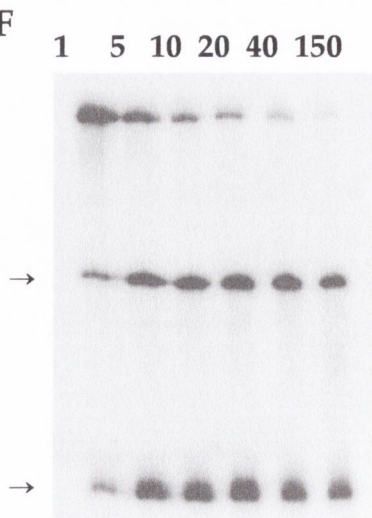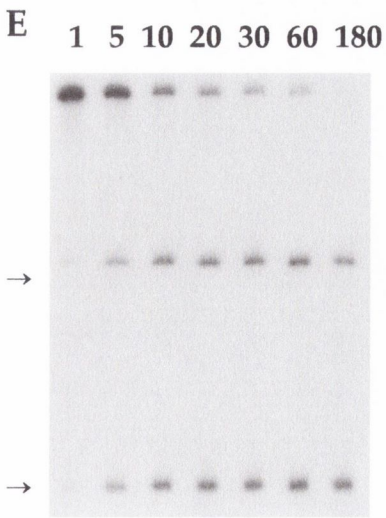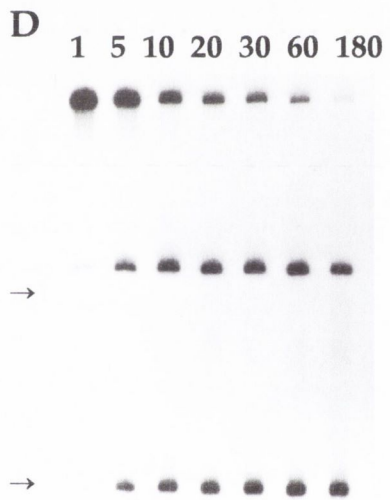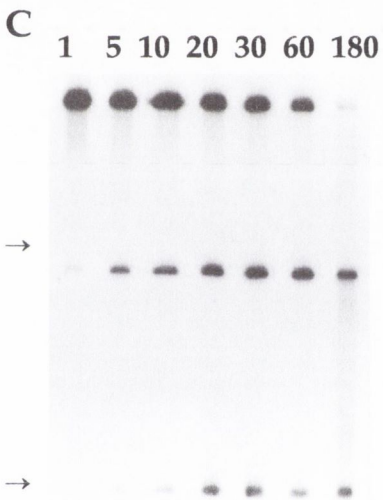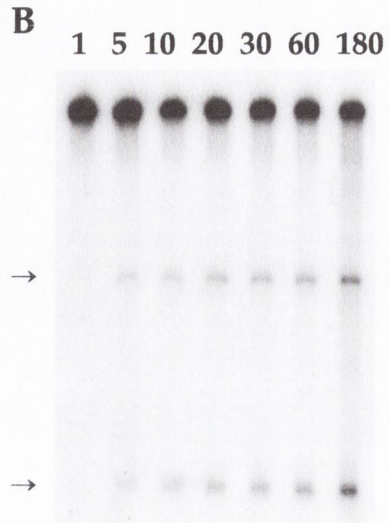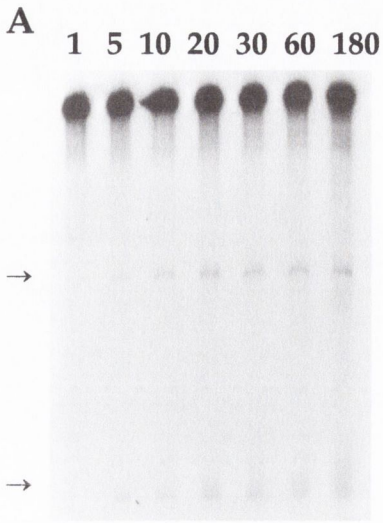
Figure 3. *A-G*, cleavage timepoints of T-allele RNA by Rzpol1a1 used to determine steady-state intervals; cleavage times (minutes) are given above the lanes and cleavage products are highlighted with arrows. T-alleleRNA:Rzpol1a1 ratios in A-G are as following 1:0.1, 1:0.3, 1:0.5, 1:1, 1:2, 1:10 and 1:100. Cleavage products were of predicted sizes.

Figure 4.
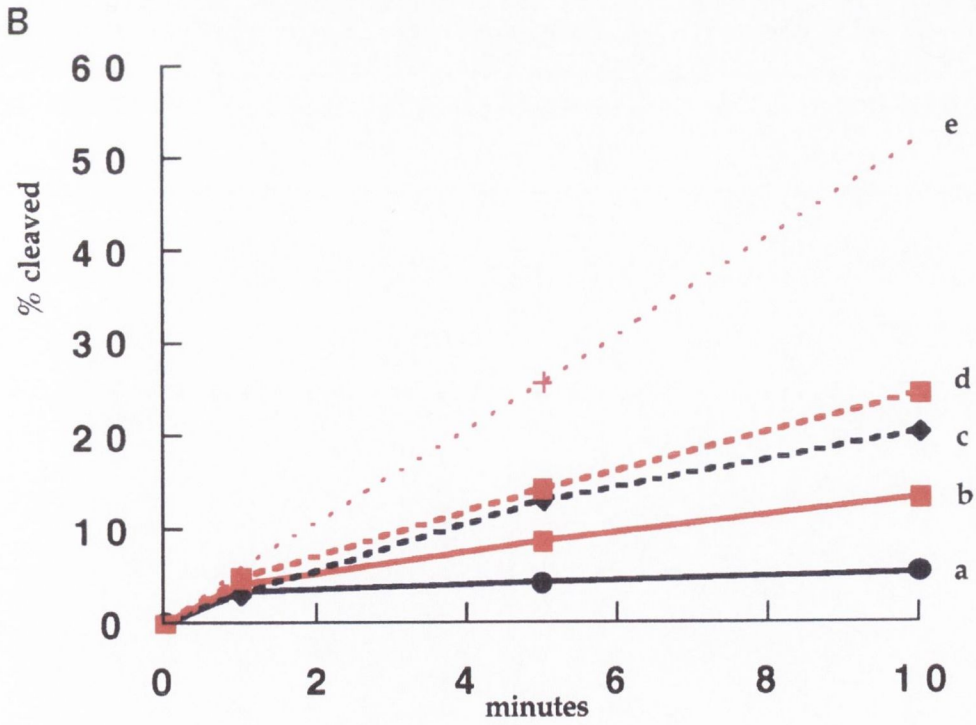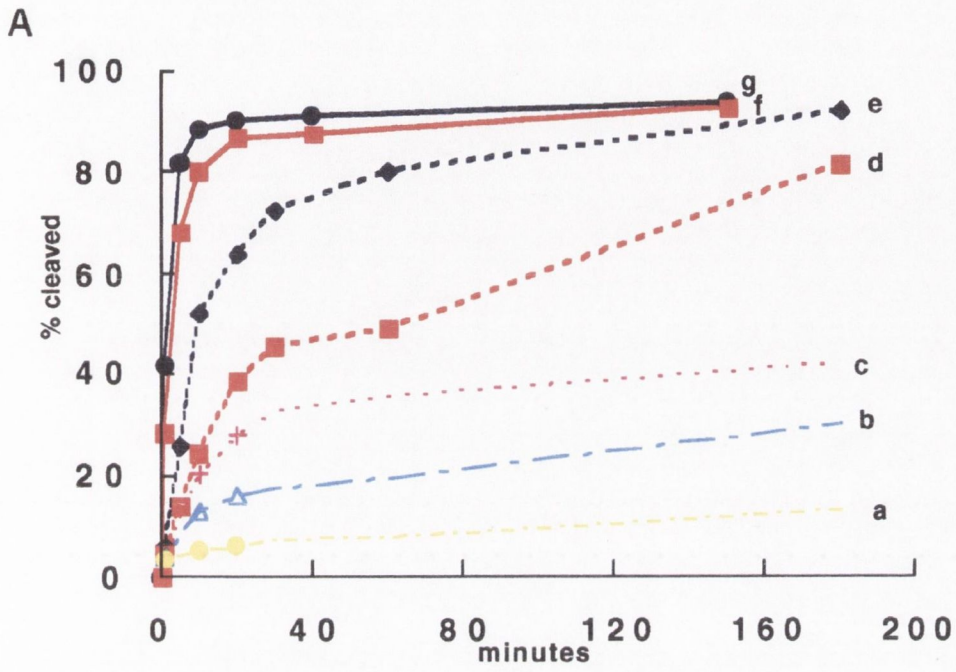
Figure 4. *A*, graph of percentage T-allele RNA cleaved by Rzpol1a1 versus time. Curves a-g depict timepoint cleavage results for molar ratios of T-allele RNA:Rzpol1a1 of 1:0.1, 1:0.3, 1:0.5, 1:1, 1:2, 1:10 and 1:100 respectively. *B*, curves a-e show the steady-state interval for ratios of T-allele RNA:Rzpol1a1 of 1:0.1, 1:0.3, 1:0.5, 1:1 and 1:2 respectively. The steady-state interval is at least 10 minutes.
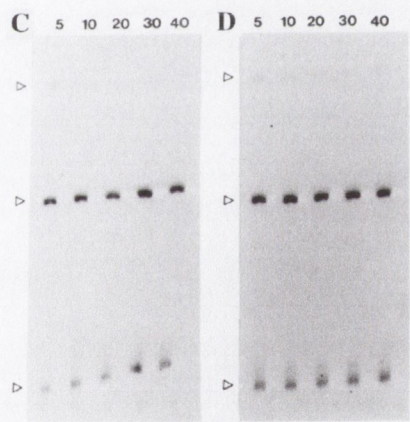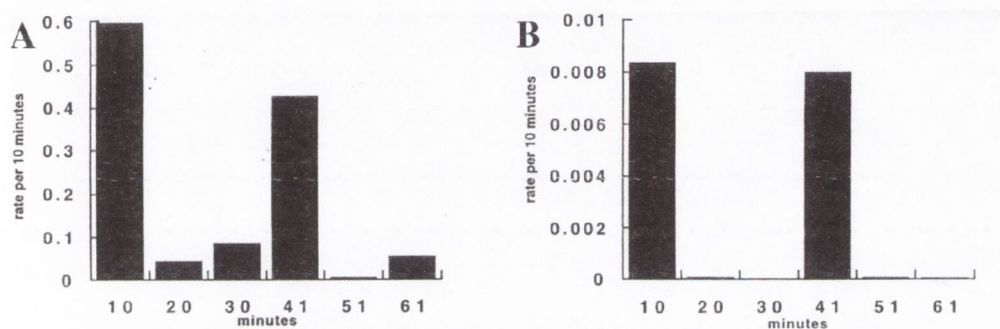
Figure 5.

Figure 5. *A*, bar chart of rates of cleavage per Rzpol1a1 molecule per 10 minutes versus time for the ratio of T-allele RNA:Rzpol1a1 of 1:0.1. Initial rates of cleavage are not achieved at 41 minutes after adding extra T-allele RNA; *B*, bar chart of rates of cleavage per Rzpol1a1 molecule per 10 minutes versus time for the ratio of T-allele RNA:Rzpol1a1 of 1:100. Initial rates of cleavage are achieved at 41 minutes after adding extra T-allele RNA. *C/D*, Timepoint reactions of T-allele RNA cleavage by Rzpol1a1 (1:100) with (*C*) and without (*D*) ribozyme pre-incubation at 37°C for 1 hour. Cleavage times (minutes) are given above the lanes. Uncleaved RNA and the two cleavage products are highlighted from top to bottom with arrows.
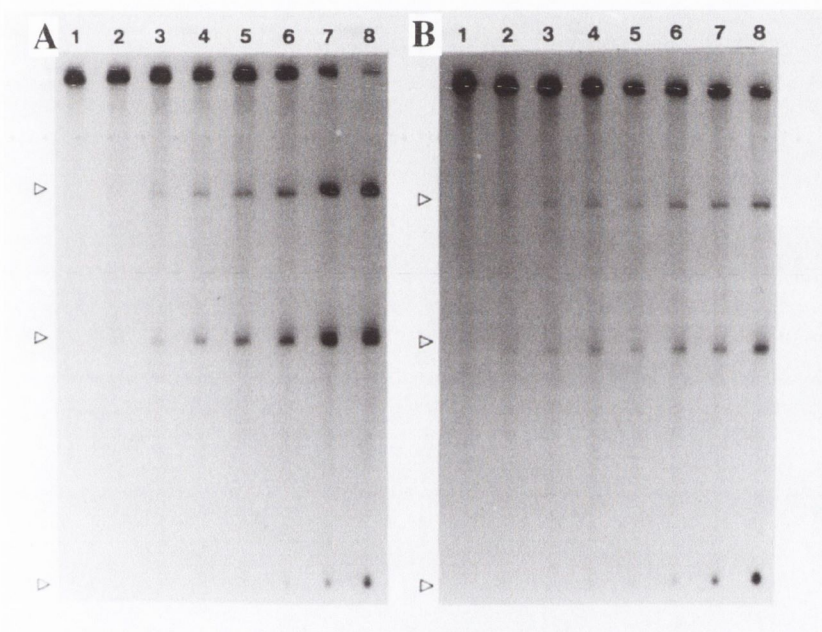
Figure 6.

Figure 6. Autoradiographs of cleavage gels without (*A*) and with Y79 RNA as inhibitor (*B*). The two cleavage products and Rzpol1a1 are highlighted from top to bottom by arrows. Molar ratios of T-allele RNA:Rzpol1a1 in lanes 1-8 are 1:0.1, 1:0.2, 1:0.5, 1:1, 1:1.25, 1:2, 1:5 and 1:10 respectively.
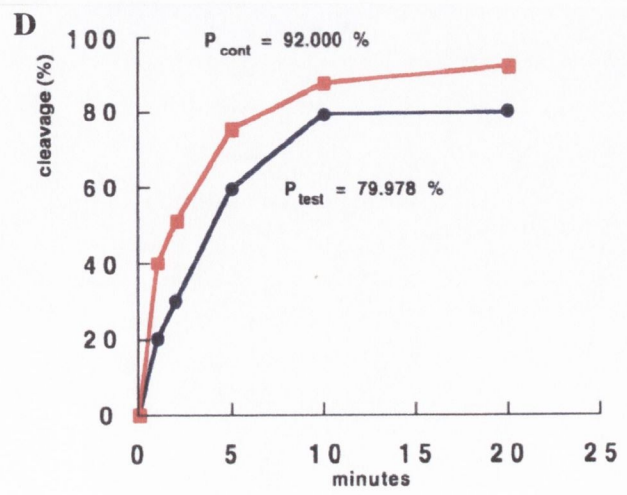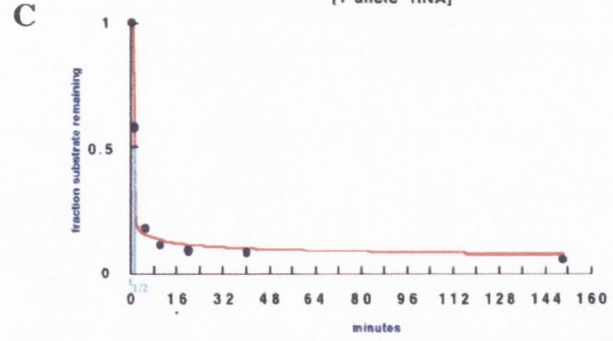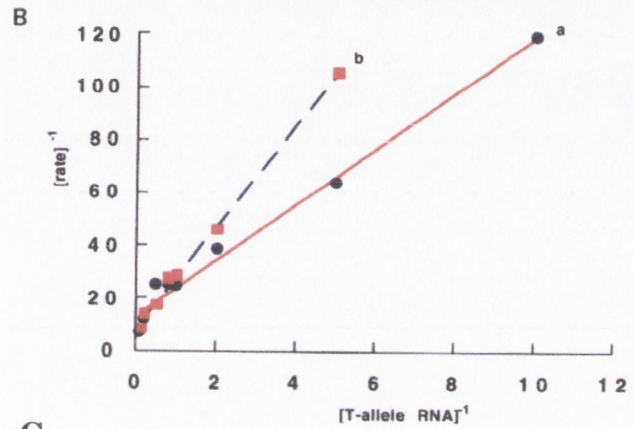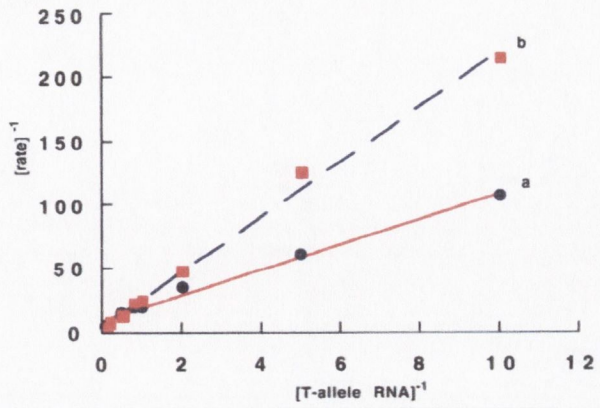
Figure 7.

Figure 7. *A*, Lineweaver-Burk plot (rate^{-1} versus [T-allele RNA]$^{-1}$) for *in vitro* cleavage of Rzpol1a1 with (curve a) and without (curve b) a 400x excess of Y79 total RNA; *B*, Lineweaver-Burk plot for *in vitro* cleavage of Rzpol1a1 in the presence of C-allele RNA. The molar ratio of Rzpol1a1:C-allele was 1:1; *C*, graph of fraction of T-allele RNA remaining versus time, under single-turnover conditions (T-allele RNA:Rzpol1a1 = 1:100). $t_{1/2}$ was used to calculate k_2. *D*, Graph of percentage T-allele RNA cleaved versus time (minutes) of control and test cleavage reactions of T-allele RNA by Rzpol1a1 (ratio 1:2.5 respectively). In the control reaction RNAs were annealed prior to initiation of the reaction with $MgCl_2$. In the test reaction RNAs were also pre-annealed, however, concurrently to initiation of the reaction with $MgCl_2$. A 100x excess of unlabeled T-allele RNA over labeled T-allele RNA was added to the reaction. Samples were taken at various times. The amount of product formed for the control and test reaction at $t = \infty$ were determined from these graphs. As can be seen, $P_{\infty cont} = 92.000\%$ and $P_{\infty test} = 79.978\%$. These figures were used to determine k_{-1}.
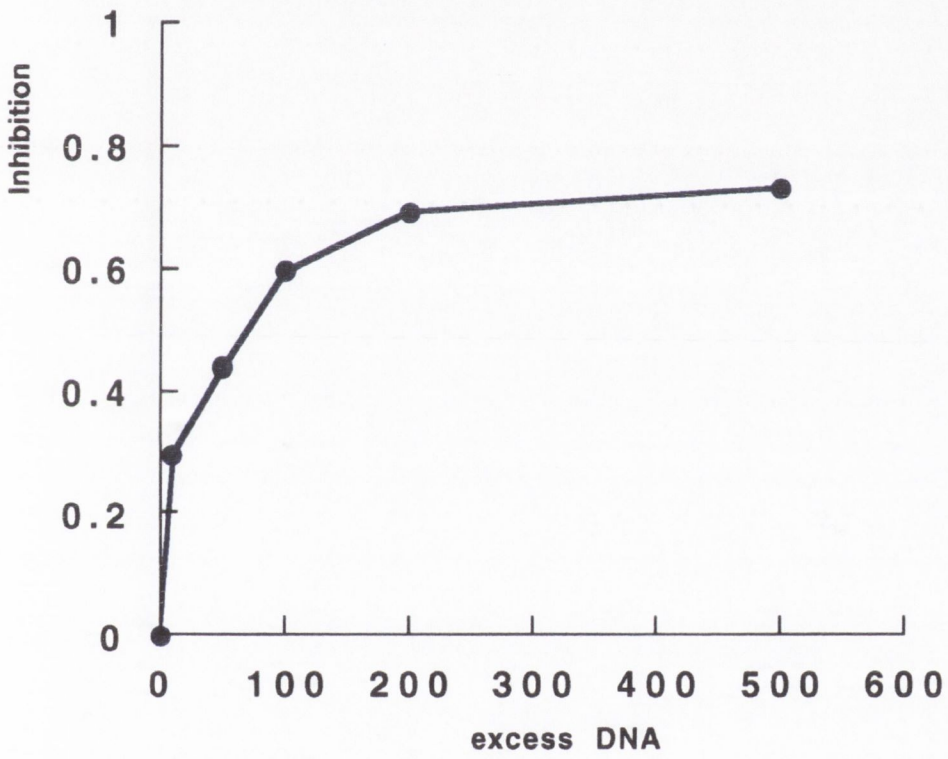
Figure 8.

Figure 8. Diagram of inhibition of ribozyme cleavage by DNA. The horizontal axis represents the weight-excess of DNA over ribozyme and the horizontal axis represents the inhibition (inhibition = 1 - (observed cleavage with DNA/expected cleavage without DNA)).

Rzpol1a1	V_{max} (min^{-1})	K_m (nM)	k_2 (min^{-1})	k_{-1} (min^{-1})
- inhibitor	0.41	9.5	0.58	0.087
+ Y79 RNA	0.42	10.3		
+ C-allele RNA	0.42	9.8		

Table 1. Kinetic parameters for *in vitro* cleavage of Rzpol1a1 on its own and in the presence of a 400x excess Y79 total RNA and C-allele RNA.

5. Rzpol1a1 studied for *in vivo* work

5.1. Introduction

Catalytic hammerhead ribozymes have been discussed in detail in chapters 3 and 4. In chapter 3 many ribozymes targeting a variety of transcripts were designed and tested *in vitro*. In addition, in chapter 4 the most efficient ribozyme, Rzpol1a1 targeting a polymorphic site in the human COL1A1 transcript, was kinetically characterised *in vitro* and found to be extremely efficient ($V_{max} = 0.41$ min^{-1}). In this chapter, Rzpol1a1 will be evaluated for future *in vivo* studies; both in cell lines and an animal model.

Many studies have been undertaken on hammerhead ribozyme structure and their *in vitro* kinetics (1.3-1.5). Efficient ribozymes then may be studied *in vivo*; either in cell culture or animal models (1.11-1.13). There are two generally accepted methods of introducing ribozymes into cells. The first is through exogenous delivery of pre-formed ribozymes and the second through endogenous delivery, which involves the expression of ribozymes from transcriptional units such as DNA plasmids. Endogenous expression has been achieved on many occasions (1.6, 1.12, 1.13), using plasmids and viruses with strong promoters driving ribozyme expression, such as the SV40, CMV, RNA polymerase II (polII) and actin, promoters or tissue specific promoters. To aid delivery of plasmids into target cells, plasmids can be associated with non-viral vectors such as lipids and synthetic polymers (sections 1.13.2.2 to 1.13.2.4).

Pre-formed ribozymes, on the other hand, can be delivered using lipids, synthetic polymers, electroporation or microinjection (sections 1.13.2.2 to 1.13.2.4). These ribozymes may require the introduction of modified nucleotides, to protect them from nucleases present in cells. There are three major target sites for modification present in RNAs: the base (A, U, C or G), the sugar, and the internucleotide phosphodiester linkage, where individual bases are linked to one another. Modified RNAs can be generated using chemical or enzymatic techniques.

For instance, all RNAs transcribed by polII contain a 5'-cap which protects them against 5'-exoribonucleases (Furuichi et al., 1977). Thus if pre-formed ribozymes are generated with the 5'-cap they are partially protected from nuclease

degradation. In addition, the 5'-end of a ribozyme (the first base) can comprise of a modified oligonucleotide containing modifications such as guanosine, guanosine 5'-monophosphate (GMP), guanosine 5'-O-(1-thiomonophosphate), ApG, CpG, AmpG, and others (reviewed in Gaur and Krupp, 1997).

Oligonucleotides (either DNA or RNA) containing phosphorothioate linkages (on the sugar) can be synthesised by either chemical or enzymatic means (Eckstein, 1985) and are protected from degradation by endonucleases.

In addition the 2'-hydroxyl groups (on the base) in RNAs can be exchanged for 2'fluoro-, 2'-amino-, 2'-O-methyl-, 2'-O-allyl or 2'-deoxy-nucleotides. These RNAs can be generated using chemical or enzymatic approaches. In addition, in chemically synthesised ribozymes 2'-modified bases can be introduced at specific sites, although only short RNAs can be synthesised chemically. In this chapter one method of RNA modification was tested for Rzpol1a1 targeting a polymorphic site in the human type I collagen transcript. In preparation for possible exogenous delivery of Rzpol1a1 to cells, the ribozyme was enzymatically generated, by *in vitro* transcription, with the incorporation of 2'-aminonucleotides; both Us and Cs. The modified ribozyme was tested both for stability in serum and cleavage of the COL1A1 transcript.

The incorporation of 2'-fluoro- and 2'-aminonucleotides into hammerhead ribozymes is one of the more successful methods of stabilising the molecule (Pieken et al., 1991a). However, the catalytic efficiency of the ribozyme may be reduced by this modification, depending on how many bases are modified and where these are located (Pieken et al., 1991b; Heidenreich and Eckstein, 1992). The exact mechanism of the inhibition of cleavage efficiency was not elucidated until 1998 when a comprehensive study in Norway demonstrated the effect(s) of each base substitution (Leirdal and Sioud, 1998). The study showed that efficient cleavage activity could be achieved for the 2'-amino modified ribozymes when their sequences were designed to contain only a few pyrimidines in helix I. Ribozymes with no pyrimidines in helix I cleave their target RNAs with almost the same efficacy as their unmodified versions. Selective 2'-amino modifications at positions 2.1 and 2.2 reduced the ribozyme cleavage activity by 8-fold, suggesting that the modifications at these positions may interfere with the formation of the ribozyme's active conformation (Leirdal and Sioud, 1998).

In preparation for either exogenous or endogenous delivery of Rzpol1a1 to cells, four primary fibroblast cell lines (C, F1, F7 and F5) were obtained from Drs. Willing and Deschenes, which were derived from OI patients and were known to express the COL1A1 gene (Willing et al., 1994). The cell lines had previously been genotyped for the C3210T polymorphism in the COL1A1 gene and were as follows:

C: heterozygous for the C-allele and the T-allele.

F1 and F7: heterozygous for the C- and T- allele, but only forming mRNA derived from the C-allele because of a null mutation in the T-allele DNA. The patient manifests type I OI, due to haploinsufficiency.

F5: heterozygous for C- and T-allele, but only forming mRNA derived from the T-allele because of a null mutation in the C-allele. The patient manifests type I OI, due to haploinsufficiency.

One of these cell lines, C, was used to optimise two (non-viral) methods of gene transfection. To this end a plasmid containing a LacZ reporter gene driven by a CMV promoter was transfected into the cell line using electroporation and a commercially available lipid, lipofectAMINE-PLUS (GibcoBRL). Neither of the methods achieved successful transfection of cell line C, although both methods were shown to work in a control COS-7 cell line. Therefore a virus was considered to be a more likely vector to achieve successful introduction of genes into this cell line. The inefficient transfection obtained with cell line C would render the exogenous approach for ribozyme delivery to this particular cell line impossible.

Initially, an Adenovirus (Ad) carrying the LacZ gene (section 1.13.1.2) driven by a CMV promoter was tested in cell line C, as this virus was available in the laboratory. Notably, in contrast to electroporation and lipofectAMINE, Ad infected over 90% of the cells from cell line C. Additionally, an MLV retrovirus (1.13.1.1) carrying a LacZ gene driven by a CMV promoter was bought from Dr. Miyanohara (Yee et al., 1994) and tested in cell line C. This virus too successfully infected cells from line C, stimulating the generation of a construct carrying Rzpol1a1 driven by a CMV promoter, which will be utilised in the generation of an MLV virus. This virus may be used to test Rzpol1a1 cleavage in cell culture or in an animal model.

Thus, in this chapter a protected ribozyme (Rzpol1a1) containing 2'-amino modified nucleotides was generated and tested *in vitro* for stability in serum and cleavage of the COL1A1 transcript. Appropriate cell lines, described above, were obtained for

testing Rzpol1a1 in cell culture. Given that these cell lines were not suitable for non-viral transfection methods, an MLV viral construct was generated containing Rzpol1a1 driven by a CMV promoter. The resulting retrovirus will be used to test if Rzpol1a1 elicits efficient cleavage of COL1A1 transcripts in cell culture or in animal models.

5.2. Materials and Methods

5.2.1. Rzpol1a1 protection

A protected version of Rzpol1a1 was generated by transcribing clone Rzpol1a1 (chapter 3.2.5.4) *in vitro* as in chapter 3.2.6, however including one change in the protocol. Instead of using the usual nucleotides provided in the Ribomax kit (Promega), 2'-NH$_2$-dUTP and 2'NH$_2$-dCTP (Amersham) were used. *In vitro* transcription reactions of the T-allele and cleavage reactions of T-allele RNA by protected Rzpol1a1 were carried out as in chapter 3.2.6/3.2.7. Extremely small quantities of Rzpol1a1 were added to T-allele RNA and incubated at 37°C for varying amounts of time. The amount of Rzpol1a1 added was too small to quantify due to inefficient transcription (discussed in sections 5.3 and 5.4).

5.2.2. Cell lines

Four primary dermal fibroblast cell lines (F1, F7, F5 and C), the first 3 derived from patients with OI and the last from a normal individual, were kindly donated by Drs. Marcia Willing and Sachi Deschenes (Willing et al., 1994). Two of the cell lines, F1 and F7, are heterozygous for the C- and the T-allele of COL1A1, but only express mRNA derived from the C-allele because of a null mutation in the T-allele DNA. In contrast, cell line F5 is heterozygous for both the C- and T-allele, but only expresses RNA derived from the T-allele because of a null mutation in the C-allele. The patients from whom these three cell lines were derived manifested the mild type I OI due to haploinsufficiency. The fourth cell line, line C, is heterozygous for the C- and T-allele and expresses both alleles. Cell line C was used in transfection studies of a plasmid carrying a reporter LacZ gene (pZeoSV/*LacZ* (Invitrogen)) using both electroporation and lipofectAMINE-PLUS (GibcoBRL). In addition, cell line C was used to assess infection of primary fibroblasts by both an Adenovirus (Ad) and a Murine Leukaemia Virus (MLV) carrying LacZ reporter genes.

5.2.3. Cell culture

All cell lines were grown in either 3 or 10 cm petridishes (Falcon or *NUNC*™) at 37°C and 5% or 6% CO_2 in a Forma Scientific infrared CO_2 incubator (Bio-Sciences). The media used was Dulbecco's Modified Eagle's Medium (DMEM) (GibcoBRL) supplemented with various substances including bovine foetal calf serum (FCS) (for recipe, Appendix A). Prior to addition of FCS to the DMEM, the FCS was incubated at 55°C for 30 minutes. DMEM which has been supplemented with the items mentioned in Appendix A will be referred to as DMEM+.

Cells, grown in 10 cm petridishes, were harvested in the following manner. The medium was removed in a class two laminar flow cabinet and the cells were rinsed with 3-4 ml of PBS (GibcoBRL) (Appendix A). 2 ml of trypsin (GibcoBRL) was added and the plate was incubated at 37°C for 5 minutes to loosen cells from the plate. The cells in the trypsin were transferred to a universal tube (Sterilin) with 8 ml of DMEM+ and spun for 5 minutes at 1000 revolutions per minute (rpm). For re-plating purposes, cells were split four times.

Cells were stored at −80°C in the following manner. 0.5 ml ($2x10^7$) of cells resuspended in PBS were combined with 0.5 ml of 2x freezing medium (1 ml DMSO, 1 ml FCS, 2 ml DMEM+). This was aliquoted into pre-cooled ampules and initially stored at −80°C. Subsequently, ampules were transferred to liquid nitrogen and stored indefinitely.

5.2.4. Cell transfections using lipofectAMINE-PLUS

Cell transfections, undertaken in 6 well (3 cm) plates (Falcon), using cell line C were optimised for cell density ($1x10^5$-$5x10^5$ cells), lipofectAMINE concentration (GibcoBRL) (2.5-20 µl), PLUS concentration (3-20 µl) (GibcoBRL), quantity of DNA (0.5-5.0 µg), transfection time (3-5 hours) and time of assay (from 24-48 hours after transfection) according to the manufacturer's protocols. Transfections, in 6 well (3 cm) plates (Falcon), were carried out in serum and antibiotic free DMEM+. The plasmid used to optimise the assay was pZeoSV/*LacZ* (Invitrogen), driven by a CMV promoter. A COS7 cell line, known to transfect well using lipofectAMINE-PLUS was transfected under similar conditions and used as a control for the transfection and LacZ assays.

5.2.5. Electroporation of mammalian cells

Cells, grown in monolayers in 10 cm petridishes, were washed twice in PBS (Appendix A). Subsequently, 2.5 ml of trypsin (GibcoBRL) was added to each plate and incubated at 37°C for 5 minutes. 10 ml of DMEM+ (GibcoBRL) (Appendix A) was added and cells were spun at 1000 rpm for 5 minutes. The pellet was resuspended in PBS and counted with the aid of a haemocytometer. $5x\ 10^6$ cells were put in a 0.4 cm gene pulser electroporation cuvette (BioRAD) and left on ice for 20-30 minutes. Cells were then electroporated at 300V and 500μF. Subsequently cells were left on ice for 20 minutes and plated out on a 10 cm petridish in 10 ml of DMEM+. 300V was chosen as a suitable voltage to use for the electroporation because a deathcurve had established that at 300V half the cells are killed. The deathcurve was carried out on 6 identical cell samples. Samples were electroporated as above at 250V, 300V, 350V, 400V, 450V and 500V (figure 1).

5.2.6. Viral infection of cell cultures

$5x10^5$ mammalian cells from cell line C were infected with $1x\ 10^9$ or $1x10^7$ plaque forming units (pfu) of either Ad or MLV respectively carrying a LacZ gene driven by a CMV promoter. In the case of Ad infection, cells were grown at 37°C for 24 hours and assayed for LacZ expression (5.2.7). In the case of MLV infection, cells were grown at 37°C for 48 hours and assayed for LacZ expression. The Ad virus was kindly donated by Dr. H. Bueler. The MLV retrovirus was commercially obtained from Dr. Miyanohara (Yee et al., 1994).

5.2.7. LacZ assay

Cell culture monolayers in 10 cm petridishes were tested for the presence of the LacZ reporter protein as follows. Cells were washed twice with PBS (Appendix A) and fixed twice at room temperature for ten minutes in 10 ml of fix solution (Appendix A). Subsequently the cells were washed twice at room temperature in 10 ml of rinse solution (Appendix A). Cell were then stained over night at 37°C with 2.5 ml of stain solution (Appendix A). After colour development cells were rinsed twice for 10 minutes with rinse solution and stored indefinitely at 4°C.

5.2.8. Cloning viral construct

The pLRNL plasmid, kindly donated by Dr. Miyanohara, was used to clone Rzpol1a1, driven by a CMV promoter. pLRNA is the plasmid which was used to generate the MLV virus carrying the LacZ reporter gene (5.6.2) (Yee et al., 1994).

The insert, CMV driven Rzpol1a1, was generated by a PCR amplification (as in section 2.2.3) of the pcDNA3 clone carrying Rzpol1a1 (section 3.2.5.4). Primers used for PCR amplification were the following:

pLRNL F: 5′ GATCA<u>GTCGAC</u>CGATGTACGGGCCAGATATA 3′

pLRNL R: 5′ GATCA<u>GGATCC</u>ACCCCCTTTCGTCCTCACGGA 3′

The SalI and BamHI site in the forward and reverse primers respectively are underlined. The sequences 3' to the restriction sites in the forward and reverse primers are part of the CMV and Rzpol1a1 sequence respectively, present in clone Rzpol1a1. The five nucleotides 5' of the restriction sites are random bases which were included to aid in subsequent restriction digests. The PCR product, using these two primers and plasmid pLRNL were digested with SalI and BamHI. The insert was subsequently ligated into the pLRNL as in section 2.2.9. Ligations were transformed into Xl1 blue-MRA cells as in section 2.2.9, resulting colonies picked, grown in LB broth supplemented with suitable antibiotics (Appendix A) and miniprepped as in section 2.2.9. Minipreps were subjected to restriction digest analysis with SalI and BamHI and checked on agarose gels for the presence of inserts. Positive clones were sequenced by an automated sequencer using the primers pLRNL F and pLRNL by the author and Dr. Sophie Kiang as in section 3.2.4.

5.3. Results

Rzpol1a1, targeting a common polymorphic site in the human COL1A1 transcript, was initially tested for cleavage specificity (chapter 3) and efficiency (chapter 4). In this chapter, Rzpol1a1 was assessed for in *vivo* work; both through exogenous and endogenous means of delivery.

Ribozymes, such as Rzpol1a1, that are highly efficient *in vitro* may, due to a short *in vivo* half-life, not be so efficient when they are delivered in cell culture or animal models. Thus, ribozymes which are delivered in an exogenous manner, are often protected from ribonucleases by the incorporation of a wide range of chemical modifications such as, the incorporation of phosphorothioates, 2'-aminonucleotides and 2'-O-alkyl groups, (Zhang et al., 1998; Pieken et al., 1991a; Ludwig et al.,

1998; see paragraph 5.1). The addition of 2'-aminonucleotides has the advantages of not only stabilising ribozymes over 14,000-fold compared to unmodified versions (Sioud and Sorensen, 1998), but also of being easy to generate *in vitro* in the laboratory by simply adding protected nucleotides to transcription reactions. For these reasons the author decided to protect Rzpol1a1 with pyrimidines containing 2'-amino uridine and cytidine. Both the cleavage efficiency of protected Rzpol1a1 and its stability in DMEM+ was tested *in vitro*. Rzpol1a1 proved to be difficult to transcribe *in vitro* with protected nucleotides and the protected ribozyme yield was so low that it was hardly detectable in the usual manner on a polyacrylamide gel (3.2.6). Protected and normal Rzpol1a1 were incubated in DMEM+ for up to 30 minutes and run on a polyacrylamide gel. After one minute about half of the unprotected ribozyme had degraded, leaving no intact ribozyme after 30 minutes. The protected ribozyme, however, remained fully intact for at least 30 minutes (figure 2a/b). Due to the small quantity of protected Rzpol1a1 generated, an unknown and very small amount of protected Rzpol1a1 was added to timepoint cleavage reactions of the T-allele RNA of COL1A1 (figure 2c). Protected Rzpol1a1 cleaved the target transcript specifically. The efficiency of the cleavage reaction was difficult to determine, given an inability to quantify the amount of protected ribozyme used in cleavage reactions. However, due to the difficulties encountered in generating the protected Rzpol1a1, this method of RNA protection may not be suitable for Rzpol1a1. Other methods of protection such as the incorporation of phosphorothioates and 2'-*O*-allyl groups (Zhang et al., 1998; Ludwig et al., 1998; see 5.1 for details) or indeed protected ribozymes could be chemically synthesised. However, the latter approach was not tested in this study due to cost considerations. Thus, endogenous methods of gene delivery of Rzpol1a1 to cell cultures and animal models were considered; two viral constructs were evaluated in the primary fibroblast cell lines.

A number of human primary fibroblast cell cultures, known to express human COL1A1 and previously genotyped for the presence of the 3210 COL1A1 polymorphism were available in the laboratory (5.2.2). One of these cell lines, C, which is heterozygous for the 3210C/T polymorphism was tested in a series of transfection experiments. Firstly a commercially available lipid, lipofectAMINE-PLUS (GibcoBRL) reagent was used to test transfection of a reporter plasmid carrying a LacZ gene driven by a CMV promoter. A range of parameters including the concentration of PLUS and lipofectAMINE, the cell density, transfection time and assay time were varied in order to optimise the transfection procedure.

However, under all circumstances no transfection of fibroblasts by the LacZ reporter plasmid was observed although a control COS-7 cell line expressed the reporter gene under the same transfection conditions (data not shown). Thus an alternative method of gene delivery to the fibroblasts had to be devised. Hence, electroporation was evaluated as a possible method of gene delivery to fibroblasts. First an electroporation death-curve was carried out on cell line C, in which the voltage of the electroporation was varied. The optimal voltage, after which 50% of cells die, was determined to be 300V and used in further experiments. Electroporation was carried out using either the reporter plasmid with the LacZ gene or the plasmid carrying Rzpol1a1. Fibroblast cells were either tested for LacZ gene expression or selected for three to four weeks with G418 (neomycin marker present on the plasmids) in an attempt to generate stable cell lines carrying Rzpol1a1. A second deathcurve was established to optimise the concentration of G418 for selection of stable fibroblast cell lines. However, unfortunately no cells either expressed LacZ or survived selection with G418. Given the lack of success with both lipofectAMINE-PLUS and electroporation another method of transfection of the fibroblast cell lines had to be considered.

Cell line C was therefore infected with an Ad virus carrying a LacZ reporter gene driven by a CMV promoter, which was available in the laboratory. After 24 hours the cells were assayed for LacZ gene expression (figure 3a). Over 90% of the cells turned blue, showing efficient viral infection. In addition an MLV retrovirus carrying the LacZ reporter gene driven by a CMV promoter was ordered commercially from Dr. Miyanohara (Yee et al., 1994) and tested on cell line C. The cells were assayed for LacZ expression after 48 hours and some blue cells were identified (figure 3b). Control cells remained unstained (figure 3c). The MLV retrovirus, which unlike the Ad virus integrates into host genomes, was therefore thought to be a good virus for stably delivering Rzpol1a1 to cell cultures and animal models for OI.

To make an MLV virus carrying Rzpol1a1 driven by a CMV promoter, clone Rzpol1a1 was PCR amplified over the CMV promoter and Rzpol1a1. The resulting amplified product was cloned into the pLRNL plasmid. This is the same plasmid which was used by Drs. Yee and Miyanohara to generate the MLV virus carrying the LacZ gene discussed above. Resulting colonies were picked, grown in LB medium and miniprepped. The resulting DNAs were sequenced by an automated sequencer and a number of clones carrying the appropriate insert were identified.

Clones carrying the correct insert will be used to generate an MLV retrovirus carrying Rzpol1a1. This recombinant virus will subsequently be used in cell line C and the other primary fibroblast cell lines described above and effects on levels of expression of the C and T3210- polymorphic alleles evaluated. In addition the MLV virus may be used in studies on an animal model for OI; either using ex vivo methods of gene delivery or systemic methods. Fortunately, a transgenic mouse model for OI was generated in 1991 (Olsen et al., 1991; Khillan et al., 1991). This animal is discussed in detail in 5.4. Translating results obtained with ribozymes in vitro to cell or animal systems may involve significant modifications to ribozyme design and methods of delivery. A number of such modifications and delivery methods have been evaluated for fibroblast cells in the current study.

5.4. Discussion

5.4.1. Results

Rzpol1a1, known *in vitro* to specifically cleave the human COL1A1 transcript efficiently at a polymorphic site (3210T) was studied for *in vivo* work. With an exogenous method of gene delivery in mind, Rzpol1a1 was protected from nucleases by the incorporation of 2'-amino pyrimidines in the RNA structure. This was achieved by *in vitro* transcription from a T7 promoter of the ribozyme in the presence of the modified nucleotides. Although the ribozyme still cleaved the T-allele of the COL1A1 transcript specifically and ribozyme stability in DMEM+ was enhanced significantly, the transcription reaction was somewhat problematic and protected Rzpol1a1 yields were low.

The incorporation of 2'-fluoro and 2'-aminonucleotides into hammerhead ribozymes was first discussed in 1991 (Pieken et al., 1991a). In this study the presence of 2'-fluorouridines, 2'-fluorocytidines or 2'-aminouridines did not significantly decrease the catalytic efficiencies of the ribozymes. However, the incorporation of 2'-aminonucleotides decreased ribozyme activity approximately by a factor of 20 and the replacement of all adenosines with 2'-fluoroadenosines abolished detectable catalysis. The 2'-fluoro and 2'-amino modifications conferred resistance toward ribonuclease degradation by a factor of at least 10^3 compared to unmodified ribozymes. An advantage of the incorporation of 2'-aminonucleotides over 2'-fluoronucleotides in ribozymes in terms of ribozyme-protection against nucleases is that 2'-aminonucleotides protect RNAs from not only RNases but also from alkaline cleavage, whereas 2'-fluoronucleotides only protect RNAs from RNases (Janik et al., 1972; Hobbs et al., 1973; Pieken et al., 1991a).

In 1992 another group tested the influence of 2'-modified pyrimidine nucleotides on hammerhead ribozymes. 2'-fluorocytidine substitutions as well as four terminal phosphorothioate internucleotidic linkages influenced the catalytic efficiency of ribozymes only negligibly. However, the substitution of uridine by 2'-fluorouridine resulted in a 5-fold decrease in cleavage efficiency. A ribozyme containing all these modifications revealed only a 7-fold lower catalytic efficiency than the unmodified ribozyme but had a markedly increased stability in cell culture supernatant (Heidenreich and Eckstein, 1992).

In 1993 the same group found that replacement of the 2'-fluoro-2'deoxyuridines in the conserved region of a ribozyme at positions 4 and 7, by 2'-amino-2'-deoxyuridines fully restored catalytic activity of the ribozymes, while the ribozyme remained stable in fetal calf serum and in cell culture supernatant.

Another group of researchers also studied the effects of 2'-amino pyrimidine modification on hammerhead ribozyme activity and stability. They found good cleavage activity can be achieved with ribozymes with uniform 2'-pyrimidine modifications, provided the ribozyme has no pyrimidines in helix 1. Interestingly, selective 2'-amino modifications at positions 2.1 and 2.2 reduced the ribozyme cleavage activity by 8-fold, suggesting that the 2'-amino groups at these two positions may interfere with the formation of the ribozyme secondary structure (Leirdal and Sioud, 1998). A hammerhead ribozyme with 2'-amino pyrimidine modifications, which targeted the protein kinase C alpha (PKC alpha) transcript was found to inhibit glioma cell growth *in vitro* as a result of the inhibition of PKC alpha gene expression. In addition, the modified ribozyme had a 14,000-fold longer half-life in serum compared to an unmodified version of the ribozyme (Sioud and Sorensen, 1998).

In regard to the low transcriptional yield of protected Rzpol1a1, which was obtained during the study, the author contacted Dr. M. Sioud for advice on this issue. His unpublished results, which he kindly discussed with the author, indicate that the efficiency of transcription using 2'-modified pyrimidines and a T7 promoter depend on the sequence of the ribozyme. In order to achieve a high yield, a ribozyme sequence should contain at least 5 purines (although 7 are preferable) near the start of transcription at the 5' end of the ribozyme. Unfortunately Rzpol1a1 contains many pyrimidines at these positions, which may account for the low transcriptional yield obtained for Rzpol1a1. Thus exogenous delivery of Rzpol1a1 protected with 2'-modified pyrimidines may not be a good option due to

the low transcriptional yield. However, it would be possible in principle to synthesise the ribozyme with protected bases commercially. This was not undertaken during the study due to cost. However, alternative methods of protection could be explored, such as the incorporation of 2'-O-methyl, 2'-O-allyl or 2'-deoxy-nucleotides. This can be achieved both chemically or, less expensively, enzymatically. In addition, the ribozyme can be generated containing phosphorothioate linkages; either chemically or enzymatically. Various different chemical modifications are discussed in detail in 5.1. In addition to difficulties with levels of transcription of protected ribozyme , plasmid gene delivery to fibroblast cell line C, heterozygous for the 3210C/T polymorphism in COL1A1, was unsuccessful using both lipofectAMINE-PLUS (GibcoBRL) and electroporation. Therefore, exogenous gene delivery of protected Rzpol1a1 into cell line C may not be a viable option. However, endogenous gene expression, of for example plasmid DNA carrying the ribozyme, using non-viral methods of gene delivery would also not be a good option as primary fibroblast cells are in some way impenetrable to DNAs. Ribozymes have on many occasions successfully been delivered to cell cultures using similar methods outlined in this chapter, including using lipids and electroporation, for either transient expression of the ribozyme or for generating stable cell lines (Ohta et al., 1996; Cameron and Jennings, 1989; Prasmickaite et al., 1998; Kariko et al., 1994; Kijima et al., 1998; Gonzalez et al., 1998; Sakamoto et al., 1996). However, Professor D.J. Prockop and Dr. J. Marini both mentioned, in a personal communication, that they had encountered the same difficulties in transfecting primary fibroblast cell lines as those encountered in this study. The author therefore suggests that primary fibroblasts may be in some way protected against the uptake of nucleic acids, perhaps as a method of cellular protection due to their dermal function or due to the fact they are undifferentiated cells, whose integrity must be carefully maintained. Dr. Marini mentioned that after trying to transfect a primary fibroblast cell line with a plasmid using lipofectAMINE (GibcoBRL), one or two stable cell lines were obtained. However, there is significant concern that these few stable cell lines, which took 6 months to generate, may be in some way defective and may not represent normal fibroblast behavior. As an alternative to non-viral methods of transfection viral modes of endogenous gene delivery were considered.

Initially, an Ad virus, available in the laboratory was evaluated in cell line C and was found to infect these cells extremely efficiently. Additionally an MLV virus was obtained from Dr. Myanohara (Yee et al., 1994) to test its ability to infect cell line

C. This virus, unlike Ad viruses, integrates into host genomes and therefore only expresses in dividing tissues. However, integration ensures prolonged expression of any transgene carried by the MLV virus (section 1.13 for details). The MLV virus infected cell line C successfully and could therefore in principle be used to carry any transgene, including Rzpol1a1, into cell C. As MLV was found to infect cell line C, a vector has been constructed to enable generation of an MLV virus carrying Rzpol1a1 driven by a CMV promoter.

5.4.2. Future work

Interestingly, the resulting MLV virus carrying Rzpol1a1 could be used for a variety of studies. For example, the virus could be used for *ex vivo* studies with a transgenic animal model for OI, expressing the human T-allele of the COL1A1 gene. In addition the virus could be used to study systemic delivery of Rzpol1a1 into a suitable animal model.

In terms of *ex vivo* gene delivery, it is of note that a method has recently and successfully been investigated for the delivery of transplants into bone marrow precursor cells; the cells that specialise into osteoblasts, chondrocytes and other cells involved in OI (Horwitz et al., 1999). In the study, the effects of transplantation of allogenic bone marrow, derived from donors, led to engraftment of functional mesenchymal progenitor cell in three children with severe forms of OI. Three months after the transplantation (DNA analysis showed a presence of 1.5-2% of donor cells), the bone density of the children was significantly increased (on average the bone density went up 26 grams, compared to the predicted 1.3 grams in normal children with similar changes in weight). Also growth velocity was increased and patients manifested reduced frequencies of bone fracture. This method of therapy for dominant OI is very attractive in that it circumvents the allelic heterogeneity of the disease (i.e. that many different mutations in the type 1 collagen genes cause the disease phenotype). In addition, the same therapy may be used in a range of different diseases involving bone marrow cells, such as Ehlers Danlos Syndrome and OI. However, it is based on the introduction of healthy donor stem cells into patients' bone marrow, not removing mutant cells or suppressing mutant genes; hence the ratio of mutant protein (the patients') versus normal protein (the donors') is altered. This, unfortunately, makes the use of immunosuppressing agents necessary for patients treated in this manner. It is of note that mesenchymal progenitor stem cells may also be utilise in future as vehicles of *ex vivo* gene delivery. Therapeutic genes could be stably introduced into

a patient's bone marrow precursor cells and these reintroduced into the patient's bone marrow.

A second study investigated the multilineage potential of adult human mesenchymal stem cell (Pittenger et al., 1999) and for the first time demonstrated their ability to replicate as undifferentiated cells in cell culture and to have the potential to differentiate to different lineages of mesenchymal tissues such as bone, cartilage, fat, tendon, muscle and marrow stroma. The cells were extracted from bone marrow taken from the illiac crest of human donors and could be cultured *in vitro* for up to 12 passages. Between approximately 0.001 and 0.01% of bone marrow cells were estimated to be mesenchymal progenitor cells (Pittenger et al, 1999).

Finally, a group of researchers was able to transduce human marrow-derived osteogenic mesenchymal progenitors with retroviruses containing LacZ and human interleukin-3 (hIL-3) *in vivo*. In this study syeloproliferative sarcoma virus containing the LacZ and neo genes were stably transduced in cell cultures of mesenchymal progenitor cells and 18% of cells manifested gene expression. After culture expansion and selection with G418, approximately 70% of the neo resistant cells co-expressed LacZ. These cells were seeded into porous calcium phosphate ceramic cubes and implanted subcutaneously in SCID mice. LacZ expression was observed in osteoblasts and osteocytes in bone developing within the ceramics 6 and 9 weeks after implantation, demonstrating firstly that transduced progenitor cells retain their ability to differentiate into bone cells and secondly that expression of LacZ remains stable for at least 9 weeks (Allay et al., 1997). A similar experiment was carried out in which mesenchymal progenitor cells were transduced with hIL-3 cDNA, adhered to ceramic cubes and implanted in SCID mice. Bone, which was subsequently formed, secreted detectable levels of hIL-3 into the systemic circulation for at least 12 weeks (Allay et al., 1997).

Thus as a method of gene delivery for disorders of mesenchymal tissue or recessive disorders, which arise from mutant protein which is excreted, such as hormonal disorders, it may in future be possible to extract a patients bone marrow, grow bulk quantities of mesenchymal stem cells from this and carry out *ex vivo* gene therapy. Subsequently, the patient's mesenchymal stem cells, carrying a therapeutic gene would be transplanted back into the patient, hopefully leading to successful transplantation of functional mesenchymal progenitor cells. Such an *ex vivo* approach may be used in a gene therapy study of OI using the MLV virus with

Rzpol1a1 and a suitable animal model. Another method to test the functionality of Rzpol1a1 *in vivo* involves the generation of transgenic mice or rats carrying the Rzpol1a1 transgene and a mutant human COL1A1 transgene with the T-allele. The animal should, in the absence of the ribozyme, manifest a severe form of OI due to a dominant negative mutation. Possible benefits of the Rzpol1a1 transgene could be assessed in mice carrying the disease causing transgene and the therapeutic transgene. A mouse model carrying a human COL1A1 minigene has existed since 1991 and displays a lethal form of OI (Olsen et al., 1991; Khillan et al., 1991). This animal may prove valuable in future gene therapy studies for OI.

A minigene version of the human COL1A1 gene has previously been generated (Olsen et al., 1991) which contained -2.3 kilobases of the 5' upstream sequence, exons and introns 1-5 of the gene, the last 6 exons and introns of the gene and about 3 kilobases of 3' sequence. The construct lacks 41 of the exons and introns of COL1A1. This minigene was shown by northern and western analysis to be expressed in mouse fibroblast cell line NIH 3T3. The minigene construct was then used to generate a transgenic mouse that expressed the minigene version of COL1A1; the mouse developed a phenotype resembling a lethal form of OI (Khillan et al., 1991). Additionally, a second transgenic mouse was generated expressing the minigene construct in a reverse orientation. This antisense mouse was bred onto the minigene mouse and rescue of the disease was demonstrated; the lethal fragile bone phenotype of the progeny was reduced from 93% to 27% (Khillan et al., 1994).

A COL1A1 minigene OI mouse, expressing the T-allele of COL1A1, could be used to test Rzpol1a1 in four ways. Firstly, systemic delivery of the MLV virus with Rzpol1a1 could be investigated. In this regard it is of note that systemic delivery, either through oral means or through injection into the bloodstream, has not been a very successful method of gene delivery to date. There are however, some success stories involving systemic delivery. For example, Adeno-associated viral (AAV) vectors have been shown to preferentially transduce hepatocytes after systemic administration in adult mice and to provide long-term expression of introduced genes. In one study this characteristic was utilised by injecting into mouse tail veins AAV vectors encoding human granulocyte colony-stimulating factor (G-CSF), which increases mature neutrophil numbers in humans and animals and has therapeutic effects in disorders featuring chronic neutropenia. High levels of G-CSF and marked elevation of neutrophil counts were detected for at least 5 months subsequent to viral administration. A therapeutically relevant amount of G-CSF

production was obtained when the liver-specific mouse albumin promoter-enhancer was used to drive G-CSF expression (Koeberl, 1999).

In addition to systemic delivery, the MLV vector encoding Rzpol1a1 and the minigene mouse could be used to explore injection of the virus into bones of the OI mouse. It would be extremely difficult to treat all bones, however, initially more fragile and accessible bones, such as thigh bones could be studied. There are a number of studies, which demonstrate that viral delivery of a therapeutic ribozyme to a target tissue has provided a beneficial effect. As mentioned on pages 45 and 46 of this Ph.D. thesis one of the more recent studies involved ribozyme delivery to retinal tissues of a transgenic rat model for adRP. The rate of photoreceptor degeneration was considerably slowed in the rat for at least three months after a single administration of virus. (Kimberly et al., 1998; Lewin et al., 1998).

A third manner in which the MLV vector encoding Rzpol1a1 could be tested using the minigene mouse is through *ex vivo* delivery of the virus. Mesenchymal progenitor cells (see above) from the OI mouse could be extracted from bone marrow, purified and grown in bulk in cell culture with the MLV virus, selected in cell culture for MLV expression and re-injected into the OI mouse (see above; Allay et al., 1997; Hurwitz et al., 1997). Re-injection could either be directly into the bone or systemically (see above). It is of note that mesenchymal progenitor cells have a homing instinct and that a small percentage of these cells, when injected into the bloodstream will find their way to bone marrow (Prockop, 1998). One large advantage of this *ex vivo* method of gene delivery is that theoretically the mouse should not suffer an immune response against the therapeutic cells, as these are derived from the mouse's own tissue.

The fourth manner in which Rzpol1a1 could be tested for functionality, using the minigene mouse, involves the generation of a second transgenic mouse expressing Rzpol1a1. This mouse could then be bred with the OI mouse model. Subsequent progeny would express both the minigene and the therapeutic agent somatically. Transgenic mice have previously been used to test the functionality of ribozymes. For example this approach was tested in 1996, when researchers generated a double transgenic mouse expressing the bovine α-lactalbumin and a specific ribozyme targeting this gene. Heterozygous expression of the ribozyme resulted in a reduction in the levels of target mRNA to 78%, 58% and 50% of that observed in the non-ribozyme transgenic littermate controls for three independent lines (L'Huillier et al., 1996).

Given the potential usefulness of the OI mouse described above, the author genotyped the OI construct, kindly donated by Dr. A. Fertala, used in generating the OI minigene mouse and discovered that the mouse contains 3210C in the COL1A1 gene and thus is not suitable for Rzpol1a1 cleavage. However Dr. Fertala has kindly given us permission to mutagenise the minigene construct and use this to generate a second minigene mouse or indeed other animal model, carrying the 3210T version of the minigene. So we can mutagenise the construct and generate a second animal with the cleavable T-allele at position 3210, which we can utilise in the manners described above.

5.5. Summary

In this chapter, Rzpol1a1 targeting a common polymorphic site in the human COL1A1 gene (the T-allele) and known to be specific and efficient at cleaving its target was evaluated for *in vivo* studies; both in cell culture and an animal model. A suitable primary fibroblast cell line expressing both COL1A1 polymorphisms was characterised in terms of its ability to be transfected and found to be transfectable by viral means only. A plasmid was therefore generated with Rzpol1a1 driven by a CMV promoter which will be utilised in the generation of an MLV retrovirus. This recombinant virus carrying Rzpol1a1 can be tested for cleavage of COL1A1 (T-allele) transcripts in cell culture and in an animal model. Fortuitously, a dominant OI mouse model with a human COL1A1 mini-transgene has preciously been generated and is available for this study. However, in the current study it has been established that the OI mouse expresses the non-cleavable polymorphism (the C-allele) at position 3210 of COL1A1, making the generation of a new OI animal model expressing the T-allele necessary. The minigene plasmid has kindly been donated by Dr. A. Fertala and can be mutagenised at position 3210 of COL1A1 for this purpose. In addition to the exploration of viral delivery to primary fibroblasts, the suitability of delivering Rzpol1a1 in an exogenous manner was investigated. Rzpol1a1 was protected with 2'-amino pyrimidines and tested for T-allele cleavage and stability in DMEM+. The protected Rzpol1a1 was both specific at cleaving its target and stable in the presence of serum, however, the ribozyme was somewhat problematic to transcribe in large quantities *in vitro*. This may be due to the presence of pyrimidines near the start of transcription. There are a number of ways to overcome this difficulty including synthesising the ribozyme commercially or altering the bases near the start of transcription. In summary, given that the next step towards the ultimate goal of therapeutic ribozymes for OI is *in vivo* evaluation

of the ribozymes studied in sections 3 to 5, both viral and non-viral methods of ribozyme delivery to primary fibroblasts have been explored. The results of these studies have been presented here in chapter 5 of the Ph.D. thesis.

5.6. Bibliography

Allay JA, Dennis JE, Haynesworth SE, Majumdar MK, Clapp DW, Shultz LD, Caplan AI, Gerson SL. LacZ and interleukin-3 expression in vivo after retroviral transduction of marrow-derived human osteogenic mesenchymal progenitors. Hum Gene Ther. 1997 Aug 10;8(12):1417-27.

Cameron FH, Jennings PA. Specific gene suppression by engineered ribozymes in monkey cells. Proc Natl Acad Sci U S A. 1989 Dec;86(23):9139-43.

Drenser KA, Timmers AM, Hauswirth WW, Lewin AS. Ribozyme-targeted destruction of RNA associated with autosomal-dominant retinitis pigmentosa. Invest Ophthalmol Vis Sci. 1998 Apr;39(5):681-9.

Eckstein F. Nucleoside phosphorothioates. Annu Rev Biochem. 1985;54:367-402.

Furuichi Y, LaFiandra A, Shatkin AJ. 5'-Terminal structure and mRNA stability. Nature. 1977 Mar 17;266(5599):235-9.

Gaur RK, Krupp G. Chemical and enzymatic approaches to construct modified RNAs. Methods Mol Biol. 1997;74:99-110.

Gonzalez MA, Serrano F, Llorente M, Abad JL, Garcia-Ortiz MJ, Bernad A. A hammerhead ribozyme targeted to the human chemokine receptor CCR5. Biochem Biophys Res Commun. 1998 Oct 20;251(2):592-6.

Heidenreich O, Eckstein F. Hammerhead ribozyme-mediated cleavage of the long terminal repeat RNA of human immunodeficiency virus type 1. J Biol Chem. 1992 Jan 25;267(3):1904-9.

Hobbs J, Sternbach H, Sprinzl M, Eckstein F. Polynucleotides containing 2'-amino-2'-deoxyribose and 2'-azido-2'-deoxyribose. Biochemistry. 1973 Dec 4;12(25):5138-45.

Horwitz EM, Prockop DJ, Fitzpatrick LA, Koo WW, Gordon PL, Neel M, Sussman M, Orchard P, Marx JC, Pyeritz RE, Brenner MK. Transplantability and therapeutic effects of bone marrow-derived mesenchymal cells in children with osteogenesis imperfecta. Nat Med. 1999 Mar;5(3):309-13.

Hurwitz DR, Kirchgesser M, Merrill W, Galanopoulos T, McGrath CA, Emami S, Hansen M, Cherington V, Appel JM, Bizinkauskas CB, Brackmann HH, Levine PH,

Greenberger JS. Systemic delivery of human growth hormone or human factor IX in dogs by reintroduced genetically modified autologous bone marrow stromal cells. Hum Gene Ther. 1997 Jan 20;8(2):137-56.

Janik B, Kotick MP, Kreiser TH, Reverman LF, Sommer RG, Wilson DP. Synthesis and properties of poly 2'-fluoro-2'-deoxyuridylic acid. Biochem Biophys Res Commun. 1972 Feb 16;46(3):1153-60.

Kariko K, Megyeri K, Xiao Q, Barnathan ES. Lipofectin-aided cell delivery of ribozyme targeted to human urokinase receptor mRNA. FEBS Lett. 1994 Sep 19;352(1):41-4.

Khillan JS, Li SW, Prockop DJ. Partial rescue of a lethal phenotype of fragile bones in transgenic mice with a chimeric antisense gene directed against a mutated collagen gene. Proc Natl Acad Sci U S A. 1994 Jul 5;91(14):6298-302.

Khillan JS, Olsen AS, Kontusaari S, Sokolov B, Prockop DJ. Transgenic mice that express a mini-gene version of the human gene for type I procollagen (COL1A1) develop a phenotype resembling a lethal form of osteogenesis imperfecta. J Biol Chem. 1991 Dec 5;266(34):23373-9.

Kijima H, Tsuchida T, Kondo H, Iida T, Oshika Y, Nakamura M, Scanlon KJ, Kondo T, Tamaoki N. Hammerhead ribozymes against gamma-glutamylcysteine synthetase mRNA down-regulate intracellular glutathione concentration of mouse islet cells. Biochem Biophys Res Commun. 1998 Jun 29;247(3):697-703.

Koeberl DD, Bonham L, Halbert CL, Allen JM, Birkebak T, Miller AD. Persistent, therapeutically relevant levels of human granulocyte colony-stimulating factor in mice after systemic delivery of adeno-associated virus vectors. Hum Gene Ther. 1999 Sep 1;10(13):2133-40.

Leirdal M, Sioud M. High cleavage activity and stability of hammerhead ribozymes with a uniform 2'-amino pyrimidine modification. Biochem Biophys Res Commun. 1998 Sep 8;250(1):171-4.

Lewin AS, Drenser KA, Hauswirth WW, Nishikawa S, Yasumura D, Flannery JG, LaVail MM. Ribozyme rescue of photoreceptor cells in a transgenic rat model of autosomal dominant retinitis pigmentosa. Nat Med. 1998 Aug;4(8):967-71.

L'Huillier PJ, Soulier S, Stinnakre MG, Lepourry L, Davis SR, Mercier JC, Vilotte JL. Efficient and specific ribozyme-mediated reduction of bovine alpha-lactalbumin expression in double transgenic mice. Proc Natl Acad Sci U S A. 1996 Jun 25;93(13):6698-703.

Ludwig J, Blaschke M, Sproat BS. Extending the cleavage rules for the hammerhead ribozyme: mutating adenosine15.1 to inosine15.1 changes the cleavage site specificity from N16.2U16.1H17 to N16.2C16.1H17. Nucleic Acids Res. 1998 May 15;26(10):2279-85.

Ohta Y, Kijima H, Ohkawa T, Kashani-Sabet M, Scanlon KJ. Tissue-specific expression of an anti-ras ribozyme inhibits proliferation of human malignant melanoma cells. Nucleic Acids Res. 1996 Mar 1;24(5):938-42.

Olsen AS, Geddis AE, Prockop DJ. High levels of expression of a minigene version of the human pro alpha 1 (I) collagen gene in stably transfected mouse fibroblasts. Effects of deleting putative regulatory sequences in the first intron. J Biol Chem. 1991 Jan 15;266(2):1117-21.

Pieken WA, Olsen DB, Aurup H, Williams DM, Heidenreich O, Benseler F, Eckstein F. Structure-function relationship of hammerhead ribozymes as probed by 2'-modifications. Nucleic Acids Symp Ser. 1991;(24):51-3.

Pieken WA, Olsen DB, Benseler F, Aurup H, Eckstein F. Kinetic characterization of ribonuclease-resistant 2'-modified hammerhead ribozymes. Science. 1991a Jul 19;253(5017):314-7.

Pittenger MF, Mackay AM, Beck SC, Jaiswal RK, Douglas R, Mosca JD, Moorman MA, Simonetti DW, Craig S, Marshak DR. Multilineage potential of adult human mesenchymal stem cells. Science. 1999 Apr 2;284(5411):143-7.

Prasmickaite L, Hogset A, Maelandsmo G, Berg K, Goodchild J, Perkins T, Fodstad O, Hovig E. Intracellular metabolism of a 2'-O-methyl-stabilized ribozyme after uptake by DOTAP transfection or asfree ribozyme. A study by capillary electrophoresis. Nucleic Acids Res. 1998 Sep 15;26(18):4241-8.

Prockop DJ. What holds us together? Why do some of us fall apart? What can we do about it? Matrix Biol. 1998 Mar;16(9):519-28.

Sakamoto N, Wu CH, Wu GY. Intracellular cleavage of hepatitis C virus RNA and inhibition of viral protein translation by hammerhead ribozymes. J Clin Invest. 1996 Dec 15;98(12):2720-8.

Sioud M, Sorensen DR. A nuclease-resistant protein kinase C alpha ribozyme blocks glioma cell growth. Nat Biotechnol. 1998 Jun;16(6):556-61.

Willing MC, Deschenes SP, Scott DA, Byers PH, Slayton RL, Pitts SH, Arikat H, Roberts EJ. Osteogenesis imperfecta type I: molecular heterogeneity for COL1A1 null alleles of type I collagen. Am J Hum Genet. 1994 Oct;55(4):638-47.

Yee JK, Miyanohara A, LaPorte P, Bouic K, Burns JC, Friedmann T. A general method for the generation of high-titer, pantropic retroviral vectors: highly efficient infection of primary hepatocytes. Proc Natl Acad Sci U S A. 1994 Sep 27;91(20):9564-8.

Zhang X, Iwatani Y, Shimayama T, Yamada R, Koito A, Xu Y, Sakai H, Uchiyama T, Hattori T. Phosphorothioate hammerhead ribozymes targeting a conserved sequence in the V3 loop region inhibit HIV-1 entry. Antisense Nucleic Acid Drug Dev. 1998 Dec;8(6):441-50.
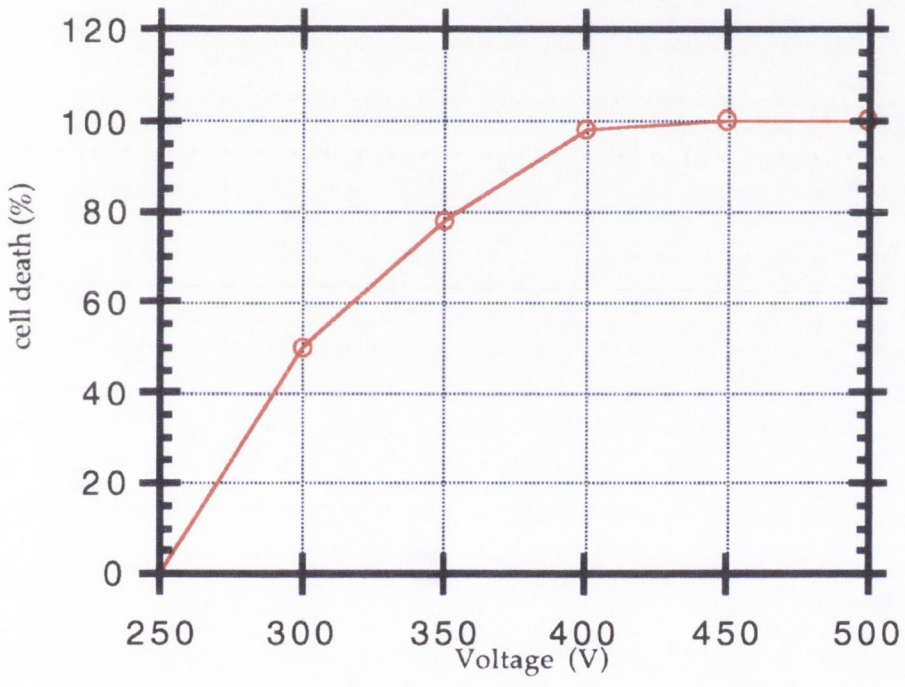
Figure 1.

Figure 1. Electroporation deathcurve of primary fibroblast cell line C. The horizontal axis represents the voltage of the electroporation. The vertical axis represents the percentage of cell death after electroporation.

Figure 2.
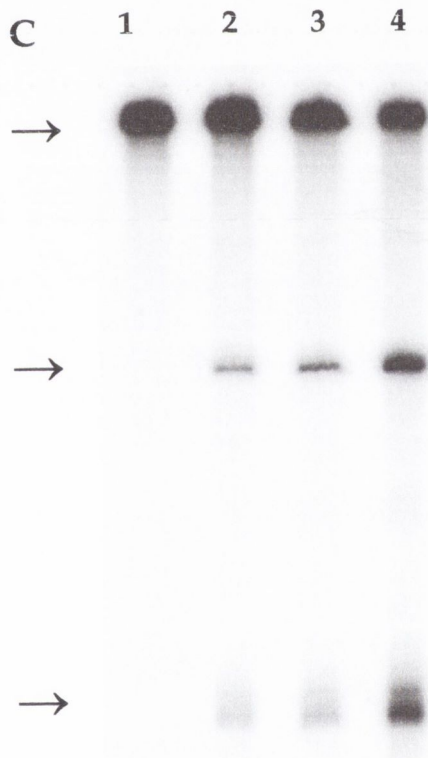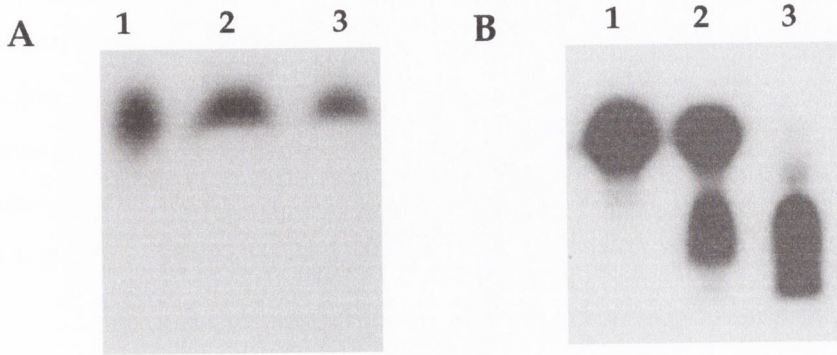
Figure 2. Protected Rzpol1a1 stability in DMEM+ and cleavage of the T-allele transcript. *A*, lanes 1-3 represent protected Rzpol1a1 incubated in DMEM+ for 0, 1 and 30 minutes. No degradation is observed after 30 minutes. *B*, lanes 1-3 represent unprotected Rzpol1a1 incubated in DMEM+ for 0, 1 and 30 minutes. No intact Rzpol1a1 is visible after 30 minutes. *C*, timepoint cleavage reactions of protected Rzpol1a1 and the T-allele RNA of COL1A1. Lanes 1-4 represent cleavage reactions for 0, 30, 60 and 180 minutes respectively. T-allele RNA and cleavage products are highlighted with arrows from top to bottom.

Figure 3.
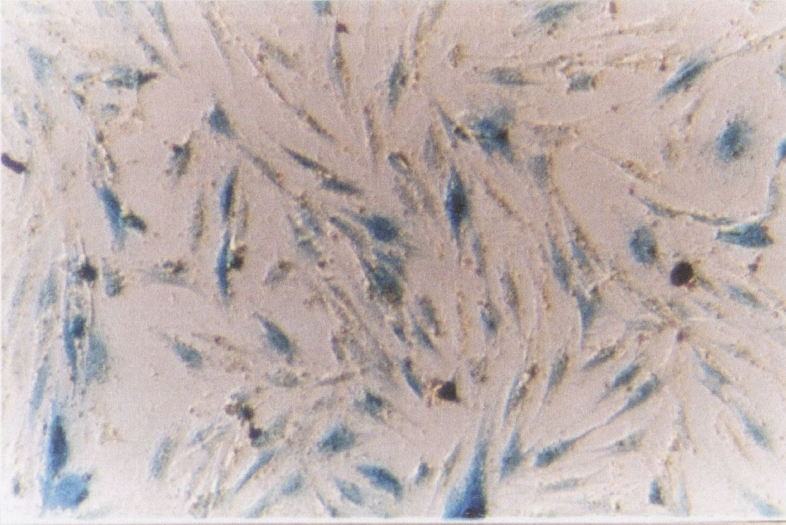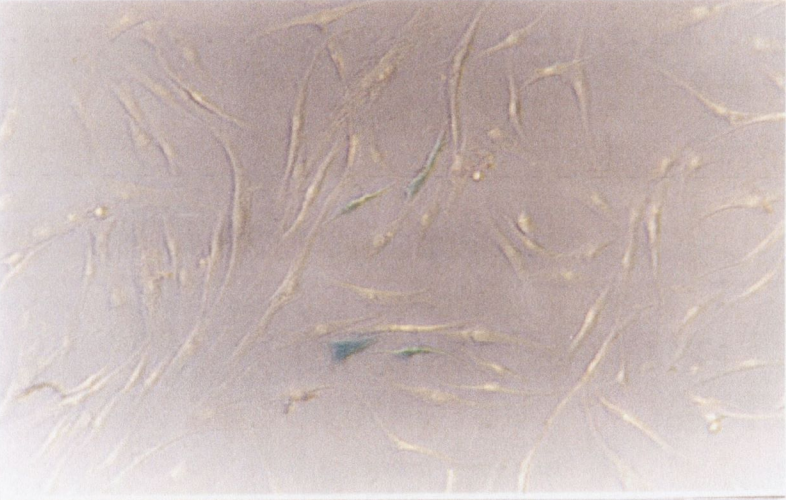
Figure 3. *A*, Ad LacZ expression in cell line C, assayed after 24 hours. Over 90% of cells are expression the reporter gene. *B*, MLV virus driving LacZ expression in cell line C, assayed after 48 hours. A small portion of cells expressed the LacZ reporter gene. *C*, Control fibroblast C cells which have not been infected with virus.

Concluding remarks

The aim of the study presented in this Ph.D. thesis has been to contribute towards the eventual generation of therapies for genetic disorders such as retinitis pigmentosa (RP) and osteogenesis imperfecta (OI). To enable the generation of such therapies, a disease gene must first be localised and characterised. In chapter 2 of this thesis a novel mitochondrial disease mutation, causing RP and sensorineural deafness in an Irish family, was identified in the second mitochondrial serine tRNA, highlighting yet again the immense heterogeneity associated with disorders such as RP. In addition to knowledge of the genetic pathogenesis of diseases, to enable the generation of gene therapies for many dominantly inherited disorders (although not recessive disorders) suppression agents will be required, which can selectively switch off mutant alleles while leaving wildtype alleles intact. However, many dominantly inherited disorders are genetically heterogeneous. For instance, there are over 150 different mutations in the human COL1A1 and COL1A2 genes known to cause OI and similarly well over 100 mutations in the rhodopsin gene give rise to adRP. Thus, the use of mutation-independent suppressors for such disorders is likely to present a more realistic therapeutic approach. In chapters 3 and 4 of this Ph.D. thesis 12 mutation-specific and mutation-independent hammerhead ribozymes, targeting the human rhodopsin, peripherin/*RDS*, COL1A1 and COL1A2 transcripts, were designed and tested *in vitro*. All ribozymes elicited sequence specific cleavage of target RNAs, although cleavage efficiencies varied widely. Therefore, in chapter 4 of this Ph.D. thesis the most efficient ribozyme identified in chapter 3, Rzpol1a1, which targets a polymorphic site in the COL1A1 transcript was characterised in terms of its kinetic profile and was found to be extremely efficient with a V_{max} of 0.41 min^{-1}. Additional steps involved in generating gene therapies, suitable for humans, include testing therapeutic agents in cell culture and suitable animal models and to design a means of delivering therapies to appropriate tissues. In chapter 5 of this Ph.D. thesis suitable primary human fibroblast cell lines expressing the polymorphic variants of human COL1A1 were characterised and subsequently used to evaluate various methods of gene delivery. In this study in fibroblast cells, the cell lines were found to be resistant to non-viral means of gene delivery (lipofectAMINE PLUS and electroporation) but were susceptible to viral gene delivery, including viruses such as Ad and MLV.

Thus a viral MLV plasmid carrying Rzpol1a1 under the control of a CMV promoter was generated, which will be used to construct an MLV retrovirus carrying the ribozyme. The virus may be used to deliver Rzpol1a1 to cells or into a suitable animal model for OI, expressing the cleavable polymorphic variant of COL1A1. A similar animal model, expressing a human COL1A1 minigene was designed in 1991 by Khillan and Olsen (see chapter 5 for details), but unfortunately carries the non-cleavable variant of COL1A1. The animal manifests a phenotype similar to human OI. The plasmid, which was used to generate the minigene mouse, was kindly donated to the author and will be mutagenised and used to generate a second animal model for OI carrying the cleavable variant of the COL1A1 gene. This animal could subsequently be used in two studies briefly described below.

Firstly, the animal could be crossed with a transgenic animal carrying and expressing Rzpol1a1 and subsequent beneficial effects on the disease phenotype evaluated. Secondly, viral delivery using the MLV virus with Rzpol1a1 could be studied, perhaps using an *ex vivo* approach involving infection of bone marrow mesenchymal progenitor cells, the undifferentiated cells which give rise to cells involved in OI, with recombinant virus. Again, subsequently, the OI phenotype and COL1A1 expression profile could be studied in these animals.

In addition, in chapter 5 of the thesis, the ability of Rzpol1a1 to be protected from ribonuclease degradation by incorporating 2'amino-pyrimidines into the ribozyme was assessed. This was carried out with a view to delivering Rzpol1a1 in an exogenous manner into cell cultures and perhaps, at a later stage into an appropriate animal model of OI. Having undertaken a number of transfection assays using the primary fibroblast cell lines obtained for the study it would now seem that delivery in an exogenous (non-viral) manner to these fibroblast cell lines may not be possible as these cells are highly resistant to transfection. Exogenous delivery of protected Rzpol1a1 to primary fibroblasts may prove difficult, however, it may be possible for example to transfect bone marrow progenitor cells. These cells would, in principle, be an ideal target cell for an *in vivo* approach to OI therapy. In this regard it is notable that Rzpol1a1 when protected with 2'amino-pyrimidines was stable in the presence of serum for at least 30 minutes and still elicited sequence specific cleavage of target RNA.

Thus during the course of this Ph.D. a novel mitochondrial disease mutation, causing RP in conjunction with sensorineural deafness was identified, highlighting the large levels of heterogeneity inherent in human inherited retinopathies. In

addition mutation independent hammerhead ribozymes, targeting retinal and collagen transcripts (rhodopsin, peripherin/*RDS*, COL1A1 and COL1A2), implicated in RP and OI, were designed and tested *in vitro*. In chapter 5 of this thesis, various studies were initiated which will be required to test the most efficient ribozyme, Rzpol1a1 targeting the COL1A1 transcript at a polymorphism, in cell culture and animal models. However, the evaluation of a gene therapy in an animal model represents only the beginning of the path leading towards a functional gene therapy, which is suitable for human patients. The development of such therapies is labor intensive and indeed extremely costly. Some elements involved in this process are outlined below.

Subsequent to testing therapeutic agents in an animal model for a genetic disorder such as a rodent, typically such agents must be tested in larger animals such as transgenic pigs and primates. Only after these tests have been carried out can human trials of the gene therapeutic drugs be attempted. In addition, to minimize risks in terms of safety, human experimental drug trials proceed through four phases. In phase I clinical trials, a drug or treatment is tested in a small group of people (20-80 patients, who have not reacted well to any drugs on the market) for the first time to evaluate its safety, determine a safe dosage range and identify possible side effects. Phase II clinical trials involve testing the study drug or treatment in a larger group of people (100-300) and evaluating the efficacy and safety further. In phase III studies the drug or treatment is tested in an even larger group of people (1,000-3,000) to confirm the efficacy, monitor side effects, compare it to commonly used treatments and collect information that will allow the drug or treatment to be used in a safe manner. Phase IV studies are carried out after the drug or treatment has been marketed and involves continued evaluation to collect information about beneficial effect(s) in various populations and any side effects associated with long-term use.

Thus, to develop a therapy from a concept into a product involves carrying out essential studies including animal studies, human trials, product development and marketing and is estimated to take about 10 years and cost at least 100 million dollars (estimates vary from about 100-500 million dollars). Such vast quantities of money are hardly ever available in university environments and must therefore frequently come from various investors, initially often involving venture capitalists, but latterly involving large multinationals. However, investors typically will only invest in a potential product if there is a good chance of monetary return in the

future. For this reason, many scientists developing therapies have found it necessary to apply for patents in order to generate appealing intellectual property, often required to tempt investors. In this regard, three patents have arisen from research undertaken during the course of this Ph.D.

The patents describe the three mutation-independent strategies of gene suppression (outlined in chapter 3) using hammerhead ribozymes and based on suppressing transcripts at polymorphic sites, in UTRs or at wobble positions. In the latter two cases, replacement genes would be generated and concurrently administered, which have been altered at the target cleavage site and which are thereby protected from ribozyme cleavage. In the case of the polymorphism approach, gene replacement may only be necessary, where haploinsufficiency plays a large role in disease pathology. These mutation-independent methods of gene suppression may help overcome the immense heterogeneity inherent in many dominant-negative disorders, including OI and RP. Other mutation-independent methods of therapy for disorders such as RP that could be considered would include the use of growth factors, the suppression of apoptotic genes involved in photoreceptor cell death and retinal transplants. The ability to overcome genetic heterogeneity will be one of the many components required to develop successful therapies for these disorders.

Gene therapies for dominant negative disorders, such as RP, which involve complex target tissues such as neurons (both rod and cone photoreceptor cells), which must survive throughout a person' s lifetime, as they are post-mitotic, will possibly involve combination therapies. Combination therapies may comprise of gene suppressors, for example hammerhead ribozymes, growth factors and anti-apoptotic agents. In addition retinal transplantation may be required. It is of note that the relatively late onset of RP, in theory, gives patients time in which to seek therapy. In the case of therapies for simpler disorders such as OI, which involves dividing cells, an *ex vivo* approach of gene therapy, involving viral delivery of a therapeutic suppressor to mesenchymal progenitor cells present in bone marrow, may be a viable approach to eventually treating OI. In the study presented in chapters 4 and 5, an extremely efficient hammerhead ribozyme, Rzpol1a1, has been designed and tested *in vitro*, which targets a common polymorphic site in COL1A1. Rzpol1a1 may be a suitable and novel suppression agent for 20% of all OI patients with a dominant negative mutation in the COL1A1 gene and for this reason warrants further investigation in cell culture and animal models.

Another essential component required for the development of gene therapies will undoubtedly be the availability of safe and efficient vector systems for delivery to the tissues involved in disorders such as RP and OI. Novel developments in vectorology should expedite the overall development of successful gene therapies.

Agarose Loading Dye
0.25% bromophenol blue
0.25% xylene cyanol
30% glycerol
69.5% H_2O

MgCl$_2$ Buffer (Promega)
500mM KCl
100m TrisCl pH 9.0
0.1% gelatin
1% tritonX100
10, 12.5, 15, 20 or 25mM
$MgCl_2$

PBS
8g NaCl
0.2g KCl
1.44g $NaHPO_4$
0.24g KH_2PO_4

Formamide Loading Dye
1mg/ml bromophenol blue
1mg/ml xylene cyanol
10mM EDTA pH8.0
80% formamide

20% Acrylamide
96.5g acrylamide
3.35g bis-acrylamide
233.5g urea
50ml 10x TBE
H_2O to 500ml

LB broth and plates
10g NaCl
10g tryptone
5g yeast extract
10mM Mg SO_4
0.2% maltose
H_2O to 1L
(plates: 15g bactoagar)
0.05g ampicillin
0.025g tetracycline
H_2O to 500ml

10X TBE
55g boric acid
108g trizma base
40ml 0.5M EDTA pH8.0
H_2O to 1L

7.75M Urea mix
233.5g urea
50ml 10x TBE

Hot NTP mix
10 ml dGTP
10 ml dTTP
10 ml dATP
12.5 ml 1/100 dil dCTP
717.5 ml H_2O

Cold NTP mix
10 ml dGTP
10 ml dCTP
10 ml dTTP
10 ml dATP
760 ml H_2O

TES
10mM TrisCl pH8.0
1mM EDTA pH8.0
0.1% SDS

DMEM+

500 ml DMEM (GibcoBRL)

5 ml L-glutamine (GibcoBRL)

5 ml penicillin/streptomycine (GibcoBRL)

5 ml sodium pyruvate (GibcoBRL)

50 ml fetal calf serum (GibcoBRL)

Fix solution

25 % gluteraldehyde

0.5 M sodiumphosphate buffer pH7.3

0.1 M EGTA pH8.0

1.0 M $MgCl_2$

Rinse solution (500 ml)

0.5 M sodium phosphate buffer pH7.3

1.0 M $MgCl_2$

50 mg sodium deoxycholate

10 ml nonidet P-40

H_2O

Stain solution (100 ml)

96 ml rinse solution

0.165 g potassium ferricyanide

0.165 g potassium ferrocyanide

4 ml X-gal solution

X-gal solution

25 mg X-gal per ml dimethylformamide

Appendix B

Modified from the online Retnet database maintained by Dr. S.P. Daiger.

http://www.sph.uth.tmc.edu/Retnet.disease.htm

Cloned and/or Mapped Genes Causing Retinal Diseases

Listed by chromosome

Chromosome 1			
Symbol	*Location*	*Disease, protein*	*Mapping method, comment*
LCA2, RP20, RPE65	1p31	Recessive Leber congenital amaurosis; recessive RP; protein: retinal pigment epithelium-specific 65 kD protein	Cloned gene; accounts for 2% of recessive RP and 16% of recessive Leber congenital amaurosis; 'RP20' withdrawn; same as Swedish Briard-Beagle dog retinal degeneration
STGD1, RP19, ABCR	1p21-p22	Recessive Stargardt disease, juvenile and late onset; recessive MD; recessive RP; recessive fundus flavimaculatus; Recessive combined RP and cone-rod dystrophy; protein: ATP-binding cassette transporter - retinal	Linkage mapping, cloned gene; may be involved in age-related macular degeneration but controversial; same as ROS1.2 and rim protein, expressed only in rod outer segment
RP18	1q13-q23	Dominant RP	Linkage mapping; Danish family; early onset night blindness
ARMD1	1q25-q31	Dominant MD, age-related	Linkage mapping; possible model for acquired age-related macular degeneration
AXPC1	1q31-q32	Recessive ataxia, posterior column with RP	Linkage mapping
RP12	1q31-q32.1	Recessive RP with para-arteriolar preservation of the RPE (PPRPE)	Linkage mapping; Dutch family; close to mouse *rd3*
USH2A	1q41	Recessive Usher syndrome, type 2a; protein: novel protein with similarity to laminins and cell adhesion molecules	Linkage mapping, cloned gene; may be either an extracellular-matrix protein or cell adhesion molecule; USH2B at same site; common 2314delG mutation with atypical phenotype

Chromosome 2

Symbol	Location	Disease, protein	Mapping method, comment
EFEMP1, DHRD, MTLV	2p16-p21	Dominant radial, macular drusen; dominant Doyne honeycomb retinal degeneration (Malattia Leventinese); Protein: EGF-containing fibrillin-like extracellular matrix protein 1	Linkage mapping, cloned gene; single mutation (Arg345Trp) found in all affected individulals to date; possible model for age-related macular degeneration
ALMS1, ALSS	2p14-p13	Recesssive Alström syndrome	Homozygosity and linkage mapping; sympotms include RP, deafness, obesity and diabetes (like BBS)
RP28	2p11-p16	Rrecessive RP	Homozygosity mapping; Consanguinous Indian family
ACHM2, RMCH2, CNCG3, CNGA3	2q11	Recessive achromatopsia; protein: cone photoreceptor cGMP-gated cation channel, alpha subunit	Homozygosity mapping, cloned gene; total color blindness and other cone-related abnormalities (rod monochromacy)
RP26	2q31-q33	Recessive RP	Linkage mapping
BBS5	2q31	Recessive Bardet-Biedl syndrome	Linkage mapping
SAG	2q37.1	Recessive Oguchi disease; recessive RP; protein: arrestin (s-antigen)	Cloned gene; CSNB and fundus palor in Japanese primarily; recessive RP in Japanese

Chromosome 3

Symbol	Location	Disease, protein	Mapping method, comment
GNAT1	3p22	dominant CSNB, Nougaret type; protein: rod transducin alpha subunit	cloned gene; missense mutation in a single large French family, may affect taste perception
SCA7, OPCA3, ADCA2	3p13-p12	dominant spinocerebellar ataxia w/ MD or retinal degeneration; protein: SCA7 protein	linkage mapping, cloned gene; Moroccan, Belgian, French, Swedish, American and African-American families; shows anticipation with expanding CAG repeat in coding sequence of protein with unknown function
BBS3	3p13-p12	recessive Bardet-Biedl syndrome	homozygosity and linkage mapping
RP5	3q	not distinct from RHO/RP4	linkage mapping; mapping error: was dropped
RHO, RP4	3q21-q24	dominant RP; dominant CSNB; recessive RP; protein: rhodopsin	linkage mapping, cloned gene; accounts for 30 to 40% of autosomal dominant RP; more than 100 distinct mutations but RhoPro23His cause s 15% of adRP in US Caucasians; 'RP4' withdrawn
USH3A, USH3	3q21-q25	recessive Usher syndrome, type 3	linkage mapping; USH3 withdrawn

OPA1	3q28-q29	dominant optic atrophy, Kjer type	linkage mapping; little or no genetic heterogeneity

Chromosome 4			
Symbol	*Location*	*Disease, protein*	*Mapping method, comment*
STGD4	4p	dominant Stargardt-like macular dystrophy	linkagemapping; Caribbean family
CSNB3, PDE6B	4p16.3	recessive RP; dominant CSNB; protein: rod cGMP phosphodiesterase beta subunit	linkage mapping, cloned gene; same as mouse *rd*, mouse *r* and *rcd1*Irish Settter dog retinal degeneration
WFS1	4p16.1	recessive Wolfram syndrome; protein: wolframin	linkage mapping, cloned gene; symptoms include diabetes, optic atrophy and deafness; often associated with multiple mitochondrial deletions
CNGA1, CNCG, CNCG1	4p12-cen	recessive RP; protein: rod cGMP-gated channel alpha subunit	cloned gene; nonsense, missense and deletion mutations in four RP families
ABL, MTP	4q24	recessive abetalipoproteinemia; protein: microsomal triglyceride transfer protein	cloned gene; multiple lipid abnormalities including pigmentary retinal degeneration

Chromosome 5			
Symbol	*Location*	*Disease, protein*	*Mapping method, comment*
WGN1, ERVR	5q13-q14	dominant Wagner disease and erosive vitreoretinopathy	linkage mapping
PDE6A	5q31.2-q34	recessive RP; protein: cGMP phosphodiesterase alpha subunit	cloned gene; homozygote and compound heterozygote mutations

Chromosome 6			
Symbol	*Location*	*Disease, protein*	*Mapping method, comment*
RP14, TULP1	6p21.3	recessive RP; protein: tubby-like protein 1	linkage mapping, cloned gene; two Dominican families and others; same as mouse *tub* which causes obesity, deafness and retinal degeneration
RDS, RP7	6p21.2-cen	dominant RP; dominant MD; digenic RP with ROM1; dominant adult vitelliform MD; protein: peripherin/RDS	linkage mapping, cloned gene; dominant mutations; also, compound heterozygotes with ; accounts for 5% of autosomal dominant RP; same as mouse *rds*; 'RP7' withdrawn
COD3, GCAP1, GUCA1A	6p21.1	dominant cone dystrophy; protein: guanylate cyclase activating protein 1A	linkage mapping, cloned gene; British family with constitutively active mutant
CORD7	6q	dominant cone-rod dystrophy	linkage mapping

RP25	6cen-q15	recessive RP	homozygosity mapping; Spanish families (10-20% of arRP); mapped to region containing GABA receptors
STGD3	6q11-q15	dominant MD, Stargardt-like	linkage mapping; excluded from MCDR1; Griesinger 98 may be distinct
MCDR1, PBCRA	6q14-q16.2	dominant MD, North Carolina type; dominant progressive bifocal chorioretinal atrophy	linkage mapping; North Carolina, German, Belizean and British families; PBCRA is clinically distinct from MCDR1
RCD1	6q25-q26	dominant retinal-cone dystrophy 1	deletion mapping

Chromosome 7

Symbol	Location	Disease, protein	Mapping method, comment
CYMD	7p21-p15	dominant MD, cystoid	linkage mapping; distinct from RP9
RP9	7p15-p13	dominant RP	linkage mapping
PEX1, IRD	7q21-q22	recessive Refsum disease, infantile; protein: peroxisome biogenesis factor 1	cloned gene; symptoms include RP, retardation and hearing deficit
RP10	7q31.3	dominant RP	linkage mapping; Spanish, Scottish and American families
BCP, CBT	7q31.3-32	dominant tritanopia; protein: blue cone opsin	cloned gene; several mutations; progressive retinopathy not observed

Chromosome 8

Symbol	Location	Disease, protein	Mapping method, comment
RP1	8q11-q13	dominant RP; protein: RP1 protein	linkage mapping, cloned gene; causes 5 to 10% of adRP; protein is photoreceptor-specific with unknown function but similarity over short region to doublecortin; distinct from mouse *Rd4*; large Kentucky family and others
TTPA	8q13.1-q13.3	recessive RP and/or recessive or dominant ataxia; protein: alpha-tocopherol-transfer protein	cloned gene; TPA mutations found in patients with vitamin E deficiency
ACHM3	8q21-q22	recessive achromatopsia Pingelapese	linkage mapping; includes total color blindness, photophobia and nystagmus; affects 4 to 10% of Pingelapese people on the Eastern Caroline Islands
VMD1	not 8q24	dominant MD, atypical vitelliform	linkage exclusion; linked to GPT but later excluded

Chromosome 9

Symbol	Location	Disease, protein	Mapping method, comment
RP21	not 9q34-qter	dominant RP with sensorineural deafness	linkage mapping; RP21 withdrawn; later mapped to in mitochondrion

Chromosome 10

Symbol	Location	Disease, protein	Mapping method, comment
USH1F	10	recessive Usher syndrome, type 1f	homozygosity mapping; inbred Hutterite family; distinct from USH1D
RDPA, PHYH, PAHX	10p15.3-p12.2	recessive Refsum disease; protein: phytanoyl-CoA hydroxylase	homozygosity mapping, cloned gene; symptoms include RP, peripheral neuropathy and cerebellar ataxia; same proteins with different names
USH1D	10q	recessive Usher syndrome, type 1d	homozygosity mapping; Pakistani family
(- - -)	10q21	recessive nonsyndromal congenital retinal nonattachment	homozygosity mapping; Iranian population
RBP4	10q24	recessive RPE degeneration; protein: retinol-binding protein 4	cloned gene; RPE atrophy with night blindness and reduced visual acuity; carrier protein for serum retinol
ONCR, PAX2	10q25	dominant renal-coloboma syndrome; protein: paired homeotic gene 2	cloned gene; optic nerve colobomas with renal abnormalities; similar malformations in mouse *Pax2(1Neu)* mutation
OAT	10q26	recessive gyrate atrophy; protein: ornithine aminotransferase	cloned gene; many mutations reported

Chromosome 11

Symbol	Location	Disease, protein	Mapping method, comment
AA	11p15	dominant atrophia areata; dominant chorioretinal degeneration, helicoid	linkage mapping
USH1C	11p15.1	recessive Usher syndrome, Acadian	linkage mapping; possibly same as mouse *rd5*
BBS1	11q13	recessive Bardet-Biedl syndrome	linkage mapping; approximately 40% ofBBS families
ROM1	11q13	dominant RP; digenic RP with RDS; protein: retinal outer segment membrane protein 1	cloned gene; compound heterozygote with ; dominant RP is rare and doubtful
VMD2	11q13	dominant MD, Best type; protein: bestrophin	linkage mapping, cloned gene; bestrophin is retinal-specific, expressed in the RPE, possibly involved in metabolism/transport of polyunsaturated fatty acids

EVR1, FEVR	11q13-q23	dominant familial exudative vitreoretinopathy	linkage mapping; distinct from VRNI
VRNI	11q13	dominant neovascular inflammatory vitreoretinopathy	linkage mapping; distinct from EVR1
MYO7A, DFNB2, USH1B	11q13.5	recessive Usher syndrome, type 1; recessive congenital deafness without RP; recessive atypical Usher syndrome (USH3-like); protein: myosin VIIA	linkage mapping, cloned gene; MY07A is a common component of cilia and microvilli; same as mouse *sh1* shaker-1 (but no RP); 'USH1B' withdrawn

Chromosome 12

Symbol	Location	Disease, protein	Mapping method, comment
RDH5, RDH1	12q13-q14	recessive fundus albipunctatus; protein: 11-*cis* retinol dehydrogenase 5	cloned gene; stationary night blindness with subretinal spots and delayed dark adaptation; protein is an RPE microsomal enzyme involved in converting 11-*cis* retinol to 11-*cis* retinal

Chromosome 13

Symbol	Location	Disease, protein	Mapping method, comment
RB1	13q14.2	dominant germline or somatic retinoblastoma; benign retinoma; pinealoma; osteogenic sarcoma; protein: retinoblastoma protein 1	deletion mapping, cloned gene; requires 'second hit' loss of heterozygosity; 5 to 10% inherited, 20 to 30% new mutation, remainder sporadic; preferential loss of maternal chromosome; protein is cell-cycle regulatory element
STGD2	13q34	dominant MD, Stargardt type	linkage mapping; large American family
RHOK, RK	13q34	recessive CSNB, Oguchi type; protein: rhodopsin kinase	cloned gene; several mutations in Japanese

Chromosome 14

Symbol	Location	Disease, protein	Mapping method, comment
(RP16)	14	recessive RP (possibly)	linkage mapping
ACHM1, RMCH	14	recessive rod monochromacy or achromatopsia	uniparental isodisomy; total color blindness or 'day blindness'
NRL, RP27	14q11.2	dominant RP; protein: neural retina lucine zipper	linkage mapping, cloned gene; NRL is a retinal transcription factor which interacts with and promotes transcription of rhodopsin and other retinal genes
LCA3	14q24	recessive Leber congenital amaurosis	homozygosity mapping; consanguineous Saudi Arabian family
USH1A, USH1	14q32	recessive Usher syndrome, French	linkage mapping; was 'USH1'

Chromosome 15

Symbol	Location	Disease, protein	Mapping method, comment
BBS4	15q22.3-q23	recessive Bardet-Biedl syndrome	homozygosity and linkage mapping; approximately 30% of BBS families
MRST	15q24	recessive retardation, spasticity and retinal degeneration	linkage mapping; inbred Pakistani family
RLBP1, CRALBP	15q26	recessive RP; recessive Bothnia dystrophy; recessive retinitis punctata albescens; protein: cellular retinaldehyde-binding protein	cloned gene; consanguineous Indian family, Swedish families and others

Chromosome 16

Symbol	Location	Disease, protein	Mapping method, comment
CLN3, JNCL	16p12.1	recessive Batten disease (ceroid-lipofuscinosis, neuronal 3), juvenile; protein: Batten disease protein	linkage mapping, cloned gene; symptoms include early-onset retinal pigmentary degeneration with later mental deterioration
RP22	16p12.1-p12.3	recessive RP	homozygosity mapping; Indian families
BBS2	16q21	recessive Bardet-Biedl syndrome, type 2	linkage mapping; Bedouin family; approximately 20% of BBS families

Chromosome 17

Symbol	Location	Disease, protein	Mapping method, comment
CORD5, RCD2	17p13-p12	dominant cone dystrophy, progressive; recessive cone-rod dystrophy	linkage mapping; several families with dominant CORD map to this region, as does a family with recessive CORD -- these may or may not be allelic
CACD	17p13	dominant central areolar choroidal dystrophy	linkage mapping
RP13	17p13.3	dominant RP	linkage mapping; South African and English families; not recoverin
GUCY2D, CORD6, LCA1, RETGC1	17p13.1	recessive Leber congenital amaurosis; dominant cone-rod dystrophy; protein: retinal-specific guanylate cyclase	linkage mapping, cloned gene; North African families and several mutations; same as chicken *rd/rd*
CORD4	17q	cone-rod dystrophy	association with neurofibromatosis; presumed dominant like NF
PDE6G, PDEG	17q21.1	mouse recessive retinal degeneration; protein: cGMP phosphodiesterase gamma subunit	cloned gene; targeted disruption transgene

RP17	17q22	dominant RP	linkage mapping; South African and Dutch families; PDEG excluded; same location as dog *prcd* progressive rod-cone degeneration

Chromosome 18			
Symbol	*Location*	*Disease, protein*	*Mapping method, comment*
CORD1	18q21.1-q21.3	cone-rod dystrophy; de Grouchy syndrome	deletion mapping; isolated case; symptoms include COD, retardation and hearing impairment

Chromosome 19			
Symbol	*Location*	*Disease, protein*	*Mapping method, comment*
OPA3, MGA3	19q13.2-q13.3	recessive optic atrophy with ataxia and 3-methylglutaconic aciduria	linkage mapping; Iraqi-Jewish families
CORD2, CRX	19q13.3	dominant cone-rod dystrophy; recessive, dominant and 'de novo' Leber congenital amaurosis; dominant RP; protein: cone-rod otx-like photoreceptor homeobox transcription factor	linkage mapping, cloned gene; meiotic drive suggested; CRX also activates pineal genes; interacts with
RP11	19q13.4	dominant RP	linkage mapping; distinct from CORD2; high frequency in British Isles (21%), highly variable; some cases may involve protein kinase C gamma (PRKCG)

Chromosome 20			
Symbol	*Location*	*Disease, protein*	*Mapping method, comment*
AGS, PLCB4	20p12	dominant Alagille syndrome; protein: phospholipase-C-beta-4	deletion mapping, cloned gene; multiple affected organs; same as Drosophila *norpA* retinal mutant

Chromosome 21			
Symbol	*Location*	*Disease, protein*	*Mapping method, comment*
USH1E	21q21	recessive Usher syndrome, type 1	linkage mapping

Chromosome 22			
Symbol	*Location*	*Disease, protein*	*Mapping method, comment*
SFD, TIMP3	22q12.1-q13.2	dominant Sorsby's fundus dystrophy; protein: tissue inhibitor of metalloproteinases-3	linkage mapping, cloned gene; model for ARMD; common British mutation; vitamin A reverses night blindness

X Chromosome			
Symbol	*Location*	*Disease, protein*	*Mapping method, comment*

RP23	Xp22	X-linked RP	linkage mapping; distinct from RP2 and RP3
RS1, XLRS1	Xp22.2	retinoschisis; protein: X-linked retinoschisis 1 protein	linkage mapping, cloned gene
RP15	Xp22.13-p22.11	X-linked RP, dominant	linkage mapping; distinct from COD1, RP2, RP3, RP6 and RS
(- - -)	Xp21-q21	RP with mental retardation	linkage mapping; may be contiguous gene syndrome including RP2
RP6	Xp21.3-p21.2	X-linked RP	linkage mapping
DMD	Xp21.2	Oregon eye disease (probable cause); protein: dystrophin	cloned gene; exons 20-28 involved in retinal disease
RPGR, RP3	Xp21.1	X-linked RP; X-linked CSNB (possibly); protein: retinitis pigmentosa GTPase regulator	linkage mapping, cloned gene; RPGR mutations are found in roughly 20% of RP3 cases; protein homologous to RCC1 and binds PDE-delta; mutations may affect protein localization
AIED, OA2	Xp11.4-q21	Åland island eye disease	linkage mapping
CSNB4	Xp11.4-p11.3	X-linked CSNB	linkage mapping; distinct from RP2, RP3, CSNB1 and CSNB2; overlaps with COD1; 'CSNB4' also refers to rhodopsin
CSNB1	Xp11.4-p11.3	X-linked CSNB	linkage mapping
OPA2	Xp11.4-p11.2	X-linked optic atrophy	linkage mapping; large Dutch family
COD1	Xp11.4	X-linked cone dystrophy, 1	linkage mapping; RP2 and RP3 excluded
PRD	Xp11.3-p11.23	retinal dysplasia, primary	linkage mapping; linked to Norrie disease, may be same locus
NDP, EVR2	Xp11.3	Norrie Disease; familial exudative vitreoretinopathy; protein: Norrie disease protein	linkage mapping, cloned gene; expressed in multiple tissues, function unknown; some mutations cause FEVR but evidence of genetic heterogeneity; associated with retinopathy of prematurity
RP2	Xp11.3	X-linked RP; protein: novel protein with similarity to human cofactor C	linkage mapping, cloned gene; human cofactor C is involved in beta-tubulin folding; accounts for 10% of XlRP
CSNB2, CSNBX2, CACNA1F	Xp11.23	X-linked CSNB, incomplete; protein: L-type voltage-gated calcium channel, alpha-1 subunit	linkage mapping, cloned gene; distinct from CSNB1; includes large Mennonite family; CACNA1F is retinal-specific
PGK1	Xq13.3	RP with myopathy; protein: phosphoglycerate kinase	cloned gene; one case only - RP is not usually found with PGK deficiency

CHM, REP1	Xq21.1-q21.3	choroideremia; protein: geranylgeranyl transferase Rab escort protein 1	linkage mapping, cloned gene; ubiquitously expressed protein (REP2 can substitute); attaches isoprenoids to Rab (e.g, Rab 27) proteins
RP24	Xq26-q27	X-linked RP	linkage mapping; single large family; RP2, RP3 and RP15 excluded
COD2, XLPCD	Xq27	X-linked progressive cone dystrophy, 2	linkage mapping
CBP, RCP	Xq28	protanopia and rare dystrophy in blue cone monochromacy; protein: red cone opsin	cloned gene; Ala180Ser polymorphism with spectral shift
CBD, GCP	Xq28	deuteranopia and rare retinal dystrophy in blue cone monochromacy; protein: green cone opsin	cloned gene; one to five copies 3' to red pigment gene or more complex organization

Mitochondrion			
Symbol	*Location*	*Disease, protein*	*Mapping method, comment*
KSS	mitochondrion	Kearns-Sayre syndrome including retinal pigmentary degeneration	sequencing; mutations in ATPase subunit 6 or multiple large deletions
LHON	mitochondrion	Leber hereditary optic neuropathy; protein: several mitochondrial proteins	sequencing; three mutations (nt 3460, 11778 and 14484) account for 95% of European cases and one (11778) for 80% of Japanese cases; penetrance influenced by mtDNA haplotype; uncertain role of rare variants; spontaneous recovery possible
MTTL1, DMDF	mitochondrion	macular pattern dystrophy with type II diabetes and deafness; protein: leucine tRNA 1 (UUA/G)	sequencing; one of two mitochondrial leucine tRNAs; often caused by heteroplasmic A3243G mutation; other mutations can cause a similar disease
MTTS2	mitochondrion	RP with progressive sensorineural hearing loss; protein: serine tRNA 2 (AGU/C)	linkage mapping, sequencing; one of two mitochondrial serine tRNAs; Irish family; previously mapped to 9q as

For references to the above table please see http://www.sph.uth.tmc.edu/Retnet.disease.htm